Nuclear Safety
NEA/CSNI/R(2015)15
July 2015
www.oecd-nea.org

Workshop on Testing Probabilistic Seismic Hazard Analysis Results and the Benefits of Bayesian Techniques

Pavia, Italy
4–6 February 2015

OECD
BETTER POLICIES FOR BETTER LIVES

NEA
NUCLEAR ENERGY AGENCY

Organisation de Coopération et de Développement Économiques
Organisation for Economic Co-operation and Development

07-Sep-2015

English text only

NUCLEAR ENERGY AGENCY
COMMITTEE ON THE SAFETY OF NUCLEAR INSTALLATIONS

CSNI Workshop on Testing PSHA Results and Benefit of Bayesian Techniques for Seismic Hazard Assessment

Pavia, Italy, 4-6 February 2015

This document only exists in PDF.

JT03381323

Complete document available on OLIS in its original format

NEA/CSNI/R(2015)15
Unclassified

English text only

ORGANISATION FOR ECONOMIC CO-OPERATION AND DEVELOPMENT

The OECD is a unique forum where the governments of 34 democracies work together to address the economic, social and environmental challenges of globalisation. The OECD is also at the forefront of efforts to understand and to help governments respond to new developments and concerns, such as corporate governance, the information economy and the challenges of an ageing population. The Organisation provides a setting where governments can compare policy experiences, seek answers to common problems, identify good practice and work to co-ordinate domestic and international policies.

The OECD member countries are: Australia, Austria, Belgium, Canada, Chile, the Czech Republic, Denmark, Estonia, Finland, France, Germany, Greece, Hungary, Iceland, Ireland, Israel, Italy, Japan, Korea, Luxembourg, Mexico, the Netherlands, New Zealand, Norway, Poland, Portugal, the Slovak Republic, Slovenia, Spain, Sweden, Switzerland, Turkey, the United Kingdom and the United States. The European Commission takes part in the work of the OECD.

OECD Publishing disseminates widely the results of the Organisation's statistics gathering and research on economic, social and environmental issues, as well as the conventions, guidelines and standards agreed by its members.

NUCLEAR ENERGY AGENCY

The OECD Nuclear Energy Agency (NEA) was established on 1 February 1958. Current NEA membership consists of 31 countries: Australia, Austria, Belgium, Canada, the Czech Republic, Denmark, Finland, France, Germany, Greece, Hungary, Iceland, Ireland, Italy, Japan, Korea, Luxembourg, Mexico, the Netherlands, Norway, Poland, Portugal, Russia, the Slovak Republic, Slovenia, Spain, Sweden, Switzerland, Turkey, the United Kingdom and the United States. The European Commission also takes part in the work of the Agency.

The mission of the NEA is:

- to assist its member countries in maintaining and further developing, through international co-operation, the scientific, technological and legal bases required for a safe, environmentally friendly and economical use of nuclear energy for peaceful purposes;
- to provide authoritative assessments and to forge common understandings on key issues, as input to government decisions on nuclear energy policy and to broader OECD policy analyses in areas such as energy and sustainable development.

Specific areas of competence of the NEA include the safety and regulation of nuclear activities, radioactive waste management, radiological protection, nuclear science, economic and technical analyses of the nuclear fuel cycle, nuclear law and liability, and public information.

The NEA Data Bank provides nuclear data and computer program services for participating countries. In these and related tasks, the NEA works in close collaboration with the International Atomic Energy Agency in Vienna, with which it has a Co-operation Agreement, as well as with other international organisations in the nuclear field.

THE COMMITTEE ON THE SAFETY OF NUCLEAR INSTALLATIONS

The NEA Committee on the Safety of Nuclear Installations (CSNI) is an international committee made up of senior scientists and engineers with broad responsibilities for safety technology and research programmes, as well as representatives from regulatory authorities. It was created in 1973 to develop and co-ordinate the activities of the NEA concerning the technical aspects of the design, construction and operation of nuclear installations insofar as they affect the safety of such installations.

The committee's purpose is to foster international co-operation in nuclear safety among NEA member countries. The main tasks of the CSNI are to exchange technical information and to promote collaboration between research, development, engineering and regulatory organisations; to review operating experience and the state of knowledge on selected topics of nuclear safety technology and safety assessment; to initiate and conduct programmes to overcome discrepancies, develop improvements and reach consensus on technical issues; and to promote the co-ordination of work that serves to maintain competence in nuclear safety matters, including the establishment of joint undertakings.

The priority of the committee is on the safety of nuclear installations and the design and construction of new reactors and installations. For advanced reactor designs, the committee provides a forum for improving safety-related knowledge and a vehicle for joint research.

In implementing its programme, the CSNI establishes co-operative mechanisms with the NEA Committee on Nuclear Regulatory Activities (CNRA), which is responsible for issues concerning the regulation, licensing and inspection of nuclear installations with regard to safety. It also co-operates with other NEA Standing Technical Committees, as well as with key international organisations such as the International Atomic Energy Agency (IAEA), on matters of common interest.

TABLE OF CONTENTS

EXECUTIVE SUMMARY

This workshop was the fourth in a series of NEA meetings (Tokyo, Japan, August 1999, Jeju, Korea, November 2006, Lyon, France, April 2008), dedicated to probabilistic approach of seismic hazard or seismic risk. The main objectives were to foster exchanges between earth scientists, statisticians and engineers so as to share experiences in progress related to developments in testing the results of probabilistic seismic hazard analyses (PSHA) with special focus on assessing the benefits of using Bayesian techniques for such a purpose. The goal was to address the current status of the regulatory arena, identifying and recommending good practices for member countries and exploring R&D to be developed on this topic.

The workshop was held in Pavia, Italy on 4-6 February 2015, hosted by EUCENTRE/IUSS (European Centre for Training and Research in Earthquake Engineering / University Institute for Advanced Studies). The workshop was attended by about 65 specialists from 12 countries. It means that, although the subject could appear as rather narrow, the workshop clearly met a scientific community expectation. The scientific content consisted of 3 invited lectures and 25 contributions from the participants.

During this workshop and previous PSHA workshops' it was unanimously acknowledge that observations are necessary to test or assess consistency (or more precisely, lack of bias) of PSHA results. Different kinds of consistency checking were presented in the workshop. The testing phase is especially useful and efficient in the process of PSHA maps revision as well as in the process to defining the seismic margins in the power plant siting process. Theoretical ground motion simulation is a promising tool for filling the gap in existing data, but their results need to be tested and validated before they use in real applications. Uncertainty at every step of the process shall be carefully evaluated.

The main findings and recommendations can be summarised as follows:

- Although this workshop was held under the auspices of the NEA, it
- is clear that its conclusions and recommendations reflect the state of the art on the subject of the workshop, and are not limited to the hazard assessment of nuclear facilities only.
- As already stated by the previous workshops, it is recommended that comparison between results of PSHA studies performed in regions of high seismicity and those from PSHA performed in regions of moderate or low seismicity be carried out at a future NEA workshop. The comparison is necessary for better understanding of the methodological differences of regional PSHA's.
- A state-of-the-art PSHA should include a testing phase against any available observation, including any kind of observation and any period of observation, including instrumental seismicity, historical seismicity and paleoseismicity data if available. It should include testing not only against its median hazard estimates but also against their entire distribution (percentiles).

- The PSHA results should be realistic; therefore, use of Bayesian techniques in PSHA is strongly encouraged in order to take into consideration any available observation. It is recommended to develop common guidelines for systematic implementation of Bayesian updating approaches in PSHA, including a clear description of possible techniques, ways to implement them and including special care on sensitive issues (e.g. correlation between ground motion intensity at different stations, stability tests, high quality "open" data, risk on double counting data, and treatment of uncertainties).

1 INTRODUCTION

This is a summary report from the "Testing PSHA Results and Benefit of Bayesian Techniques for Seismic Hazard Assessment", held in Pavia, Italy on 4-6 February 2015. About 65 specialists from 12 countries attended this workshop.

The Meeting was sponsored by the NEA and hosted by EUCENTRE/IUSS (European Centre for Training and Research in Earthquake Engineering / University Institute for Advanced Studies).

This was the fourth in a series of NEA meetings that began in Tokyo, Japan, in August 1999, followed by a second meeting in Jeju, Korea, in November 2006 and a third meeting in Lyon, France, in April 2008.

2 OBJECTIVES

The main objectives of the Meeting were to foster exchanges between earth scientists, statisticians and engineers so as to share experiences in progress related to developments in testing the results of probabilistic seismic hazard analyses (PSHA) with special focus on assessing the benefits of using Bayesian techniques for such a purpose. The goal was to address the current status of the regulatory arena, identifying and recommending good practices for member countries and exploring future research and development (R&D) to be developed on this topic.

In recent years, increasing efforts have been devoted to the assessment of the reliability of PSHA results. Different kinds of procedures have been tested and many papers have provided useful information on this subject. Consistent with the pattern of previous CSNI workshops, the deliverables and expected results were the following:

- a description of the state-of-the-art methodologies for testing the reliability of PSHA results;
- a presentation of application studies conducted in different areas concerning the testing of PSHA results versus available observations in order to get, to the extent allowed by the uncertainty implicit in such observations, an objective comparison and to improve the confidence in the results;
- a description of the state-of-the-art Bayesian techniques for testing seismic hazard estimates;
- a presentation of application studies conducted in different contexts to determine the benefit of Bayesian techniques for testing seismic hazard estimates;

The workshop accomplished the following targeted recommendations:

- which testing procedure is appropriate depending on the available data;
- good practices and recommendations to implement procedures for testing PSHA results;
- good practices for the implementation of Bayesian techniques in the field of seismic hazard assessment;
- R&D activities to be developed on the subject.

3 RECALL OF PREVIOUS RECOMMENDATIONS

The previous OECD workshop conclusions were presented in order to point out the main advances or findings on the topic available before this workshop.

3.1 Main conclusions and recommendations from the 2006 Jeju Workshop

- "PSHA must be performed in as realistic a way as possible, in order to reach a probabilistic result in the form of a realistic distribution, including all of the uncertainties."

- "In addition, PSHA results should be compared to all available observations, especially for return periods where records are available, in order to get an objective comparison and to improve the confidence in the results, at least in that range of return periods."

- "Finally, an extensive comparison should be performed between PSHA results conducted in different regions, including low to moderate seismicity regions as well as high seismicity regions, especially in the range of return periods where observed data are available."

- "A well-executed PSHA would normally include these three desirable features described above, as for instance required in the ANS Standard. However, discussions at the meeting revealed that this may not always be the case. Since seismic hazard analysis forms a key element of seismic PSA with major safety and cost impact on nuclear power plants, future PSHAs are encouraged to meet these requirements."

3.2 Main conclusions and recommendations from 2008 Lyon Workshop

- "The recommendations concerning PSHA from the 2006 NEA workshop in Jeju, Korea remain valid. Specifically, it remains important that any PSHA be as realistic as feasible, and that it tries to include consistency checks against all available data."

- "… it is very important to undertake "consistency checks", which provide valuable information even though a consistency check is a lesser standard than a validation would be."

- "The Workshop included several papers and extensive discussion about using Bayesian methods in PSHA. While Bayes' classic theorem on updating prior information with newer information is of course rigorously correct, and some presentations demonstrated its potential efficiency in PSHA, its application is not mature enough for routine use in PSHA without special care."

- "Despite these difficulties, using Bayesian updating methods can be of important value and further work (both research work and applications) in this area is to be encouraged."

- "Among the subjects within the scope of this Workshop was the issue of the value of comparisons between PSHA studies performed in regions of high seismicity and other studies

performed in regions of moderate or low seismicity. This was also an explicit recommendation of the earlier Workshop in Jeju, Korea, in 2006. However, only one paper was submitted to the Workshop on this topic, and very little discussion took place about such comparisons. It is recommended that this subject be given special attention at a future NEA workshop."

4 FINDINGS AND RECOMMENDATIONS

Although this workshop was held under the auspices of the NEA, it is clear that the hereunder conclusions and recommendations reflect the state of the art on the subject of the workshop, and are not limited to the hazard assessment of nuclear facilities only.

The objectives defined for workshop recommendations were as follows:

1. Comparison between PSHA studies performed in regions of high seismicity and other studies performed in regions of moderate or low seismicity
2. Use of observations to test or assess consistency of PSHA results
3. Use of Bayesian techniques in the development of PSHA

For these targets the following recommendations of the workshop are presented.

4.1 Comparison between PSHA studies performed in regions of high seismicity and other studies performed in regions of moderate or low seismicity

Previous workshops (Jeju, 2006 and Lyon, 2008) already pointed out the fact that seldom do studies focus on a comparison between PSHA performed in regions of high seismicity and those performed in regions of moderate or low seismicity.

No papers dealing with this issue were presented during this workshop. However, it was pointed out that this recommendation remains valid.

Recommendation 1.1 - It is recommended that comparison between results of PSHA studies performed in regions of high seismicity and those from PSHA performed in regions of moderate or low seismicity be carried out at a future NEA workshop

4.2 On the use of observations to test or assess consistency of PSHA results

During this workshop, it was unanimously acknowledge that observations are necessary to test or assess consistency (or more precisely, lack of bias) of PSHA results. This is fully in line with previous workshops' recommendations that a PSHA should be carried out in an unbiased manner following clearly formulated assumptions. This recommendation is still valid.

Different kinds of consistency checking were presented, showing that many institutions are now performing such assessments. Presentations covered different kind of checking or scoring and different

kind of observations (e.g. instrumental seismicity, historical seismicity and paleoseismicity observations, which were treated as direct or indirect observations, depending on the proposed testing or scoring method). The quality of papers in this field indicates the significant improvements that have been made since the previous workshop.

The following conclusions were shared among the participants:

- For consistency checking or scoring of PSHA results, observations coming from any available time horizon (i.e. instrumental seismicity, historical seismicity, and paleoseismicity) are of interest.

- To assess consistency of PSHA results with historical data, in many parts of the world the wealth of macroseismic Intensities can be an indicator of the historical hazard as accurately as instrumental PGA recordings or better. A possible way to incorporate macroseismic intensity observations is to translate them into "imperfect" PGA observations (i.e. affected by some uncertainty).

- Another option is to use fragility curves appropriate for conventional buildings so as to derive a seismic risk estimate from the PSHA outputs. This risk can then be compared to the historically observed seismic risk.

- The different components of PSHA, such as source modeling, ground motion evaluation, uncertainties, can be tested individually.

- Although site specific PSHA is necessary at the nuclear installation site, PSHA at a regional scale should also be considered with the purpose of testing the credibility of probabilistic hazard estimates.

- The testing (or scoring) phase is especially useful and efficient in the process of PSHA maps revision, because, to a certain extent, data collected at the scale of a territory can compensate for lack of data at the scale of individual sites. Different papers pointed out that, recent maps do not necessarily perform better than earlier ones in comparison with the available observations.

- Theoretical ground motion simulation is a promising tool for filling the gap in existing data (e.g. recordings close to large M earthquakes), but their results need to be fully tested and validated before they can be confidently used in real applications.

- Theoretical ground motion estimates from physically based independent models can also be considered for the purpose of comparison to probabilistic hazard estimates outputs.

- Modeling of uncertainty at every step of the process and its effect on the final PSHA results shall be carefully evaluated.

In addition, it was observed that different kinds of observations can, and should, be used for testing the credibility of PHSA results. The first kind comprise "direct" observations, namely those that can be directly compared to traditional measures of seismic hazard,, such as recordings of peak ground acceleration (or other ground motion intensity parameters), while a second kind is "indirect" observations,

such as the presence of precariously balanced rocks or other fragile geologic formations (e.g. stalactites and stalagmites in caves) close to faults, that can be compared to PSHA results only after they are appropriately manipulated. There is a third, intermediate kind of observation made from macroseismic intensities. They can be treated as direct observations and directly compared to PSHA results expressed in that quantity or as indirect observations, in which case they should be also appropriately manipulated (transformed first into PGA or other traditional ground motion intensity measure used in PSHA) before the comparison can be made or combined with fragility curves appropriate for conventional buildings).

In this regard, although this item was not the core of the workshop, it was recalled by the participants that the PGA (and its associated response spectrum) is a very poor indicator of the seismic input motion damaging capacity. Better alternate indicators should be proposed by the earthquake engineering community and used in the future for the implementation of PSHA.

Recommendation 2.1 – A state-of-the-art PSHA should include a testing (or scoring) phase against any available observation (including any kind of observation and any period of observation) and should include testing not only against its median hazard estimates but also against their entire distribution (percentiles).

Recommendation 2.2 – When "direct" observations are used, comparison with PSHA results, while taking into consideration the aleatory variability involved, should properly consider the correlation between the observations at different recording stations in the same earthquake.

Recommendation 2.3 – When "indirect" observations are used for testing the credibility of probabilistic seismic hazard estimates, the comparison should take into consideration the uncertainty included in the process of converting the original observation (e.g. macroseismic intensity or existence of a precariously balanced rock of a given acceleration capacity) into the parameter used for reporting the PSHA results used for the comparison.

4.3 On the use of Bayesian techniques in the development of PSHA

During this workshop, many papers were presented showing that Bayesian techniques are now fully matured, some of them being used for more than 30 years. It was also pointed out that many studies were performed in the past and should be neither disregarded nor forgotten due to new studies or data (new result does not necessarily imply better quality!). It was especially pointed out that Bayesian approaches offer the opportunity to update past assessment considering new data or observations.

Following conclusions were shared among participants:

- It was recognised that Bayesian approaches, which consider different types of posterior information and local observations, are largely used within the international scientific community to test and, sometimes, update PSHA results.
- Bayesian techniques provide an objective method for attributing weights to the branches of a logic tree.
- Obviously, if prior PSHA is poorly executed (e.g. due to sparse seismic data) or plainly wrong, updating will not resolve it!

- Finally, it was shown that the performance of Bayesian updating improves with increasing amount of data, but even in case of low amount of data updating is still possible but less efficient.

Recommendation 3.1 – Use of Bayesian techniques in PSHA is strongly encouraged in order to take into consideration any available observation.

Recommendation 3.2 – It is recommended to develop common guidelines for systematic implementation of Bayesian updating approaches in PSHA, including a clear description of possible techniques, ways to implement them and including special care on sensitive issues (e.g. correlation between ground motion intensity at different stations, stability tests, high quality "open" data, risk on double counting data, and treatment of uncertainties). Such an action could be included in NEA Medium-Term Strategy for the WGIAGE Seismic Sub-group.

Recommendation 3.3 – It is also recommended to share experience with other probabilistic hazard estimates for other natural perils (i.e. volcano, tsunami, flood, tropical cyclone wind) in order to go towards a systematic approach of estimating and comparing risks from different natural perils.

Recommendation 3.4 - Finally, as a general conclusion, it is recommended that past observations, data and studies should not be forgotten nor obliterated by new ones, but considered as references and experience feedback.

APPENDIX 1 - LIST OF PARTICIPANTS

Name	Company
John Anderson	Nevada Seismological Laboratory
Roger Musson	British Geological Survey
Jacopo Selva	Istituto Nazionale di Geofisica e Vulcanologia
Pierre Labbé	EDF
Y. Fukushima	IAEA
Paolo Bazzurro	IUSS / Eucentre Foundation
Gloria Senfaute	EDF
Massimiliano Stucchi	Eucentre Foundation
Olli Nevander	NEA
Emanuel Viallet	EDF
Ricardo Monteiro	IUSS / Eucentre Foundation
Götz Bokelmann	University of Wien
Katalin Gribovszki	Geodetic and Geophysical Institute
Hongjun Si	Seismological Research Institute Inc
Philippe L.A. Renault	Swissnuclear
Antonella Peresan	University of Trieste
Iunio Iervolino	Università degli Studi di Napoli Federico II
Nicolas Kuehn	University of California, Berkeley
Norman A. Abrahamson	Pacific Gas Electric
Dario Albarello	Università degli Studi di Siena
Vera D'Amico	Istituto Nazionale di Geofisica e Vulcanologia
Marco Mucciarelli	Istituto Nazionale di Oceanografia e Geofisica
Agnès Helmstetter	Université Grenoble Alpes
Sum Mak	GFZ German Research Centre for Geosciences
Janne Laitonen	STUK – Radiation and Nuclear Safety Authority, Finland
Yong Li	U.S. Nuclear Regulatory Commission
Danijel Schorlemmer	GFZ German Research Centre for Geosciences
Fabrice Cotton	GFZ German Research Centre for Geosciences
Pierre Labbé	EDF
Annalisa Rosti	Eucentre Foundation
Maria Rota	Eucentre Foundation
Andrea Penna	Eucentre Foundation
Emilia Fiorini	Eucentre Foundation
Gordon Woo	RMS, UK
Maria Crespo	PRINCIPIA Ingenieros Consultores, Madrid, Spain
José G. Sanchez-Cabañero	Consejo de Seguridad Nuclear
Jean-Michel Thiry	AREVA
Laura Peruzza	Istituto Nazionale di Oceanografia e Geofisica
Agostino Goretti	Dipartimento Protezione Civile
Francesca Pacor	Istituto Nazionale di Geofisica e Vulcanologia
Ramon Secanell Gallart	GEOTER SAS
Merlin Keller	EDF / CEIDRE-TEGG
Nicolas Humbert	EDF
Kris Vanneste	Royal Observatory of Belgium
Tania Del Giudice	

Name	Company
Carlo Meletti	Istituto Nazionale di Geofisica e Vulcanologia
Matteo Taroni	Istituto Nazionale di Geofisica e Vulcanologia
Marco Zei	Georisk Engineering S.r.l.
Marco Uzielli	Georisk Engineering S.r.l.
Alain Pecker	Géodynamique et Structure
Pamela Poggi	D'Appolonia SpA
Gernot Thuma	Gesellschaft für Anlagen- und Reaktorsicherheit (GRS) mbH
David Heeszel	U.S. Nuclear Regulatory Commission
Maria Lancieri	Institut de Radioprotection et Sûreté Nucléaire
Daniela Tonoli	Studio Geotecnico Italiano
Gary Gibson	Seismology Research Centre
Mario Ordaz	Universidad Nacional Autónoma de México
Christophe Durouchoux	EDF
Mauro Dolce	Dipartimento Protezione Civile
Daniela Di Bucci	Dipartimento Protezione Civile
Marco Pagani	GEM Foundation
Graeme Weatherill	GEM Foundation
Julio Garcia	GEM Foundation
Luis Rodriguez	UME Graduate School
Yen-Shin Chen	UME Graduate School
Robin Gee	GEM Foundation / InOGS

APPENDIX 2 - WORKSHOP PROGRAM

Introduction and Objectives of the workshop
O. Nevander (NEA) (only presentation)

Session 1, Chairman: P. Labbé (EDF) and Y. Fukushima (IAEA)

Keynote lecture: Precarious rocks and related fragile geological features to test or to improve seismic hazard assessment. (only presentation)
John Anderson. Nevada Seismological Laboratory, USA

1-1 Constraints on Long-Term Seismic Hazard From Vulnerable Stalagmites
G. Bokelmann1, K. Gribovszki

1-2 Validation of GMPE on very hard rock using global database (copy of presentation is missing)
Hongjun Si, Seismological Research Institute Inc., 705-6-525, Minami-Ohya, Machida City, Tokyo 194-0031, Japan (only presentation, no full paper)

1-3 Testing and centering of ground motion models for use in PSHA based on available intensity data
Philippe L.A. Renault and Luis A. Dalguer. Swissnuclear, P.O. Box 1663, 4601 Olten, Switzerland

1-4 Seismic hazard assessments: a comparative analysis - A new probabilistic shift away from seismic hazard reality in Italy?
A. Peresan; A. Nekrasova; V.Kossobokov; G.F. Panza

1-5 Metrics, observations, and biases in quantitative assessment of seismic hazard model predictions
Edward Brooks, Seth Stein, Bruce D. Spencer, Antonella Peresan

1-6 The effect of dependence of observations on hazard validation studies
Iunio Iervolino; Massimiliano Giorgio

Session 2, Chairman: P. Bazzurro (IUSS, EUCENTRE) and G. Senfaute (EDF)

Keynote lecture: Statistical tests of PSHA models. (only presentation)
Roger Musson. British Geological Survey, UK

2-1Non-Ergodic Seismic Hazard: Using Bayesian Updating for Site-Specific and Path-Specific Effects for Ground-Motion Models
Nicolas Kuehn, Norman Abrahamson

2-2 Some steps forward in confronting probabilistic seismic hazard with observations in Italy
Laura Peruzza

2-3 The scoring test on Italian Probabilistic Seismic Hazard Estimates developed in the frame of S2-2012 DPC-INGV Project
D.Albarello, L.Peruzza, V.D'Amico

2-4 Revision of earthquake catalogues on probabilistic terms: consequences on PSHA validation
M. Mucciarelli

2-5 Testing Probabilistic Seismic Hazard Estimates Against Accelerometric Data in two countries: France And Turkey
Hilal Tasan, Céline Beauval, Agnès Helmstetter, Abdullah Sandikkay, Philippe Guéguen.

2-6 Direct verification of seismic hazard maps
Sum Mak; Danijel Schorlemmer (only presentation, no full paper)

Session 3, Chairman: M. Stucchi (EUCENTRE) and O. Nevander (NEA)

3-1 Regulatory View on Challenges in PSHA in Low Seismicity Areas
Janne Laitonen and Jorma Sandberg, STUK – Radiation and Nuclear Safety Authority, Finland

3-2 Testing PSHA while there are large uncertainties in input data
Yong Li, U.S. Nuclear Regulatory Commission (only presentation, no full paper)

3-3 Testing & Evaluation in the Global Earthquake Model
Danijel Schorlemmer, Sum Mak, Thomas Beutin, Robert Clements, Max Schneider, Fabrice Cotton, Jochen Zschau (only presentation, no full paper)

3-4 A method for testing PSHA outputs against historical seismicity at the scale of a territory; example of France
Pierre Labbé, EDF Div Ingénierie Nucléaire, Paris, France.

3-5 Comparison of PSHA results with historical macroseismic observations in south-east France
Annalisa ROSTI, Maria ROTA, Andrea PENNA, Emilia FIORINI and Guido MAGENES, EUCENTRE, Pavia.

3-6 An Application Of Bayes Theorem To Test Macroseismic Intensity Data
Emilia FIORINI, Paolo BAZZURRO

Session 4, Chairman : E. Viallet (EDF) and R. Monteiro (IUSS, EUCENTRE)

Keynote lecture: Probabilistic Seismic Hazard Assessment: Combining Cornell-Like Approaches and Data at Sites through Bayesian Inference. (only presentation)
Jacopo Selva. INGV, Italy.

4-1 Thirty-Year Bayesian Updating of PHSA for Hinkley Point NPP PSHA testing
Gordon Woo, RMS, 30 Monument Street, London EC3R 8NB, England

4-2 Past is the Key of the Present. A Geological Principle as Bayesian Philosophy Applied for Seismic Hazard Analysis - Bayesian Philosophy Applied for Seismic Hazard Analysis; Examples

José G. Sanchez, Cabañero; Raúl Pérez; Maria J. Crespo

4-3 Bayesian update of a simplified PSHA model, description of updating methods
L. Vaseux and J.M. Thiry, AREVA, France (only presentation, no full paper)

4-4 A Bayesian methodology to update the Probabilistic Seismic Hazard Assessment
Ramon SECANELL, Christophe MARTIN, E. Viallet, Gloria SENFAUTE

4-5 Bayesian Estimation of the Earthquake Recurrence Parameters for Seismic Hazard Assessment
Merlin KELLER , Marine MARCILHAC, Thierry YALAMAS; Ramòn SECANELL3, Gloria SENFAUTE

4-6 PSHA updating technique with a Bayesian framework
Nicolas Humbert, EDF, Centre d'Ingénierie Hydraulique Structure / Génie Civil, France

APPENDIX 3 - PAPERS

APPENDIX 3 - WORKSHOP PAPERS

Session 1, Chairman: P. Labbé (EDF) and Y. Fukushima (IAEA)

1-1 Constraints on Long-Term Seismic Hazard From Vulnerable Stalagmites
G. Bokelmann1, K. Gribovszki

1-2 Validation of GMPE on very hard rock using global database (copy of presentation is missing)
Hongjun Si, Seismological Research Institute Inc., 705-6-525, Minami-Ohya, Machida City, Tokyo 194-0031, Japan (only presentation, no full paper)

1-3 Testing and centering of ground motion models for use in PSHA based on available intensity data
Philippe L.A. Renault and Luis A. Dalguer. Swissnuclear, P.O. Box 1663, 4601 Olten, Switzerland

1-4 Seismic hazard assessments: a comparative analysis - A new probabilistic shift away from seismic hazard reality in Italy?
A. Peresan; A. Nekrasova; V.Kossobokov; G.F. Panza

1-5 Metrics, observations, and biases in quantitative assessment of seismic hazard model predictions
Edward Brooks, Seth Stein, Bruce D. Spencer, Antonella Peresan

1-6 The effect of dependence of observations on hazard validation studies
Iunio Iervolino; Massimiliano Giorgio

Session 2, Chairman: P. Bazzurro (IUSS, EUCENTRE) and G. Senfaute (EDF)

2-1 Non-Ergodic Seismic Hazard: Using Bayesian Updating for Site-Specific and Path-Specific Effects for Ground-Motion Models
Nicolas Kuehn, Norman Abrahamson

2-2 Some steps forward in confronting probabilistic seismic hazard with observations in Italy
Laura Peruzza

2-3 The scoring test on Italian Probabilistic Seismic Hazard Estimates developed in the frame of S2-2012 DPC-INGV Project
D.Albarello, L.Peruzza, V.D'Amico

2-4 Revision of earthquake catalogues on probabilistic terms: consequences on PSHA validation
M. Mucciarelli

2-5 Testing Probabilistic Seismic Hazard Estimates Against Accelerometric Data in two countries: France And Turkey
Hilal Tasan, Céline Beauval, Agnès Helmstetter, Abdullah Sandikkay, Philippe Guéguen.

2-6 Direct verification of seismic hazard maps
Sum Mak; Danijel Schorlemmer (only presentation, no full paper)

Session 3, Chairman: M. Stucchi (EUCENTRE) and O. Nevander (OECD/NEA)

3-1 Regulatory View on Challenges in PSHA in Low Seismicity Areas
Janne Laitonen and Jorma Sandberg, STUK – Radiation and Nuclear Safety Authority, Finland

3-2 Testing PSHA while there are large uncertainties in input data
Yong Li, U.S. Nuclear Regulatory Commission (only presentation, no full paper)

3-3 Testing & Evaluation in the Global Earthquake Model
Danijel Schorlemmer, Sum Mak, Thomas Beutin, Robert Clements, Max Schneider, Fabrice Cotton, Jochen Zschau (only presentation, no full paper)

3-4 A method for testing PSHA outputs against historical seismicity at the scale of a territory; example of France
Pierre Labbé, EDF Div Ingénierie Nucléaire, Paris, France.

3-5 Comparison of PSHA results with historical macroseismic observations in south-east France
Annalisa ROSTI, Maria ROTA, Andrea PENNA, Emilia FIORINI and Guido MAGENES, EUCENTRE, Pavia.

3-6 An Application Of Bayes Theorem To Test Macroseismic Intensity Data
Emilia FIORINI, Paolo BAZZURRO

Session 4, Chairman : E. Viallet (EDF) and R. Monteiro (IUSS, EUCENTRE)

4-1 Thirty-Year Bayesian Updating of PHSA for Hinkley Point NPP PSHA testing
Gordon Woo, RMS, 30 Monument Street, London EC3R 8NB, England

4-2 Past is the Key of the Present. A Geological Principle as Bayesian Philosophy Applied for Seismic Hazard Analysis
José G. Sanchez, Cabañero; Raúl Pérez; Maria J. Crespo

4-3 Bayesian update of a simplified PSHA model, comparison of different academic cases
L. Vaseux and J.M. Thiry, AREVA, France (only presentation, no full paper)

4-4 A Bayesian methodology to update the Probabilistic Seismic Hazard Assessment
Ramon SECANELL, Christophe MARTIN, E. Viallet, Gloria SENFAUTE

4-5 Bayesian Estimation of the Earthquake Recurrence Parameters for Seismic Hazard Assessment

Merlin KELLER , Marine MARCILHAC, Thierry YALAMAS; Ramòn SECANELL3, Gloria SENFAUTE

4-6 PSHA updating technique with a Bayesian framework: Innovations

Nicolas Humbert, EDF, Centre d'Ingénierie Hydraulique Structure / Génie Civil, France

CSNI Workshop on "*Testing PSHA Results and Benefit of Bayesian Techniques for Seismic Hazard Assessment*"
4-6 February 2015, Eucentre Foundation, Pavia, Italy

Constraints on Long-Term Seismic Hazard From Vulnerable Stalagmites

Götz Bokelmann
Department of Meteorology and Geophysics, University of Vienna, Austria,
Goetz.Bokelmann@univie.ac.at

Katalin Gribovszki
Department of Meteorology and Geophysics, University of Vienna, Austria and
Geodetic and Geophysical Institute, Research Centre for Astronomy and Earth Sciences,
HAS, Hungary, gribovk2@univie.ac.at

SUMMARY

As for any model/theory, a probabilistic seismic hazard analysis (PSHA) model is best tested by comparing its predictions with observations that are independent, e.g. which have not been used for creating the model. Arguably, the most valuable information in the context of seismic hazard analysis is information on long-term hazard, namely maximum intensities (or magnitudes) occuring over time intervals that are at least as long as a seismic cycle. Such long-term information can in principle be gained from intact stalagmites in natural caves, and we outline the approach here. Sensitive stalagmites have survived all earthquakes that have occurred over their long time span, e.g. over thousands of years or more - depending on the age of the stalagmite. Their "survival" requires that the horizontal ground acceleration has never exceeded a certain critical value within that period. Such information is very valuable, even if it concerns only a single site, namely that of a particularly sensitive infrastructure.

Keywords: *speleology, speleoseismology, stalagmite, prehistoric earthquake, cantilever beam, seismic hazard, PGA, PSHA.*

1. Introduction

Earthquakes hit urban centers in Europe infrequently, but occasionally with disastrous effects. This raises the important issue for society, how to react to the natural hazard: potential damages are huge, and infrastructure costs for addressing these hazards are huge as well. Furthermore, seismic hazard is only one of the many hazards facing society. Societal means need to be distributed in a reasonable manner - to assure that all of these hazards (natural as well as societal) are addressed appropriately. Obtaining an unbiased view of seismic hazard (and risk) is very important therefore.

In principle, the best way to test a PSHA model is to compare its predictions with observations that are entirely independent of the procedure used to produce the PSHA models. Arguably, the most valuable information in this context should be information on long-term hazard, namely maximum intensities (or magnitudes) occuring over time intervals that are at least as long as a seismic cycle – if that exists. Such information would be very valuable, even if it concerns only a single site, namely that of a particularly sensitive infrastructure. Such a request may seem hopeless – but it is not.

Long-term information can in principle be gained from intact, vulnerable, candle-stick type stalagmites (IVS) in natural caves. These have survived all earthquakes that have occurred, over thousands of years, or longer - depending on the age of the stalagmite. Their "survival" requires that the horizontal ground acceleration has never exceeded a certain critical value within that period.

This paper is based on case studies in Austria (e.g., Gribovszki et al., 2013), which has moderate seismicity, but a well-documented history of major earthquake-induced damage, e.g., Villach in 1348 and 1690, Vienna in 1590, Leoben in 1794, and Innsbruck in 1551, 1572, and 1589. Seismic intensities have reached levels up to 10. It is clearly important to know which "worst-case" damages to expect.

We have identified sets of particularly sensitive stalagmites in the general vicinity of two major cities in Austria (Vienna and Graz). Non-destructive in-situ measurements have been performed for these and other caves in Austria and Slovakia, in order to determine the horizontal ground accelerations that would result in failure of these stalagmites. These specially-shaped intact stalagmites allow estimating the upper limit on horizontal peak ground acceleration (HPGA) generated by paleoearthquakes. Such information can help make the right strategic decisions.

2. Seismic hazard estimation by intact vulnerable stalagmites (IVS)

Several studies have considered "speleoseismology" throughout the last thirty years (Forti and Postpischl, 1984, 1988; Delaby and Quinif, 2001; Cadorin et al., 2001; Lacave et al., 2000, 2004; Kagan et al., 2005; Becker et al., 2006; Bednárik 2009; Szeidovitz et al., 2005, 2007, 2008, 2008a; Paskaleva et al., 2006, 2008; Gribovszki et al., 2008, 2013, 2013a, Shanov and Kostov, 2015).
Results of Forti and Postpischl (1984, 1988), and Delaby and Quinif (2001) have shown that examining the broken and tilted speleothems can indeed be useful for revealing historic and paleoearthquakes. Cadorin et al. (2001) have performed laboratory measurements and theoretical computations to determine the horizontal acceleration that was necessary to break the broken speleothems in the Hotton cave (Belgium). For the small speleothems in that cave, relatively strong values of acceleration were required to break them. Hence, in that case these (relatively small) speleothems appear to not be indicators of paleoearthquakes, or the earthquakes were considerably stronger than expected.
Lacave et al. (2000) have determined by in-situ measurements the natural frequencies of various types of speleothems, estimated curves describing the natural frequency as a function of the type and length of the speleothem, and computed the speleothems' viscous equivalent damping. Furthermore, Lacave et al. (2004) have constructed vulnerability curves (probability of breaking vs. peak ground acceleration [PGA] functions) for classes of differently shaped stalactites. Kagan et al. (2005) have dated broken speleothems by UTh and oxygen isotope methods in two caves in

Israel, in order to determine the age of large earthquakes affecting the territory and broke the examined speleothems.
Becker et al. (2006) have given a comprehensive critical review of speleoseismology. They describe processes other than earthquakes that can have the same or very similar effects on speleothems, and they conclude that, before a decision is made on the seismic origin of deformations and damages found in caves, alternative explanations must be taken into account as well. Bednárik (2009) has modelled numerically the displacement of stalactites excited by seismic ground motion. Shanov and Kostov (2015) have given a comprehensive study about traces of paleoseismicity and active tectonics in karst taking into account the investigation of broken and unbroken stalagmites with case studies in Bulgarian caves as well.
In the Central European region, speleothem examinations for paleoearthquake research have begun with a series of research projects named "Comprehensive investigation of recent and paleoearthquake occurred in the Carpathian Basin" between 2000-2005 in Hungary and subsequently in Bulgaria and Slovakia (Szeidovitz et al., 2005, Szeidovitz et al., 2007, Szeidovitz et al., 2008, Szeidovitz et al., 2008a, Paskaleva et al., 2006, Paskaleva et al., 2008, Gribovszki et al., 2008, Gribovszki et al., 2013, Gribovszki et al., 2013a). The results gave new and more constraining (lower) horizontal ground acceleration values for Northern Hungary. These examinations have impact on the seismic hazard assessment of the Middle-European region, as well as neighboring territories. The estimated horizontal ground acceleration results of the Bulgarian stalagmite investigation were improved by finite element numerical model calculation using SAP software as well (Paskaleva et al., 2006). In these numerical calculations the approximate shape of the stalagmite could be taken into account.

At the second part of this chapter we outline the approach how can long-term information of seismic hazard in principle be gained from intact, vulnerable, candle-stick type stalagmites (IVS) in natural caves.

Estimation of upper limit on horizontal peak ground acceleration
Values of the horizontal peak ground acceleration (HPGA) that can break IVS can be estimated by theoretical calculations based on cantilever beam theory, if we know the exact dimensions of the stalagmite and its geo-mechanical and elastic parameters. The geo-mechanical and elastic parameters of the stalagmite can be measured by using broken stalagmite samples (lying on the ground at the same hall of the cave, as the investigated stalagmite) in mechanical laboratory. The dimensions and the eigenfrequency of the stalagmite can be measured in situ in the cave.

Estimation of age, growing rate, and past shape of IVS
The next step in our method is to determine the age of the IVS at different heights. These age measurements constrain the shape of IVS during its growth period, and help to assign critical HPGA values backward into the past. If core samples can be drilled from the axis of IVS for at least two different heights the age of these core samples constrain the age and the growing rate of the IVS. Based on the age determination a simplified model of the changing shape of the investigated stalagmite going backward in the past can be constructed. If we know that the stalagmite is still growing (because it is wet) and if we assume a constant value of the growth rate (this is the determined one by using age determination results of two core samples) then we can determine the height of stalagmite backward into the past. Furthermore the results of the investigations done by Dreybrodt and Romanov (2008) have to be taken into account as well. They pointed out that candle-stick type stalagmites grow with more or less constant diameter.
Taking into account all of the above (facts and assumptions) the height of IVS going backward into the past (and the shape of the stalagmite as well, because the diameter is constant at the cross section) can be calculated as a function of the age. With the shape of IVS in the past the critical

horizontal ground acceleration of the IVS can be estimated for the past (Fig. 1, 'in the cave' curve).

Attenuation of seismic waves with depth

It is known that for deeper caves, the amplification of seismic waves is weaker, or in other words, the attenuation increases (Becker et al., 2006). Therefore, it is important to know the depth of the cave, where the investigated IVS is located. If the depth of the cave is known, then the next step is to evaluate the attenuation of seismic waves by direct measurement in the cave and at the surface, or by collected data from the literature (results of measurements performed previously by others), and to multiply the critical horizontal ground acceleration (CHGA), depending on the height of the IVS, in the cave by the attenuation factor in order to get CHGA at the surface, which corresponds to the acceleration at which failure of the stalagmite would occur in the cave (see Fig. 1).

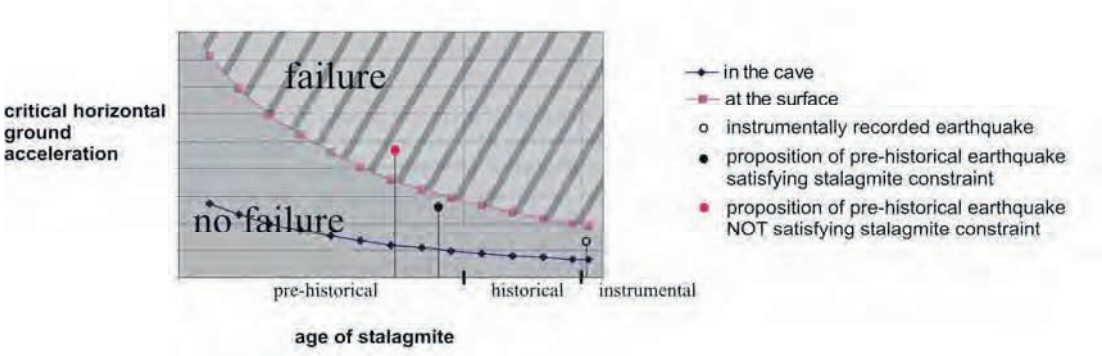

Figure 1. Illustration of the constraint on critical horizontal ground acceleration (CHGA) provided by an intact vulnerable stalagmite (IVS). As a function of stalagmite age, CHGA decreases due to increasing stalagmite height (curves), compared with measured (instrumental) and inferred (pre-historical/historical) horizontal ground accelerations.

Fig. 1 suggests how we can test propositions of pre-historical earthquakes using intact vulnerable stalagmites, and in which sense we can provide long-term upper bounds on horizontal ground acceleration. Furthermore, we can test seismic hazard models such as SHARE, and we will document this in the following, followed by a brief discussion on how this can provide constraints on seismic hazard for sites of specific interest, such as towns or critical infrastructures (dams, nuclear power plants, etc.).

3. Testing seismic hazard models (e.g., SHARE)

Seismic hazard is defined as the probable level of ground shaking associated with the recurrence of earthquakes. Basically two different types of seismic hazard models exist: probabilistic and deterministic.

The main elements of modern probabilistic seismic hazard assessment can be grouped into four main categories. The first element is the compilation of a uniform database and catalogue of seismicity for the historical, early-instrumental, and instrumental periods. The second is the creation of a master seismic source model to describe the spatial-temporal distribution of earthquakes, integrating the earthquake history with evidence from seismotectonics,

paleoseismology, mapping of active faults, geodesy, and geodynamic modeling. The third is the evaluation of ground shaking as a function of earthquake size and distance, taking into account propagation effects in different tectonic and structural environments. He fourth is the computation of the probability of occurrence of ground shaking in a given time period, to produce maps of seismic hazard and related uncertainties at appropriate scales (Giardini, 1999).

In deterministic seismic hazard studies the principal objective is to determine the design ground acceleration values at different parts of the target area, which is usually a smaller area, than in probabilistic seismic hazard assessments. The knowledge of the seismic source and wave propagation process – together with the known geological structure – makes it possible to calculate by computer programs the ground motions associated with a given earthquake scenario. Using modern deterministic seismic hazard assessments the focal source, path and site effects can be all taken into account and therefore it is possible to carry out a detailed study of the propagating wave field at even large distances from the epicentre.
As a result of the modern deterministic seismic hazard computations synthetic seismograms are created and the PGA values can be determined directly from the seismograms (Panza et al., 1999).

Over the last decades, most countries in Europe have set up probabilistic seismic hazard assessment for the whole territory of the country and deterministic seismic hazard studies for smaller regions such as towns or critical infrastructures.
Four main project frameworks have aimed at improving regional seismic hazard assessment in the European-Mediterranean region, by integrating earthquake catalogues, seismic source zoning, and hazard assessment in the last fifteen years.
The Global Seismic Hazard Assessment Program (GSHAP), a UN/IDNDR demonstration project, produced the first seismic hazard map for the European-Mediterranean region as part of the Global Seismic Hazard Map (Giardini, 1999), based on the compilation and assemblage of hazard results obtained independently in different test areas and multinational programs.
The International Geological Correlation Program project n.382 Seismotectonics and seismic hazard assessment of the Mediterranean basin (SESAME) developed in 2000 the first integrated seismic source model and homogeneous hazard mapping for the Mediterranean region (Jaménez et al., 2001).
The European Seismological Commission (Working Group on Seismic Hazard Assessment) has completed the first unified seismic source model and seismic hazard mapping for Europe and the Mediterranean.
About ten years later the SHARE Project (Danciu et al., 2013) was launched. The main objective of SHARE was to provide a community-based seismic hazard model for the Euro-Mediterranean region with update mechanisms. The project aimed to establish new standards in Probabilistic Seismic Hazard Assessment (PSHA) practice by a close cooperation of leading European geologists, seismologists and engineers. The project and the resulting maps cover the whole European territory, including Turkey.
The project built a framework for integration across national borders, compiled relevant earthquake and fault data, and developed a sustainable, high-impact authoritative community-based hazard model assembled by seeking extensive expert elicitation and participation through multiple community feedback procedures.
SHARE produced among others more than sixty time-independent European Seismic Hazard Maps spanning spectral ordinates of PGA to 10 seconds and exceedance probabilities ranging from 10^{-1} to 10^{-4} yearly probability. SHARE introduced an innovative weighting scheme that reflects the importance of the input data sets considering their time horizon, thus emphasizing the geologic knowledge for products with longer time horizons and seismological data for shorter ones.

5

We`re using the SHARE code to extract horizontal ground accelerations for a number of different exceedence probability of earthquake, and compare them with the stalagmite-derived CHGA. This comparison is illustrated in Figure 2. In this case, the SHARE-derived values would be considerably larger than the new constraint from the stalagmites. We refer the reader to a subsequent study, where we give the specifics of this comparison for the case studies indicated above.

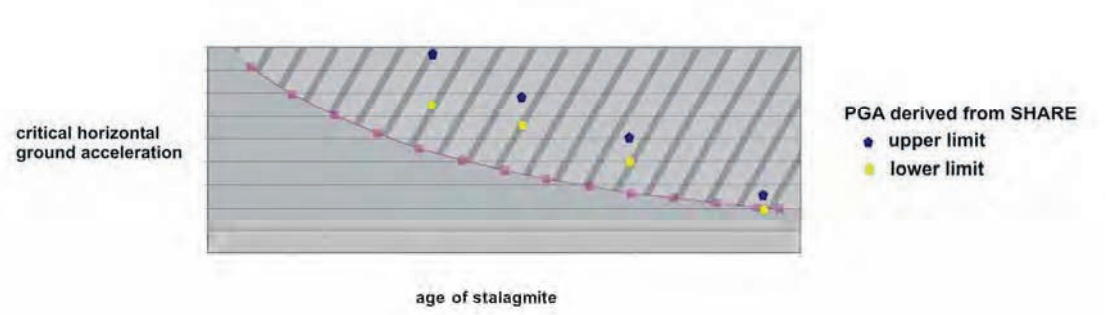

Figure 2. Comparison between stalagmite-derived critical horizontal ground acceleration and PGA derived from SHARE (illustration).

4. Local nature of the stalagmite constraint

From the stalagmite we obtain constraints on seismic hazard through model calculations. The basic concept is illustrated in Figure 3a): an intact stalagmite constrains CHGA at its location that can arise from (all) earthquakes in the area, which is just enough to break the stalagmite. The main purpose of this model calculation is to redistribute that CHGA onto potential sites of earthquakes. Figure 3b) illustrates this redistribution, showing that the constraint acts more strongly on closer sites than more distant ones. The redistribution requires (at least approximate) knowledge of propagation properties of seismic waves, especially their attenuation with distance.

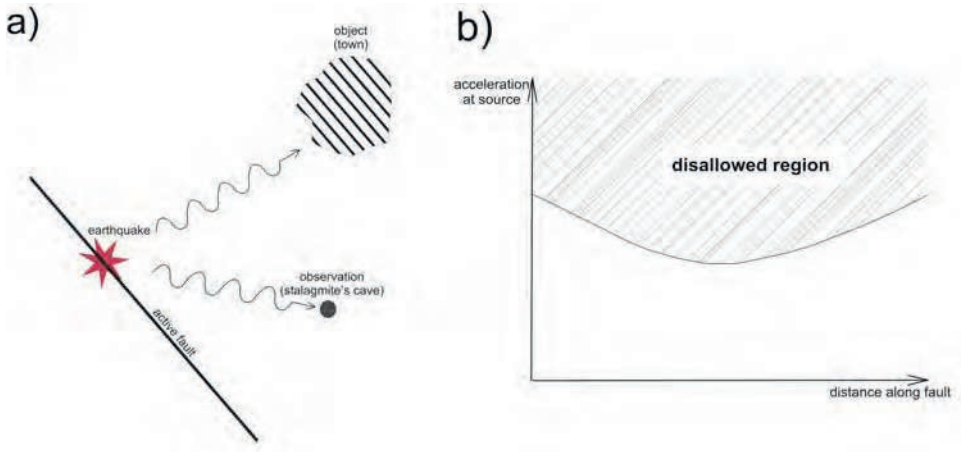

Figure 3. a) Sketch of the three-site seismic hazard model calculation (seismic waves propagate from an earthquake source to the object and the observation cave); b) type of constraint offered by the intactness of a stalagmite on maximum acceleration at the position of potential earthquake sources.

REFERENCES

Becker A, Davenport CA, Eichenberger U, Gilli E, Jeannin P-Y, Lacave C (2006) Speleoseismology: a critical perspective. ***J Seismol.***, 10, 371–388

Bednárik, M (2009) Seismometric portrayal of calcite tubular stalactites. Ph.D. thesis. Geophysical Institute, Slovak Academy of Sciences

Cadorin, J, Jongmans, D, Plumier, A, Camelbeeck, T, Delaby, S, Quinif, Y (2001) Modelling of speleothems failure in the Hotton cave (Belgium). Is the failure earthquake induced? ***Netherlands Journal of Geosciences - Geologie en Mijnbouw***, 80, 315–321

Danciu, LJ, Woessner, D, Giardini and the SHARE consortium (2013) A community-based probabilistic seismic hazard model for the European region. ***Proceedings of the Vienna Congress on Recent Advanced in Earthquake Engineering and Structural Dynamics & 13. D-A-CH Tagung***, Vienna, Paper No. 496

Delaby, S, Quinif, Y (2001) Palaeoseismic investigations in Belgian caves. ***Geologie en Mijnbouw***, 80, 323–332

Dreybrodt, W, Romanov, D (2008) Regular stalagmites: Theory behind their shape. ***Acta Carsologica***, 37, 2-3, 175-184

Forti, P, Postpischl, D (1984) Seismotectonic and paleoseismic analyses using karst sediments. ***Marine Geology***, 55, 145–161

Forti, P, Postpischl, D (1988) Seismotectonics and radiometric dating of karst sediments. ***Proc Hist Seismol of Central-eastern Mediterranean Region***, ENEAIAEA Roma, 312–322

Giardini, D (ed.) (1999) The Global Seismic Hazard Assessment Program 1992-1999. Special Issue. ***Annali Geofis.***, 42, 6

Gribovszki, K, Bokelmann, G, Szeidovitz, Gy, Varga, P, Paskaleva, I, Brimich, L, Kovacs, K (2013) Comprehensive investigation of intact, vulnerable stalagmites to estimate an upper limit on prehistoric ground acceleration. ***Proceedings of the Vienna Congress on Recent Advanced in Earthquake Engineering and Structural Dynamics & 13. D-A-CH Tagung***, Vienna, Paper No. 445

Jiménez, MJ, Giardini, D, Grünthal, G and the SESAME Working group (2001) Unified Seismic Hazard Modeling throughout the Mediterranean region. ***Boll. Geof. Teor. Appl.***, 42, 3-18

Kagan, EJ, Agnon, A, Bar-Matthews, M, Ayalon, A (2005) Dating large infrequent earthquakes by damaged cave deposits. ***Geology***, 33, 261–264

Lacave, C, Levret, A, Koller, M (2000) Measurements of natural frequencies and damping of speleothems. ***Proc. of the 12th World Conference on Earthquake Engineering***, Auckland, New-Zealand, Paper No. 2118.

Lacave, C, Koller, M, Egozcue, J (2004) What can be concluded about seismic history from broken and unbroken speleothems? ***Journal of Earthquake Engineering***, 8, 431–455

Panza, GF, Vaccari, F, Cazzaro, R (1999) Deterministic seismic hazard assessment. In Wenzel, F and Lungulu, D (eds) Vrancea Earthquakes; Tectonics, hazard and risk mitigation. Kluwer Academic Publishers, The Netherlands, 269-286

Paskaleva, I, Gribovszki, K, Kostov, K, Varga, P, Nikolov, G (2008) Peak ground acceleration assessment using the parameters of intact speleothems in caves situated in NW and SW Bulgaria. ***Proc. of the International Conference on Civil Engineering Design and Construction***, Varna, Bulgaria, 249–264

Paskaleva, I, Szeidovitz, G, Kostov, K, Koleva, G, Nikolov, G, Gribovszki, K, Czifra, T (2006) Calculating the peak ground horizontal acceleration generated by paleoearthquakes from failure tensile stress of speleothems, ***Proc. of International Conference on Civil Engineering Design and Construction***, Varna, Bulgaria.

Shanov, S, Kostov, K (2015) Dynamic Tectonics and Karst, Cave and Karst Systems of the World. Springer-Verlag Berlin Heidelberg, 123p

Szeidovitz, G, Leél- ″Ossy, S, Surányi, G, Czifra, T, Gribovszki, K (2005) Calculating the peak ground horizontal acceleration generated by paleoearthquakes from failure tensile stress of speleothems. ***Hungarian Geophysics*** (in Hungarian), 46, 91–101

Szeidovitz, G, Gribovszki, K, Bus, Z, Surányi, G, Leél- ″Ossy, S, Scharek, P (2007) Comprehensive investigation of recent and paleoearthquakes occurred in the Carpathian Basin. ***Hungarian Geophysics*** (in Hungarian), 47, 155–159.

Szeidovitz, G, Paskaleva, I, Gribovszki, K, Kostov, K, Surányi, G, Varga, Z, Nikolov, G (2008) Estimation of an upper limit on prehistoric peak ground acceleration using the parameters of intact speleothems in caves situated at the western part of Balkan Mountain Range. ***Acta Geod. Geoph. Hung.***, 43, 249–266.

Szeidovitz, G, Surányi, G, Gribovszki, K, Bus, Z, Leél- ″Ossy, S, Varga, Z (2008a) Estimation of an upper limit on prehistoric peak ground acceleration using the parameters of intact speleothems in Hungarian caves. ***Journal of Seismology***,12, 21–33.

CSNI Workshop on "*Testing PSHA Results and Benefit of Bayesian Techniques for Seismic Hazard Assessment*"
4-6 February 2015, Eucentre Foundation, Pavia, Italy

Testing and Centering of Ground Motion Models for Use in PSHA Based on Available Intensity Data

Philippe L.A. Renault
Swissnuclear, P.O. Box 1663, 4601 Olten, Switzerland, philippe.renault@swissnuclear.ch

Luis A. Dalguer
Swissnuclear, P.O. Box 1663, 4601 Olten, Switzerland, luis.dalguer@wissnuclear.ch

SUMMARY

Recent PSHA studies have raised an increasing need for testing of PSHA results and its intermediate products. This contribution discusses the various testing approaches which have been used in the framework of the PEGASOS Refinement Project (PRP) (www.pegasos.ch). A key evaluation tool for checking the centering of the weighted ground motion logic trees has been based on testing with intensity data and by development of so called mixture models. The available ground motion data from Switzerland are for M<5 earthquakes, mostly in the range of M2-M3. The historical intensity data provide a rough measure of the ground motion from large historical earthquakes. This provides a basis and method to test and update the logic tree in order to check if the model selected by the experts is centered on the observed large magnitude data. Although there are large uncertainties when converting intensity data to spectral accelerations, these data are important because they allow testing of the large magnitude scaling, which are usually lacking in low seismicity regions.
Furthermore, the use of Sammon's maps and self-organizing maps is presented and discussed in the context of guidance for selecting and weighting ground motion prediction equations. This approach was iterative and provided means of justification for specific choices by the experts. Even if the presented framework has not been applied to test the PSHA end results, it provides means to test the main ingredients used in the hazard assessment. Testing was understood in this context as expert tool to increase confidence in the robustness of the key contributors used in hazard assessment and thus, also in the results.

Keywords: *Probabilistic seismic hazard analysis, Nuclear power plants, Switzerland, Testing.*

1. Introduction

The PEGASOS study (German acronym for: Probabilistic Seismic Hazard Analysis for Swiss Nuclear Power Plant Sites) was carried out from 2000 to 2004 and evaluated the seismic hazard considering the broad knowledge of the international expert community in earthquake science and geotechnical engineering [1]. The PEGASOS project, carried out as a SSHAC Level 4 study [2],

documents the available scientific knowledge related to the occurrence of earthquakes in Switzerland, ground motion models for Switzerland, and site response at the four Swiss nuclear power plant sites at that time [3][4].
A key aspect of the PEGASOS study was the quantification of the aleatory variability and epistemic uncertainty in seismic hazard at the four Swiss NPP sites. The epistemic uncertainties are due to the very limited data for ground motions from large magnitude earthquakes, and soil properties at the NPP sites. After completion of the PEGASOS Project, the review team of the Swiss Federal Nuclear Safety Inspectorate (ENSI, formerly HSK) and the project sponsor found that the uncertainty range was rather broad, and that this spread could possibly be reduced by further investigations. The epistemic uncertainties are usually due to the very limited data on (i) strong earthquakes, (ii) ground motion attenuation, and (iii) soil properties at the NPP sites. Thus, the PEGASOS Refinement Project (PRP) represents an update of the PEGASOS Project, with the objective of improved quantification of the epistemic uncertainties in the hazard through the collection of new data and use of improved models and methods [5]. This interdisciplinary project – which started in 2008 – involved 25 key experts from 8 European countries and the USA and was completed in 2013 [6].

The project is sub divided into five subprojects (SP) based on the main technical topics of a PSHA (Figure 1), its numerical evaluation and post-processing:

- Subproject 1 (SP1): Seismic source characterization, with 4 expert groups each with 3 experts
- Subproject 2 (SP2): Ground motion characterization, with 5 experts
- Subproject 3 (SP3): Site response characterization, with 4 experts
- Subproject 4 (SP4): Seismic hazard calculations, with 3 experts
- Subproject 5 (SP5): Scenario earthquakes, with 4 experts

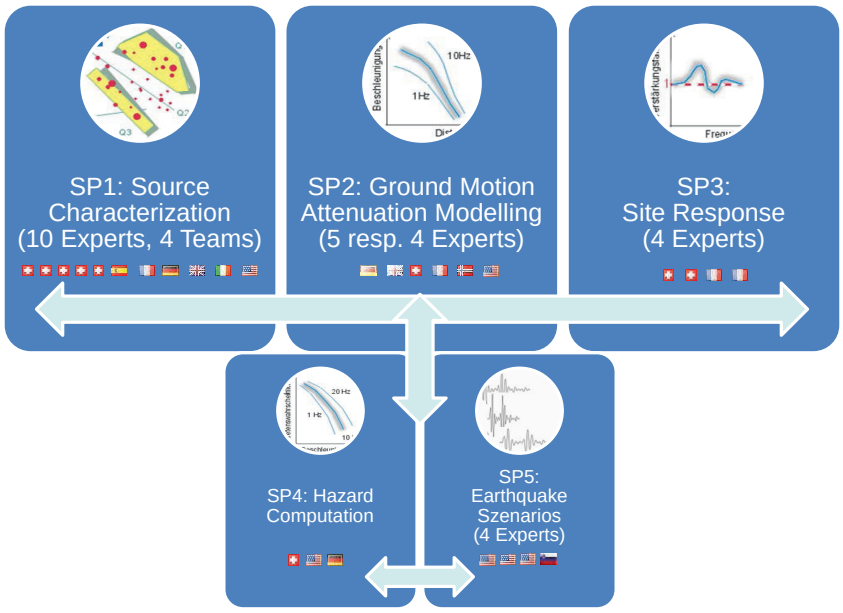

Figure 1. Structure of the PRP with its subprojects. The flags indicate the nationalities of the participating experts in each subproject.

This paper is intended to give an insight of the activities within the project on testing model choices. Testing of the resulting final results in form of the hazard curves or response spectra at a

given annual level of probability was not performed in the framework of the PRP, as in our opinion such a comparison will always be incomplete and questionable if one tries to compare a real occurred earthquake (of usually small magnitude) to the large range of results emerging from a probabilistic hazard study. Promising approaches in this respect are e.g. investigated in [2].

2. General Approach

2.1 Testing and Sammon's and Self-Organizing Maps

Within the PRP, the ground motion experts used new techniques [8] [9][10][11][12] to support the selection and quantitative comparison of ground-motion prediction models for seismic hazard analysis. Scherbaum et al. [11] proposed the use of Sammon's maps and self-organizing maps (SOMs) from the field of high-dimensional information visualization to evaluate the candidate ground motion prediction equations (GMPE). Both techniques allow the projection of high-dimensional vectors onto two-dimensional maps such that the mutual distances between these vectors and even their topological neighborhood can be preserved. These techniques allowed the experts to make more objective decisions during the selection and evaluation phase.

In Figure 2 the Sammon's maps which are directly computed from the high-dimensional feature vectors are shown. Since the SOMs and Sammon's maps are initialized at random staring points, each run produces a new map with new locations for the models. For details on the methodology, see [11].

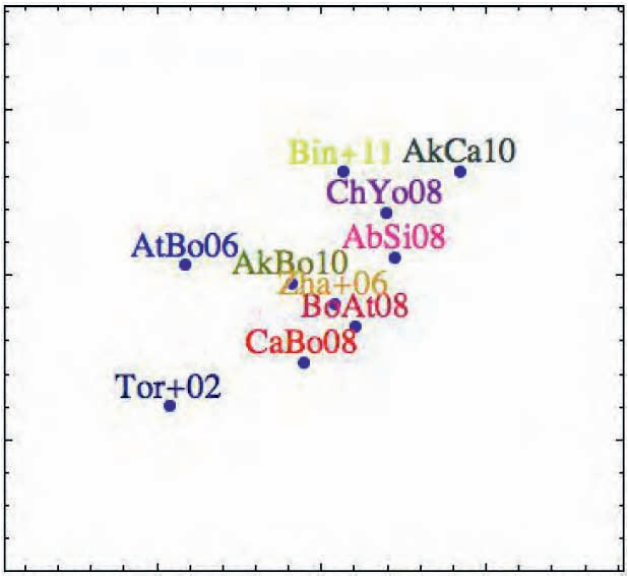

Figure 2. Sammon's map for the candidate GMPEs evaluated for PGA and the magnitude range from 4.5-7.

In Figure 3 the SOMs are shown. These are topology-preserving, i.e. if the feature vectors lie on a high-dimensional manifold, the distance is evaluated along this manifold. The distances are then visualized by plotting the GMPEs on a grid, where the grey-scale of each nodes represents the average distance between this node and its neighbouring nodes (darker means larger distance). The nodes between different GMPE nodes can be thought of as interpolations between the GMPEs.

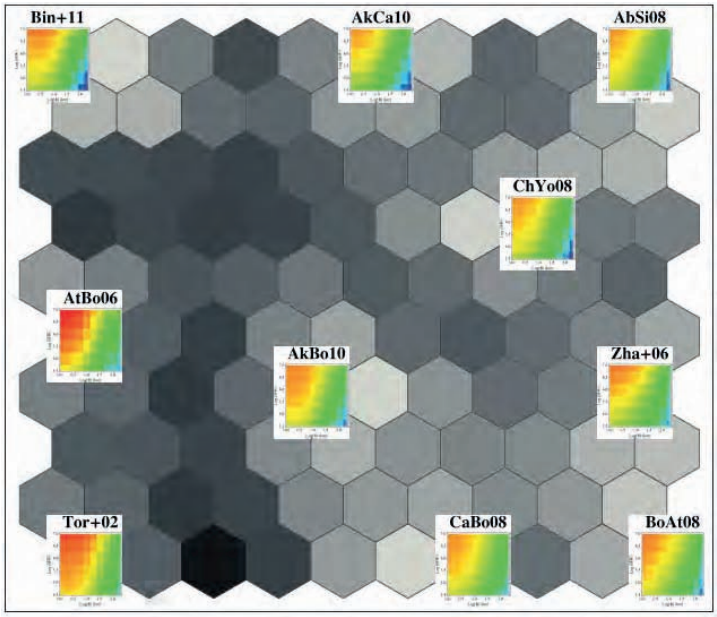

Figure 3. SOM (log-median variance) for the GMPEs evaluated for PGA and the magnitude range from 4.5-7.

A SOM visualizes the distance between adjacent nodes. Thus, the distance between two GMPEs on a SOM can be calculated by summing up the distances along the shortest path between the nodes corresponding to the GMPEs. With these distances one can calculate Sammon's maps, which are shown in Figure 4.

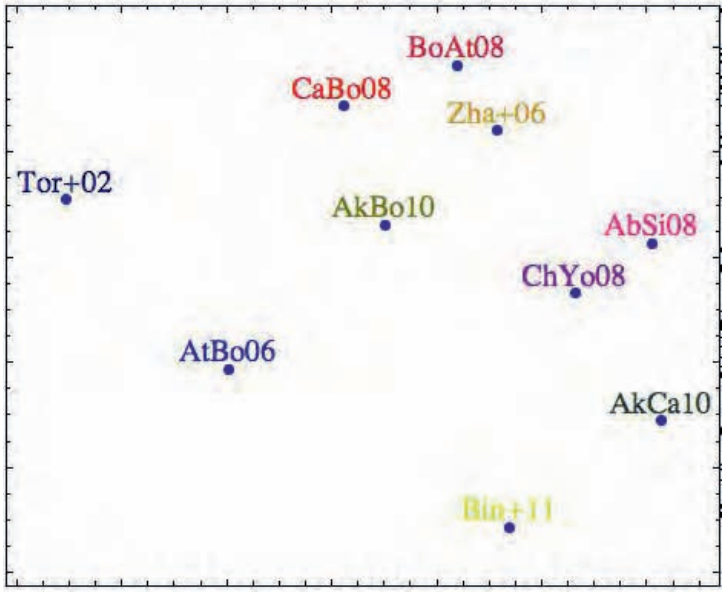

Figure 4. Sammon's map (log-median variance) for PGA and the whole magnitude range, calculated from the SOM of Figure 3.

Furthermore, several ways were used to test the preselected GMPEs against the Swiss macroseismic intensity observations. These comparisons were mainly based on building a so-called mixture model (see Section 3). The comparison with intensity data was not used to discard models, but rather to support the experts in their evaluation of weights for the candidate GMPEs.

2.2 Comparison with Finite-Fault Simulations

Beside the selection and comparison techniques mentioned above, the project also decided to compare the proposed ground motion models to physics-based simulation results which is also a kind of independent test. For this the magnitude and distance scaling from the Finite-Fault Simulations (FFS) were compared to the scaling from the resulting weighted GMPEs. For the PRP simulations, two different values for site κ were considered as input parameters for the broad band ground motion simulations: 0.01 s and 0.03 s, based on [13], who performed a detailed study at the beginning of the project on the site κ values at or close to the NPP-sites of interest.

An example of this comparison is shown in Figure 2 for a magnitude ~6.5 strike-slip earthquake and κ=0.010 s. For this example, the median curves from the FFS are within the range of the ground motion expert models for frequencies greater than 1 Hz, but are much lower at 1 Hz. The distance scaling from the FFS tends to be stronger from 5-50 km but similar for distances less than 5 km. For another case of a M6.75 earthquake (not shown), the 1 Hz curve is within the range of the SP2 expert models, so the 1 Hz difference is not systematic. The SP2 experts did not directly use the FFS results as it appears that additional calibration of the method is needed.

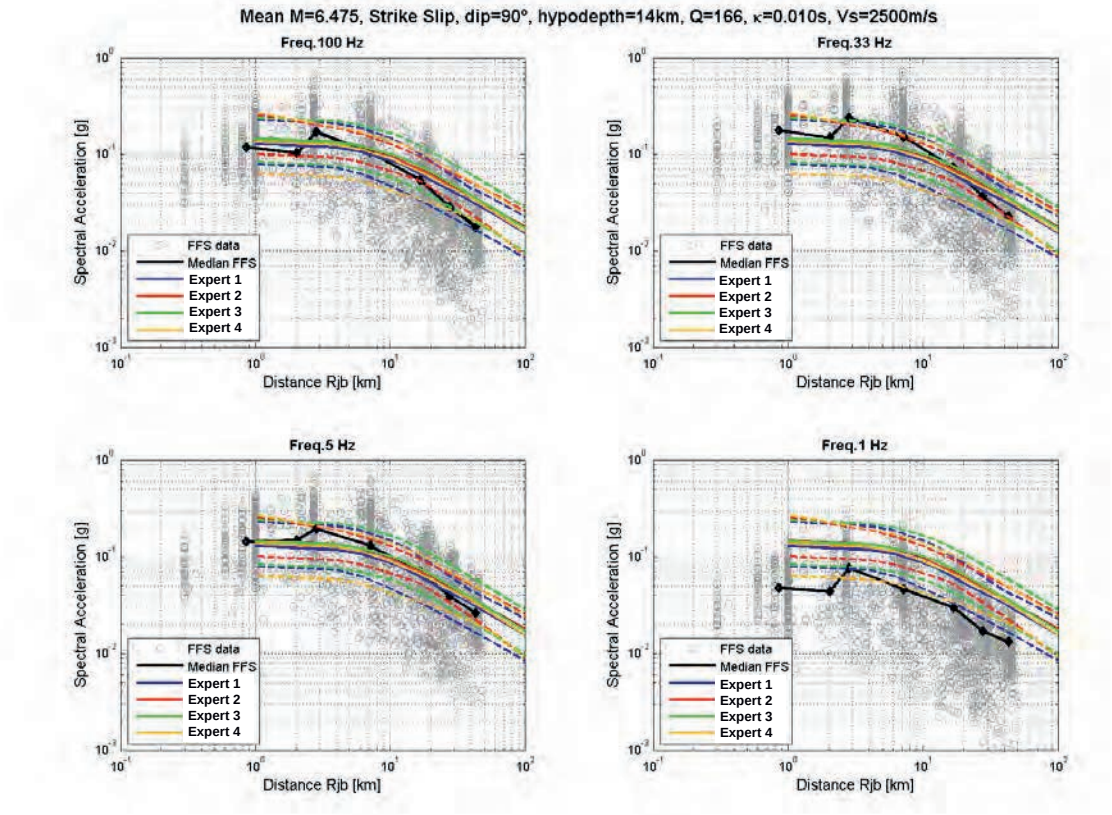

Figure 5. Comparison of FFS results with the range of ground motion expert models for 100 Hz, 33 Hz, 5 Hz and 1 Hz, for events with M~6.5.

3. Testing and Centering of Models with intensity data

A key evaluation tool for checking the centering of the weighted logic trees is the intensity testing and the mixture model. The available ground motion data from Switzerland are for M<5

earthquakes, mostly in the range of M2-M3. The historical intensity data provide a rough measure of the ground motion from large historical earthquakes. This provides a method to test the logic tree to check if the model is centered on the observed large magnitude data. Although there are large uncertainties when converting intensity data to spectral accelerations, these data are important because they allow testing of the large magnitude scaling.

3.1 Intensity testing

The testing is based on comparisons of Swiss intensities with the predictions of the GMPEs (including the Swiss stochastic model [13]). Conversion between spectral accelerations and intensities are done using the relations of Faenza & Michelini [14]. After a careful evaluation, this specific equation was selected by the ground motion experts as being the most defendable and representative one for being applied in the specific context of the study. It is acknowledged that there is no unique way to define the relationship between intensities and spectral accelerations and that all the relationships come along with a large uncertainty.

For testing, it is assumed that the selected models form a so-called "mixture model" $p(y_i|x)$

$$p(y|x) = \sum_{i=1}^{M} w_i p_i(y|x)$$

where M is the number of tested candidate models (e.g. specified by the ground motion experts) and the w_i are the individual weights with $\Sigma_i\ w_i = 1$, which are estimated using Bayesian inference. In this notation, y is the target variable (i.e. intensity), and x are the predictors such as magnitude, distance, spectral acceleration and so on.

In this case, the mixture model is a weighted average of the empirical GMPEs and parametrized Swiss stochastic model versions (PSSM) that best fit the observed intensity data. In total, more than 1000 sets of weights were calculated, for different magnitude/distance ranges, period combinations and priors. To compare different models and distributions, the so-called LLH value (from log-likelihood value) is often calculated (see [10] for details). It is defined as

$$LLH := -\frac{1}{N}\sum_{i=1}^{N} log_2\ g(x_i)$$

where N is the number of data and g is the probability density function defined by the GMPE. The LLH value is a measure of how much information is lost if "reality" (i.e. the data generating distribution) is replaced by the GMPE. It can be used as a ranking criterion for GMPEs, with a larger LLH-value implying a better model.

The testing was done in two different ways. First, residual plots were evaluated for each of the tested models. Then, mixture weights were calculated, with different values for the prior distribution, different period combinations and different data ranges (see Figure 3. The testing was done for 4 period combinations: using all periods but PGA (i.e. T=0.3, 1, 2 s), and using each PGA, 0.3 s, 1 s and 2 s individually. Four data ranges were considered, which are shown in Table 1.

Table 1. Data ranges and scenarios used for the testing.

Scenario	SC1	SC2	SC3	SC4
Magnitude range	3-7.5	4-5.5	5-7.5	5.5-7.5
Distance range [km]	0-200	10-100	10-100	100-200

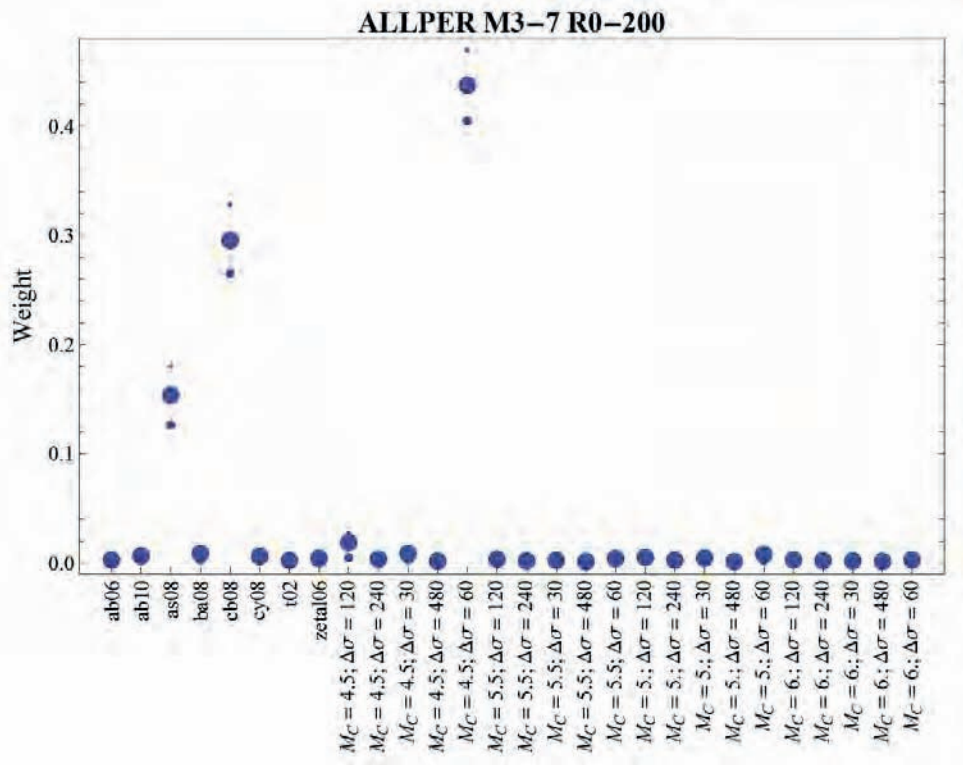

Figure 6. Example plot for means and interquartile range for the posterior distribution of the weights for the GMPEs and different PSSMs given a subset of the converted intensities. Here the weights were calculated using all periods, for the full M and R range. The first eight points are related to the candidate empirical GMPEs and the other 20 points are representing the different PSSMs.

In Figure 3 the method results in higher weights for the AS08, CB08 models and the PSSM with a stress drop of 60 bar (for *Mc*=4.5, which is the magnitude onset for the constant stress drop). This means that those three models are necessary (considering of course their relative weight) in order to represent best the given intensity data. This doesn't mean that the other models are wrong or can be discarded (their weight is non-zero most of the time), simply that they are not required by the test to embody the given dataset. As this result is period dependent, one needs to carefully evaluate the low and high period behavior in order to get the full picture.

3.2 Mixture model comparisons

The goal of the mixture model comparison was to check to what degree the observed macroseismic intensity data are consistent or inconsistent with the set of candidate ground motion models of each expert. The comparisons are only available for the periods 0.01 s, 0.3 s, 1 s and 2 s, as these are the periods for which the intensity relationship [14], relating spectral acceleration to intensity, is defined.

The mixture model and the intensity testing is based on the generic Swiss rock conditions (V_S=1000 m/s, κ=0.017 s) and there is, therefore, no NPP-specific dependence in the presented results and NPP-specific small magnitude adjustments of the GMPEs are not needed. For this comparison, a new equivalent and representative GMPE is generated that is a linear combination of the candidate GMPEs which are centered on the observed intensity data. The weighted ground motion models from the experts can then be compared to the mixture model to help evaluate if

the model is properly centered. Centered can be understood in this context as an average predicted ground motion value compared to a converted intensity, which are both not necessarily completely representative for the analyzed site, but still being the best available information.

In order to evaluate the robustness of the mixture model, it was tested using four different sets of magnitude and distance ranges shown below:

- M_W = 5.5-6.6; R = 100-200 km
- M_W = 5.5-6.6; R = 10-100 km
- M_W = 4.0-5.5; R = 10-100 km
- M_W = 4.0-6.6; R = 10-200 km

The sets of magnitude and distance ranges listed above were selected for use in determining the average mixture model and are slightly different to the magnitude distance ranges used to evaluate the weights for the candidate models shown in Table 1.

The intensity to spectral acceleration conversions were defined by the ground motion experts. The different strategies are repeated here:

- Assuming Italian intensity is equivalent to Swiss intensity (raw intensity data)
- Assuming Italian intensity needs to be adjusted to Swiss intensity on rock using an average value of 0.38 intensity units (converted intensities are 0.38 units lower)
- Applying site condition corrections from the site geology to rock site conditions to the raw intensity data (providing a "rock intensity").

For the final mixture model approach, the converted intensities adjusted by -0.38 intensity units have been used.

Figure 4 shows an example of the expert-specific weighted mean model compared to the mixture model versus distance for one expert. The expert-specific weighted mean model is based on the evaluation of the GMPEs and PSSMs used by the expert with their corresponding V_S-κ corrections and weights. The weighted average of the GMPE and PSSM (shown by the black line) is similar to the mixture model (shown by the blue line), indicating that the expert model is centered with respect to the intensity data. The expert model was decomposed into the GMPE and PSSM parts in order to see if the two groups are systematically low or high compared to the mixture model. For this example, the average PSSMs are lower than the mixture model and average GMPEs are higher than the mixture model

A sensitivity to the median, lower and upper bound V_S-κ corrections (out of the five branches of the 5-point distribution), as specified by the individual expert approach was evaluated, but is not discussed within this paper. Furthermore, these plots were later updated by also splitting the GMPEs and PSSMs into their individual models in order to check if certain stress-drop and target κ combinations could be identified as extreme cases not supported by the data. An example plot comparing different alternative mixture models to the individual GMPEs and PSSMs as a function of the expert-specific target κ is shown in Figure 5.

In this figure, on the left hand side, the intensity based mixture model is compared with the overall weighted prediction, based on a combination of weighted GMPEs and PSSMs. The right hand side of the figure shows as solid lines the weighted average GMPE or PSSM, respectively. The dashed lines are representing the individual non-weighted empirical GMPEs and alternative stochastic models which are behind the solid lines. The dashed lines allow seeing the scatter of the models compared to the “center” and if they are biased high or low compared to the intensity data.

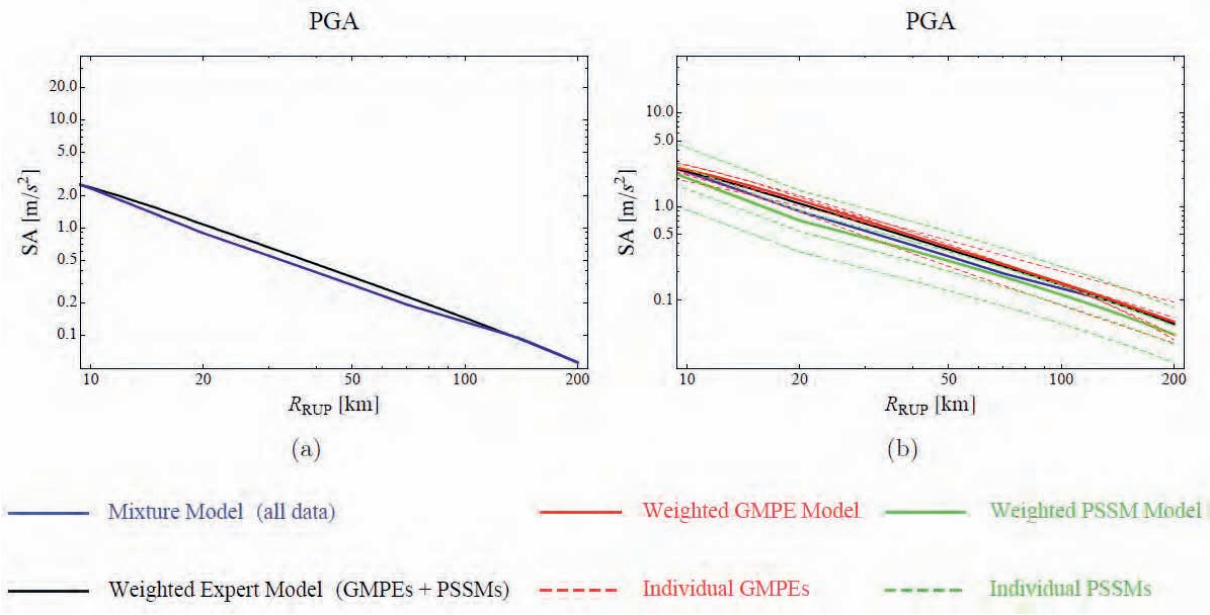

Figure 7. Example plots for mixture model comparisons for one expert. (a) Comparison of the mixture model (blue) with the expert's average (black) at PGA as spectral acceleration versus distance. (b) Comparison of the mixture model (blue) with the expert's average (black) and the different GMPEs (red) and PSSMs (green) at PGA.

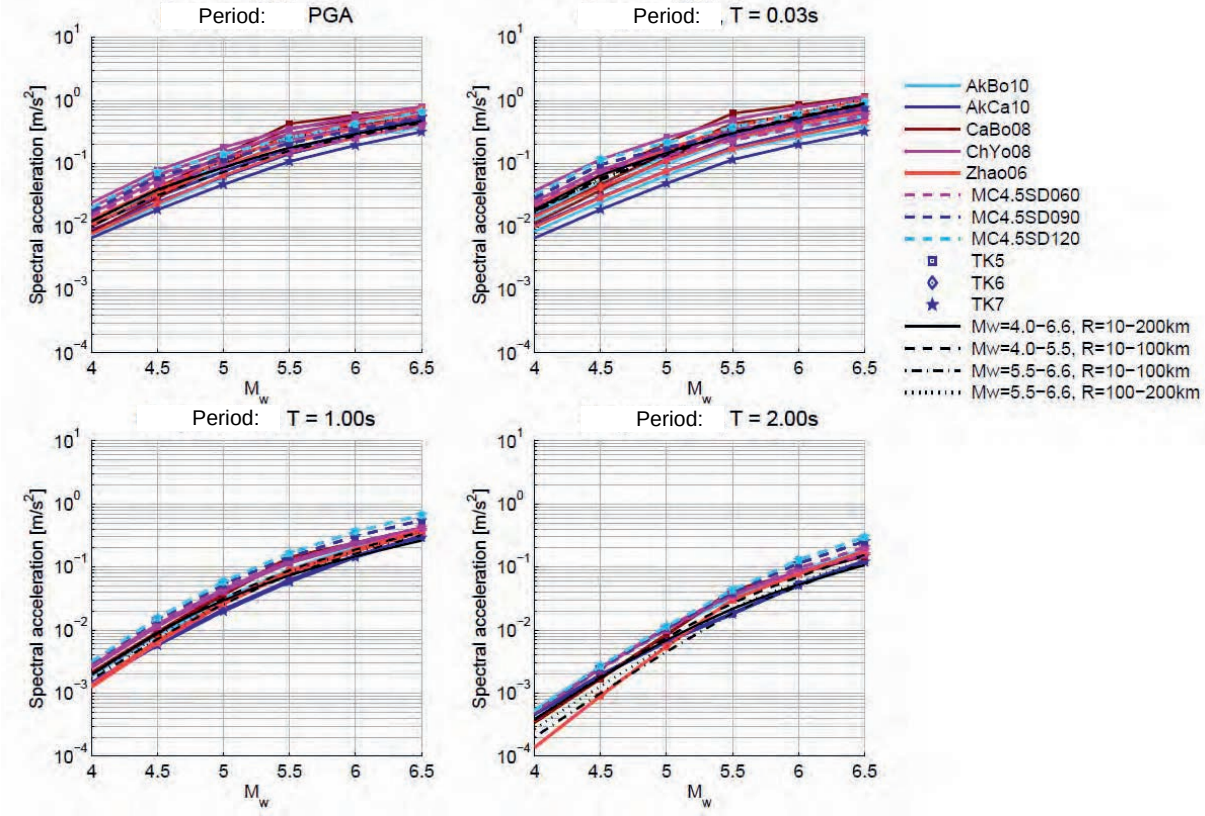

Figure 8. Example plot comparing different alternative mixture models (black lines) for R_{jb}=40 km to the individual GMPEs (solid colored lines) and PSSMs (dashed colored lines) in dependence of the expert-specific target κ (denoted TK).

Another approach is to compute the residuals of the intensity data by GMPE or PSSM directly. This allows for a check of the centering of the models in a similar, but different, way. An example of the residuals from the intensity data from the Cambell & Bozorgnia (2008) [13] model adjusted GMPE is shown in Figure 6. As this comparison needs to be done for each candidate model, spectral period and intensity conversion strategy the resulting amount of plots to analyze gets easily overwhelming. The latter lead to the fact that this approach was classified as informative but not really useful and thus, not all experts made big use of it.

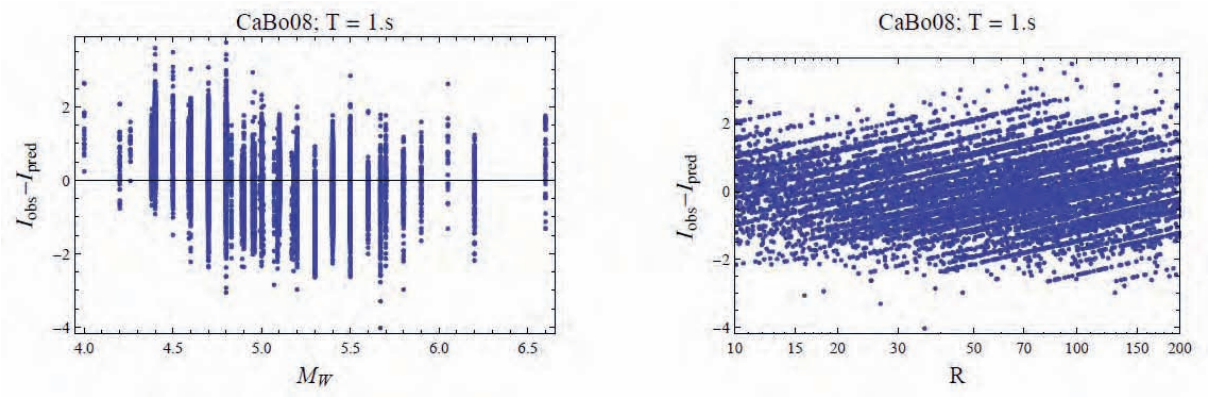

Figure 9. Example plot for residuals of the intensity data and the Campbell & Bozorgnia (2008) candidate model depending on magnitude and distance at 1 Hz.

The ground motion experts used the comparisons between the GMPE and the intensity data in very different ways. Some experts used the intensity data to constrain the mixture model and then evaluated the candidate GMPEs in terms of their consistency with the mixture model. Other members of the ground motion expert team evaluated the residuals from the intensity in the traditional method of residual analysis.

An interesting conclusion of the project was that all of the PRP ground motion experts found that the Eastern United States models were inconsistent with the Swiss specific intensity data (either checking the mixture model or checking the residuals), so these models were not part of the range of technically defensible interpretations. This led all of the experts to set the logic tree weights for the Eastern United States models to zero.

The ground motion experts also used the intensity data testing to constrain the stress-drops for large magnitude for the PSSM (see e.g. Figure 3). Overall, this led to an increase in the stress-drop for the PSSM from near 60 bars from the initial proponent model [13] to an average close to 90 bars.

4. Conclusions

The testing presented and discussed in this paper is not directly testing the hazard results, but rather all the components and facets of the models used to compute the hazard, which at the end is simply a numerical exercise if the hazard integral is acceptable as a solution for the problem. Nevertheless, testing at the ground motion level allows having some insight in the behavior of the various pieces contribution to the ground motion and thus, a better way to understand the results. A couple of approaches used within the PEGASOS Refinement Project were discussed in this paper and show the additional information which can be provided but also the burden of the interpreting expert to deal with dependencies on period, magnitude and distance.

STATEMENT

Statements of facts and opinions expressed are those of the authors and, unless expressly stated to the contrary, are not the opinion or position of swissnuclear, its sponsors, or its committees. Swissnuclear does not necessarily endorse or approve, and assumes no responsibility for, the content, accuracy or completeness of the information presented.

REFERENCES

[1] Abrahamson, N.; Birkhäuser, P.; Koller, M.; Mayer-Rosa, D.; Smit, P.; Sprecher, C.; Tinic, S. & Graf, R. (2002) PEGASOS - A comprehensive probabilistic seismic hazard assessment for nuclear power plant in Switzerland. *12th European Conference on Earthquake Engineering*, Elsevier Science Ltd

[2] SSHAC - Senior Seismic Hazard Analysis Committee (1997). Recommendations for Probabilistic Seismic Hazard Analysis: Guidance on Uncertainty and Use of Experts, U.S. Nuclear Regulatory Commission, NUREG/CR-6372

[3] NAGRA (2004). Probabilistic Seismic Hazards Analysis for Swiss Nuclear Power Plant Sites (PEGASOS Project). Final Report, Vol. 1-6. prepared for Unterausschuss Kernenergie der Überlandwerke (UAK). URL: http://www.swissnuclear.ch/en/pegasos-reports-_content---1--1070--80.html.

[4] Zuidema, P. (2006). PEGASOS: A PSHA for Swiss nuclear power plants – Some comments from a managerail point of view. *OECD-IAEA, CSNI Workshop: Specialist meetin on the Seismic Probabilistic Safety Assessment of Nuclear Facilities*, Seogwipo, Jeju Island, Korea

[5] Renault, P.; Heuberger, S. & Abrahamson, N. A. (2010). PEGASOS Refinement Project: An improved PSHA for Swiss nuclear power plants. *14th European Conference on Earthquake Engineering* - 30. August to 3. September 2010, Ohrid, Republic of Macedonia

[6] Swissnuclear (2013). Probabilistic Seismic Hazard Analysis for Swiss Nuclear Power Plant Sites - PEGASOS Renement Project. Final Report, Vol. 1-5. URL: http://www.swissnuclear.ch

[7] Albarello, D.; Peruzza, L. & D'Amico, V. (2014) A scoring test on probabilistic seismic hazard estimates in Italy. *Natural Hazard and Earth System Sciences Discuss.*, 2, 5721-5757

[8] Delavaud, E.; Scherbaum, F.; Kühn, N. & Riggelsen, C. (2009). Information-Theoretic Ground-Motion Model Selection for Seismic Hazard Analysis: An Applicability Study Using Californian Data. *Bulletin of the Seismological Society of America*, 99:6, 3248-3263

[9] Riggelsen, C.; Gianniotis, N. & Scherbaum, F. (2011). Learning Aggregations of Ground Motion Models from Data. *Institute of Earth and Environmental Science, Geophysics/Seismology, Potsdam University*, Potsdam, Germany

[10] Scherbaum, F.; Delavaud, E. & Riggelsen, C. (2009). Model Selection in Seismic Hazard Analysis: an Information-Theoretic Perspective. *Bulletin of the Seismological Society of America*, 99, 3234-3247

[11] Scherbaum, F.; Kühn, N. M.; Ohrnberger, M. & Koehler, A. (2010). Exploring the Proximity of Ground-Motion Models using High-Dimensional Visualization Techniques. *Earthquake Spectra*, 26, 1117-1138

[12] Scherbaum, F. & Kühn, N. M. (2011). Logic tree branch weights and probabilities: Summing up to one is not enough. *Earthqake Spectra*, Opinion Paper, 27:4, 1237-1251

[13] Edwards, B. & Fäh, D. (2013) A Stochastic Ground-Motion Model for Switzerland. *Bulletin of the Seismological Society of America*, 103:1, 78-98

[14] Faenza, L. & Michelini, A. (2011) Regression analysis of MCS Intensity and ground motion spectral accelerations (SAs) in Italy. *Geophysical Journal International*, 186:3, 1415-1430

[15] Campbell, K. W. & Bozorgnia, Y. (2008) NGA Ground Motion Model for the Geometric Mean Horizontal Component of PGA, PGV, PGD and 5% Damped Linear Elastic Response Spectra for Periods Ranging from 0.01 to 10 s. *Earthquake Spectra*, 24:1, 139-171

In press in "Nonlinear Mathematical Physics and Natural Hazards"
B. Aneva and M. Kouteva-Guentcheva (eds.)
Springer Proceedings in Physics, 163
DOI 10.1007/978-3-319-14328-6_7

A new probabilistic shift away from seismic hazard reality in Italy?

A. Nekrasova[1,2], A. Peresan[2,3,5], V.G. Kossobokov[1,2,4,5], G.F. Panza[2,3,5,6]

[1] Institute of Earthquake Prediction Theory and Mathematical Geophysics, Russian Academy of Sciences, Moscow, Russian Federation
[2] The Abdus Salam International Centre for Theoretical Physics, SAND Group, Trieste – Italy
[3] Department of Mathematics and Geosciences, University of Trieste, Trieste, Italy. E-mail: aperesan@units.it
[4] Institut de Physique du Globe de Paris, Paris, France
[5] International Seismic Safety Organization (ISSO) - www.issoquake.org
[6] Institute of Geophysics, China Earthquake Administration, Beijing, People's Republic of China

Abstract

Objective testing is a key issue in the process of revision and improvement of seismic hazard assessments. Therefore we continue the rigorous comparative analysis of past and newly available hazard maps for the territory of Italy against the seismic activity observed in reality. The final Global Seismic Hazard Assessment Program (GSHAP) results and the most recent version of Seismic Hazard Harmonization in Europe (SHARE) project maps, along with the reference hazard maps for the Italian seismic code, all obtained by probabilistic seismic hazard assessment (PSHA), are cross-compared to the three ground shaking maps based on the duly physically and mathematically rooted neo-deterministic approach (NDSHA). These eight hazard maps for Italy are tested against the available data on ground shaking. The results of comparison between predicted macroseismic intensities and those reported for past earthquakes (in the time interval 1000 – 2014) show that models provide rather conservative estimates, which tend to over-estimate seismic hazard at the ground shaking levels below the MCS intensity IX. Only exception is represented by the neo-deterministic maps associated with a fixed return period of 475 or 2475 years, which provide a better fit to observations, at the cost of model consistent 10% or 2% cases of exceedance

respectively. In terms of the Kolmogorov-Smirnov goodness of fit criterion, although all of the eight hazard maps differ significantly from the distribution of the observed ground shaking reported in the available Italian databases, the NDSHA approach appears to outscore significantly the PSHA one.

Keywords Earthquake catalogs – Peak ground acceleration – Macroseismic intensity – Probabilistic seismic hazard assessment – Neo-deterministic seismic hazard assessment – Seismic hazard maps

1. Introduction

A reliable and comprehensive characterization of expected seismic ground shaking, in a anticipatory perspective, is essential in order to develop effective risk mitigation strategies, including the adequate engineering design of earthquake-resistant structures.

A common belief is that a probabilistic assessment of the seismic hazard (PSHA), accounting for the probability of occurrence of a given ground shaking within a specified time interval, is needed for any rational decision making and for optimal allocation of resources (Marzocchi, 2013). However, since data are often insufficient to constrain the probability models and to test them, ground shaking probabilities turn out highly uncertain and unreliable, particularly for the large, sporadic and most destructive earthquakes. Comparison of observed numbers of fatalities with those calculated based on expected ground shaking from GSHAP maps (Wyss et al., 2012; Kossobokov and Nekrasova, 2012), show that seismic hazard maps based on the standard probabilistic method do not allow to reliably estimate the risk to which the population is exposed due to large earthquakes in many regions worldwide.

Although testing should be a necessary step in any scientific process of seismic hazard assessment, it is not a standard practice and there is not yet a commonly agreed procedure for models evaluation and comparison. Recently Mak et al. (2014) pointed out that, depending on the limited time span of available observations (compared with the selected return period of PSHA map), the probability of failing to reject an inadequate model can be high. Even if formal testing does not guarantee the adequacy of a model, a quantitative analysis of performances may allow comparing different models and spotting out possible problems. Objective testing, in fact, may have different purposes, ranging from purely scientific verification of model distributions and parameters to the assessment of maps predictive capability for moderate to extreme shaking, which may require specific metrics and tests.

In spite of the evidenced shortcomings and of its poor performances (see Panza et al., 2014 for an in depth discussion), PSHA is still widely applied in the framework of several large scale projects at regional and global scale (e.g. Global Earthquake Model). Most of such attempts in improving seismic hazard maps, however, basically rely on the collection and revision of the input data and, so far, did not include a formal procedure to assess the improved capability of the revised maps in describing ground shaking. By analogy with medicine testing, in fact, the adequacy of the proposed maps should be established before their publication and control should be performed by the proponents as a primary test of reliability of the new results.

A possible alternative to the conventional PSHA approach is provided by the Neo-Deterministic Seismic Hazard Assessment, NDSHA (Panza et al. 2001; 2012; 2013), a methodology that allows for the consideration of a wide range of possible seismic sources as the starting point for deriving scenarios via full waveforms modeling. Besides the standard NDSHA maps, which provide reliable estimates of maximum seismic ground motion from a wide set of possible scenario earthquakes, the flexibility of NDSHA allows to account for earthquake recurrence and it permits to compute ground shaking maps at specified return periods (Peresan et al., 2013). A systematic comparative analysis was carried out for the territory of Italy between the NDSHA and PSHA maps (the last is at the base of current seismic regulation), investigating their performances with respect to past earthquakes, so as to better understand the performances and possible limits of the two different approaches to seismic hazard assessment (Nekrasova et al., 2014).

In this study the comparative analysis is extended to additional hazard maps for the Italian territory, which are available from large scale projects (i.e. GSHAP), including the most recent probabilistic map, which has been compiled for the territory of Europe in the framework of Seismic Hazard Harmonization in Europe (SHARE) project (Giardini et al., 2013). The new European Seismic Hazard Map (ESHM13), in fact, has been released recently by Giardini et al. (2014) with the following declared intent:

> “SHARE's main objective is to provide a community-based seismic hazard model for the Euro-Mediterranean region with update mechanisms. The project aims to establish new standards in Probabilistic Seismic Hazard Assessment (PSHA) practice by a close cooperation of leading European geologists, seismologists and engineers.”

Regretfully, the new SHARE map does not seem to address most of the limits of the PSHA approach (e.g. Stein et al., 2012, Panza et al., 2014) and repeats the errors of its predecessors, possibly (mis)leading to unexpected economic and human life losses from future earthquakes.

2. Data

In this study we consider ground shaking estimates for the territory of Italy within the boundaries from 36°N to 48°N and from 6°E to 20°E provided by the following eight seismic hazard assessment maps.

(a) The final Global Seismic Hazard Assessment Program (GSHAP) map that depicts peak ground acceleration (PGA) values with a 10% chance of exceedance of in 50 years (GSHAP10%) corresponding to a return period of 475 years.

The GSHAP PGA values obtained by the probabilistic seismic hazard analysis (PSHA) methodology and presented as the final Global Seismic Hazard Map (Shedlock et al., 2000; Giardini et al., 2003) and Table (GSHPUB.dat, http://www.seismo2009.ethz.ch/GSHAP/) are provided on a 0.1°×0.1° regular grid for seismically active regions of the Globe, including the territory of Italy.

(b) The SHARE PGA values as defined by a 10% chance of exceedance in 50 years (SHARE10%) corresponding to a return period of 475 years.

(c) The SHARE PGA values for a probability of exceedance of 2% in 50 years (SHARE2%) associated with a 2475-year return period.

The SHARE PGA values, obtained by the, claimed, improved PSHA methodology, are given at the grid points of a regular 0.1°×0.1° mesh, which data can be downloaded from http://www.efehr.org:8080/jetspeed/portal/hazard.psml.

(d) The current Italian official seismic hazard map PGA values as defined by a 10% chance of exceedance of in 50 years (PGA10%) corresponding to a return period of 475 years

(e) The Italian official seismic hazard map PGA values for a 2% probability of exceedance in 50 years (PGA2%) associated with a return period of 2475 years.

Both the official seismic hazard maps for Italy are based on PSHA (Meletti and Montaldo, 2007; the data file http://esse1.mi.ingv.it/d2.html) at the grid points of a regular 0.2°×0.2° mesh.

(f) The maximum design ground acceleration (DGA) map for Italy, estimated by the standard NDSHA approach.

(g) The NDSHA DGA values estimated for a return period of 475 years, corresponding to a 10% chance of exceedance of in 50 years (DGA10%).

(h) The NDSHA DGA values estimated for a return period of 2475 years, corresponding to a 2% chance of exceedance of in 50 years (DGA2%).

The three design ground acceleration (DGA) maps are based on the neo-deterministic seismic hazard assessment, NDSHA (Panza et al., 2012 and references therein), which provides ground shaking estimates at the grid points of a regular 0.2°×0.2° mesh. From the complete synthetic seismograms associated to each grid point, the DGA estimates are extracted, which can be

compared to PGA (Zuccolo et al., 2011). The DGA map defined by the standard NDSHA method does not depend on temporal properties of earthquakes occurrence, whereas the DGA10% and DGA2% maps are obtained by incorporating earthquake recurrence information into NDSHA (Peresan et al., 2013; Magrin, 2012), and correspond to return periods of 475 and 2475 years, respectively (i.e. same as considered in compilation of the PSHA maps). The application of NDSHA variant that computes ground shaking at a fixed return period implies additional requirements to the input data, which are not fulfilled in the parts of the Italian territory delineated as blank areas in Fig.1 g, h. In turn, the limits of available data in adequately constraining ground shaking recurrence, as evidenced by NDSHA analysis (Peresan et al. 2013), cast doubts on the meaning and validity of PSHA values given for these blank areas, if based on the same data.

For the purpose of comparison between different grids we enhance the regular 0.2°×0.2° mesh into a 0.1°×0.1° one, so that each PGA value from the original grid point is attributed to four points on the fine grid (i.e. the original point, plus its three nearest neighbors to the east, south, and south-east).

The observed seismic activity data are taken from the SHARE European Earthquake Catalogue (SHEEC), as reported by Stucchi et al. (2012) for historical events in 1000-1899 and by Grünthal et al. (2013) for earthquakes in 1900-2006. The data set covering more than a millennium (a time interval about ten times longer than that available in most of the regions worldwide), with a completeness level satisfactory for this kind of analysis, is quite a unique property of the territory of Italy and fully warrants the following analysis. The SHEEC data provides records on macroseismic intensity at epicenter, I_0. In our analysis we have used integer values of I_0, attributing the upper limit when in SHEEC the reported I_0 is a range. This is a conservative natural choice of seismic hazard estimate, adequate to analysis aimed at the largest possible ground shaking. The observed intensity map, I_{obs}, is compiled by attributing to a grid point of a regular 0.1°×0.1° mesh the maximum of I_0 for earthquakes from SHEEC within the 0.25°-side square centered at this grid point. This resulting map of the observed ground shaking intensity gives us an opportunity for a quantitative comparison of the eight seismic hazard maps of the Italian territory with the seismic reality.

3. Cross-comparison of the PGA maps for Italy.

We repeat the analysis reported in (Nekrasova et al., 2014), expanding the comparison to the probabilistic seismic hazard maps for the Italian territory obtained in the framework of large scale projects: the Global Seismic Hazard Assessment Programme (GSHAP) map published 15 years ago (Giardini et al., 1999), and its new offspring for Europe (SHARE), which became available recently (Giardini et al., 2013, 2014).

Table 1 gives an overall summary on the PGA values for each of the eight SHA maps (Fig. 1). Evidently, the SHARE maps increase dramatically both the lower and the upper limits of the expected seismic hazard in Italy. In particular, the minimum of the SHARE PGA is about 2 and 4 times larger than the corresponding estimates of the earlier probabilistic SHA. In comparison to the NDSHA maps the minimum values of ground shaking by the SHARE maps are about 5 and 10 times larger. The increase of the maximum PGA on the SHARE maps accounts to about 10-50% of the corresponding previously suggested values.

Table 1 The parameters of the eight SHA ground acceleration maps for Italian territory.

Map	GSHAP	SHARE10%	SHARE2%	PGA10%	PGA2%	DGA	DGA10%	DGA2%
Number of points	3066	3066	3066	3044	3044	3066	1739	2266
min(mGA), m/s^2	0.39	0.74	1.72	0.30	0.43	0.20	0.16	0.18
max(mGA), m/s^2	2.97	4.19	8.82	2.71	5.98	5.83	3.74	5.83

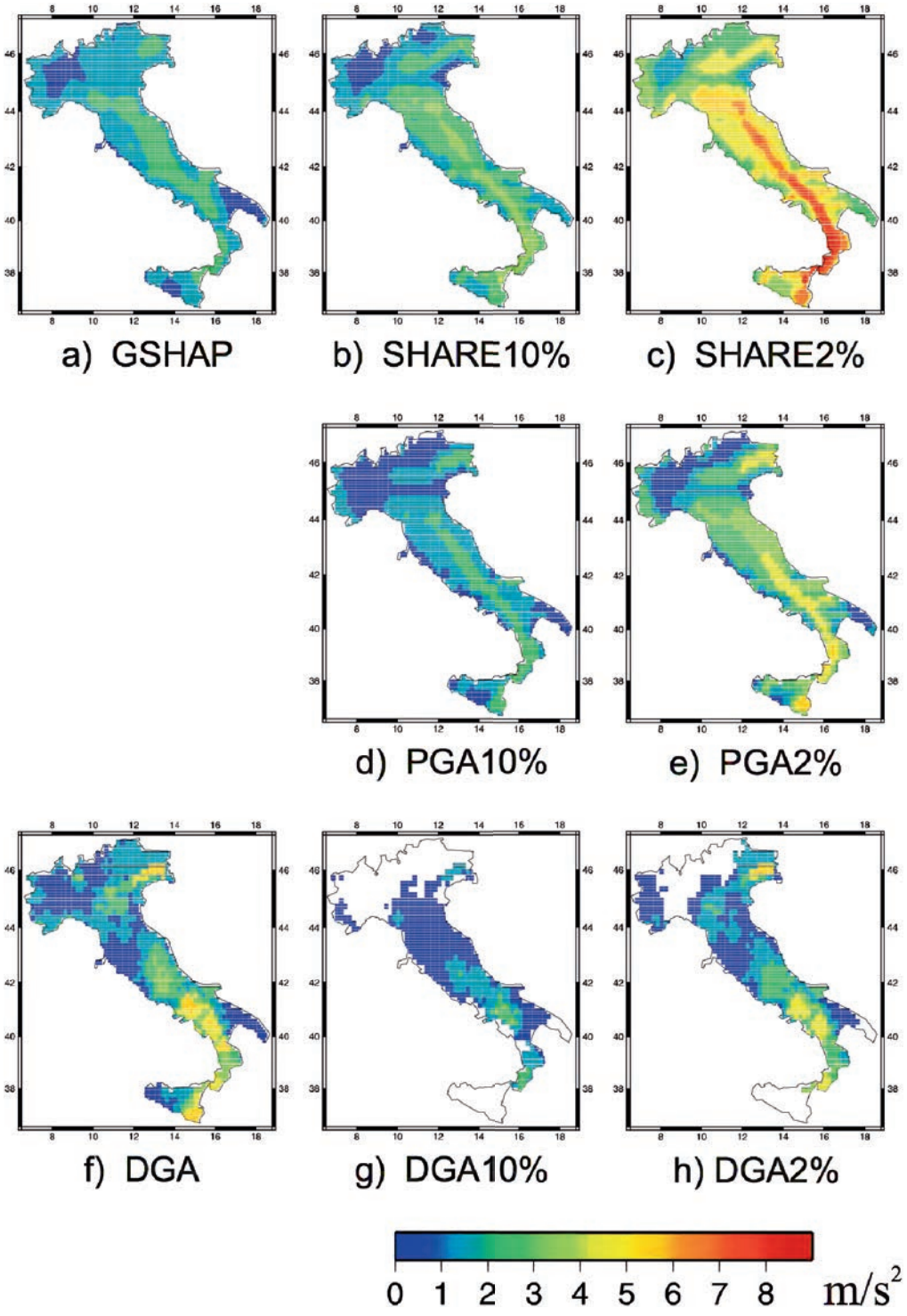

Fig. 1 Comparison of model ground acceleration maps: a) GSHAP corresponding to a return period of 475 years; b) SHARE10% corresponding to a return period of 475 years; c) SHARE2% corresponding to a return period of 2475 years; d) PGA10% corresponding to a return period of 475 years; e) PGA2% corresponding to a return period of 2475 years; f) DGA not depending on time; g) DGA10% corresponding to a return period of 475 years; h) DGA2% corresponding to a return period of 2475 years.

Table 2 provides a more refined comparison, based upon the percentage of PGA values ratio at a grid point (mGA1/mGA2), for a number of pairs of model maps mGA1 and mGA2. SHARE map values at a grid point exceed those of the previous maps by a factor of 2 or more in 4% of cases, for the GSHAP map, in 17% and 40% of cases, for the corresponding national PSHA maps, and to up to more than 75% of cases, for the NDSHA estimates. The SHARE estimate is less than any previous hazard estimates in 2%-3% of grid points. Specifically, as can be concluded from the maps of the ratio of the PGA values for different pairs of models, a selection being provided in Figure 2, just about 2% of the grid points of the Italian official SHA maps have higher PGA values than that of SHARE; these are all located in the Friuli-Venezia-Giulia region (Figure 2 c-d). In comparison to the previous hazard maps, the SHARE PGA values corresponding to a return period of 475 years increase by a factor of 2 or more in the regions of Trentino, Lombardia, Eastern Sicily, and Puglia; for Liguria PGA increases more than 4 times. The misfit of the SHARE maps with respect to the NDSHA ones is even more dramatic (Figure 2 e-g): e.g. the SHARE2% values are larger than the DGA2% by a factor of 4 or more in about 40% of the Italian territory.

Table 2 The percentage of the grid points from different ranges of the ratio mGA1/mGA2 of the PGA values from selected pairs of SHA maps.

mGA1 / *mGA2* range	GSHAP / PGA10%	SHARE10%– / GSHAP	SHARE10% / PGA10%	SHARE2% / PGA2%	SHARE10% / DGA	SHARE10% / DGA10%	SHARE2% / DGA2%
≥4	-	-	0.26	1.25	4.04	30.82	39.81
≥2	6.73	4.21	17.05	40.31	26.65	75.79	78.60
≥1	78.58	85.32	97.40	97.96	65.04	97.99	97.04
<1	21.42	14.68	2.60	2.04	34.96	2.01	2.96

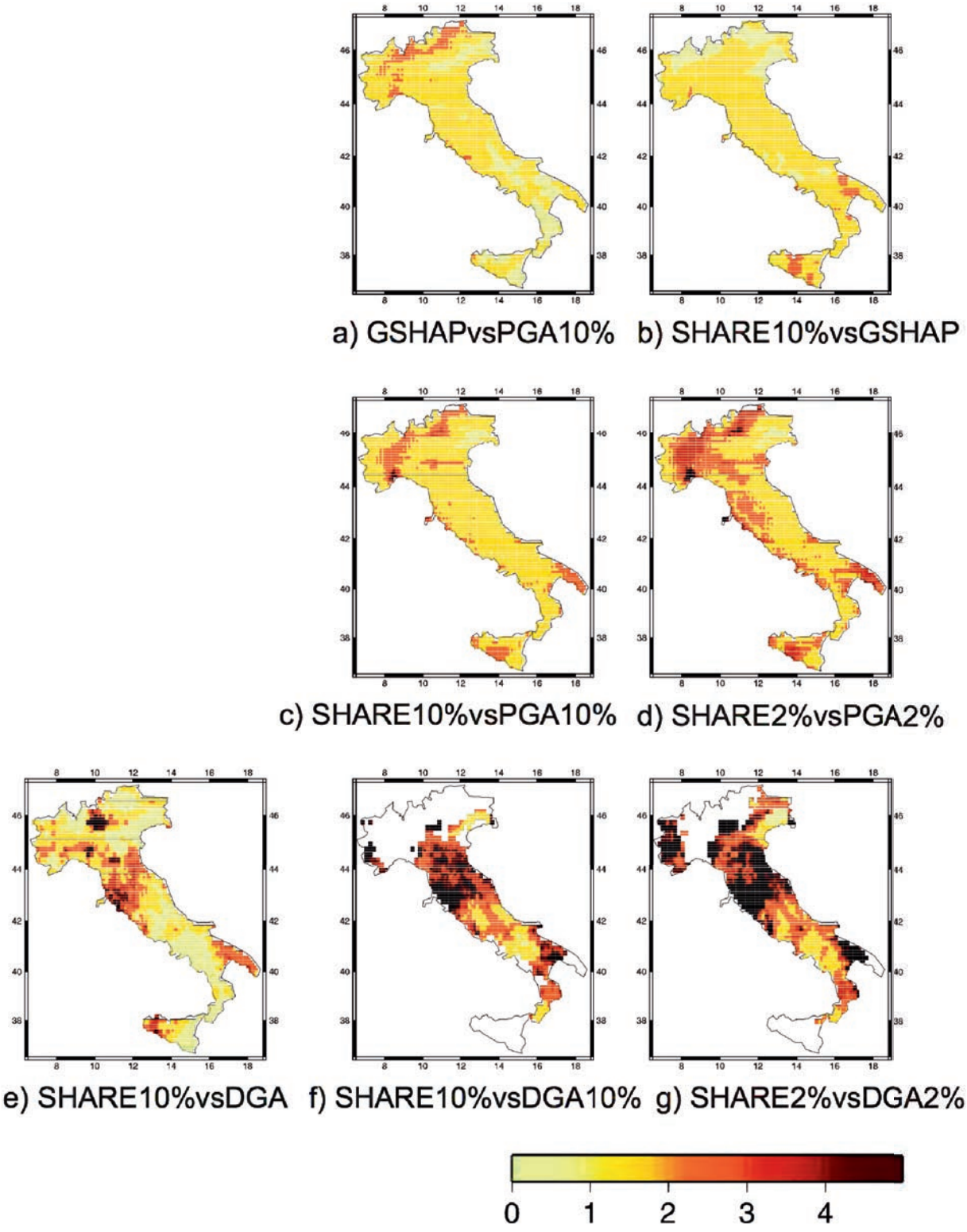

Fig. 2 Selected maps of the ratio between PGA values from different pairs of SHA maps: a) GSHAP divided by PGA10%; b) SHARE10% divided by GSHAP; c) SHARE10% divided by PGA10%; d) SHARE2% divided by PGA2%, e) SHARE10% divided by DGA f) SHARE10% divided by DGA10%, g) SHARE2% divided by DGA2%.

Each of the six graphs in Figure 3 shows the correlation diagram between a pair of seismic hazard maps of Italy, displaying the PGA values on a grid point of one map versus the PGA values on the same grid point of another map. These are all possible pairs of maps corresponding to a return period of 475 years (i.e. probabilistic GSHAP, SHARE10%, PGA10%, and neo-deterministic DGA10%). It is evident that the most recent map reviewed by the probabilistic approach to seismic hazard assessment (SHARE10%) evidently provides a gross overestimation of PGA values, compared to all of the other maps. The neo-deterministic map (DGA10%) is the most optimistic in providing low PGA values, under 1 m/s^2, but conservative in expecting high accelerations, above 2 m/s^2.

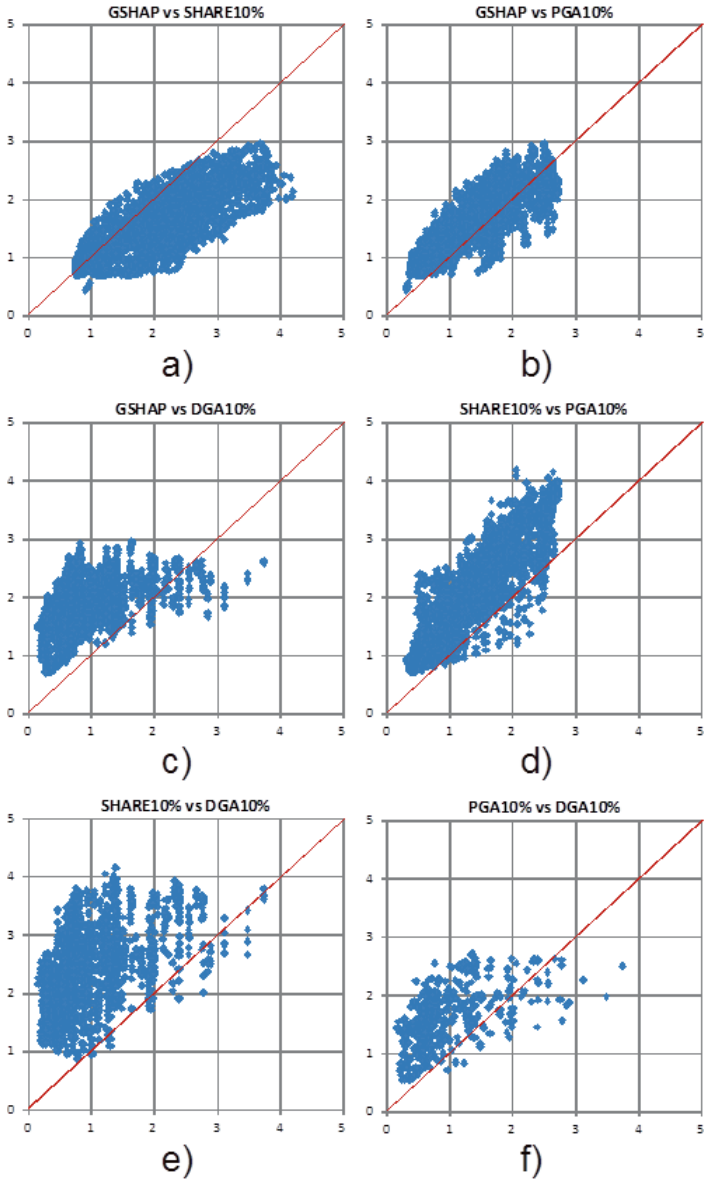

Fig. 3 Correlation diagrams of the PGA values (in m/s^2) on the four hazard maps of Italy corresponding to a return period of 475 years: a) GSHAP (ordinate) versus SHARE10% (abscissa); b) GSHAP versus PGA10%; c) GSHAP versus DGA10%; d) SHARE10% versus PGA10%; e) SHARE10% versus DGA10%; f) PGA10% versus DGA10%. These are all possible pairs of maps corresponding to a return period of 475 years (i.e. probabilistic GSHAP, SHARE10%, PGA10%, and adjusted neo-deterministic DGA10%).

Of course, any cross-comparison of the maps obtained by different models and/or series of correlation diagrams does not answer to the key question of a model adequacy to reality. In the next section we address this pivotal question in hazard assessment by comparisons of the model maps with the available observations.

4. Comparison of the hazard maps for Italy against registered ground shaking.

The two currently official seismic hazard maps for Italy PGA10% and PGA2% and the three neo-deterministic maps DGA, DGA10% and DGA2% were already subject of comparison in (Nekrasova et al, 2014). Here we update and expand the comparison with the observed ground shaking to the European Seismic Hazard Maps 2013 - SHARE10% and SHARE2%, issued recently (Giardini et al. 2014), along with their predecessor, GSHAP map (Giardini et al. 1999). Table 3 lists the conversion rules between PGA and MCS for the territory of Italy after Indirli et al. (2011). These rules are used to convert the estimated ground shaking from SHARE10%, SHARE2%, PGA10%, PGA2%, DGA, DGA10%, DGA2% into the corresponding macroseismic intensity MCS values. Figure 4 shows the eight model intensity maps subject to comparison along with the map I_{obs} compiled from the SHEEC reported data. All the nine intensity maps refer to the same regular 0.1°×0.1° mesh within the borders of Italy. For the purposes of comparison the recurrence adjusted DGA10% and DGA2% neo-deterministic maps were expanded to the grid points of no recurrence determination, following the empirical linear regression equation that links the DGA map values and the existing estimates on the DGA2% and DGA10% maps. The resulting model intensity maps are DGA2%* and DGA10%*, respectively.

Figure 4 presents the eight intensity maps obtained (i) from the real seismicity I_{obs} (Figure 4a) as well as (ii) from the ground motion estimates $I_{\mathrm{SHARE10\%}}$, $I_{\mathrm{SHARE2\%}}$, $I_{\mathrm{PGA10\%}}$, $I_{\mathrm{PGA2\%}}$, I_{DGA}, $I_{\mathrm{DGA10\%*}}$, $I_{\mathrm{DGA2\%*}}$ (Figure 4b-h, respectively).

Table 3 Relation between I_{MCS} and model ground motion, mGA, after Indirli et al. (2011)

I_{MCS}	VI	VII	VIII	IX	X	XI
mGA, (g)	0.01-0.02	0.02-0.04	0.04 – 0.08	0.08 – 0.15	0.15-0.3	0.3-0.6

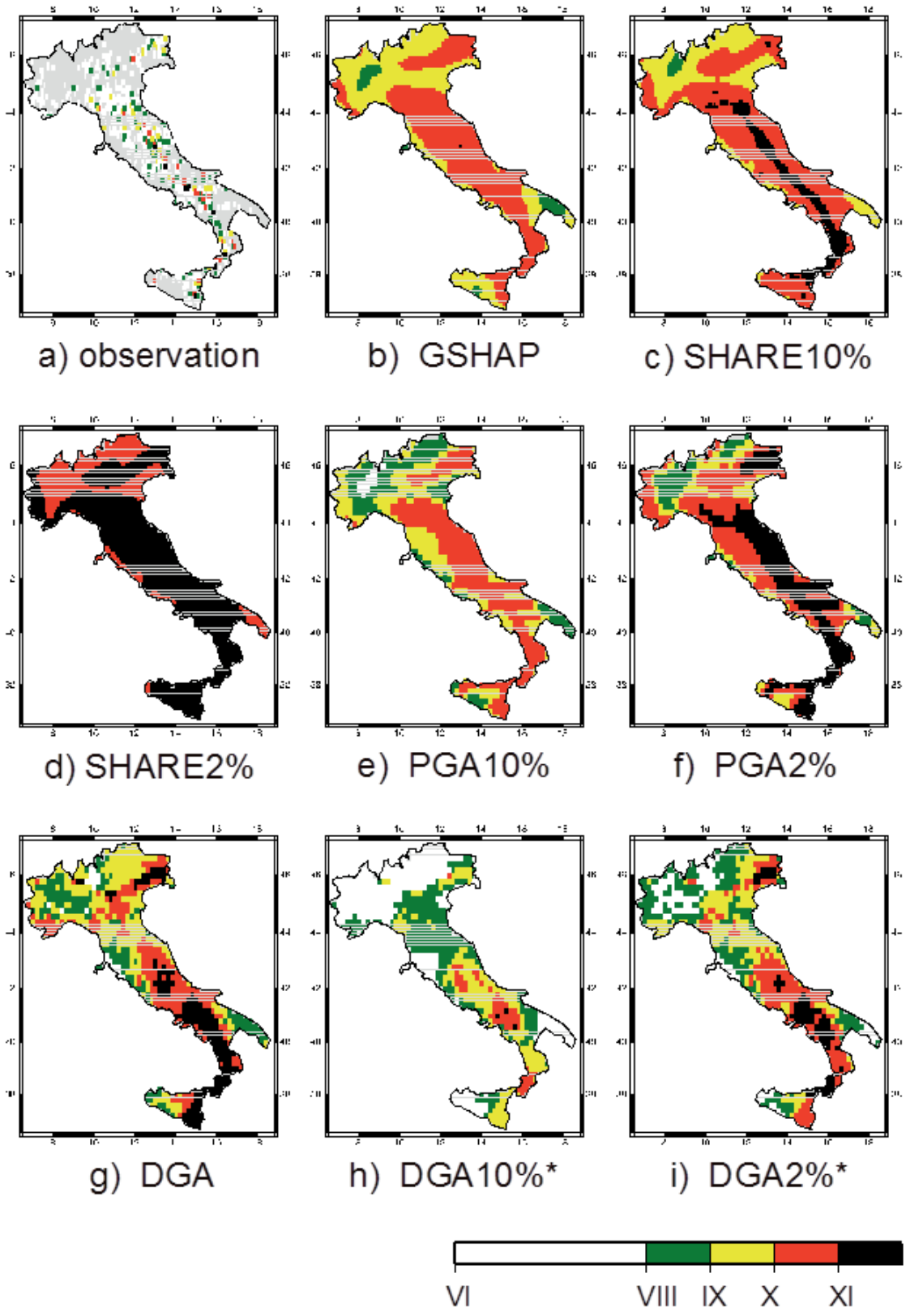

Fig.4 The intensity maps under comparison: a) I_{obs} map obtained from the reported seismicity data in 1000-2006; model intensity corresponding to PGA maps – b) GSHAP, c) SHARE10%, d) SHARE2%, e) PGA10%, f) PGA2%, g) DGA, h) DGA10%*, and i) DGA2%*.

Table 4 The percentage of I_{MCS} from different ranges in real observation map (I_{obs}) and in the model intensity maps corresponding to the eight hazard maps considered.

I_{MCS} range	I_{obs}	GSHAP	SHARE10%	SHARE2%	PGA10%	PGA2%	DGA	DGA10%*	DGA2%*
≥ XI	2.76	0.03	14.58	75.28	-	33.84	19.28	0.39	10.21
≥ X	11.63	56.20	72.70	100	44.48	74.15	45.66	8.06	34.93
≥ IX	21.40	94.98	98.56	100	76.74	90.57	78.90	31.12	59.52
≥ VIII	41.69	100	100	100	97.77	100	97.23	61.42	86.82
≥ VII	74.27	100	100	100	100	100	100	86.43	98.47
≥ VI	100								

The percentage of the points with intensity VI or more for each of these maps is summarized in Table 4. Remarkably, the SHARE2% assigns all the territory to “extreme” ground shaking of intensity X or larger, while the I_{obs} map of macroseismic intensities reports such intensity, in about two thousand years of observations, for less than 12% of the territory. At this “extreme” level of ground shaking the DGA10%* with its 8% appear to be the nearest to I_{obs}, and, in general, the neo-deterministic maps are closer to reality than all the probabilistic ones but PGA10%, which predicts (about 45% of intensity X) for a return period of 475 years similar values to those of the time unlimited DGA. Similar situation exists at the “severe”, intensity VIII level of ground shaking: it is attributed to 100% of the Italian territory by all the probabilistic maps except PGA10%, which attributes it to 98% of the territory, still too large in comparison to 42% of I_{obs}. Once again the DGA10%* with its 61.42% is the closest to I_{obs}.

More rigid comparison with respect to the I_{obs} map can be performed by applying the Kolmogorov-Smirnov test that quantifies the distance between the empirical distribution functions. The maximum absolute difference between the empirical distributions is commonly used in the Kolmogorov-Smirnov two-sample criterion to distinguish whether or not the values from the two samples are drawn from the same statistical distribution of independent variables. We apply the two sample Kolmogorov-Smirnov statistic $\lambda_{K\text{-}S}$ to the empirical distribution functions of MCS values on a model map and the observed SHEEC reported data map:

$$\lambda_{K\text{-}S}(D, n, m) = [nm/(n+m)]^{1/2} D,$$

where D = max | $F_i(I)$ - $F_0(I)$ | is the maximum of the absolute difference between the empirical distributions of the i-th model map $F_i(I)$ and the I_{obs} map $F_0(I)$, whose sample sizes are n and m, respectively; I = VI, VII, VIII, IX, X, XI, XII. Figure 5a shows the empirical distribution functions used in the comparison. For the purposes of additional testing and qualitative uncertainty estimation, the empirical distribution function of the MCS values from the publicly available database of direct macroseismic observations DBMI04 (Stucchi et al. 2007) is also object of comparison with the I_{obs} map. Figure 5b shows the nine differences $F_i(I)$ - $F_0(I)$ and it illustrates the departure of a model from the zero-line of reality; the departure of direct MCS observations from DBMI04 characterizes the realistic dispersion of the real data. Table 5 summarizes the results of the comparison in terms of computed D and $\Delta_{K\text{-}S}$.

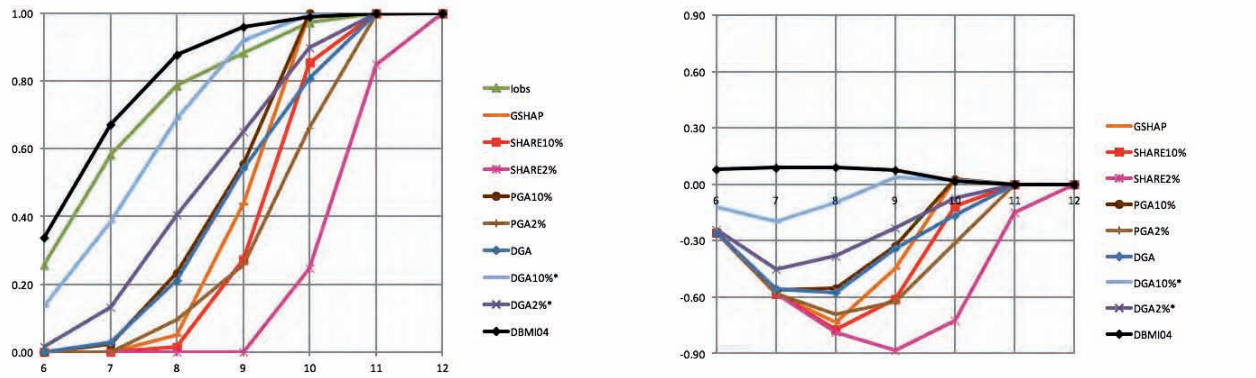

Fig. 5 The empirical probability functions of macroseismic intensity (a) and the difference between a model and the real intensities $F_i(I)$ - $F_0(I)$ (b).

Table 5 The Kolmogorov-Smirnov two-sample statistic $\Delta_{K\text{-}S}$ applied to a model map and the real seismic intensity map (I_{obs}, sample size 1341). Sample size indicates the number of grid points analysed.

Statistic	Model seismic intensity map								
	GSHAP	SHARE10%	SHAE2%	PGA10%	PGA2%	DGA	DGA10%*	DGA2%*	DBMI04
Sample size	3066	3066	3066	3044	3044	3066	3066	3066	19713
D	0.74	0.77	0.88	0.56	0.69	0.57	0.20	0.45	0.09
$\Delta_{K\text{-}S}$	22.47	23.57	26.99	17.11	21.10	17.56	6.03	13.79	1.82

The K-S test results confirm quantitatively the conclusions that could have been already reached from Table 4: the values of seismic intensity assigned by any of the models considered and reported in SHEEC do not come from the same distribution. The $D_{K\text{-}S}$ for the two representatives of the observed ground shaking, i.e. at epicenter (the I_{obs} map) and at site of direct observation (the DBMI04 data), provides an empirical estimate of admissible departure of real intensity distributions as a reference for claiming consistency of a model. Nekrasova et al (2014) have shown that the DGA10% map appears to be “the best fit” among the five model intensity maps for Italy (i.e., the two official and the three neo-deterministic maps). The investigation expanded to the eight model maps confirms this conclusion. Moreover, it becomes evident that the GSHAP and most recent SHARE maps for Italy are hardly consistent with observations and overestimate dramatically the seismic hazard in the region. Apparently the SHARE maps keep moving away from reality, even more than GSHAP.

Tables 6 and 7 disclose the quality of a model map in predicting the maximum of the macroseismic intensity, in particular, the expectation of ”a 10% or 2% chance of exceedance in 50 years”. Table 6 indicates clearly that for SHARE maps the number of exceedances, by a unit of MCS intensity or larger, is by far smaller than one should expect from the number of trials represented by the intensity VIII or larger records in DBMI04. Once again the fit of the adjusted neo-deterministic DGA10%* and DGA2%* (11.6% and 1.9% exceedances, correspondingly) is more consistent with expectations than that of the probabilistic maps, both for a return period of 475 years (GSHAP is exceeded in 4.4%, SHARE10% in 0.1% and PGA10% in 4.5% of cases, respectively) and for a return period of 2475 years (SHARE2% and PGA2% are never exceeded, thus it is 0.0%). The small sample of $I_0 \geq$ VIII earthquakes from SHEEC (Table 7) does not permit, although does not contradict, the conclusion on a model map consistency, as clear as with the macroseismic records from DBMI04.

Table 6. Number of grid points where the difference Δ, between the intensity $I \geq$VIII records in DBMI04 and the maximum of the model map values at the distance of 1/8° or less, has been computed.

Model	GSHAP	SHARE10%	SHARE2%	PGA10%	PGA2%	DGA	DGA10%*	DGA2%*
Total	4421	4421	4421	4421	4421	4421	4421	4421
Δ = 2	1	0	0	0	0	0	81	6
Δ = 1	193	3	0	200	0	9	434	76
Δ = 0	589	236	0	620	189	276	1194	430
Δ = -1	1562	706	257	1611	633	963	1444	1125
Δ = -2	2009	1790	914	1990	1670	1616	1049	1557
Δ = -3	67	1686	1711	0	1924	1557	213	1227
Δ = -4	0	0	1539	0	5	0	0	0

Table 7. Number of earthquakes with $I_0 \geq$ VIII from SHEEC for which the difference Δ, between I_0 and the maximum of the model map values at the distance of 1/8° or less, has been computed.

Model	GSHAP	SHARE10%	SHARE2%	PGA10%	PGA2%	DGA	DGA10%*	DGA2%*
Total	42	42	42	42	42	42	42	42
Δ = 2	0	0	0	0	0	0	3	1
Δ = 1	2	0	0	1	0	1	5	1
Δ = 0	8	2	0	9	1	5	8	5
Δ = -1	12	10	4	13	9	9	19	12
Δ = -2	20	16	9	19	16	13	6	14
Δ = -3	0	14	18	0	16	14	1	9
Δ = -4	0	0	11	0	0	0	0	0

5. Conclusions

The comparison of the model intensity maps against the real seismic activity in Italy, made over a time interval of more than a millennium, reveals many discrepancies in several aspects of the models seismic ground shaking distribution in space and size.

We did repeat the analysis reported in (Nekrasova et al., 2014) and expanded it to the Global Seismic Hazard Assessment Programme (GSHAP) map and its new offspring for Europe (SHARE), which became available recently (Giardini et al., 2014). The results of the analysis described in this paper confirm the following conclusions:

- the estimates of seismic intensity attributed by any of the eight models considered, including the official and most recent SHARE seismic hazard maps, and those reported in the Italian databases of empirical observations could hardly arise from the same distribution;
- models (except for the recurrence adjusted neo-deterministic DGA10% and DGA2%, at the cost of model consistent 10% or 2% cases of exceedance) generally provide rather conservative estimates with respect to reality. They tend to over-estimate seismic hazard particularly at the levels below violent (MCS intensity IX) ground shaking events and yet most of them do not guarantee avoiding underestimations for the largest earthquakes;
- probabilistic maps have a higher tendency to overestimate the hazard, with respect to the corresponding deterministic maps and reality; in particular, the newly published SHARE maps assign all the territory of Italy to extreme ground shaking of intensity $I \geq IX$;
- in terms of the goodness of fit measured by the Kolmogorov-Smirnov two-sample statistic, the NDSHA models appear to outscore the probabilistic ones and might be a better representation of the real seismicity. In particular, the minimum value of $\square_{K\text{-}S}$ obtained for DGA10%* is 3-4 times smaller than for any of the probabilistic models, while it is 3 times larger than for the reference misfit of the observed ground shaking at epicenters and at sites of direct observations.

The study of the statistical significance of the detected inconsistencies between model and observed intensities and their interpretation should be addressed in further investigation of earthquake phenomenon, in particular for the predictability of the maximum ground shaking.

What is often the problem with probabilistic approaches is that probability is a purely mathematical concept and, by the law of large numbers, the frequency approaches the probability only in an infinite collection of independent identically distributed random occurrences. It is clear, therefore, that all methods that mix these two terms (frequency and probability) without computing the deviations with sufficient number of moments are bound to fail sooner or later. As expected, an oversimplified model computation of the minimum time interval required for reliable occurrence rate estimates with reasonable uncertainty for a return period of 475 years (Beauval et al. 2008; Mak et al. 2014) suggests the geological time span of 12,000 years. In the case of Italy, on account of the millennial earthquake catalogue available, a reliable and physically sound alternative is represented by NDSHA hazard estimations, which in their standard definition do not depend on the probability of earthquake occurrence, but can be adjusted by recurrence if the data allow.

The obtained results might be indicative of a fundamental misfit of the generally accepted uniform rules of homogeneous smoothing applied to observations on top the naturally fractal system of blocks-and-faults with evidently heterogeneous structure and rheology. Any model for SHA aimed, presumably, at predicting disastrous ground shaking that would actually occur must pass series of rigid testing against the available real seismic activity data before being suggested as a practical seismic hazard and risk estimation. Otherwise, similar to medical malpractice, although at much higher level of simultaneous losses (Wyss et al. 2012), the use of untested seismic hazard maps would eventually mislead to crime of negligence.

Acknowledgements

This paper was completed during the visit of A.K. Nekrasova at the Structure and Nonlinear Dynamics of the Earth (SAND) Group of the Abdus Salam International Centre for Theoretical Physics, Miramare - Trieste, Italy. AKN and VGK acknowledge the support from the Russian Foundation for Basic Research (RFBR grants № 13-05-91167 and № 14-05-92691).

References

Beauval C., P-Y. Bard P-Y, S. Hainzl, Guguen (2008) Can strong motion observations be used to constrain probabilistic seismic hazard estimates? Bull Seismol Soc Am 98(2): 509-520.

Giardini D., G. Grünthal, K.M. Shedlock, P. Zhang (1999) The GSHAP Global Seismic Hazard Map. Annali di Geofisica 42 (6): 1225-1228.

Giardini D., G. Grünthal, K.M. Shedlock, P. Zhang (2003) The GSHAP Global Seismic Hazard Map. In: Lee, W., Kanamori, H., Jennings, P. and Kisslinger, C. (eds.): International Handbook of Earthquake

& Engineering Seismology, International Geophysics Series 81 B, Academic Press, Amsterdam, 1233-1239.

Giardini D., J. Woessner, L. Danciu, F. Cotton, H. Crowley, G. Grünthal, R. Pinho, G. Valensise, S. Akkar, R. Arvidsson, R. Basili, T. Cameelbeck, A. Campos-Costa, J. Douglas, M. B. Demircioglu, M. Erdik, J. Fonseca, B. Glavatovic, C. Lindholm, K. Makropoulos, C. Meletti, R. Musson, K. Pitilakis, A. Rovida, K. Sesetyan, D. Stromeyer, M. Stucchi, (2013) Seismic Hazard Harmonization in Europe (SHARE): Online Data Resource, doi:10.12686/SED-00000001-SHARE

Giardini D., J. Woessner, L. Danciu (2014) Mapping Europe's Seismic Hazard, Eos Trans. AGU, Eos, Vol. 95, No. 29, 22 July 2014

Grünthal G., R. Wahlström, D. Stromeyer (2013) The SHARE European Earthquake Catalogue (SHEEC) for the time period 1900-2006 and its comparison to the European Mediterranean Earthquake Catalogue (EMEC). Journal of Seismology. 17, 4, 1339-1344. DOI: 10.1007/s10950-013-9379-y

Indirli M, H. Razafindrakoto, F. Romanelli, C. Puglisi, L. Lanzoni, E. Milani, M. Munari, S. Apablaza (2011) Hazard Evaluation in Valparaiso: the MAR VASTO Project. Pure Appl Geophys 168(3-4):543-582

Kossobokov V.G., A.K. Nekrasova (2012). Global seismic hazard assessment program maps are erroneous. Seismic Instrum., 48 (2). http://dx.doi.org/10.3103/S0747923912020065. Allerton Press, Inc., 2012162-170.

Magrin A. (2012) Multi-scale seismic hazard scenarios., PhD Thesis. Univ. degli Studi di Trieste, Italy.

Mak S., R.A. Clements, D. Schorlemmer (2014) The statistical power of testing probabilistic seismic-hazard assessments. Seismological Research Letters 85(4): 781-783.

Marzocchi W. (2013), Seismic Hazard and Public Safety. Eos, Vol. 94, No. 27, 240-241.

Meletti C., V. Montaldo (2007) Stime di pericolosità sismica per diverse probabilità di superamento in 50 anni: valori di ag. http://esse1.mi.ingv.it/d2.html, Deliverable D2

Nekrasova A., V. Kossobokov, A. Peresan, A. Magrin (2014) The comparison of the NDSHA, PSHA seismic hazard maps and real seismicity for the Italian territory, Natural Hazards 70 (1), pp.629–641 DOI 10.1007/s11069-013-0832

Panza G.F., F. Romanelli, F. Vaccari (2001) Seismic wave propagation in laterally heterogeneous anelastic media: Theory and applications to seismic zonation. Advances in Geophysics, 43:1-95.

Panza G.F, La Mura C, Peresan A, Romanelli F, Vaccari F. (2012). Seismic Hazard Scenarios as Preventive Tools for a Disaster Resilient Society. In: Dmowska R (Ed) Advances in Geophysics, Elsevier, London, 93–165.

Panza G.F., A. Peresan A., C. La Mura (2013). Seismic Hazard and Strong Ground Motion: an Operational Neo-deterministic Approach from National to Local Scale. [Eds.UNESCO-EOLSS Joint Commitee], in Encyclopedia of Life Support Systems (EOLSS), Geophysics and Geochemistry, Developed under the Auspices of the UNESCO, Eolss Publishers, Oxford ,UK, p. 1-49.

Panza G.F., V. Kossobokov, A. Peresan, A. Nekrasova (2014). Why are the standard probabilistic methods of estimating seismic hazard and risks too often wrong? In: Earthquake Hazard, Risk, and Disasters. M. Wyss Ed., Chapter 12, 309-357. http://dx.doi.org/10.1016/B978-0-12-394848-9.00012-2.

Peresan A., A. Magrin, A. Nekrasova, V.G. Kossobokov, G.F. Panza (2013) Earthquake recurrence and seismic hazard assessment: a comparative analysis over the Italian territory. In: Proceedings of the ERES 2013 Conference. WIT Transactions on The Built Environment, Vol 132, pp 23-34. doi:10.2495/ERES130031, ISSN 1743-3509 (on-line)

Shedlock K.M., D. Giardini., G. Grünthal, P. Zhang (2000). The GSHAP Global Seismic Hazard Map. Seismol. Res. Letters 71 (6), 679-686.

Stucchi M, R. Camassi, A. Rovida, M. Locati, E. Ercolani, C. Meletti, P. Migliavacca, F. Bernardini, R. Azzaro (2007) DBMI04, il database delle osservazioni macrosismiche dei terremoti italiani utilizzate per la compilazione del catalogo parametrico CPTI04. Quad. Geof. 49: 38 (available at http:// emidius.mi.ingv.it/DBMI04/).

Stucchi et al., (2012) The SHARE European Earthquake Catalogue (SHEEC) 1000–1899. Journal of Seismology, doi: 10.1007/s10950-012-9335-2.

Stein S., R. Geller, M. Liu (2012) Why earthquake hazard maps often fail and what to do about it, Tectonophysics, 562-563, 1–25.

Wyss M., A. Nekrasova, V. Kossobokov (2012) Errors in expected human losses due to incorrect seismic hazard estimates, Nat. Hazards, 62, 927–935.

Zuccolo E., F. Vaccari, A. Peresan, G.F. Panza (2011) Neo-deterministic and probabilistic seismic hazard assessments: a comparison over the Italian territory. Pure Appl. Geophys., 168:69–83.

OPINION

Bayes and BOGSAT: Issues in When and How to Revise Earthquake Hazard Maps

INTRODUCTION

Recent large earthquakes that caused ground shaking larger than anticipated have generated interest in how to improve earthquake hazard mapping. Issues under discussion include how to evaluate maps' performance, how to assess their uncertainties, how to make better maps, and how to best use maps given their limitations.

An important question is what to do after an earthquake yielding shaking larger than anticipated. Hazard mappers have two choices. One is to regard the high shaking as a low-probability event allowed by the map, which used estimates of the probability of future earthquakes and the resulting shaking to predict the maximum shaking expected with a certain probability over a given time (Hanks *et al.*, 2012; Frankel, 2013). The usual choice, however, is to accept that high shaking was not simply a low-probability event consistent with the map, and revise the map to show increased hazard in the heavily shaken area (Fig. 1).

Whether and how much to revise a map is complicated, because a new map that better describes the past may or may not better predict the future. For example, increasing the predicted hazard after an earthquake on a fault will make better predictions if the average recurrence time is short compared to the map's time window but will overpredict future shaking if the average recurrence time is much longer than the map's time window.

BAYES' RULE

For insight into whether and how to remake a hazard map, imagine tossing a coin, which comes up heads four times in a row. How likely do you think it is to come up heads on the next toss? You started off assuming that the coin is fair—equally likely to land heads or tails. Should you change that assumption?

Either choice runs a risk. If the coin is severely biased, staying with the assumption that it is fair will continue to yield poor predictions. However, if the coin is fair and the four heads were just a low-probability event, changing to the assumption that the coin is biased does a better job of describing what happened in the past but will make your prediction worse.

Your choice would depend on how confident you were in your assumption, prior to the tosses, that the coin was fair. If you were confident that the coin was fair, you would not change your model and continue to assume that a head or tail is equally likely. However, if you got the coin at a magic show, your confidence that it is fair would be lower, and you would be more apt to change your model to one predicting a head more likely than a tail.

A statistical approach that combines preconceptions with observations to decide how to update forecasts as additional information becomes available uses Bayes' Rule (Rice, 2007). In this formulation

$$\text{revised or posterior probability} \propto \text{likelihood of observations given the prior model} \times \text{prior probability}$$

omitting a normalization. This starts by assuming an initial or prior probability model based on information available prior to the additional observations, calculating how likely the observations were given that model, and using the product as the revised or posterior probability model to account for the additional observations.

We can describe a coin's probability of landing heads by a parameter from 0 (always tails) to 1 (always heads) and represent our beliefs about the parameter by a probability distribution. If, prior to observing the four heads, we are confident the coin is fair or nearly fair, our prior probability distribution is tightly clustered around 0.5 (although to allow surprises, it assigns nonzero probability throughout the interval). If we think the coin may be biased, our prior distribution would have a much larger spread and might be skewed toward 0 or 1.

After some tosses, the revised model depends on both the observations and the prior model. If we had high confidence that the coin was fair, a few low-probability observations would not change it much. However, if we had little confidence in the prior model, these low-probability observations change it a lot.

In the Bayesian approach, probability represents our belief in how a system works based on the information we have. This probability is subjective, because given the little information we know about the coin, we have no way to know the actual probability of a head on the next toss. Once we have chosen a model, we can calculate this probability precisely. However, because this probability assumes that the model is true, it also is subjective and subject to revision after the next toss.

This view differs from the frequentist view in which an event's probability is the frequency in which it occurs in a large number of trials. After a thousand independent tosses under standard conditions, the fraction of heads would be a good estimate of the probability of a head on the next toss. However, because we only have four tosses, we factor in our preconcep-

doi: 10.1785/0220140215

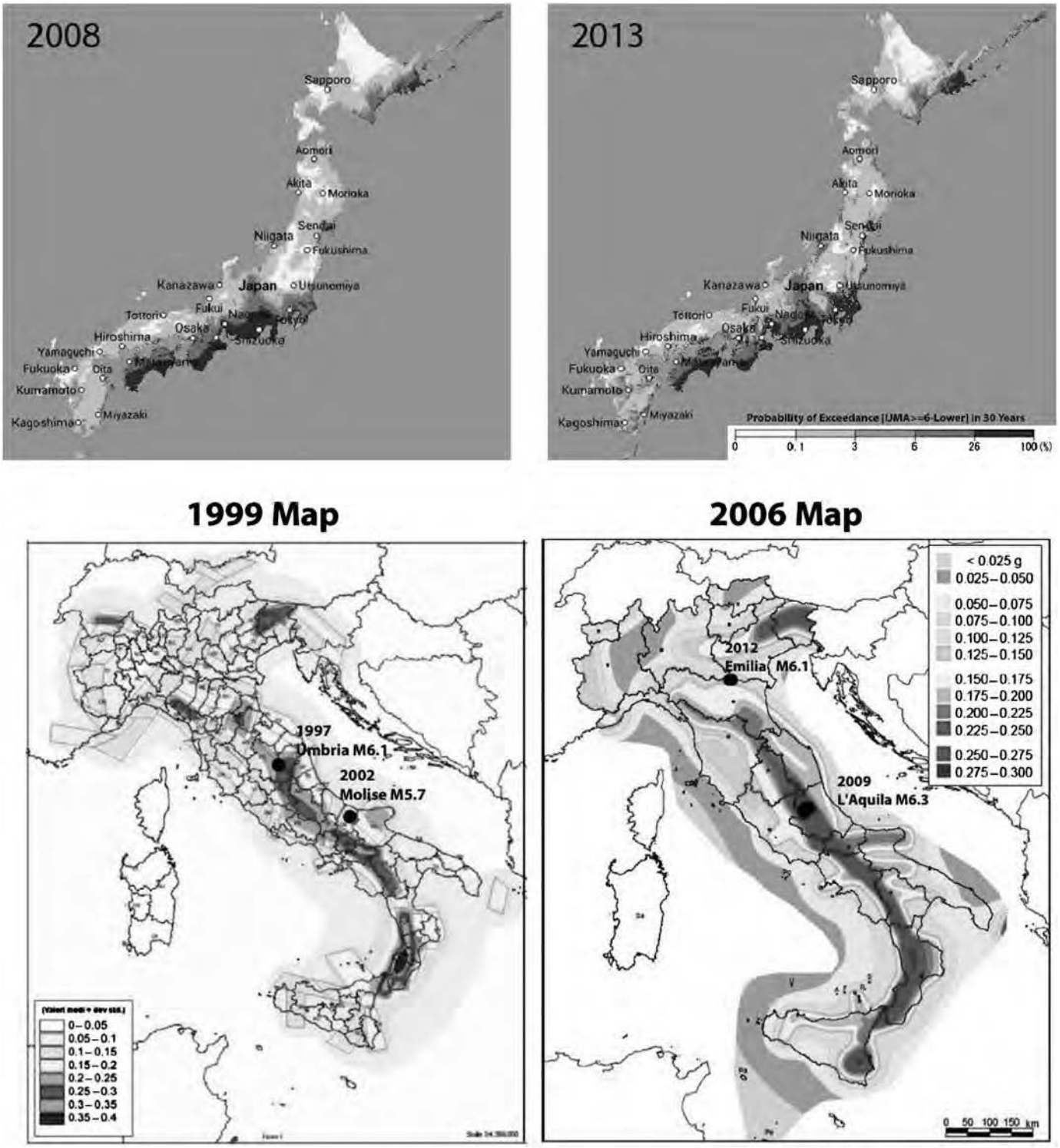

▲ **Figure 1.** (top) Japanese seismic-hazard maps before and after the 2011 Tohoku earthquake. The predicted hazard has been increased both along the east coast, where the 2011 earthquake occurred, and on the west coast. (http://www.j-shis.bosai.go.jp/map/?lang=en; last accessed December 2014.) (bottom) Comparison of successive Italian hazard maps (Stein *et al.*, 2013). The 1999 map was updated to reflect the 2002 Molise earthquake, and the 2006 map will likely be updated after the 2012 Emilia earthquake.

tions rather than automatically assume that four heads prove that the probability of one in the next toss is near 1.

Although the Bayesian approach requires assuming a prior probability distribution, this assumption's effect is reduced as more data become available, provided the prior distribution does not assign zero probability to parameter values that include the true state of nature. After enough observations, the posterior distribution does not depend on the assumed prior distribution.

EARTHQUAKE PROBABILITIES

Seismologists often approach estimating earthquake hazards in the spirit of Bayes' Rule, because this involves assuming probability models based on limited data and then using new data to improve them (Marzocchi and Jordan, 2014). To see this, consider a simple example in which we assume that the probability of a large earthquake on a fault is described by a Poisson process with parameter $\lambda = 1/T$, corresponding to an average return time of T years. Following Campbell (1982), we represent our uncertainty about λ using a gamma distribution with mean μ and standard deviation σ as our prior probability distribution. If an earthquake occurs only one year after the last, the prior distribution is updated to the posterior distribution, and the prior mean μ updates to the posterior mean $\mu' = \mu(1 + \sigma^2/\mu^2)/(1 + \sigma^2/\mu)$ (Rice, 2007).

Consider μ to be specified as 0.02, that is $T = 50$ yrs. If we are highly confident about λ when the forecast is made, σ is small, so the posterior mean μ' and prior mean μ are close. We treat the new observation that did not fit the model well as a rare event that does not change our preconception much. However, if we were uncertain that λ would be near the prior mean μ, σ is large so the new observation changes our view, making the posterior mean very different (larger) than the prior mean.

Figure 2 shows how the updated forecast, described by the posterior mean, increasingly differs from the initial forecast (prior mean) when the uncertainty in the prior distribution is larger. The less confidence we have in the prior model, the more a new datum can change it.

This example is useful because inferring earthquake probabilities, which are crucial inputs for hazard mapping, is very difficult given the poorly understood faulting process and the limitations of the earthquake record (Savage, 1994; Parsons, 2008). It is unclear whether to assume earthquake recurrence is described by a Poisson process with no memory, so the probability is constant with time, or by time-dependent models based on an earthquake cycle in which the probability is small shortly after the past one, and then increases. Numerical simulation shows that these two are difficult to distinguish even in a simple case (Stein and Stein, 2013a). Moreover, using a time-dependent model requires choosing many parameters that are poorly constrained by the available earthquake history.

From a statistical view, Stark and Freedman (2003) concluded that earthquake probability estimates are "shaky." In their view, "the interpretation that probability is a property of a model and has meaning for the world only by analogy seems the most appropriate.... The problem in earthquake forecasts is that the models have not been tested against relevant data. Indeed, the models cannot be tested on a human time scale, so there is little reason to believe the probability estimate." Savage (1991) concluded that earthquake probability estimates for California are "virtually meaningless" and that it would be meaningful only to quote broad ranges, such as low (< 10%), intermediate (10%–90%), or high (> 90%). In other words, it seems reasonable to say that earthquakes of a given size are more likely on some faults than others, but quantifying this involves large uncertainty.

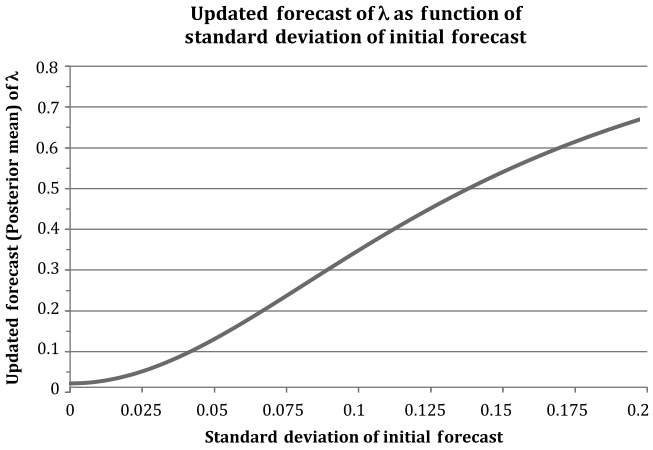

▲ **Figure 2.** Sensitivity of updated forecast of λ, initially assumed to equal 0.02, to assumed prior uncertainty. The lower our confidence in the initial forecast, the more the new datum changes it.

HAZARD MAPS

The earthquake probability example illustrates the challenge for hazard maps: choosing hundreds or thousands of parameters to predict the answers to four questions over periods of 500–2500 yr: Where will large earthquakes occur? When will they occur? How large will they be? How strong will their shaking be?

Some of the parameters required are reasonably well known, some are somewhat known, some are essentially unknown, and some may be unknowable (e.g., Stein *et al.*, 2012). As a result, mappers combine data and models with their sense of how the earth works. Stark and Freedman (2003) note that this involves "geological mapping, geodetic mapping, viscoelastic loading calculations, paleoseismic observations, extrapolating rules of thumb across geography and magnitude, simulation, and many appeals to expert opinion. Philosophical difficulties aside, the numerical probability values seem rather arbitrary."

Such models, which involve subjective assessments and choices among many poorly known or unknown parameters, are sometimes termed BOGSATs, from "Bunch Of Guys Sitting Around a Table" (Kurowicka and Cooke, 2006). Not surprisingly, sometimes the resulting maps do well at predicting what occurs in future earthquakes, and sometimes they do poorly. However, at this point, there is no way to avoid BOGSAT. Although some parameters could be better estimated, and knowledge of some will improve as new data and models become available, major uncertainties seem likely to remain (Stein and Friedrich, 2014).

Nonetheless, despite their large uncertainties, hazard maps have some useful information. From a mitigation policy standpoint, inaccurate hazard (and loss) estimates are still useful unless they involve gross misestimates (Stein and Stein, 2013b). For example, a highway department would likely use its limited funds to preferentially strengthen bridges in predicted high-hazard areas.

In our view, one should consider the BOGSAT process from a Bayesian perspective. This recognizes that the predicted hazard reflects mapmakers' view of the world based on their assessment of diverse data and models, and that when and how maps are revised once new data become available depends on the mapmakers' preconceptions. Because this is the case, how can it be done better?

At a fundamental level, we need to learn more about when and how revising maps makes them better or worse predictors of the future. In some cases revisions should make the map work better, and in others, worse. In particular, raising the predicted hazard where a large earthquake recently occurred may improve the match of the model to past data (though this is rarely quantified using a previously defined metric) but degrade its fit to future events.

On a working level, we suggest several changes to current procedures.

First, maps should specify what they seek to predict and how their performance should be measured. Various metrics can be used, so users can know what the mappers' goals are and be able at later time to assess how well the map met them. For example, how well did the map perform compared to one that assumed a much smoother variation in the predicted hazard (Geller, 2011)?

Second, hazard map documentation should list the parameters used and estimates of their uncertainties. Often much of this information is available in the documentation (e.g., Field *et al.*, 2008). In particular, weights assigned to logic tree branches are a discretized version of the prior probability density function assumed for that parameter. It would be useful to list model assumptions in a consistent form to make changes between successive maps easier to identify and discuss.

Third, estimates of the expected uncertainty in the predicted hazard should be presented and explained. Forecasts with significant economic and policy implications typically present

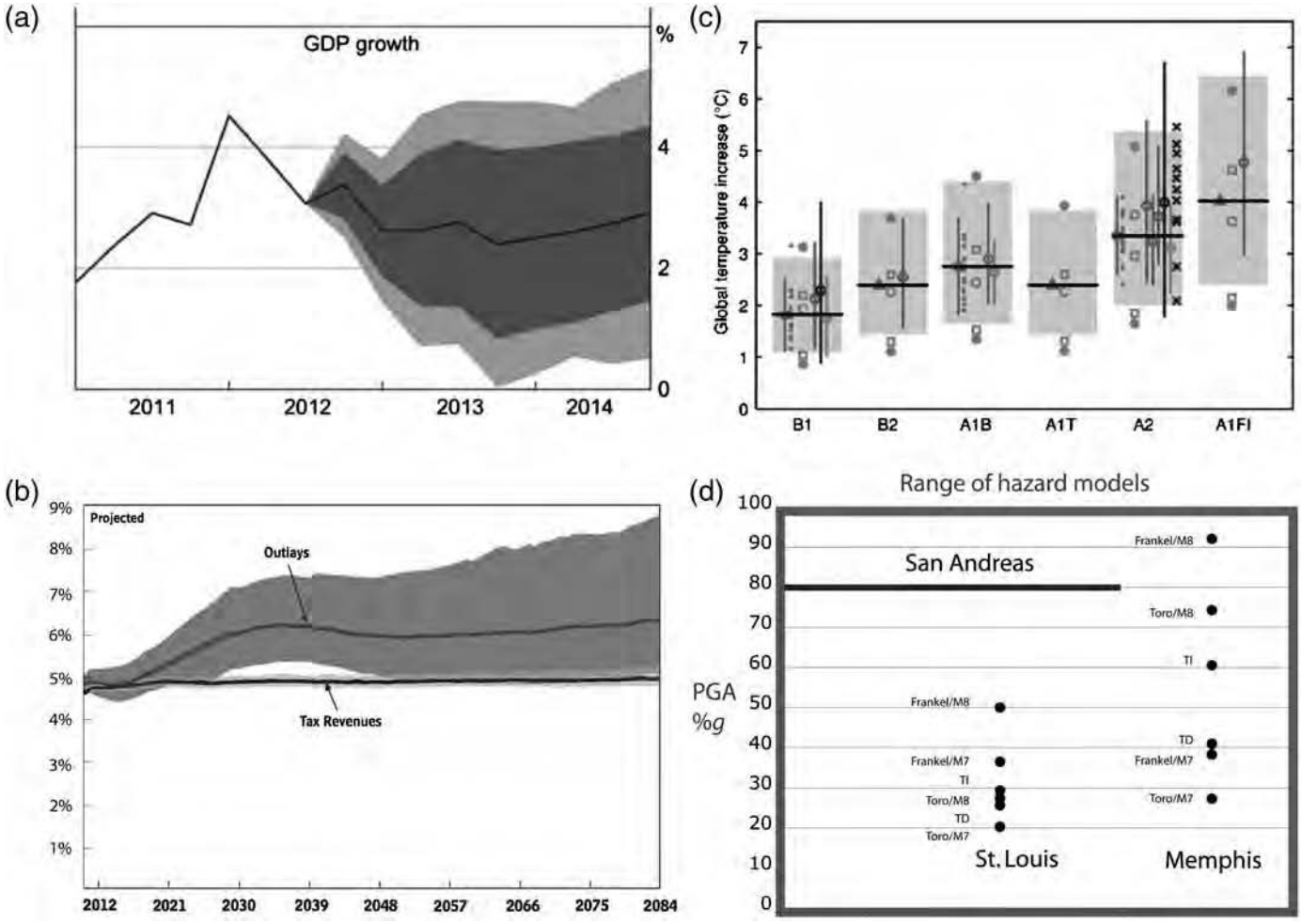

▲ **Figure 3.** Presenting forecast uncertainties. (a) Forecast of Australian Gross Domestic Product (GDP) growth. Uncertainty bounds are 70% and 90% (Reserve Bank of Australia, 2013). (b) Forecast of U.S. Social Security expenditure as percentage of GDP (Congressional Budget Office, 2010) (c) Comparison of the rise in global temperature by the year 2099 predicted by various climate models. For various carbon emissions scenarios, for example, B1, the vertical band shows the predicted warming (Intergovernmental Panel on Climate Change [IPCC], 2007). (d) Comparison of earthquake hazard, described as peak ground acceleration as a percentage of the acceleration of gravity expected with 2% risk in 50 yr, predicted by various assumptions for two sites in the central United States (Stein *et al.*, 2012).

uncertainties (Fig. 3). Although forecasts sometimes miss their targets (Stein and Stein, 2014), uncertainty estimates are still useful. This would involve generating hazard curves and maps for different parameter values within their assumed uncertainties. The resulting range of estimates could be presented via uncertainty maps or tabulations at sites. These uncertainties could be factored in policy making, as is done for other forecasts.

Fourth, changes in parameter values between successive maps should be listed and explained. Some will likely reflect what happened in earthquakes after the map was made whereas others will reflect data not used in the earlier map, because they were not recognized, not appreciated, or unavailable. The criteria used to decide when parameters were changed should be defined (Ramsey, 1926).

Deciding when and how to revise hazard maps would combine Bayes and BOGSAT. Conceptually, changing parameters would reflect Bayes' Rule, because those previously thought to have greater uncertainty would be most easily changed by new data or ideas. Operationally, because most parameters are estimated via a combination of data, models, and assumptions, the actual values would come from BOGSAT rather than explicit calculation. Even so, the Bayesian approach would add value because it is systematic. If BOGSAT leads to big changes in the map, one can assess what that implies about prior confidence in the forecasts.

This approach would give users information about the uncertainties to make better decisions. Meteorologists (Hirschberg *et al.*, 2011) have adopted a goal of "routinely providing the nation with comprehensive, skillful, reliable, sharp, and useful information about the uncertainty of hydrometeorological forecasts." Although seismologists have a tougher challenge and a longer way to go, we should try to do the same.

ACKNOWLEDGMENTS

Stein thanks the U.S. Geological Survey John Wesley Powell Center for Analysis and Synthesis for hosting a working group under auspices of the Global Earthquake Model project, whose stimulating discussions inspired this work. Spencer thanks the Institute for Policy Research for supporting his research. We also thank Sandy Zabell for helpful comments.

REFERENCES

Campbell, K. W. (1982). Bayesian analysis of extreme earthquake occurrences, *Bull. Seismol. Soc. Am.* **72,** 1689–1705.

Congressional Budget Office, Washington, D.C. (2010). *Long-Term Projections for Social Security.*

Field, E., T. E. Dawson, K. R. Felzer, A. D. Frankel, V. Gupta, T. H. Jordan, T. Parsons, M. D. Petersen, R. S. Stein, R. J. Weldon II, and C. J. Wills (2008). The uniform California earthquake rupture forecast, Version 2, *U.S. Geol. Surv. Open-File Rept. 2007-1437.*

Frankel, A. (2013). Comment on "Why earthquake hazard maps often fail and what to do about it," by S. Stein, R. J. Geller, and M. Liu, *Tectonophysics* **592,** 200–206.

Geller, R. J. (2011). Shake-up time for Japanese seismology, *Nature* **472,** 407–409.

Hanks, T. C., G. C. Beroza, and S. Toda (2012). Have recent earthquakes exposed flaws in or misunderstandings of probabilistic seismic hazard analysis? *Seismol. Res. Lett.* **83,** 759–764.

Hirschberg, P., E. Abrams, A. Bleistein, W. Bua, L. D. Monache, T. W. Dulong, J. E. Gaynor, B. Glahn, T. M. Hamill, J. A. Hansen, D. C. Hilderbrand, R. N. Hoffman, B. H. Morrow, B. Philips, J. Sokich, and N. Stuart (2011). An implementation plan for generating and communicating forecast uncertainty information, *Bull. Am. Meteorol. Soc.* **92,** 1651–1666.

Intergovernmental Panel on Climate Change (IPCC) (2007). *Climate Change*, Cambridge Univ. Press, New York.

Kurowicka, D., and R. M. Cooke (2006). *Uncertainty Analysis with High Dimensional Dependence Modeling*, Wiley, Hoboken, New Jersey.

Marzocchi, W., and T. H. Jordan (2014). Testing for ontological errors in probabilistic forecasting models of natural systems, *Proc. Natl. Acad. Sci. Unit. States Am.* **111,** 11973–11978.

Parsons, T. (2008). Earthquake recurrence on the south Hayward fault is most consistent with a time dependent, renewal process, *Geophys. Res. Lett.* **35,** doi: 10.1029/2008GL035887.

Ramsey, F. P. (1926). Truth and probability. in *Foundations of Mathematics.*, R. B. Braithwaite (Editor), Littlefield, Adams & Co, Totowa, New Jersey, 156–198.

Reserve Bank of Australia, Sydney, Australia (2013). *Statement on Monetary Policy.*

Rice, J. A. (2007). *Mathematical Statistics and Data Analysis*, Duxbury, India.

Savage, J. C. (1991). Criticism of some forecasts of the national earthquake prediction council, *Bull. Seismol. Soc. Am.* **81,** 862–881.

Savage, J. C. (1994). Empirical earthquake probabilities from observed recurrence intervals, *Bull. Seismol. Soc. Am.* **84,** 219–221.

Stark, P. B., and D. A. Freedman (2003). What is the chance of an earthquake? in *Earthquake Science and Seismic Risk Reduction*, F. Mulargia and R. J. Geller (Editors), 201–213. Kluwer, Dordrecht, The Netherlands.

Stein, S., and A. Friedrich (2014). How much can we clear the crystal ball? *Astron. Geophys.* **55,** 2.11–2.17.

Stein, S., and J. L. Stein (2013a). Shallow versus deep uncertainties in natural hazard assessments, *Eos Trans AGU* **94,** no. 4, 133–140.

Stein, S., and J. L. Stein (2013b). How good do natural hazard assessments need to be? *GSA Today* **23,** nos. 4/5, 60–61.

Stein, S., and J. L. Stein (2014). *Playing Against Nature: Integrating Science and Economics to Mitigate Natural Hazards in an Uncertain World*, Wiley/AGU, Hoboken, New Jersey.

Stein, S., R. J. Geller, and M. Liu (2012). Why earthquake hazard maps often fail and what to do about it, *Tectonophysics* **562/563,** 1–25.

Stein, S., R. J. Geller, and M. Liu (2013). Reply to comment by Arthur Frankel on "Why Earthquake Hazard Maps Often Fail and What to do About It," *Tectonophysics* **592,** 207–209.

Seth Stein
Department of Earth and Planetary Sciences
and Institute for Policy Research
Northwestern University
Evanston, Illinois 60208 U.S.A.
seth@earth.northwestern.edu

Bruce D. Spencer
Department of Statistics and Institute for Policy Research
Northwestern University
Evanston, Illinois 60208 U.S.A.

Edward Brooks
Department of Earth and Planetary Sciences
Northwestern University
Evanston, Illinois 60208 U.S.A.

Published Online 31 December 2014

CSNI Workshop on "*Testing PSHA Results and Benefit of Bayesian Techniques for Seismic Hazard Assessment*"
4-6 February 2015, Eucentre Foundation, Pavia, Italy

The effect of dependence of observations on hazard validation studies

Iunio Iervolino
Università degli Studi di Napoli Federico II, Italy, iunio.iervolino@unina.it

Massimiliano Giorgio
Seconda Università degli Studi di Napoli, Italy, massimiliano.giorgio@unina2.it

SUMMARY

In countries with an advanced seismic technical culture, where best-practice probabilistic hazard studies are available along with dense seismic networks, there is an increasing interest in validation of hazard maps. This, basically, means trying to quantitatively understand whether probabilities estimated via hazard analysis are consistent with observed frequencies of exceedance of ground motion intensity thresholds. Because the exceedance events of interest are typically rare with respect to the time span covered by data from seismic monitoring networks, a common approach underlying these studies is to pool observations from different sites. The main reason for this is to collect a number of data large enough to convincingly perform a statistical analysis. However, this is often done neglecting the intrinsic stochastic dependence affecting observations at different sites in the same earthquake. On these premises, the presented study demonstrates how this may lead to potentially fallacious conclusions about inadequateness of probabilistic seismic hazard assessment. The study refers, as an example, to an ideal seismic source zone and some recording sites. It is shown, how accounting for the dependence of intensity on magnitude and source to site distance, may change the results of validation from fail to pass. Some considerations with respect to other studies, attempting to validate Italian data via thirty years of seismic observations all across the country, are also made.

Keywords: *Probabilistic seismic hazard analysis, Validation, Disaggregation, Binomial distribution.*

1. INTRODUCTION

Due to their underlying predictive meaning, probabilistic seismic hazard analysis or PSHA (e.g., Cornell, 1968; Reiter, 1990) studies are debated and often questioned (e.g., Hanks et al., 2012, Kossobokov and Nekrasova, 2012, Stein et al., 2011 and 2012, Stirling, 2012). Italy is not an exception in this sense; indeed, in the country there is a constant debate on the consistency and adequacy of the national hazard map (Stucchi et al., 2011), which serves as a basis for the definition of seismic actions for structural design according to the current building code (CS.LL.PP., 2008).

A number of studies tried to quantitatively confirm or disprove probabilistic seismic hazard estimates via observed ground motions over the years (e.g., Albarello and D'amico, 2008). The soundest studies, attempting to validate hazard maps, are based on the theory of hypothesis testing or confidence intervals (e.g., Mood et al., 1974). In fact, these studies recognize that validating hazard at a single site requires a large number of earthquake observations, which is seldom available due to very long time (on average) required to collect those (e.g., Iervolino, 2013). Therefore, they tend to pool together seismic records at different sites, in the same time span, to create a sample of sufficiently large size to make the formal comparison with PSHA. However, it seems that, in these exercises, the effect of stochastic dependency of observations at different sites, yet in the same earthquake, is often overlooked. The consequent risk is that of being led to fallacious conclusions, labelling seismic hazard estimates from PSHA as erroneous (often claimed not conservative).

Hazard maps are usually a collection of ground motion intensity measures (IMs) values, corresponding to percentiles of site-specific marginal IM distributions. This is because the civil structures are typically point-like, and therefore codes require location-specific SPHA. The aim of this paper is to recall that, due to certain basic aspects of PSHA, in the case the same earthquake affects more than one site, recordings are not independent and therefore the observed IM exceedances should be cautiously compared to hazard maps. The cause for stochastic dependency is twofold: (i) there's stochastic dependency carried by the ground motion prediction equation or GMPE, as hazard *disaggregation* shows (e.g., Iervolino et al., 2011); (ii) there may be also spatial correlation of GMPE's intraevent residuals (e.g., Esposito and Iervolino, 2011). This study will focus on (i) as it is sufficient to prove the argument that spatial dependency of observation in a single seismic event must be take into account in PSHA validation attempts. Other forms of dependency, such as spatial clustering of exceedances, are also neglected.

To this end the remainder of the paper is organized such that a brief review of site-specific and regional PSHA, is initially given. Then, simple examples of how hazard validation would quantitatively change if the dependency of observations were accounted for, are discussed. Finally, some recommendations for comparison of hazard and observed ground motions are addressed with respect to one of the approach to PSHA validation found in literature.

2. SITE-SPECIFIC AND REGIONAL PSHA ESSENTIALS

In its standard form, PSHA consists of the estimate of the mean rate (e.g., annual) of exceedance of a given value of an IM, for example peak ground acceleration or PGA, at a site of interest (e.g., the location where a building under design is to be constructed). The computation of this rate, which can be represented as λ_{IM}, is often carried out considering: at first the rate of earthquake occurrence on the source, ν; then the conditional probability of IM exceedance given event magnitude (M) and source-to-site distance (R), as well as other parameters; and finally by averaging over all possible events via the joint distribution of M and R, as in Equation (1).[1]

This articulation, is only for convenience, because the $P\left[IM \geq im \mid m \cap r\right]$ term is obtained from GMPEs, while ν and $P\left[M = m \cap R = r\right]$, the latter being the joint probability of M and R, are provided based on seismicity – historical or instrumental – and geological information about the source.

$$\lambda_{IM} = \nu \cdot P\left[IM > im\right] = \nu \cdot \sum_{m,r} P\left[IM > im \middle| m \cap r\right] \cdot P\left[M = m \cap R = r\right] \quad (1)$$

[1] For the sake of simplicity in this illustration, the probabilities are expressed for discrete random variables while, strictly speaking, these should be considered continuous. In fact, sums and probabilities should be replaced by integrals and probability density function, respectively.

In fact, it is possible to show that, if the occurrence of earthquakes on the source follows a homogeneous Poisson processes (HPP) with rate ν, then also the process describing the occurrence of events determining exceedance of the IM at the site of interest, follows a HPP. Furthermore, the rate of the latter depends on that of the former as per Equation (1). It is a *filtered* process; the occurrence of earthquakes on the source is filtered by the probability that the resulting ground motion will cause the exceedance of the *im* intensity level in question at the site. In other words, among all the earthquakes occurring on the fault, retaining only those causing the considered effect at the site, the occurrence of events belonging to this *random selection* is still described by a HPP.

If the analysis as per Equation (1) is repeated for all IM-values in a range of interest, a curve for λ_{IM}, as a function of *im*, is obtained. It is termed *hazard curve*, and for each IM-value provides the rate of the specific HPP regulating its exceedance at the site of interest.

One important consequence of the HPP assumption for earthquake occurrence[2] is that the random time elapsed between two consecutive events (i.e., the *interarrival* time), is characterized by the *exponential* distribution. Therefore, the probability that the time between two events causing the exceedance of the IM-value of interest at the site, $T(im)$, is lower than *t*, is given by Equation (2). The same distribution also provides the probability to observe at least one exceedance of *im* during *t* years.

$$P\left[\textit{at least one exceedance of } im \textit{ during } t\right] = P\left[T(im) \le t\right] = 1 - e^{-\lambda_{IM} \cdot t} \tag{2}$$

In the case of *regional* seismic hazard, one may want to calculate, for example, the ground motion intensity, which has a specific *annual rate of exceedance in at least one of several* sites of interest. Let the objective of *regional* probabilistic seismic hazard analysis (e.g., Esposito and Iervolino, 2011) be to compute the annual rate of the event, which causes the exceedance of a certain IM-value in at least one of two sites, $\{1,2\}$, in the same region. Such a calculation could be carried out by implementing Equation (3). In the equation $\{R_1, R_2\}$ are the earthquake distances from sites 1 and 2 respectively.

$$\lambda_{IM_1 \cup IM_2} = \\ = \nu \cdot \left\{ 1 - \sum_{m, r_1, r_2} P\left[IM_1 \le im_1 \cap IM_2 \le im_2 \mid m \cap r_1 \cap r_2\right] \cdot P\left[M = m \cap R_1 = r_1 \cap R_2 = r_2\right] \right\} \tag{3}$$

The need for the joint probability, $P\left[IM_1 \le im_1 \cap IM_2 \le im_2 \mid m \cap r_1 \cap r_2\right]$, in Equation (3), recalls that GMPEs always imply stochastic dependency of IMs at different sites. This is because the mean of IM at the two sites changes with the value of M and with the earthquake location, which affects the distances, and also because there could be spatial dependency of intraevent residuals of the ground motion prediction model (neglected in the rest of this paper, as mentioned earlier on).

To understand this issue, in Figure 1 an ideal, $20 \times 80\ km^2$, seismic source is considered. It is discretized in sixty-eight possible earthquake source locations. It is also imagined that four recording stations are located in the sites indicated by triangles labeled 1-4 in the figure. It is assumed that event rate of earthquakes is $\nu = 1\left[events/yr\right]$, globally over the source zone. The distribution of magnitude is a truncated exponential one, defined in the $\left[4.5, 7\right]$ range. The *b*-

[2] In this work, considerations regarding the choice – however frequent – of the HPP to model earthquake occurrence are omitted, as well as any discussion of possible alternatives.

value of the Gutenberg-Richter relationship is equal to one. The considered GMPE is that of Ambraseys et al. (1996).[3]

For each (equally likely) possible earthquake location in the picture, 10^4 values of magnitude were generated via a montecarlo simulation. These simulations where used to compute the site-specific hazard curves for sites $\{1,2\}$ via Equation (1), and the joint hazard via Equation (3). Resulting hazard curves are shown in Figure 2. It is to note that the joint hazard may not be lower than those corresponding to hazard for each individual site.

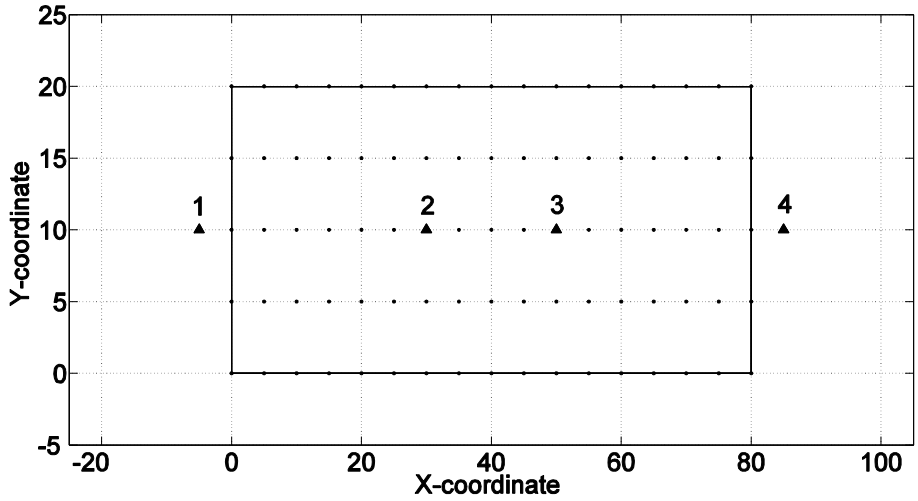

Figure 1. Ideal seismic source zone and considered sites (distances in km).

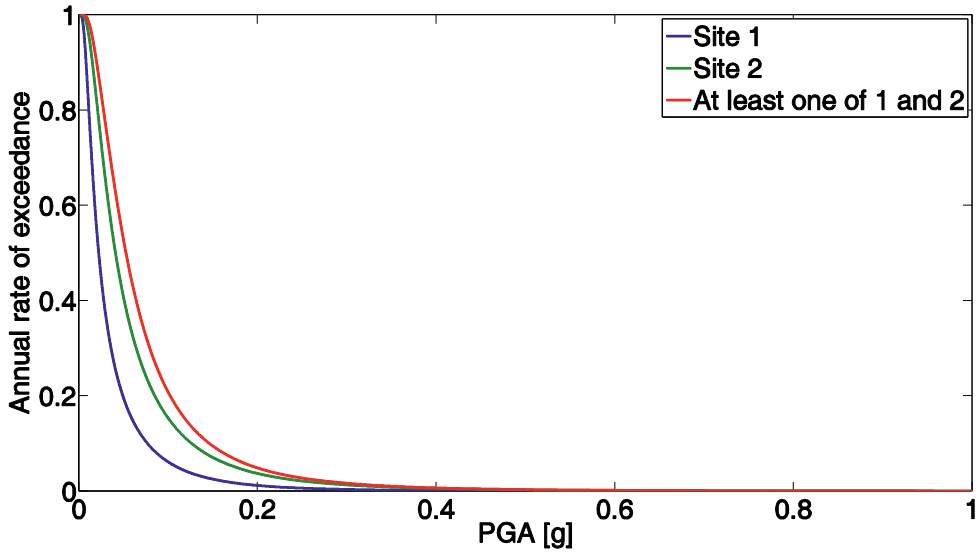

Figure 2. Site-specific (marginal) and regional (joint) hazard for sites 1 and 2 in Figure 1.

Another, even more straightforward way to recall that IM observations at different sites, yet in the same earthquake event, cannot be considered independent random variables, is readily provided by the well-known tool of hazard disaggregation. Given a hazard curve for a specific site and a

[3] In fact, the considered GMPE uses fault distance, while herein it is used as if it was epicentral distance.

threshold in terms of IM, disaggregation results in a distribution that, given exceedance of the considered IM-level, provides the probability, for example, of each possible magnitude-distance being the causative event for such an exceedance at the considered location, $P\left[M = m \cap R = r \middle| IM > im\right]$. Such a distribution may be obtained via the Bayes' theorem (Mood et al., 1974) as in Equation (4). As an example, Figure 3 shows disaggregation of the PGA with 10% exceedance probability in thirty years, $PGA(10/30)$, for sites 1 and 2.

$$P\left[M = m \cap R = r \middle| IM > im\right] = \frac{\nu \cdot P\left[IM > im \middle| m \cap r\right] \cdot P\left[M = m \cap R = r\right]}{\lambda_{IM}} \tag{4}$$

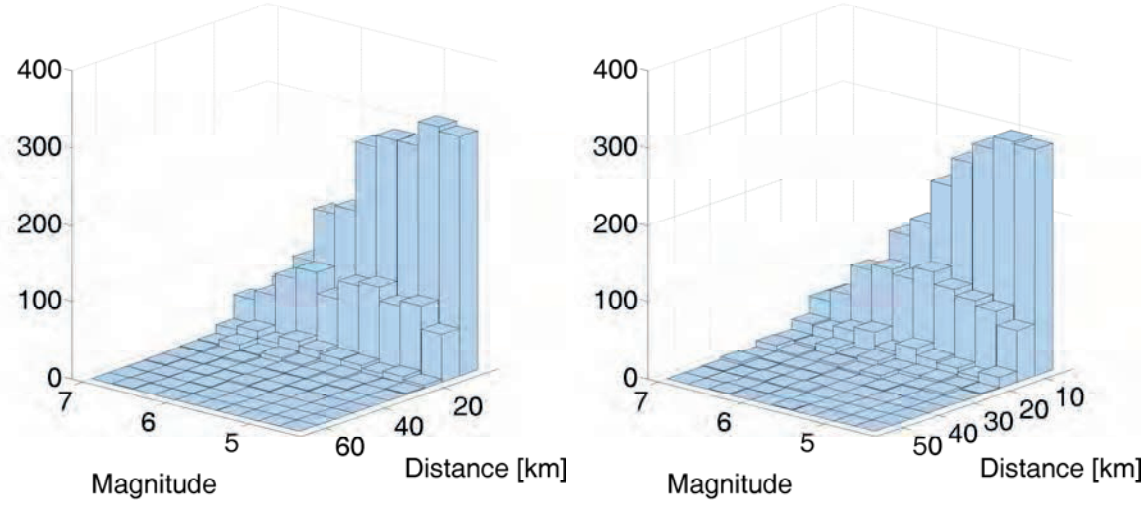

Figure 3. 10% in 30 yr PGA hazard disaggregation for site 1 (left) and site 2 (right). Vertical axis is the probability of the *M*-*R* pair being causative for the exceedance.

It follows from disaggregation, that once exceedance is observed at site 1 in one earthquake, then the probability of exceedance of site 2 changes with respect to the hazard curve for the site, which is the definition of stochastic dependency, Equation (5). As it will be clarified in the following, this has important reflections on validation of a hazard map, which includes both sites 1 and 2.

$$\begin{aligned} &P\left[IM_2 > im_2 \middle| IM_1 > im_1\right] = \\ &= \sum_{m,r} P\left[IM_2 > im_2 \middle| IM_1 > im_1 \cap m \cap r\right] \cdot P\left[M = m, R = r \middle| IM_1 > im_1\right] \neq \\ &\neq P\left[IM_2 > im_2\right] = \sum_{m,r} P\left[IM_2 > im_2 \middle| m \cap r\right] \cdot P\left[M = m \cap R = r\right] \end{aligned} \tag{5}$$

In fact, on the basis of results obtained via the montecarlo simulation described above, it is possible to calculate the probability that a generic earthquake causes exceedance of specific values of intensity, im_1 and im_2, at the sites 1 and 2. For example, im_1 and im_2 may be set equal to $PGA_1(10/30)$ and $PGA_2(10/30)$, respectively; i.e., the values of PGA which corresponds a

10% exceedance probability at each of the sites.[4] More specifically, it is possible to compute: the probability, P_0, that in one (generic) event none of the two sites experiences exceedance; the probability, P_1, to observe exceedance in (exactly) one of the two sites; and the probability, P_2, of observing an exceedance in both the sites. Then, it is easy to verify that the simulation leads to different results with respect to those one obtains in the case it is assumed that exceedances at the two sites (in a generic event) are stochastically independent. In fact, under this hypothesis, the number of exceedances of $PGA_1(10/30)$ and $PGA_2(10/30)$, being the sum of independent and equally distributed Bernoulli random variables, can be considered (by definition) a binomial, $B(n,p)$, random variable with $n=2$ and $p=0.003512$. In fact, the mean and the variance of the total number of exceedances in *t* years of $PGA_i(10/30)$, for both the dependent and the independent case, may be computed as in Equations (6).

$$\begin{cases} \mu(t) = \nu \cdot t \cdot \sum_{i=0}^{2} i \cdot P_i = \nu \cdot t \cdot (0 \cdot P_0 + 1 \cdot P_1 + 2 \cdot P_2) \\ \sigma^2(t) = \nu \cdot t \cdot \left(\sum_{i=0}^{2} i^2 \cdot P_i \right) = \nu \cdot t \cdot (0^2 \cdot P_0 + 1^2 \cdot P_1 + 2^2 \cdot P_2) \end{cases} \tag{6}$$

Means and variances obtained for $t=1$ and $\nu=1$ using the distribution obtained via montecarlo simulation, for different pairs of sites in Figure 1, and those obtained using the binomial distribution, are reported in the following Table 1. For the pairs in the second and third columns, the values considered for the $PGA_3(10/30)$ and $PGA_4(10/30)$ as well as the values of probability P_0, P_1, and P_2 are obtained adopting the same approach used for sites 1 and 2 in the example above.

Table 1. Mean and variance of the random variable counting the number of exceedances in one year for pairs of sites.

	Sites 1,2	Sites 1,4	Sites 2,3	Any two sites considered independent
Mean	0.0070	0.0070	0.0070	0.0070
Stand. Dev.	0.0839	0.0838	0.0853	0.0840

Results show that, as expected, the binomial model allows to calculate correctly the mean number of exceedances (which is the same for sites $\{1,2\}$, $\{1,4\}$, and $\{2,3\}$), yet it does not allow to calculate the *exact* (i.e., according to the considered assumptions) value of the variance, which from simulation results larger considering the pair of sites $\{2,3\}$ and smaller for $\{1,4\}$ and about equal for $\{1,2\}$. This result is due to the fact that the binomial model is not able to account for the negative correlation that exist between exceedances in sites $\{1,4\}$, which are relatively far from each other, and the positive correlation between exceedances in sites relatively close, $\{2,3\}$. It only approximates the results for sites $\{1,2\}$, at an intermediate distance.

[4] $PGA(10/30)$ implies probability of exceedance in one event equal to 0.003512. Indeed, from Equation (2): $P\{T[PGA(10/30)] \le 30\} = 1 - e^{-1 \cdot P[PGA > PGA(10/30)] 30} = 0.1$, from which $P[PGA > PGA(10/30)] = 0.003512$ derives.

3. THE EFFECT OF REGIONAL HAZARD ON SITE-SPECIFIC HAZARD TESTING

In order better clarify the importance of the arguments discussed so far, it can be worthwhile to illustrate the implications they can have in practical applications. To do so, in the next section, mathematical and conceptual details of the validation study discussed in Albarello and D'amico (2008) are recalled. Subsequently, it is finally shown how neglecting stochastic dependence can lead to erroneous conclusions.

3.1. An Italian Hazard Validation Study

In Albarello and D'amico (2008) interesting validation problem is discussed. The aim of the study was to validate the 10% in 30 yr PGA hazard from the official nationwide hazard map. To this aim, the authors gathered data from sixty-eight seismic station operating during a thirty years period across the entire Italian territory. In fact, for these stations, which recorded thirty-eight earthquakes, according to the Italian accelerometric archive or ITACA (http://itaca.mi.ingv.it/), it was observed that thirteen times (collectively) the PGA with a 10% in 30 years exceeding probability according to the hazard map of Stucchi et al. (2011), was actually exceeded. In Figure 4 the map with the stations as well as the location and year of earthquake occurrence and/or of exceedance is given.

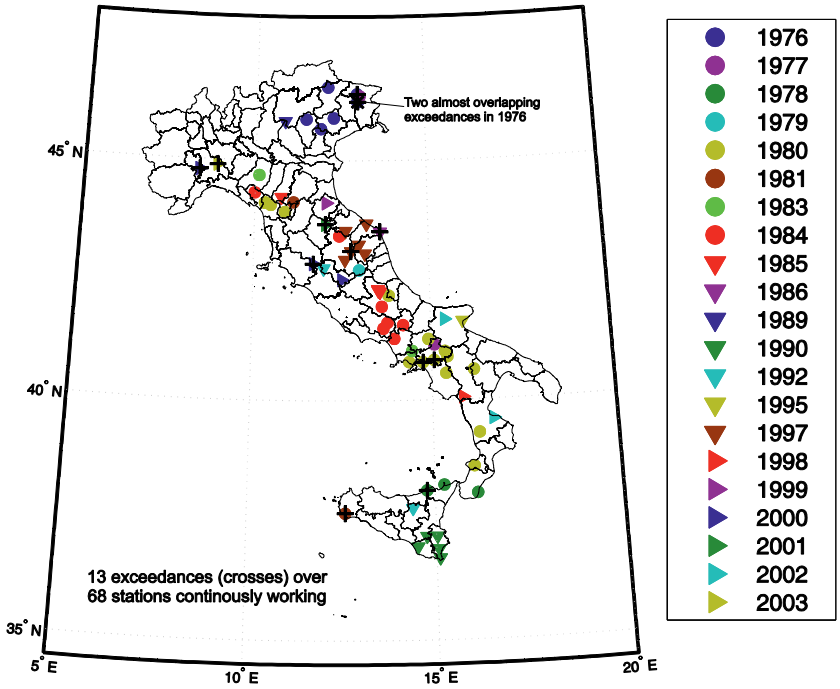

Figure 4. Seismic stations operating in a thirty years time frame, earthquake date and exceedance of PGA(10/30) indicated with crosses.

In the cited study, in order to perform the requested statistical test, authors adopt two approaches, both based on the hypothesis that exceedances in different sites, given that these are *sufficiently far away from each other*, can be considered stochastically independent. In particular, in the first approach, termed the *counting approach*, the event of exceedance of PGA with 10% in 30 years exceeding probability at each site *i*, is modeled as a

Bernoulli random variable which assumes value 0 if exceedance is not observed, and value 1 if $PGA_i(10/30)$ is exceeded *at least once* in thirty years at site *i*.[5] This random variable is characterized by 0.1 probability of observing the exceedance, which is a direct consequence of definition of $PGA_i(10/30)$.[6] Indeed, Bernoulli variables counting the exceedance of $PGA_i(10/30)$ at least once in in thirty years at different sites are equally distributed with $p = 0.1$. Then, under the independence hypothesis, the probability to observe *k* exceedances in thirty years over the sixty-eight stations is given by the binomial distribution $B(n, p)$ in Equation (7), where the number of trials, *n*, is 68 and $p = 0.1$.

$$P\left[k \text{ exceedances of } PGA(10/30) \text{ across } 68 \text{ stations in } 30 \text{ yr}\right] = \binom{68}{k} \cdot 0.1^k \cdot 0.9^{68-k} \quad (7)$$

Consequently, they computed the mean and the variance of the number of sites in which at least an exceedances in thirty years is observed as $n \cdot p = 68 \cdot 0.1 = 6.8$ and $n \cdot p \cdot (1-p) = 68 \cdot 0.1 \cdot (1-0.1) = 6.12$ respectively. Finally, they performed a formal statistical test to check the (null) hypothesis that the exceedances probability at the generic site is 0.1, as suggested by the Italian hazard map, against the (alternative) hypothesis that this probability is probability larger than 0.1. In fact, considered that from available data it results that in 30 years the discussed exceedance has been observed in thirteen of the sixty-eight sites and noted that for the central limit theorem it can assumed that:

$$P\left[\left|number\ of\ exceedances - 6.8\right| > 1.96 \cdot \sqrt{6.12}\right] \cong 0.05 \quad (8)$$

they concluded that, being $13 - 6.8 = 6.2 > 1.96 \cdot \sqrt{6.12} = 4.85$, the observed number of exceedances, give evidence (at 0.05 significance level) that the real value of the exceedances probability at the generic site is larger than 0.1.

3.2. Results obtained accounting for stochastic dependence

In this section it is shown how the presence of stochastic dependency among exceedances at different sites can invalidate decisions taken on the basis of Equation (8). In fact, the use of the binomial model in presence of the discussed form of stochastic dependency, which, ultimately, depends on the spatial distribution of the considered sites with respect to the sources zone, can give a value of the variance that can differ from the *exact* one in a way to change the result of a hypothesis test.

To further illustrate this issue, let consider the ideal seismic source introduced in Figure 1. In this case it is supposed that sixty-eight sites exist (Figure 5). The simulation in this case is performed adopting the same numerical approach and source features previously listed. For each of the 10^4 value of M and for all possible event locations (which are also sixty-eight), the PGAs at each of the sites were simulated. The obtained set of $68 \cdot 10^4$ observations was used to compute the values of $PGA_i(10/30)$, $\{i = 1,2,...,68\}$, as well as the values of probabilities $\{P_0, P_1, ..., P_{68}\}$

[5] Note that, obviously, each of the sites has different values of $PGA(10/30)$ corresponding to the same exceedance probability.

[6] This result, that rigorously applies under the common hypotheses of PSHA, neglects the case of exceedance in aftershock sequences; e.g., Iervolino et al., 2014).

that a single, generic, event causes exceedances of $PGA_i(10/30)$ at any given number of sites simultaneously.

In Figure 6 the probabilities obtained from the simulations are compared to the case it is assumed independence of exceedance events; i.e., in the case number of exceedance in a single event is modeled as a binomial $B(n, p)$ random variable with $n = 68$ and $p = 0.003512$.

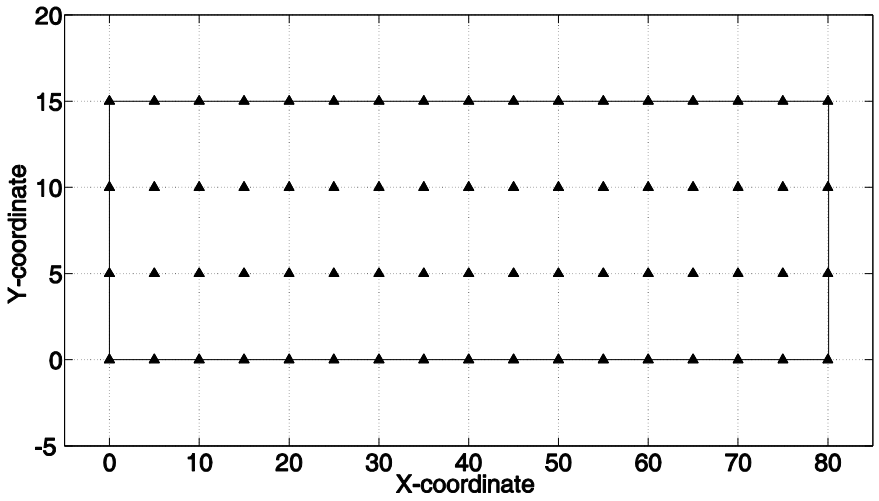

Figure 5. Ideal seismic source zone and sites (distances in km).

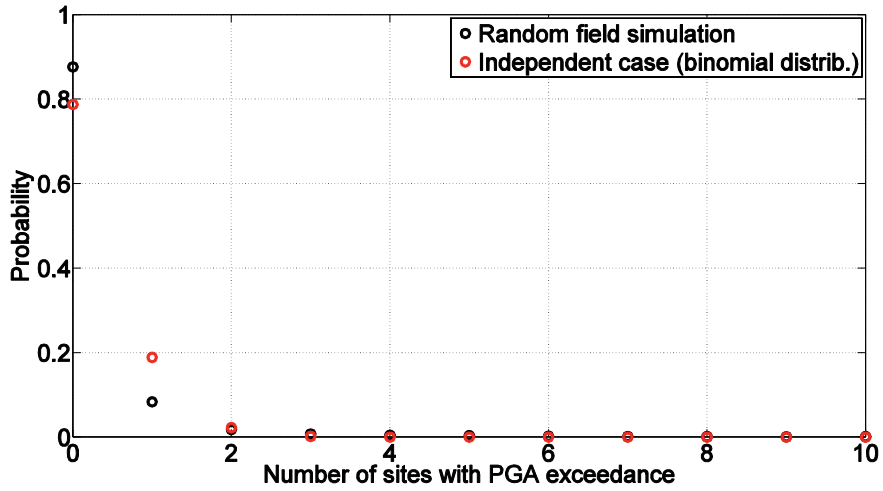

Figure 6. Distributions, in one year, of the number of sites with contemporary exceedance of the PGA with 10% exceedance probability in 30 years.

It may be seen that the spatial dependency of ground motions significantly affects the distributions. Indeed, from Equation (6), Equations (9) results. The mean computed adopting the binomial model (i.e., $68 \cdot 0.003512 \cdot 30 = 7.16$) coincides, as expected, with the mean calculated using the simulation, whereas a difference exists between the variances, which result equal to 8.85 and 26.54 for the binomial model and for the model obtained via simulation, respectively.

$$\begin{cases} \mu(t) = \nu \cdot t \cdot \left(0 \cdot P_0 + 1 \cdot P_1 + ... + 68 \cdot P_{68}\right) \\ \sigma^2(t) = \nu \cdot t \cdot \left(0^2 \cdot P_0 + 1^2 \cdot P_1 + ... + 68^2 \cdot P_{68}\right) \end{cases} \tag{9}$$

At this point, re-applying Equation (8), on the basis of these results, the decision rule in Equation (10) is obtained.

$$\begin{cases} Simulation: P\left[\left|number\ of\ \ exceedances - 7.16\right| > 1.96 \cdot \sqrt{26.54}\right] \cong 0.05 \\ Independent: P\left[\left|number\ of\ \ exceedances - 7.16\right| > 1.96 \cdot \sqrt{8.85}\right] \cong 0.05 \end{cases} \tag{10}$$

Supposing that in thirty years thirteen exceedances have been observed over sixty-eight sites, because $13 - 7.16 = 5.84$ and $1.96 \cdot \sqrt{8.85} = 5.83$, adopting the binomial model would lead to conclude, that at the significance level $\alpha = 0.05$, data give evidence that the true *p* is different from 0.1. On the other hand, because $1.96 \cdot \sqrt{26.54} = 10.1$, the simulations allow to verify that in the considered case the observed number of exceedance is consistent (at the same significance level) with the (null) hypothesis that the exceedance probability at the generic site is 0.1, as suggested by PSHA.[7]

4. CONCLUSIONS

The paper discussed some arguments, which should be taken into consideration when attempting to validate probabilistic seismic hazard studies versus observed earthquakes. In particular, it was discussed that ground motion intensity records at different seismic stations in the same earthquake are not independent. Such a form of spatial stochastic dependence arises, primarily but not only, from the ground motion prediction equation, and is confirmed by seismic hazard disaggregation. Indeed, given that the exceedance at one site is observed, the probability of exceedance at another site changes with respect to the hazard curve. As a consequence, the test statistic to validate hazard cannot rely on models that are not able to account for these form of dependence.

To quantitatively evaluate the effect of such a dependence on possible observed samples of ground motion exceedances, some simple examples were set up. They consisted of an ideal seismic source and some sites affected by its seismicity. It was shown that the variance of the number of exceedances may results larger than that obtained under the hypothesis that exceedance in different sites are independent. It is also shown, how accounting for this dependence may change the results of statistical tests adopted in validation study from reject to not-reject the hypothesis that observations are consistent with the probabilistic seismic hazard map.

It is believed that these arguments, very simple from the statistical point of view, can help the future validations of hazard studies, a field of commendable effort for earthquake engineers and engineering seismologists.

[7] Here attention is focused on the total number of exceedance in thirty years. Hence a little difference is obtained in terms of both mean and variance with respect to results obtained by Albarello e D'amico (2008), where it is considered the number of sites in which at least one exceedance is observed. This little difference doesn't affect the validity of the results obtained in this section.

ACKNOWLEDGEMENTS

This work was developed within the ReLUIS 2014-2018 framework programme. Authors wish to thank Dario Albarello and Vera D'Amico for kindly providing the data of their study.

REFERENCES

Albarello, D., and D'Amico, V., 2008. Testing probabilistic seismic hazard estimates by comparison with observations: an example in Italy, *Geophys. J. Int.* **175**, 1088–1094.

Ambraseys, N. N., Simpson, K. A., and Bommer, J. J., 1996. Prediction of horizontal response spectra in Europe, *Earthquake Eng. Struct. Dyn.* **25**, 371-400.

Cornell, C. A., 1968. Engineering seismic risk analysis, *B. Seismol. Soc. Am.* **58**, 1583–1606.

CS.LL.PP., 2008. *Decreto Ministeriale 14 gennaio 2008: Norme tecniche per le costruzioni. Gazzetta Ufficiale della Repubblica Italiana, n. 29, 4 febbraio 2008, Suppl. Ordinario n. 30.* Ist. Polig. e Zecca dello Stato S.p.a., Roma. (in Italian)

Esposito, S., and Iervolino, I., 2011. PGA and PGV spatial correlation models based on European multi-event datasets, *B. Seismol. Soc. Am.* **101**, 2532–2541.

Gutenberg. R., and Richter, C.F., 1944. Frequency of earthquakes in California, *B. Seism. Soc. Am.* **34**, 185-188.

Hanks, T. C., Beroza, G. C., and Toda, S., 2012. Have recent earthquakes exposed flaws in or misunderstandings of probabilistic seismic hazard analysis?, *Seismol. Res. Lett.* **83**, 759-764.

Kossobokov, V. G., and Nekrasova, A. K., 2012. Global Seismic Hazard Assessment Program maps are erroneous, *Seismic instruments*, **48**, 162–170,

Iervolino, I., 2013. Probabilities and fallacies: why hazard maps cannot be validated by individual earthquakes. *Earthquake Spectra,* **29**, 1125–1136.

Iervolino, I., Chioccarelli, E., and Convertito, V., 2011. Design earthquakes from multimodal hazard disaggregation, *Soil Dyn. Earthq. Eng.* **31**, 1212–1231.

Mood, A. M., Graybill, F. A., and Boes, D. C., 1974. *Introduction to the theory of statistics*, McGraw-Hill, NY, 480 pp.

Reiter, R., 1990. E*arthquake hazard analysis: issues and insights*, Columbia University Press, NY, 254 pp.

Stein, S., Geller, R. G., and Liu, M., 2011. Bad assumptions or bad luck: why earthquake hazard maps need objective testing, *Seismol. Res. Lett.* **82**, 623-626.

Stein, S., Geller, R. G., and Liu, M., 2012. Why earthquake hazard maps often fail and what to do about it, *Tectonophysics*, **562/563**, 1-25.

Stirling, M. W., 2012. Earthquake hazard maps and objective testing: the hazard mapper's point of view, *Seismol. Res. Lett.* **83**, 231-232.

Stucchi, M., Meletti, C., Montaldo, V., Crowley, H., Calvi, G. M., and Boschi, E., 2011. Seismic hazard assessment (2003-2009) for the Italian building code, *B. Seismol. Soc. Am.* **101**, 1885–1911.

Non-Ergodic Seismic Hazard: Using Bayesian Updating for Site-Specific and Path-Specific Effects for Ground-Motion Models

N. M. Kuehn[1], N. A. Abrahamson[2]

[1]Pacific Earthquake Engineering Research Center, University of California, Berkeley, CA, USA

kuehn@berkeley.edu

[2]Pacific Gas and Electric Company, San Francisco, CA, USA

abrahamson@berkeley.edu

Abstract

Traditional probabilistic seismic hazard analysis (PSHA) is based on the ergodic assumption, which means that the distribution of ground motions over time at given site is the same as their spatial distribution over all sites for the same magnitude, distance, and site condition. With large increase in the number of recorded ground motion data, there are now repeated observations at given sites and from multiple earthquakes in small regions. Evaluations of such data from Taiwan, Japan, and California have shown that the size of the repeatable site effects, ray path effects, and source effects is large, accounting for about 75% of the variance treated as aleatory variability in ergodic GMPEs, demonstrating that the ergodic assumption is not realistic. To remove the ergodic assumption requires incorporating the systematic site, path, and source effects into the GMPE. In particular, the epistemic uncertainty in these terms needs to be included. The empirical observations show that the systematic path and source effects are spatially correlated (e.g. earthquakes that are close together will have more similar path effects than earthquakes that are far apart), so the epistemic uncertainty for the path and source effects needs to account for this spatial correlation (Walling, 2009). The inclusion of the epistemic uncertainty of the site, path, and source terms in hazard calculations for a particular site leads to large uncertainties in the resulting hazard curve distribution. As an example, for a site in California, the uncertainty in the hazard for critical structures (e.g. hazard level of about 1E-4) is increased by a factor of more than 100.

However, a new event at one location relevant to the hazard at a site provides new information about the distribution of source terms at that location, as well as about path effects to the site. The Bayesian framework is particularly suited to gradually incorporate such information as it becomes available to constrain the uncertainty range. Basically, one assumes a prior distribution of (spatially correlated) GMPEs, which gets subsequently updated, thus yielding a posterior distribution of hazard curves. We show how this can be easily formulated in terms of a Bayesian non-parametric process, which accounts for both the uncertainty of the source and path terms, as well as their spatial correlation.

1 Introduction

PSHA aims to calculate the expected rate of exceedance for certain ground-motion levels at a particular site. This is done by taking into account all relevant sources (magnitudes and distances) and ground-motions that these sources can induce. There are generally two distinct parts of a PSHA – the first is the seismic source characterization, which aims to describe a joint probability distribution of magnitudes and distances. The second part is the ground-motion characterization, in which the conditional distribution of the ground-motion parameter of interest given magnitude and distance (and possibly other predictor variables) is described. These two parts are combined to calculate the expected rates of exceedances for different ground-motion levels, which is called a hazard curve. To accommodate uncertainties in models and parameters, a logic tree framework (Kulkarni et al. (1984) [8])) is employed, in which different models or parameters occupy different branches of the tree. Weights are assigned to each branch, and the weighted calculations lead to a distribution of hazard curves.

The characterization of the ground-motion distribution for PSHA is usually done via ground-motion prediction equations (GMPEs), which connect the ground-motion parameter of interest with earthquake source, path and site related parameters such as magnitude and distance. Typically, a lognormal distribution for ground motion is assumed. A key parameter in PSHA is the variance of the ground-motion distribution, since it controls the shape of the hazard curve (Bommer and Abrahamson, 2006) [5]. The variance is usually determined using empirical data and applying the ergodic assumption, which means that the distribution of ground motions over time at given site is the same as their spatial distribution over all sites for the same magnitude, distance, and site condition (Anderson and Brune, 1999) [3]. Thus, for the estimation of GMPEs, records from different events and at different sites are

"lumped" together, and a function for the median and the variance is estimated. Traditionally, the variance is separated into a between-event and a within-event part. In recent years, it has been recognized that the variance of the ground-motion distribution can be broken down into many different components (Al-Atik et al., 2010) [2]. In particular, the use of single-station sigma has become standard practice in site-specific PSHA studies (Atkinson, 2006; Rodriguez-Marek, 2011) [4, 11]. This is an example of trading aleatory variability and epistemic uncertainty, as many recordings at one particular site allow one to calculate the repeatable site amplification at that particular site. Hence, the aleatory variance of the ground-motion distribution is reduced as part of the ergodic assumption is dropped.

With the advent of more and more instrumentation, and thus with more recordings, it is possible to estimate repeatable source and path effects. This means that the aleatory variance can be reduced even further, which has important consequences for PSHA results. It is important to remember, however, that epistemic uncertainty and aleatory variability are traded. Hence, one needs to take into account the epistemic uncertainty in repeatable source and path effects in PSHA calculations. This leads to an increased epistemic uncertainty in the resulting hazard curve distribution. However, each new event provides a lot of information, which can be used to reduce this uncertainty. In the following, we show how.

2 Seismic Hazard with and without the Ergodic Assumption

The expected rate of exceedance for ground-motion level A is calculated by

$$\nu(Y > A|\ldots) = \nu_{base} \int_M \int_R P(Y > A|m, r, \ldots) P(m, r, \ldots)\, dm\, dr, \qquad (1)$$

where Y is the ground-motion parameter of interest and $P(Y > A|m, r, \ldots)$ is the conditional distribution of that Y is greater than A, given a certain value of the magnitude $M = m$ and distance $R = r$ and possible other relevant parameters. The exceedance probability can be calculated by

$$P(Y > A|m, r, \ldots) = \int_A^\infty P(Y|m, r, \ldots) dy, \qquad (2)$$

where $P(Y|m, r, \ldots)$ is the probability density function (PDF) of the conditional distribution of Y. If a lognormal distribution is assumed for Y, Equation 2 can be expressed in terms of the cumulative distribution function

(CDF) Φ:

$$P(Y > A|m, r, \ldots) = 1 - \Phi\left(\frac{\log A - \mu(m, r, \ldots)}{\sigma}\right). \quad (3)$$

The PDF for the lognormal distribution is

$$P(Y|m, r, \ldots) = \begin{cases} \frac{e^{-\frac{(\log(y)-\mu)^2}{2\sigma^2}}}{\sqrt{2\pi}\sigma y} & y > 0 \\ 0 & \text{else} \end{cases} \quad (4)$$

where μ and σ are the mean and standard deviation of the associated normal distribution, which are functions of M and R. The variance σ^2 is a measure of aleatory variability, and it is integrated out in equation 2. Thus, it is clear that the value of σ^2 influences the hazard results.

In general, the median μ is a function of magnitude, distance and other parameters, and is estimated based on a GMPE. For an individual recording, the value predicted by the GMPE, μ_{GMPE} needs to be adjusted:

$$\mu = \mu_{GMPE} + \delta_{S2S} + \delta_{P2P} + \delta_{L2L}, \quad (5)$$

where δ_{S2S} is a repeatable site effect, δ_{P2P} is a repeatable path effect, and δ_{L2L} is a repeatable source effect. These terms need to be taken into account when calculating PSHA.

With increasing data, it has been recognized that the aleatory variability can be partitioned (Al-Atik, 2010 [2]; Walling, 2009 [12]), assuming independent site, source and path terms:

$$\sigma^2 = \tau_0^2 + \tau_S^2 + \phi_0^2 + \phi_S^2 + \phi_P^2, \quad (6)$$

where τ_R, ϕ_S and ϕ_P describe repeatable source, site and path effects. In equation 6, only τ_0 and ϕ_0 describe aleatory variability, the other parts are epistemic in nature. Hence, in hazard calculations (equation 2) only the aleatory part of the variance should be used. However, it is important to still include the epistemic uncertainty associated with the repeatable source, site and path effects. These affect the median ground-motion prediction. In general, for a random location, the effects are unknown, but assumed to be distributed with a normal distribution of mean zero and the associated standard distribution.

The sizes of the different varianc components are shown in Table 1, which is reproduced from Lin et al. (2011) [9]. In addition, the sizes of the single-station standard deviation, $\sigma_{SS}^2 = \tau_0^2 + \tau_S^2 + \phi_0^2 + \phi_P^2$, and single-path standard

Table 1: Size of variances, reproduced from Table 5 from Lin et al. (2011) [9]. σ_T is the total standard deviation including all effects, $\sigma_S S$ is the single-station standard deviation, and σ_P is the single-path standard deviation.

Spectral period	τ_S	τ_0	ϕ_{S2S}	ϕ_P	ϕ_0	σ_T	σ_{SS}	σ_P
0.01	0.254	0.247	0.259	0.401	0.230	0.637	0.583	0.337
0.1	0.282	0.273	0.353	0.410	0.238	0.710	0.616	0.363

deviation, $\sigma_P^2 = \tau_0^2 + \phi_0^2$ are tabulated. The use of the single-station station standard deviation has become standard practice in hazard calculations (e.g. Rodriguez-Marek et al., 2011) [11]. It already reduces the variance by a significant amount. The use of the single-path variance is the next step in trading aleatory and epistemic variances.

As an example, we only consider path effects in the following to keep the notation clean. Let Ξ_{ik} denote the random variable associated with the repeatable path effect from a particular location i to a site k. It is distributed according to a normal distribution with mean 0 and standard deviation σ_P, and can take values $\delta_{P2P,ik}$:

$$\Xi_{ik} \sim N(\delta_{P2P,ik}; 0, \phi_P) \tag{7}$$

The distribution of ground motion (cf. equation 4) then becomes

$$P(Y|m, r, \ldots) = \begin{cases} \frac{e^{-\frac{(\log(y)-(\mu+\delta_{P2P,ik}))^2}{2\sigma^2}}}{\sqrt{2\pi}\sigma y} & x > 0 \\ 0 & \text{else} \end{cases} \tag{8}$$

In general, the specific value of $\delta_{P2P,ik}$ is unknown, and hence is associated with epistemic uncertainty. This uncertainty needs to be considered in hazard calculations, e.g. by putting several values on a logic tree, or by integrating over it. In Figure 1, the difference between the ergodic and nonergodic ground-motion distribution is shown schematically.

The epistemic uncertainty associated with the repeatable path effects can be reduced. If the path effect is known, i.e. the value of $\delta_{P2P,ki}$, then one does not need to integrate over its uncertainty. This reduces the uncertainty in the resulting distribution over exceedance probabilities, i.e. over hazard curves. The repeatable path and source effects for one particular location can be estimated if en earthquake occurs at that particular location, and is recorded both at the site and some other stations. There is one unique path effect for each location, so knowing the path effect for one location leads to a reduction in uncertainty for events at this particular location. It has

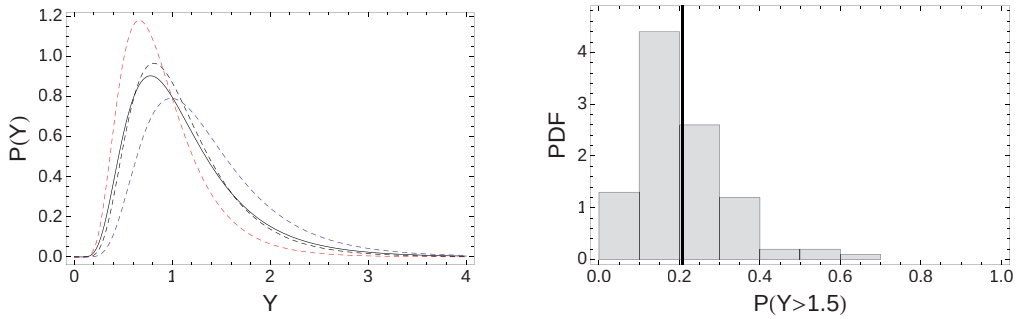

Figure 1: **Left:** Lognormal distribution for the total (ergodic) standard deviation (black line) with median $\mu_0 = 1$, and three sampled lognormal distributions with non-ergodic standard deviations, where the median is $\mu = 1+\delta$, where δ is sampled from a normal distribution. **Right:** Distribution of exceedance probabilities for the lognormal distribution with non-ergodic standard deviation, calculated from 100 samples lognormal distribution. The exceedance probability for the lognormal distribution with ergodic standard deviation is shown as a black line.

been found (e.g. Walling, 2009) [12], however, that path and source effects are spatially correlated. This allows one to learn something about path and source effects in the vicinity of an event with knwon source and path effects.

The spatial correlation of source and path effects is generally modeled by a correlation function that describes the correlation of effects between different locations. In the geostatistical literature, this is known as kriging (Goovaerts, 1997) [6]. In the statistical/machine learning community, this is called a Gaussian process (GP) (Rasmussen and Williams, 2006) [10], which is a Bayesian nonparametric technique.

3 Gaussian Process

A Gaussian process defines a distribution over functions. In the context of repeatable source and path effects, the functions define the values of the effects, dependent on the location. Before seeing any data, the distribution defined by the GP is the prior distribution. A sample function drawn from this distribution is only loosely constrained. After observing some data, the GP prior can be updated in a Bayesian way to obtain the posterior distribution of functions. The posterior distribution allows only functions that are in agreement with the data. A one-dimensional example is shown in Figure 2, where in the left panel GP prior is depicted. The shaded area shows

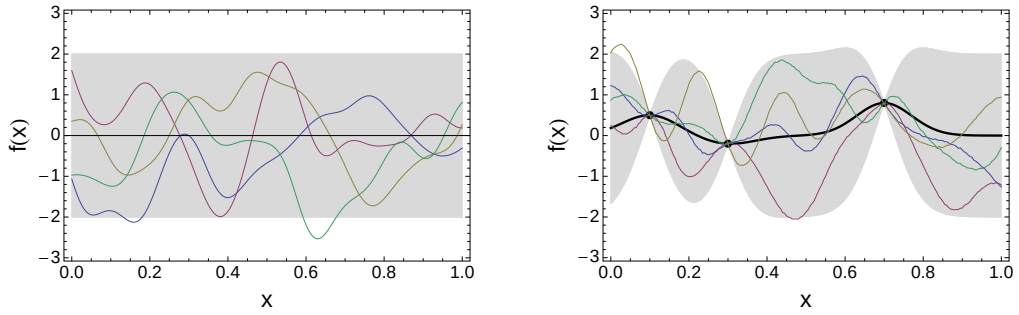

Figure 2: Four functions randomly sampled from a (one-dimensional) zero mean GP (**left**) and posterior (**right**) distribution with covariance function $k(x_i, x_j) = \exp(-100|x_i - x_j|^2)$. The observations in the right plot are marked by a black dot, the posterior mean is the thick black line. The shaded area displays the pointwise 90% confidence interval around the mean.

the pointwise 95% uncertainty, together with four randomly drawn sample functions. The black line is the mean of the prior distribution. The right panel shows the posterior distribution, after observing three (noise free) data points. Now, the uncertainty close to the observed data points is greatly reduced, and the sampled functions go through the obervations. The mean of the posterior GP distribution also changes due to the observations. In the context of source and path effects, the y-axis in Figure 2 is the value of the effect, and the x-axis is the geographical location. The shaded area, showing the uncertainty, is determined by the variance associated with each effect (ϕ_P^2 and τ_S^2). Figure 2 already shows that just a few data points can reduce the uncertainty associated with the repeatable source and path effects.

More formally, a GP defines a distribution on functions $f(\boldsymbol{x})$:

$$f(\boldsymbol{x}) \sim GP(m(\boldsymbol{x}), k(\boldsymbol{x}, \boldsymbol{x}')), \tag{9}$$

which means that the function value at location $\boldsymbol{x}$ is drawn from a GP with mean $m(\boldsymbol{x})$ and covariance function $k(\boldsymbol{x}, \boldsymbol{x}')$. These two fully specify a GP. The covariance function is an important part of the GP, since it encodes all assumptions about how the sampled functions look (smooth, linear, periodic and so on), so it needs to be chosen with care. In the following, we assume $m(\boldsymbol{x}) = 0$, since the repeatable effects are assumed to be a-priori distributed with mean zero.

Sampling function values at locations $\boldsymbol{x}_1, \ldots, \boldsymbol{x}_N$ from a GP is done by calculating the mean values at the input locations, as well as entries of the covariance matrix, $\Sigma_{i,j} = k(\boldsymbol{x}_i, \boldsymbol{x}_j)$. Then, the function values are sampled

from a multivariate normal distribution with the calculated mean and covariance.

3.1 Predictive Distribution

In this section, we describe how one can calculate predictions for a new, previously unseen input $\boldsymbol{x}_\star$, given that some n observations are available. This is done by conditioning on the available data points. Hence, we calculate the conditional distribution of the new data point, given the observations, which ill be denoted by $\mathcal{D} = (\boldsymbol{X}, \boldsymbol{y})$, where $\boldsymbol{X} = \{\boldsymbol{x}_i\}_{i=1}^n$ are the locations at which data is observed and $\boldsymbol{y} = \{y_i\}_{i=1}^n$ are the corresponding observations of the function values (or source/path effects). The predictive mean and variance of the new observation can be calculated by

$$\mu_\star = \boldsymbol{k}_{\boldsymbol{y}\star}^T \boldsymbol{K}_{\boldsymbol{y}}^{-1} \boldsymbol{y} \tag{10}$$

$$\sigma_\star^2 = k_{\star\star} - \boldsymbol{k}_{\boldsymbol{y}\star}^T \boldsymbol{K}_{\boldsymbol{y}}^{-1} \boldsymbol{k}_{\boldsymbol{y}\star} \tag{11}$$

where $\boldsymbol{K}_{\boldsymbol{y}} = k(\boldsymbol{x_i}, \boldsymbol{x_j})_{i,j}$ is the covariance matrix of the observations, $\boldsymbol{k}_{\boldsymbol{y}\star}^T = [k(\boldsymbol{x}_1, \boldsymbol{x}_\star, \ldots, k(\boldsymbol{x}_n, \boldsymbol{x}_\star)]^T$ is a vector containing the covariances between the observations and the new data point, and $k_{\star\star}$ is the auto-covariance. Equations 10 and 11 arise from the multinormal distribution, where one conditions on a subset of the set of variables. The equations have been used to calculate the mean and variance shown in the right panel of Figure 2.

4 PSHA

In this section, we show how one can calculate hazard based on a non-ergodic assumption, and update the resulting hazard curve distribution based on new data. We use a generic situation, but the concept is valid for all situations.

We assume a site-specific PSHA, with a rectangular background zone of dimensions 200 x 200 km. All points inside this zone have the same rate (probability) of generating an earthquake.

The definition of the covariance functions for the repeatable source and path terms follows Walling (2009) [12]. The covariance function for the source terms is a spherical covariance function

$$k(\boldsymbol{x}, \boldsymbol{x}') = \sigma_{sp}^2 (1 - 1.5\text{Min}\left[1, \sqrt{(\boldsymbol{x} - \boldsymbol{x}')L(\boldsymbol{x} - \boldsymbol{x}')}\right] + 0.5\text{Min}\left[1, \sqrt{(\boldsymbol{x} - \boldsymbol{x}')L(\boldsymbol{x} - \boldsymbol{x}')}\right]^3), \tag{12}$$

where σ_{sp}^2 is the variance of the spatial correlation (τ_S or ϕ_P^2 as in 1) and $L = \begin{pmatrix} 1/l^2 & 0 \\ 0 & 1/l^2 \end{pmatrix}$ is a matrix describing the extent of the spatial correlation. The parameter l is a characteristic length scale after which the correlation is zero. Theoretically, the length scales could differ in x and y-direction, but in this application it is reasonable to assume that there is no preference of correlation in either direction. The covariance function of eq. 12 models the assumption that sources that are near each other (have small distance $|\boldsymbol{x}-\boldsymbol{x}'|$) are strongly correlated, whereas the correlation decreases with increasing distance between the sources.

The covariance function for the systematic, repeatable path effects needs to accommodate two assumptions. On the one hand, the path effects for paths from sources that are close should be strongly correlated. This can be modeled with the same covariance function as for the source effects (eq. 12). On the other hand, the correlation should depend on the direction, or the difference in direction between sources. This is illustrated in Figure 3, where the two blue sources have the same distance from each other than the two red sources. However, it is obvious that path effects from the red sources to the site should be strongly correlated, as the seismic waves travel through similar medium, whereas the paths from the blue sources to the site do not overlap at all. Hence, the covariance function for the repeatable path effects needs to include a term that depends on the difference in direction, which can be parameterized by the azimuth. The covariance function for the repeatable path terms is thus

$$\begin{aligned} k(\boldsymbol{x}, \boldsymbol{x}') = \sigma_p^2 (1 - 1.5\text{Min}\left[1, \sqrt{(\boldsymbol{x}-\boldsymbol{x}')L(\boldsymbol{x}-\boldsymbol{x}')}\right] \\ + 0.5\text{Min}\left[1, \sqrt{(\boldsymbol{x}-\boldsymbol{x}')L(\boldsymbol{x}-\boldsymbol{x}')}\right]^3) \\ \times \exp\left[-\rho \sin^2\left(0.5(\alpha - \alpha')\right)\right], \end{aligned} \tag{13}$$

where α denotes the azimuth between the site and the location $\boldsymbol{x}$. The first part of eq. 13 is the same spherical covariance function as eq. 12. The second part is a modification that depends on the difference in azimuths between paths. It is a periodic covariance function that takes its maximum when the difference in azimuth is zero or 2π, and reaches its minimum for $|\alpha - \alpha'| = \pi$.

Given a covariance function, it is possible to sample the repeatable effects for each location. This is done by calculating the covariances between the points on the map, and then sampling from a multinormal distribution with mean zero and the calculated covariance. Two examples of such a map is shown in Figure 4. These are two realizations of the epistemic uncertainty

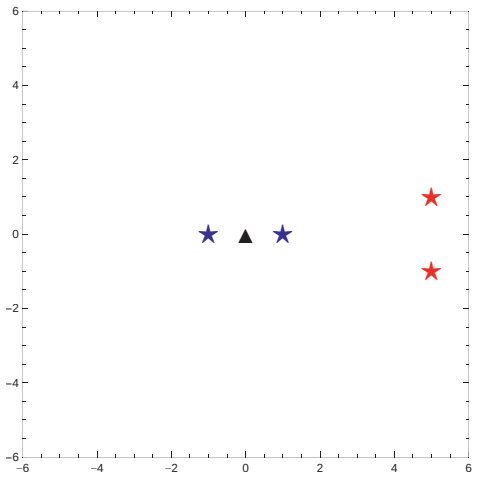

Figure 3: Schematic example of how the spatial correlation of path effects should depend both on the distance between the sources, but also on the distance in azimuth between them.

associated with the repeatable path effects, without any observations. To fully capture this uncertainty for PSHA, one needs to sample many realizations and calculate hazard curves for each of them. It is also important to remember that the effects shown in the maps of Figure 4 are epistemic in nature – they are the repeatable path effects. For hazard calculations, one needs to add the aleatory ground-motion variability. This is shown in the left part of Figure 5, which shows the same underlying map of repeatable path effects as the left part of Figure 4, but with sampled (uncorrelated) aleatory variability added. By contrast, the right part of Figure 5 shows a map of source effects that neglect the spatial correlation of the effects. The overall variance is the same in both cases.

The calculated hazard using repeatable source and path effects is shown in Figure 6. The calculations are done with one GMPE, the model of Akkar et al. (2014) [1]. For the source model, a doubly-truncated Gutenberg-Richter distribution is assumed, with $M_{min} = 5$ and $M_{max} = 7.5$, and a b-value of $b = 1$. To calculate the hazard, 100 realizations of repeatable source and path effects each are sampled. For each of the sampled maps, a separate hazard curve is calculated, which are shown as gray lines in Figure 6. The mean of of the hazard curves is plotted as a black line. In addition, the hazard curve without consideration of the spatial correlation is plotted as a red dashed curve. As one can see, the mean of the hazard curves is very close, while there is large uncertainty associated with the hazard curves in-

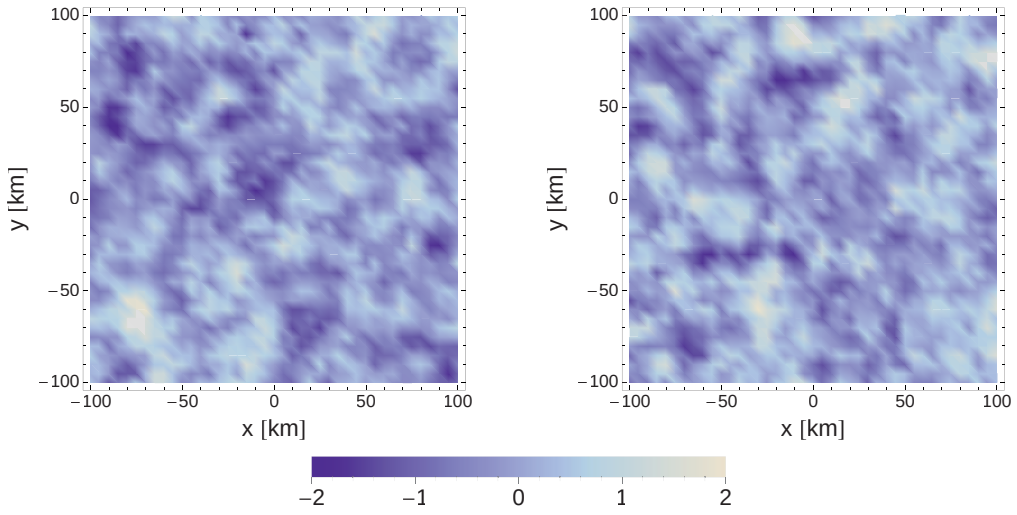

Figure 4: Example maps of spatially correlated repeatable path effects.

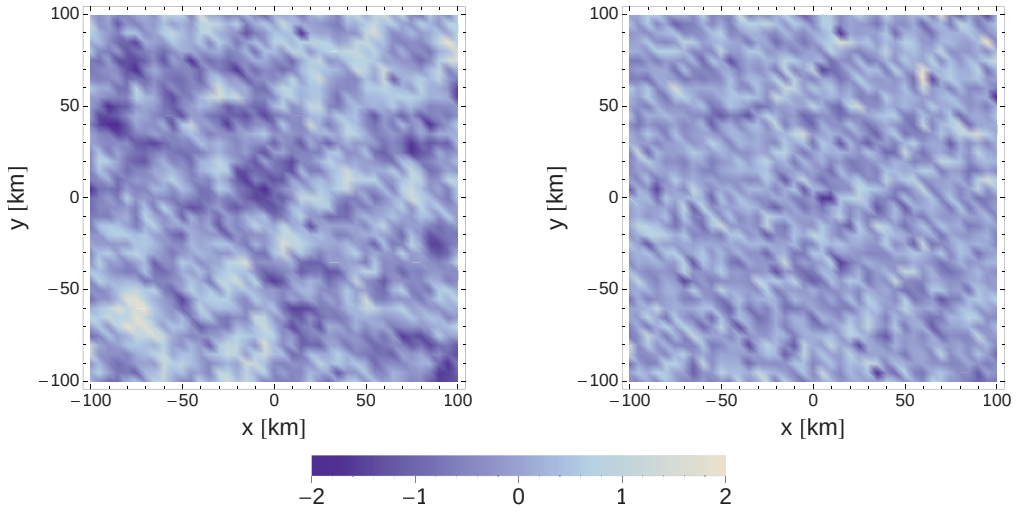

Figure 5: Left: Map of spatially correlated path effects, with added (uncorrelated) aleatory variability. Right: Map of total, uncorrelated variability.

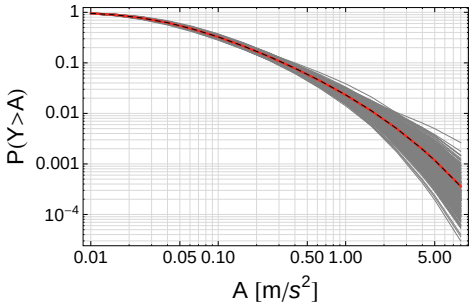

Figure 6: Exceedance probabilities, calculated for repetitive sampling of spatially correlated source and path effects (gray lines). The black line is the mean of the gray lines, while the red line is the hazard calcuclated without taking spatial correlations into account (ergodic assumption).

cluding the spatial correlation. Hence, in the absence of any information, the non-ergodic and ergodic PSHA calculations yield very similar results for the mean hazard, but the uncertainty associated with the former should not be neglected. In the following, we show how the uncertainty decreases with adding new information.

4.1 Hazard in light of new information

We have seen in section 3.1 how it is possible to calculate a posterior predictive distribution in light of a new data point. The same concept and calculations can be used to update the hazard curve distribution, once an earthquake has occurred close to the site. As an example, let us assume that there have been four events close to the site for which the hazard was calculated in the previous section. We further assume that the source and path terms of these events have been estimated. Then, we can calculate the mean of both the source terms and the path terms, given the observations (cf. eq. 10). The posterior mean and (pointwise) variance are shown in Figure 7 for path effects, after four observations. The prior mean was zero for the whole map, while the prior variance was 0.17. Corresponding maps can be calculated for the source effects. As one can see, in the vicinity of the observations variance decreases – this means that the range of possible source effects decreases. It does not decrease to zero, since the effect can only estimated from data to a certain degree () At the same time, the mean around the observations is close to the observational value. Both of these effects reflect in the calculation of the posterior hazard – the mean hazard

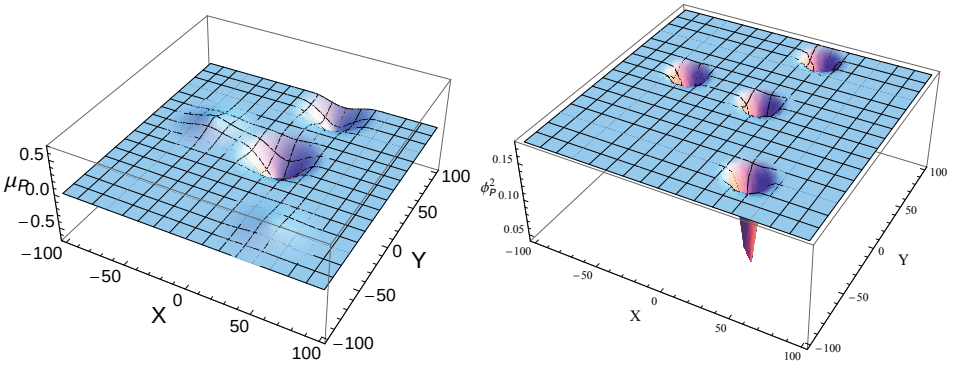

Figure 7: Posterior mean and uncertainty of the repeatable path effects, after three observations.

changes, but its uncertainty range decreases as well. This is shown in Figure 8, where the prior and posterior distributions of exceedane probabilities are compared. In the right part of Figure 8, we compare the difference in the range of exceedance probabilities for three different cases: inclusion of spatial correlations for both path and source effects, only path effects and only source effects. AS one can see, the reduction that is observed is largely due to the inclusion of spatially correlated path effects.

5 Discussion

We have seen how letting go of the ergodic assumptions leads to a large increase in the epistemic uncertainty of the hazard curve distribution, even though the mean hazard remains relatively unchanged. However, we have seen in a simple example calculation that just a few obserevations can reduce this uncertainty by a great amount. The amount of reduction, depends on the actual observations, and their location. There are some assumptions that are made when updating the hazard, and calculating the repeatable source and path effects. One assumption is that the repeatable effects are independent of the predictor variables. This is an important assumption, as it makes it possible to estimate the effects from small events. This is especially important for path effects – for the source effects, one can argue that these are uncorrelated between small and large effects. In this case, one can introduce a correlation that additionally depends on the magnitudes (cf. Hermkes et al. (2014) [7]). This makes it practical to use the approach to reduce uncertainty. However, there are practical considerations to consider. To estimate the source effect of an event, one needs to have several recordings

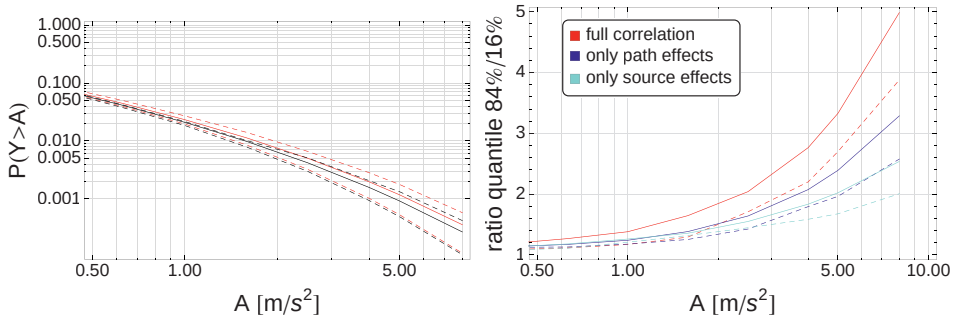

Figure 8: **Left:** (Prior) distribution of exceedance probabilities (red), calculated without observations (red lines); Posterior distribution of exceedance probabilities after four observations (black lines). The mean hazard is plotted as a solid line, the median hazard curve as a dashed line, and the 16% and 84% quantiles are plotted as dotted lines. **Right:** Ratios between the 84% and 16% quantiles of the exceedance probability distribution, without (solid lines) and with (dashed lines) observations.

of this event. Then, the source effect can be estimated from the residuals of the recordings. Therefore, it is important to have instrumentation in the vicinity of the site. To properly partition the residuals of an event into its soure, site and patheffects, however, just instruments at the site are not sufficient – one needs many isntruments to reliably estimate the source terms. This requires the deployment of many instruments, but it has great potential to reduce uncertainty in hazard calculations.

References

[1] S. Akkar, M. A. Sandkkaya, and J. J. Bommer. Empirical ground-motion models for point- and extended-source crustal earthquake scenarios in Europe and the Middle East. *Bulletin of Earthquake Engineering*, 12(1):359–387, May 2014.

[2] L. Al-Atik, N. Abrahamson, J. J. Bommer, F. Scherbaum, F. Cotton, and N. Kuehn. The Variability of Ground-Motion Prediction Models and Its Components. *Seismological Research Letters*, 81(5):794–801, August 2010.

[3] J. G. Anderson and J. N. Brune. Probabilistic seismic hazard analysis without the ergotic assumption. *Seismological research letters*, 70(1):19–28, 1999.

[4] G. M. Atkinson. Single-station sigma. *Bulletin of the Seismological Society of America*, 96(2):446–455, 2006.

[5] J. J. Bommer and N. A. Abrahamson. Why Do Modern Probabilistic Seismic-Hazard Analyses Often Lead to Increased Hazard Estimates? *Bulletin of the Seismological Society of America*, 96(6):1967–1977, 2006.

[6] P. Goovaerts. *Geostatistics for Natural Resources Evaluation.* Oxford University Press, 1997.

[7] M. Hermkes, N. M. Kuehn, and C. Riggelsen. Simultaneous quantification of epistemic and aleatory uncertainty in GMPEs using Gaussian process regression. *Bulletin of Earthquake Engineering*, 12(1):449–466, October 2014.

[8] R.B. Kulkarni, R.R. Youngs, and K.J. Coppersmith. Assessment of Confidence Intervals for Results of Seismic Hazard Analysis. In *Conf. 8th World Conf. on Earthquake Engineering*, pages 263–270, 1984.

[9] P.-S. Lin, B. Chiou, N. Abrahamson, M. Walling, C.-T. Lee, and C.-T. Cheng. Repeatable Source, Site, and Path Effects on the Standard Deviation for Empirical Ground-Motion Prediction Models. *Bulletin of the Seismological Society of America*, 101(5):2281–2295, September 2011.

[10] C. E. Rasmussen and C. K. I. Williams. *Gaussian Processes for Machine Learning.* MIT Press, Cambridge, April 2006.

[11] A. Rodriguez-Marek, G. A. Montalva, F. Cotton, and F. Bonilla. Analysis of Single-Station Standard Deviation Using the KiK-net Data. *Bulletin of the Seismological Society of America*, 101(3):1242–1258, May 2011.

[12] Melanie Anne Walling. *Non-Ergodic Probabilistic Seismic Hazard Analysis and Spatial Simulation of Variation in Ground Motion.* Phd-thesis, Berkeley, 2009.

CSNI Workshop on "*Testing PSHA Results and Benefit of Bayesian Techniques for Seismic Hazard Assessment*"
4-6 February 2015, Eucentre Foundation, Pavia, Italy

Some Steps Forward in Confronting Probabilistic Seismic Hazard with Observations in Italy

Laura Peruzza
OGS (Istituto Nazionale di Oceanografia e di Geofisica Sperimentale), Italy,
lperuzza@inogs.it

Agostino Goretti
Civil Protection Department, Seismic and Volcanic Risk Office, Italy,
agostino.goretti@protezionecivile.it

Francesca Pacor
INGV-Milano, Italy, francesca.pacor@ingv.it

Task 2 and Task 6 Working Groups[1]
S2-2014 DOC-INGV Project, https://sites.google.com/site/ingvdpc2014progettos2/home

SUMMARY

A scoring test on PSHA in Italy has been realized in the frame of the S2-2012 Project (https://sites.google.com/site/ingvdpc2012progettos2/home) "Constraining Observations into Seismic Hazard", first annual phase of researches funded in the 2012-2021 Agreement between the National Civil Defence Department (DPC) and National Institute of Geophysics and Volcanology (INGV). The scoring test has pinpointed the need of having i) high quality site response characterizations for the accelerometric stations, ii) a careful check on completeness of recordings, not fully accomplished by the information available in 2013 in the ITACA archive (http://itaca.mi.ingv.it), and iii) in depth understanding of some methodological aspects of scoring. The second (S2-2014, https://sites.google.com/site/ingvdpc2014progettos2/home) and

[1] The S2-2014 Task 2 and Task 6 Working Groups are formed by:
Research Unit RU1_M (Mucciarelli, Gallipoli leaders) OGS and CNR-IMAA, Trieste and Potenza
RU1_B (Barnaba), OGS, Udine
RU1_L (Laurenzano), OGS, Trieste
RU2_L (Luzi), INGV, Milano
RU4 (Barani), University of Genoa, Genova
RU5 (Albarello), University of Siena, Siena
RU7 (Bazzurro), Eucentre, Pavia
RU8 (Castellaro), University of Bologna, Bologna

ultimate annual phase of the project accomplishes these needs, with the coordinated work of several research groups. We will present the conceptual flowchart of analyses, the new data gathered, some thoughts developed on the validation elaborations performed so far; we suggest using Italy as test case for validation procedures of PSHA.

Keywords: *Probabilistic seismic hazard analysis, scoring test, Italy.*

1. Introduction

Project S2-2014 "Constraining Observations into Seismic Hazard" is the second and last year of projects funded in the frame of the 2012-2021 Agreement between DPC and INGV. It concerns the mid-long term Seismic Hazard Assessment in Italy, focusing on two priority areas, namely the Po Plain and peninsular Southern Italy. The planning and expected activities for this second year (https://sites.google.com/site/ingvdpc2014progettos2/) are the prosecution of the S2-2012 project, which results are available for the whole scientific community on the project's website https://sites.google.com/site/ingvdpc2012progettos2/. The 2014 project is organized into 8 main Tasks, developed by activities proposals of 8 Research Units; Task 2 is focused on high quality instrumental observations and site characterization, Task 6 is devoted to Validation and ranking of PSHA; they operate in mutual sinergy.
The first months of the S2-2014 Project permitted a global revision and the submission of the results of validation and ranking obtained in 2012-13. An HQ characterization of site stations response on the subset of ITACA stations with long recording activity is expected by the on-going project's activities (Task 2, 4), and some extensions of validation using macroseismic data are under debate, after the release of the tools to aggregate independent historical and instrumental databases (Task 3). In addition, an intense methodological discussion started among the Task 6 participants. We track here some main aspects we have been facing till now.

2. Increase and quality control of instrumental observations

Previous analyses (Albarello et al., 2014; Albarello and Peruzza, 2015) addressed the issue of improving the quality of information available at the accelerometric recording stations, as a key element in any validation procedures of PSH results.
Three activities have been planned by Task 2 of S2-2014 Project:

1) characterization of accelerometric stations through in situ measurements;
2) collection and analysis of strong-motion data recorded by coupled accelerometers at the surface and in boreholes;
3) assessment of ground motion variability at selected sites and investigation on the physical causes (e.g. geology, geophysics parameters) using available seismic data and information from microzonation studies.

The organization of a workshop (held at INGV in Milano on 29 May 2014, in which researchers and experts shared information on the on-going initiatives, promoting cooperation among different projects, minutes at https://sites.google.com/site/ingvdpc2014progettos2/documents) was the first step we did. Up to now, a close collaboration between the S2-Project has been established with:

- the GEORAN project, carried out by DPC together with the CNR-IGAG, to enlarge the number of investigated stations and to define the standards for archiving and sharing the collected data;

- the 2014 ReLUIS research program, to evaluate the waveforms at bedrock and to calculate seismic hazard at specific sites;
- the DPC activities, relative to the noise measurements at the RAN stations, to compute the horizontal and vertical spectral ration and identify the fundamental frequencies.

Side by side, ITACA (http://itaca.mi.ingv.it) database has been maintained and upgraded; the new release (v. 2.0), available since Feb 2014, accounts for accelerograms till Jan 2014. A short description of old used for PSHA testing and new data now available is given in the next section.

2.1 Dataset of accelerometric recordings versus predicted shaking

At the beginning of the Project S2-2012, the database of accelerometric data available for Italy was ITACA 1.0 (Luzi et al., 2008; Pacor et al., 2011). Several elaborations have been based on this dataset, and Ground Motion Prediction equations benefitted of these data (e.g. ITA10, Bindi et al., 2011). ITACA 1.0 collected data from the late '70ies till the early 00'ies; it does not account for relevant earthquakes recently occurred in Italy, such as the Emilia 2012 seismic sequence (Luzi et al., 2013) in Northern Italy and several aftershocks of L'Aquila, 2009 sequence (Ameri et al., 2009). During the S2-2012 an upgrade of ITACA (v. 1.1) has been released; then, in Feb 2014, a new release (ITACA 2.0) benefits not only of an expanded dataset, but also of a renovated architecture, checks and post-processing of raw data. The new version of ITACA contains more than 15.000 strong motion data and the relevant metadata, acquired by the major Italian networks till to 2013. The bulk of data comes from the National Accelerometric Network (RAN), operated by DPC, and, from the 2006, by the Italian Seismic Network (RSN) operated by INGV. ITACA 2.0 includes 7580 three-component waveforms relative to 1214 events with magnitude M>3.0 recorded in the period 1972-2013. More than 900 recording stations are present in ITACA, providing at least 1 records, but only for a few percentage of these is available a complete site characterization, including a measurement of the V_s profile (about 12%).

The validation test performed on PSHA by the S2-2012 Project have used a subset of about 70 stations, selected among the ones with a long life of continuous recording (Pacor et al., 2013); the "ON" status for a station, in the early years of the Italian accelerometric network, is documented only by informal stations reports, as the equipments have been operating in sporadic mode, based on a triggering threshold. Most of the first analogic accelerometric stations went progressively out of work in 2004-2005, and have been replaced by digital instruments, especially after the L'Aquila earthquakes.

Figure 1a shows the maximum value of Peak Ground Acceleration (PGA) observed at the previously cited subset of stations (used for validation purposes), accordingly to the initial and final releases of ITACA, and focusing on the testing period (25 years of continuous recording, from 1979 till 2004) used in the preliminary scoring test (Albarello et al., 2014). Reference PGA values of the actual Italian regulation (MPS04, 2004) are plotted too; note that they refer to reference site condition (rock, or soil type A), and to a return period of 475 years (10% of exceedance in 50 years). Note also in Figure 1b the bars that represent the global duration of recordings (interruptions are accounted for) for the same sites; about 70 stations, on 967 actually stored in ITACA, have a lifetime from 30 to 40 years, time interval not too far form the usual reference times used in PSHA.

The last decade of data contributes significantly to the maximum observed PGA value at many stations, and only 1 station (RNC, in Tuscany; BRM refer to a double siting) has values lower than 0.1 g, the commonly used triggering threshold of analogic accelerometers of the XX century.

The updated dataset of recordings, given not only in terms of PGA, will be the next benchmark for the upgrade of the scoring test, planned in the frame of S2-2014 Project activities.

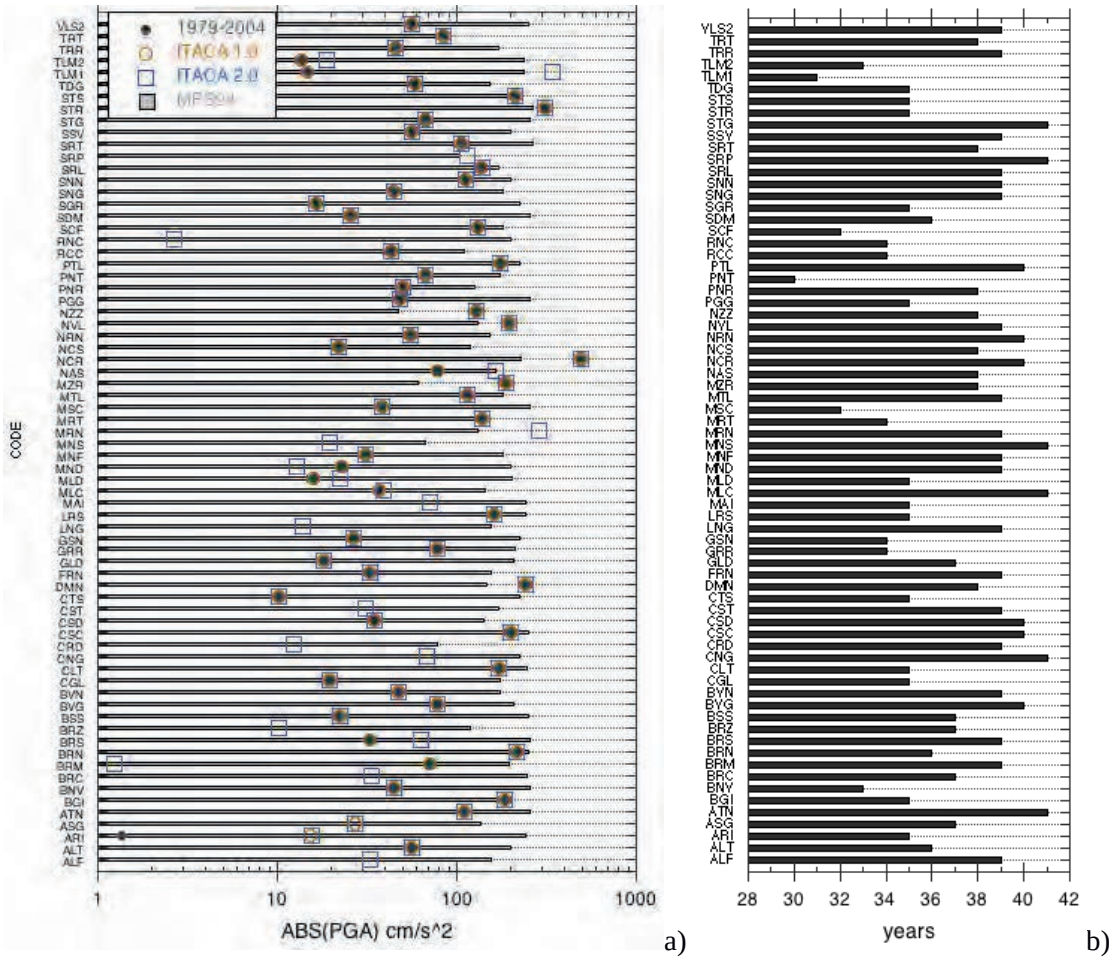

Figure 1: Subset of accelerometric station with a long lifetime of recordings: a) maximum observed PGA; b) total duration of activity.

2.2 Site characterization

The activity of the characterization of accelerometric stations through in situ measurements consists in the update of the stations metadata in the Italian strong database ITACA 2.0, with additional geological and geophysical information, which are fundamental for the site characterization. A selection among the recording stations operating during the last 40 years, identified among the one listed in Figure 1, has been made to evaluate the stations that should be characterized with the highest priority.

The five RUs (RU1 OGS; RU2 INGV-MI; RU4 UNIGE; RU5 UNISI; RU8 UNIBO) involved in this activity have been in charge of the evaluation of the shear wave velocity profile with techniques based on passive measurements (active and/or passive such us ESAC-FK, MASW) and of the collection of geophysical and geological data.

The geophysical measurements have been carried out during summer 2014 and a meeting has been held in Milan on 14 October 2014, and in Bologna on 3 November, to share the results of the measurement campaigns. A web site has been created (http://dyna.mi.ingv.it/sitechar, password protected) to upload all documents related to the field survey (including binary files such as photos, maps, and single station microtremor measurements), to homogenize the information and reduce the manual interaction for the population of the ITACA database.

Table 1 lists the stations that have been investigated by the various teams, and a synthetic classification of results obtained (given in terms of EC8 classes). Figure 2 shows also how original classes are reassigned, after the field investigation.

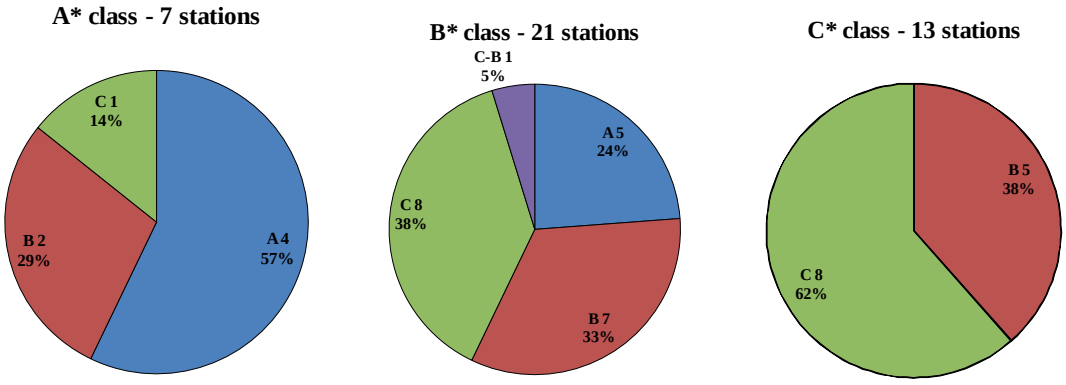

Figure 2: Distribution of EC8 soil categories obtained after the share wave profile measurements and the assignment of the Vs30 value, for the 41 selected sites initially classified as EC8-soil type classes based on large-scale geological mapping.

Notably 12 on 41 stations are on worse site conditions than expected (marked in red, in the last column of Tab. 1) while 10 on 41 are on safer soil type (green). Thus, about 50% of site-specific conditions does not correspond to the initial assignment.
These numbers are very critical if valid for other stations too, as most of the post-processing done on accelerometric recordings, done by assuming that the site classification is realistic, may be no more valid. Future investigation will give additional elements for the de-convolution of site-specific observations to standard site condition (rock, or soil type A) used in the PSHA.

3. Implications of ground motion spatial correlation on seismic hazard estimate validation

One of the aims of the S2-2012 project has been to develop and implement a methodology for the validation of probabilistic seismic hazard analysis in Italy. The methodology is based on the comparison between expected and recorded strong motion parameters in accelerometric stations that have been active for at least 30 years. The same issue of seismic hazard validation is also addressed in the second year of the S2 project in order to better develop the methodology and to make use of more accurate data.
In this context, a specific focus is devoted to the implications of the spatial correlation of the ground motion intensity parameters in different stations. In previous studies these parameters, such as PGA in the various stations, were considered as independent variables. With this assumption, the likelihood of a set of maximum values of the recorded parameters in the various stations is given by the product of the individual likelihoods.
However, when considering spatially extended systems, different sources of dependence must be considered and analysed. A first type of dependency is related to ground motion prediction equations (GMPEs) that provide the probability of exceeding a given parameter of the ground motion given a seismic event at a certain distance from the site. They provide therefore a conditional probability (upon the event) expressed, in case of multiple sites affected by the same earthquake, by a multivariate distribution with a certain degree of dependence between variables, according to the model adopted.

Table 1. List of the stations investigated during the S2-2014 project, with updated site class.

STATION CODE	RESEARCH UNIT	STATION NAME	LONG	LAT	ELEV	EC8 class geologic	$V_{S,30}$ [m/s]	EC8 update
BRC	OGS	BARCIS	12.552	46.186	453	A*	860	**A**
CRD	IMAA-CNR	CORTINA DAMPEZZO	12.118	46.525	1550	A*	880	**A**
GRR	OGS	GIARRE	15.163	37.726	240	A*	>800	**A**
MLC	OGS	MALCESINE	10.853	45.813	77	A*	580	**B**
MLD	UNIBO	MELDOLA	12.071	44.118	126	A*	230-270	**C**
NCS	UNIGE	NICOSIA	14.400	37.751	780	A*	360	**B**
SRT	UNISI	SORTINO	15.030	37.163	445	A*	>800	**A**
ARI	OGS	ARIANO IRPINO	15.091	41.153	750	B*	384	**B**
ASG	OGS	ASIAGO (ROANA)	11.474	45.856	974	B*	960	**A**
BRM	IMAA-CNR	BRASIMONE (CAMUGNANO)	11.118	44.129	842	B*	410	**B**
BRZ	UNISI	BERSEZIO	6.970	44.381	1590	B*	1103	**A**
CGL	UNISI	CAGLI	12.629	43.535	277	B*	>800	**A**
CNG	INGVMI	CONEGLIANO 5	12.288	45.883	63	B*	220	**C**
CRN	OGS	CROTONE (MONTEDISON)	17.111	39.078	60	B*	295	**C**
CSC	UNIGE	CASCIA	13.013	42.719	677	B*	>800	**A**
CSD	UNIBO	CASTEL VISCARDO	12.004	42.753	488	B*	480	**B**
FRN	UNISI	FORNOVO	10.108	44.686	275	B*	310-360	**C**
GLD	CNR-IGAG	GILDONE	14.757	41.510	755	B*	470	**B**
LRS	IMAA-CNR	LAURIA	15.835	40.046	425	B*	1010	**A**
NAS	INGVMI	NASO	14.786	38.119	470	B*	310	**C**
NZZ	IMAA-CNR	NIZZA MONFERRATO	8.357	44.782	165	B*	328	**C**
PGL	OGS	PEGLIO	12.498	43.696	465	B*	330	**C**
PNN	OGS	PENNABILLI	12.261	43.817	525	B*	340-380	**C-B**
SGR	UNIBO	S. GIORGIO LA MOLARA	14.926	41.272	635	B*	701	**B**
SNG	OGS	SENIGALLIA	13.227	43.685	100	B*	260	**C**
SRL	UNISI	SIROLO	13.619	43.517	81	B*	270	**C**
STS	UNIBO	S. SOFIA	11.905	43.942	268	B*	460	**B**
TDG	UNIBO	TORRE DEL GRECO	14.383	40.797	178	B*	435	**B**
ALF	UNIBO	ALFONSINE	12.033	44.502	6	C*	240	**C**
CST	UNIGE	CASTELFRANCO 5	11.902	45.659	42	C*	180-360	**B**
DMN	UNISI	DEMONTE	7.271	44.315	770	C*	514	**B**
GSN	UNIBO	GIOIA SANNITICA	14.446	41.302	275	C*	456	**B**
LNG	CNR-IGAG	LANGHIRANO (LESIGNANO BAGNI)	10.313	44.656	207	C*	180-360	**C**
MAI	OGS	MAIANO	13.070	46.185	164	C*	200	**C**
MNS	IMAA-CNR	MONSELICE	11.723	45.253	5	C*	190	**C**
MTL	UNISI	MATELICA	13.008	43.249	365	C*	580	**B**
MZR	IMAA-CNR	MAZARA DEL VALLO	12.611	37.653	17	C*	520	**B**
PNT	UNISI	PONTECORVO	13.683	41.499	115	C*	180-360	**C**
RCC	UNISI	ROCCAMONFINA	13.980	41.288	613	C*	242	**C**
SRP	INGVMI	SORBOLO (PEZZANI)	10.447	44.848	32	C*		**C**
VLS2	CNR-IGAG	VILLA SAN GIOVANNI - 1	15.647	38.218	144	C*	315	**C**

In the early relationships (Sabetta-Pugliese, 1987), the error associated with the ground motion estimate at a site was considered to be independent of that in other sites. The only source of error is therefore the intra-event (within-event) variance σ_{tot}^2. New generations of GMPEs (Bindi et al, 2011) provide an inter-event (between-event) variance, τ^2, and an intra-event (within-event) variance, σ^2. The first one is common to all sites suffering from the same event, the second one is independent between sites. In this case, the ground motion generated by an earthquake at two sites has total variance $\sigma^2+\tau^2$ and correlation $\rho_\tau=\tau^2/(\sigma^2+\tau^2)$.
A further source of dependence is given by the possible correlation of the intra-event error term with the distance between two sites. In this case a correlation, $\rho_D=\rho(D)$, decreasing with the distance, D, between stations, is usually assumed. By combining the two aspects, the correlation between the seismic intensity parameters at the two sites is $\rho=\rho_\tau+(1-\rho_\tau)\rho_D$. This correlation implies a dependence of the ground motion parameters caused by the same event at different sites. Therefore when performing seismic hazard assessment, the ground motion parameters multivariate joint distribution given by GMPEs at various sites give rise to joint rates of occurrence, which in turn, when associated to an occurrence model, such as the Poissonian one, leads to a multivariate distribution of the maximum intensity of the ground motion parameters at different sites.
But even considering the only intra-event error term in GMPEs, that is even considering uncorrelated ground motions parameters given an event at a certain distance from sites, joint rates of occurrence arise as the same earthquake is felt at different sites.
It is than obvious that the dependence of the ground motion maximum intensity in different stations depends on the distance between stations and on the intensity levels considered in relation to the release of energy in the seismogenetic zone. It also depends on the exposure time for which the hazard model it is intended to be validated. Finally it is noted that, in relation to the actual arrangement of the accelerometric stations on the territory, even very distant stations may in some way be correlated through stations placed between them, if not too far apart.
From the practical point of view, neglecting this dependence when validating hazard models, involves double counting some observations because, intuitively, joint occurrence are not to be considered. However, from a computational point of view the evaluation of joint rates give rise to a combinatorial analysis, making the direct approach not feasible for more than two or three stations.
In this paper we want to explore the above issues in order to assess the influence and the implications of the spatial correlation of the maximum intensity of ground motion in the validation of seismic hazard models. The proposed approach is analytical for a small number of stations and then moves to Monte Carlo simulations and copulas for a larger number of stations.

3.1 Likelihood in case of independent and dependent hazard

In the case of single station and Poisson model, the hazard is given by the well-known relationship:

$$h(a) = \Pr(A > a \mid T) = 1 - e^{\lambda(a)T}$$

where a is the maximum soil motion parameter, T is the exposure time and $\lambda(a)$ is the annual exceedance frequency of a, given by:

$$\lambda(a) = \sum_z \nu_z \iint_{M,R} \Pr(A > a \mid M, R)\, f_M\, f_R\, dm dr$$

The hazard curve, h(a), gives the complementary probability distribution function of the maximum expected ground acceleration at the site, CCDF(a). The derivative of the distribution function, CDF(a)=1-CCDF(a), provides the probability density function of the maximum ground acceleration at the site:

$$f_A = -\frac{\partial h(a)}{\partial a} = -Te^{-\lambda(a)T}\frac{\partial \lambda(a)}{\partial a}$$

When two stations, S_1 e S_2, are considered, a_1 and a_2 will be the expected maximum ground accelerations in the stations. The joint hazard is defined as:

$$h(a_1, a_2) = \Pr(A_1 > a_1 \cap A_2 > a_2 \mid T)$$

If a_1 and a_2 are independent, and T is the same at both stations, one gets:

$$\Pr(A_1 < a_1 \cap A_2 < a_2 \mid T) = \Pr(A_1 < a_1 \mid T)(A_2 < a_2 \mid T) = e^{-\lambda_1(a_1)T}e^{-\lambda_1(a_1)T} = e^{-[\lambda_1(a_1)+\lambda_2(a_2)]T}$$

From the previous equations it comes that the joint process of a_1 in S_1 and a_2 in S_2 is a Poisson process with rate given by the sum of the individual rates. The joint density distribution of a_1 and a_2, the likelihood of the model, is simply given by:

$$f_{A_1,A_2} = \frac{\partial^2}{\partial a_1 \partial a_2}\Pr(A_1 < a_1 \cap A_2 < a_2 \mid T) = \left[-Te^{-\lambda_1(a_1)T}\frac{\partial \lambda_1(a_1)}{\partial a_1}\right]\left[-Te^{-\lambda_2(a_2)T}\frac{\partial \lambda_2(a_2)}{\partial a_2}\right] = f_{A_1} f_{A_2}$$

In the general case of two dependent stations, the joint annual frequencies of exceedance are given by:

$$\lambda(a_1, a_2) = \sum\nolimits_z \nu_z \iiint_{M,X,Y} \Pr(A_1 > a_1 \mid M, R_1 \cap A_2 > a_2 \mid M, R_2)\, f_M\, f_{XY}\, dm dx dy$$

and they can be set in a 2D matrix format. Note that even in the case of independent GMPEs

$$\Pr(A_1 > a_1 \mid M, R_1 \cap A_2 > a_2 \mid M, R_2) = \Pr(A_1 > a_1 \mid M, R_1)\Pr(A_2 > a_2 \mid M, R_2)$$

the rates of exceedance are dependent as the magnitude of any event, M, is common to both stations.

The distribution of a joint bivariate Poisson process is given by:

$$\Pr(X => x, Y = y) = e^{-(\theta_1+\theta_2+\theta_o)}\frac{\theta_1^x}{x!}\frac{\theta_2^y}{y!}\sum_{i=0}^{\min(x,y)}\binom{x}{i}\binom{y}{i}i!\left(\frac{\theta_o}{\theta_1\theta_2}\right)^i$$

When X is the number of occurrence of the first variable, Y the number of occurrence of the second variable, $\theta_1+\theta_o$ the mean number of events of the first variable, $\theta_2+\theta_o$ the mean number of events of the second variable, θ_o the mean number of joint events. In our case we have $\lambda_1 T=\lambda(a_1)=\theta_1+\theta_o$, $\lambda_2 T=\lambda(a_2)=\theta_2+\theta_o$, $\lambda_{12} T=\lambda(a_1,a_2)=\theta_o$ and hence $\theta_1+\theta_2+\theta_o=(\lambda_1+\lambda_2-\lambda_{12})T$. The cumulative distribution function of a_1 and a_2 in T, is given by:

$$CDF(a_1, a_2 \mid T) = \Pr(A_1 < a_1 \cap A_2 < a_2 \mid T) = \Pr(N_1 = 0 \cap N_2 = 0 \mid T) = e^{-(\lambda_1+\lambda_2-\lambda_{12})T}$$

where N_1 and N_2 are the number of events with ground acceleration greater then a_1 in S_1 and a_2 in S_2. With respect to the case of two independent stations, it is easy to see how the joint rates, λ_{12}, are deducted from the sum of the rates, $\lambda_1+\lambda_2$. If a_1 and a_2 can be assumed bivariate Poisson, the joint density distribution of a_1 and a_2 (the likelihood of the model) is again obtained differentiating the CDF:

$$f_{A_1,A_2} = T^2 e^{-[\lambda_1(a_1)+\lambda_2(a_2)-\lambda_{12}(a_1,a_2)]T}\left[\frac{\partial \lambda_1(a_1) - \partial \lambda_{12}(a_1,a_2)}{\partial a_1}\frac{\partial \lambda_2(a_2) - \partial \lambda_{12}(a_1,a_2)}{\partial a_2} + \frac{1}{T}\frac{\partial^2 \lambda_{12}(a_1,a_2)}{\partial a_1 \partial a_2}\right]$$

and it clearly differs from the one obtained in the case of independent variables.
When there are more than two stations, the combinatory nature of the problems makes impossible to have closed form solutions. On possible solution is to separate the variability of the individual ground motions accelerations at different sites from the intrinsic dependency. This is easily performed through copulas. Copulas are functions that describe dependencies among variables, and provide a way to create distributions to model correlated multivariate data. Using a copula, a multivariate distribution can be constructed by specifying marginal univariate distributions, and choosing a particular copula to provide a correlation structure between variables. Bivariate distributions, as well as distributions in higher dimensions, are possible. In the bivariate case the likelihood of the model is given by:

$$f_{XY} = \frac{\partial^2 \Pr(X < x, Y < y)}{\partial x \partial y} = \frac{\partial^2 C(U,V)}{\partial u \partial v} \frac{\partial F(x)}{\partial x} \frac{\partial G(y)}{\partial y} = \frac{\partial^2 C(U,V)}{\partial u \partial v} f_X f_Y = c(U,V) f_X f_Y$$

where G=CDF(a_1), F=CDF(a_2), C(U,V) is the copula whose structure must be specified and U=F(x), V=G(y). To this end several measure of dependency can be used. Among them rank correlation measures the degree to which large or small values of one random variable associate with large or small values of another. However, unlike the linear correlation coefficient, they measure the association only in terms of ranks. As a consequence, the rank correlation is preserved under any monotonic transformation.
The extension to the multivariate case is straightforward. The likelihood of the model is given by:

$$f_{X_1 X_2 \ldots X_N} = \frac{\partial^N C(U_1,..,U_N)}{\partial u_1 .. \partial u_N} \prod_{i=1,N} f_{X\,i} = c^N(U_1,..,U_N) \prod_{i=1,N} f_{X\,i}$$

and the structure of C is completely defined by the correlation matrix between variables. Note also that the N-derivative of the copula is the ratio between the likelihood of the model in case of dependent and independent stations.

3.2 Evaluation of rank correlation between maximum ground motion parameters

To quantify the rank correlation between maximum expected ground motion parameters we have considered the ideal case of two stations embedded in a single seismogenic zone. As the annual rates of modest ground acceleration (acceleration threshold of instruments) are of interest, a seismogenic zone 400x400 sq km has been assumed, characterized by a Gutenber-Richter recurrence, $\log_{10}(N)=a-b(M-M_{min})$, with parameters a=1.2x10^{-4} events per sq km per year, b=1.0, M_{min}=4.0, truncated at M_{max}=7.5. The ground motion predictive relationship of Bindi et al. (2011), which contains the intra-event and inter-event error term, has been used. These assumptions imply, in a station far enough away from the edges of the area, an acceleration of 0.208 g with 475 years return period. The size of the seismogenic zone is such as to be able to move the stations within the zone (Figure 3), up to 100 Km of relative distance, without substantial changes in the marginal rates of exceedance, at least for accelerations above 0.025 g. When different hazard have to be considered in the stations, they stations are placed at one corner and then one is moved towards the centre of the seismogenetic zone.

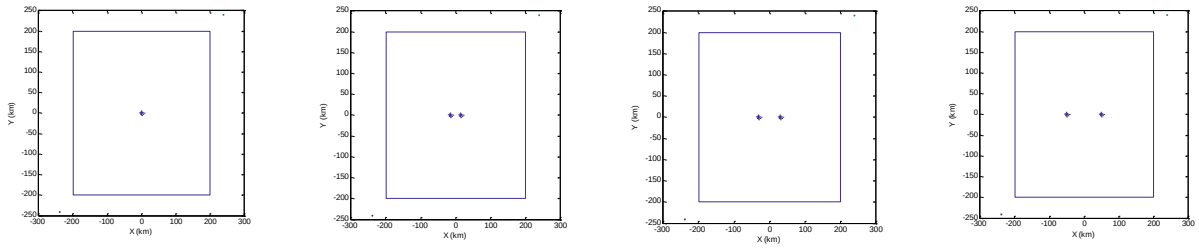

Figure 3. Seismogenetic zone and stations at distance of *D*=0-30-60-100 Km

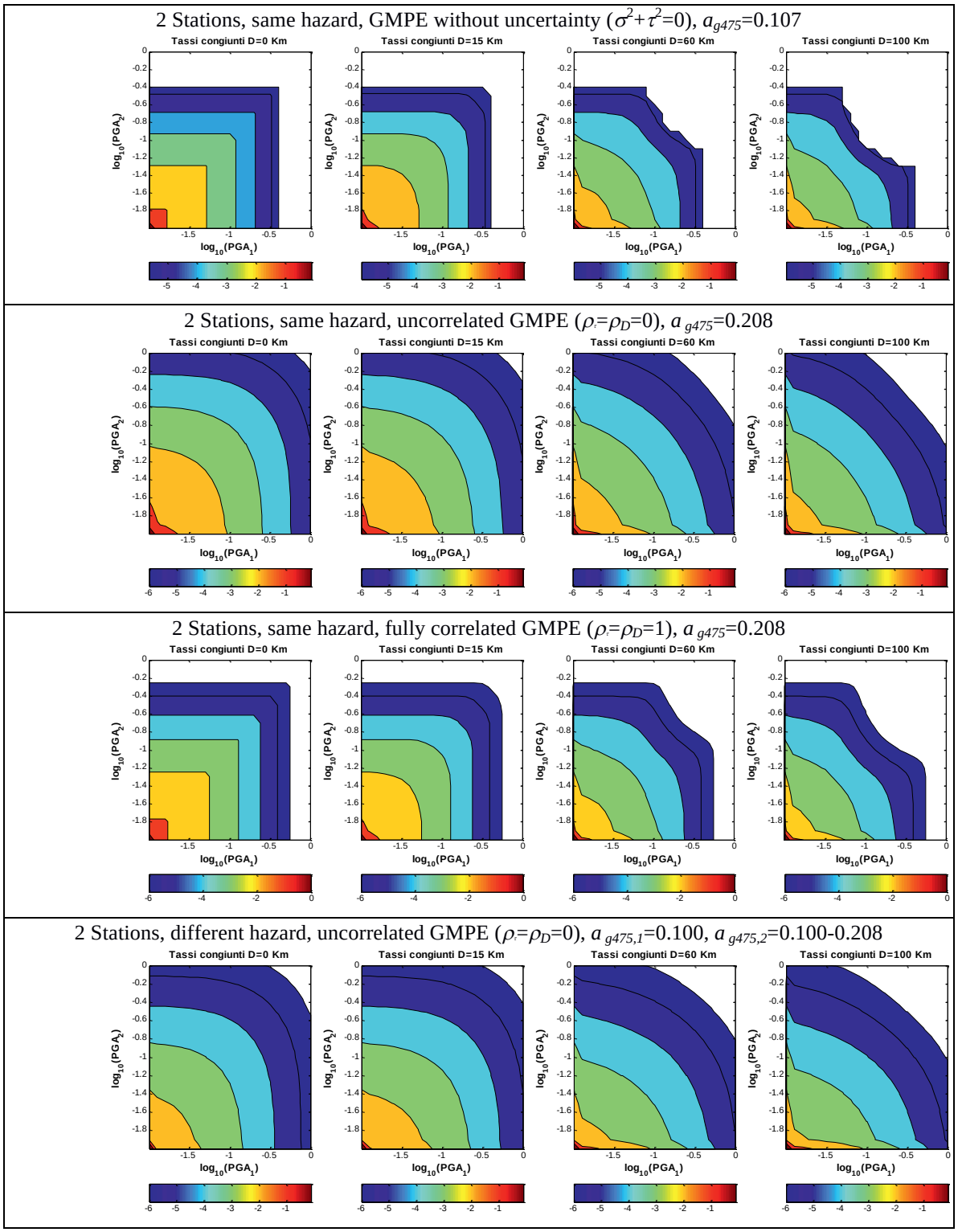

Figure 4. Joint annual rates of exceedance at 2 stations at distance *D*=0-30-60-100 Km (GMPE Bindi et al, 2010)

Figure 4 shows the joint annual rates of exceedance in two stations at different distances. The effect of distance is analysed moving the two stations within the seismogenic zone. The choices made for the two stations imply that both stations have the same marginal rates of exceedance and,

therefore, the same marginal distributions of the maximum acceleration. As the distance increases, the contour lines of the joint rates at the two stations from square tend to become triangular and, at even greater distances, not shown in the figure, but detectable in the case of stations at distance of *D*=100 Km for modest acceleration, tend to be parallel to the axes. In fact, for stations totally independent the marginal rates do not change, while the joint rates cancel out.
Therefore, the gradient of the contour lines of the joint rates in correspondence of the axes are perpendicular to the axes and no longer parallel to them.
The dependence of the maximum acceleration in two stations related to the time of exposure, *T*, is than analysed. A sample of 10,000 pairs of acceleration in the two stations is simulated according to their joint distribution for a given exposure time. The two cases of *T*=30 and *T*=500 years are shown in Figure 5, together with the contour line of the joint density distribution and the marginal density distributions.

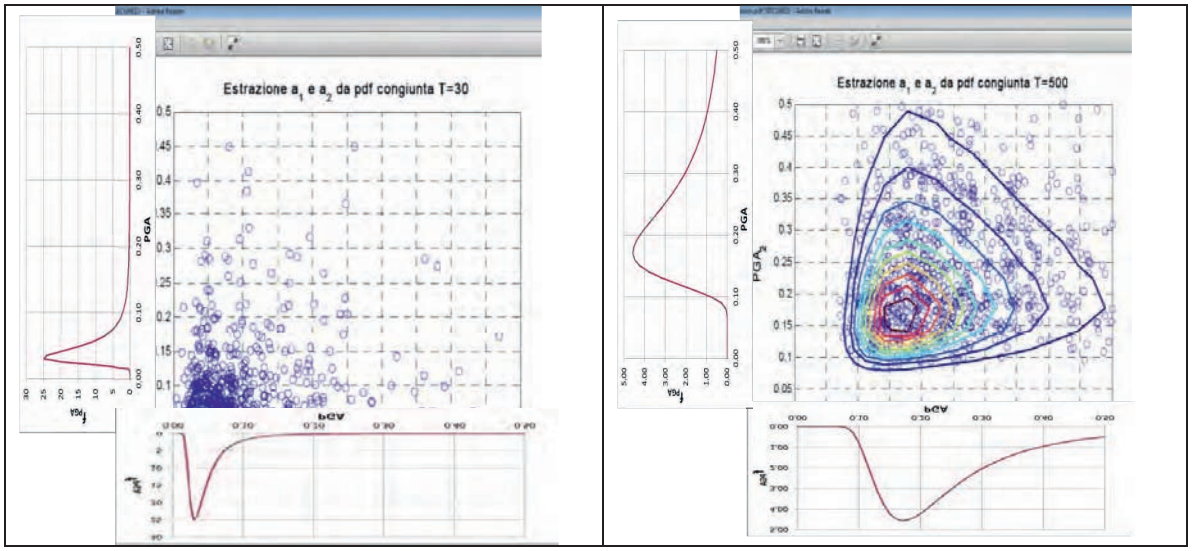

Figure 5. Contour lines of joint density distribution and marginal density distributions at 2 stations at distance *D*=0 Km, *T*=30 and *T*=500 years (GMPE Bindi et al, 2010)

From the simulated accelerations, the Spearman correlation is evaluated and reported in Figure 6 for different distances between stations and different exposure times. One can note some common trends in the analysed cases:
The correlation of the maximum accelerations in the stations reduces with distance. In general at *D*=30 Km it still not negligible, while at distance greater than *D*=50 Km can be neglected;

- The correlation of the maximum accelerations in the stations reduces with exposure time. In general the correlation decreases significantly for *T*<100 years. For *T*>100 years the decrease is less significant;
- The correlation of the maximum accelerations in the stations decreases as the GMPE uncertainty ($\sigma^2+\tau^2$) increases;
- The trend of the correlation of the maximum accelerations in the stations with the GMPE correlation (ρ_{ε}, ρ_D) is not very clear. Some additional analysis is needed.

A possible functional form that reflects the above trend is given by:

$$\rho(a_1,a_2)=e^{-a_D D_{12}}e^{-a_\sigma \sigma_{t\alpha}}e^{-\alpha_{r\varepsilon D}\rho_{\varepsilon D}}e^{-a_T T}$$

The parameters obtained by means of least square optimisation are α_D=0.0295, α_ε=1.3647, $\alpha_{\varepsilon D}$=1.1680, and α_T=0.0030.

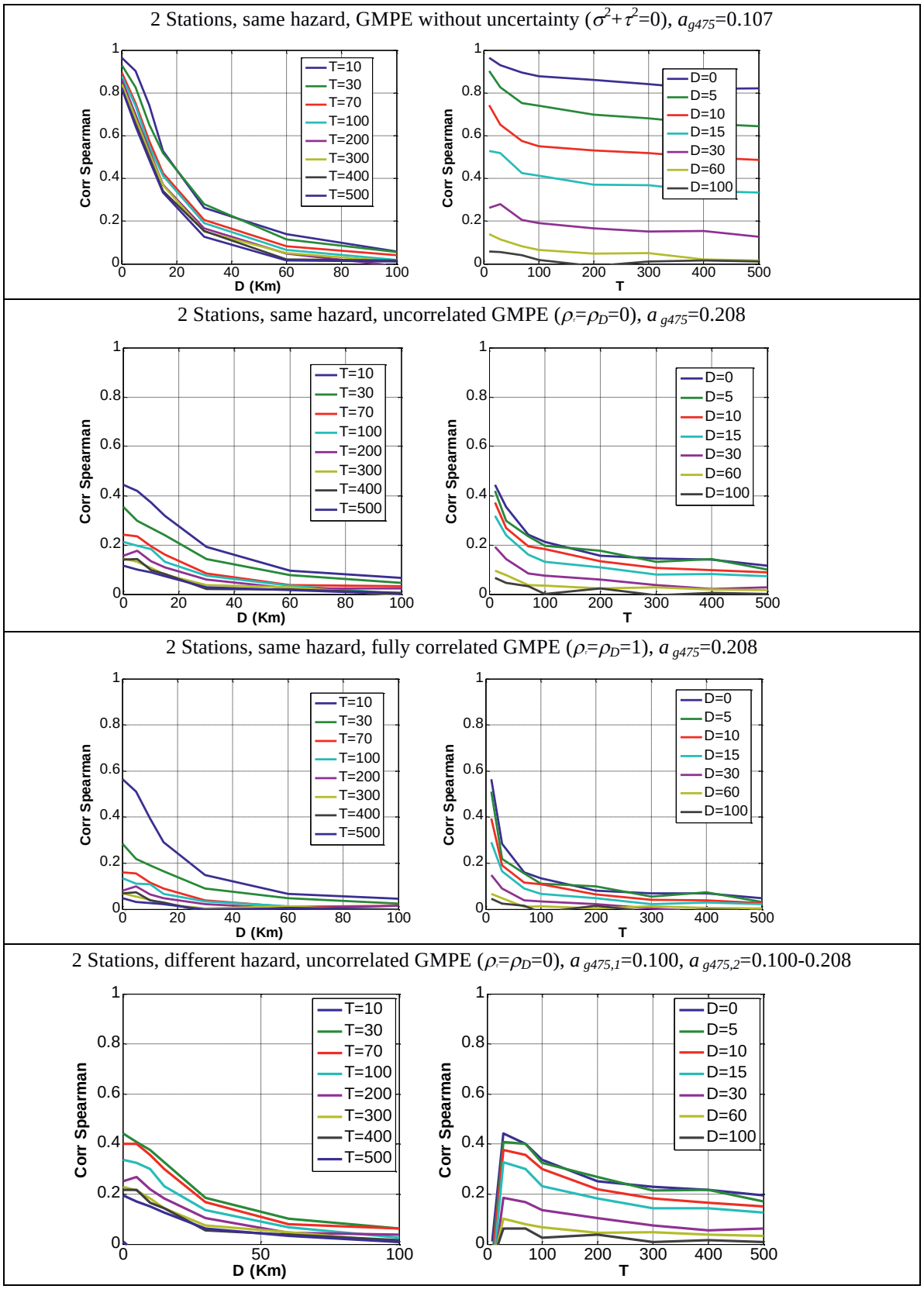

Figure 6. Spearman correlation of maximum acceleration at two stations at different distances and for different exposure times (GMPE Bindi et al., 2010)

The standard deviation of the estimated Spearman correlation is σ_ρ=0.159. The explained variance is 47.8%. From the previous equation, it is possible to evaluate the correlation between maximum accelerations at pairs of stations and the correlation between maximum accelerations at all *N* stations. From there one can evaluate the copula distribution. Given also the marginal density distributions of the maximum acceleration in the stations, evaluated for the maximum recorded acceleration in the exposure time, one gets the likelihood of the hazard model.

4. Conclusive remarks

The first months of the S2-2014 Project permitted a global revision and the publication of the first results of validation and ranking obtained in the previous S2-2012 Project (Albarello et al., 2014). Waiting for the fulfilment of the high-quality characterization of site response on the subset of 41 ITACA stations with a long recording activity, some sensitivity tests have been performed; in addition, an intense methodological discussion started among the Task6 participants. Some of these aspects have been brought to the attention during several conferences (Albarello et al., 2014a-c) and will be faced and deepened during this meeting too.
In the next and conclusive months the S2-2014 activities will be focussed on the re-evaluation of the scoring tests, given the new experimental data available (especially those obtained for site-specific seismic response), and the methodological enhancements proposed till now. We suggest an "international" scoring test on the already available Italian dataset of models' results and observations (Supplementary Materials to Albarello et al., 2014, available on Task 6 folder of S2-2014 Project website too); if the interest on the comparison of methods and results on this test case will raise, a webinar for should be organized in the frame of the S2-2014 activities.

Acknowledgements This study has benefited from funding provided by the Italian Presidency of the Council of Ministers – Civil protection Department (DPC), Project S2-2012. This paper does not necessarily represent DPC official opinion and policies.

REFERENCES

Albarello D., L. Peruzza, and V. D'Amico (2014) A scoring test on probabilistic seismic hazard estimates in Italy. Nat. Hazards Earth Syst. Sci. Discuss., 2, 5721–5757, 2014, www.nat-hazards-earth-syst-sci-discuss.net/2/5721/2014/, doi:10.5194/nhessd-2-5721-2014; in print on NHESS

Albarello D., D'Amico V., Peruzza L., Pacor F. (2014a) Testing probabilistic seismic hazard estimates by comparison with observations. Workshop: Results of the European Project SHARE: Seismic Harmonization in Europe © 2014, DGEB E.V., Frankfurt, Apr 25, 2014

Albarello D., D'Amico V., Peruzza L. (2014b) Testing and scoring probabilistic seismic hazard estimates Second European Conference on Earthquake Engineering and Seismology, Istanbul, Aug 25-29, 2014.

Albarello D., D'Amico V., Peruzza L. (2014c) Controllo e valutazione comparativa di stime di pericolosità sismica in forma probabilistica. XXXIII GNGTS, Bologna, Nov 25-27, 2014

Albarello D. and Peruzza L. (2015) The Scoring Test on Italian Probabilistic Seismic Hazard Estimates Developed in the Frame of S2-2012 DPC-INGV Project Scoring and testing procedures devoted to Probabilistic Seismic Hazard Assessment. Workshop on TESTING PSHA RESULTS AND BENEFIT OF BAYESIAN TECHNIQUES FOR SEISMIC HAZARD ASSESSMENT, Pavia 4-6 February, 2015

Ameri G., Massa M., Bindi D., D'Alema E., Gorini A., Luzi L., Marzorati S., Pacor F., Paolucci R., Puglia R. and C. Smerzini (2009) The 6 April 2009, Mw 6.3, L'Aquila (Central Italy) earthquake: strong-motion observations. Seismol. Res. Lett., 80, 951-966

Bindi D., Pacor F., Luzi L., Puglia R., Massa M., Ameri G. & Paolucci R. (2011) Ground Motion Prediction Equations Derived from the Italian Strong Motion Data Base, Bull Earthquake Eng, 9:1899–1920

Gruppo di Lavoro MPS (2004) Redazione della mappa di pericolosità sismica prevista dall'Ordinanza PCM 3274 del 20 marzo 2003, Rapporto conclusivo per il dipartimento di Protezione Civile, INGV, Milano—Roma, 65 pp. +5 appendici. Website: http://zonesismiche.mi.ingv.it/elaborazioni/ - in Italian

Luzi, L., S. Hailemikael, D. Bindi D, F. Pacor, F. Mele, and F. Sabetta (2008) ITACA (ITalian ACcelerometric Archive): A Web Portal for the Dissemination of Italian Strong-motion Data, Seismological Research Letters, 79(5), 716–722, doi: 10.1785/gssrl.79.5.716

Luzi L., F. Pacor, G. Ameri, R. Puglia, P. Burrato, M. Massa, P. Augliera, G. Franceschina, S. Lovati, R. Castro (2013) Overview on the Strong‐Motion Data Recorded during the May–June 2012 Emilia Seismic Sequence, Seismological Research Letters, 84(4), 629-644

Pacor, F., R. Paolucci, L. Luzi, F. Sabetta, A. Spinelli, A. Gorini, M. Nicoletti, S. Marcucci, L. Filippi, and M. Dolce (2011) Overview of the Italian strong motion database ITACA 1.0, Bull Earthquake Eng, 9(6), 1723–1739, doi: 10.1007/s10518-011-9327-6

Pacor F., Luzi L., Puglia R., D'Amico M., Bindi D. (2013) D2.3 – Strong motion parameters of selected events (update the national database ITACA v1.1), revised GMPE. Internal Report of DPC-INGV S2-2012 Project available at https://sites.google.com/site/ingvdpc2012progettos2/deliverables/d2-3-updated-strong-motion-data

CSNI Workshop on "*Testing PSHA Results and Benefit of Bayesian Techniques for Seismic Hazard Assessment*"
4-6 February 2015, Eucentre Foundation, Pavia, Italy

The Scoring Test on Italian Probabilistic Seismic Hazard Estimates Developed in the Frame of S2-2012 DPC-INGV Project

Dario Albarello
Università degli Studi di Siena, Italy, dario.albarello@unisi.it

Laura Peruzza
OGS (Istituto Nazionale di Oceanografia e di Geofisica Sperimentale), Italy, lperuzza@inogs.it

SUMMARY

An empirical scoring test on PSHA in Italy has been realized in the frame of the Project S2-2012 (https://sites.google.com/site/ingvdpc2012progettos2/home), the first annual phase of researches funded by the 2012-2021 Agreement between the National Civil Defence Department (DPC) and National Institute of Geophysics and Volcanology (INGV). The test is based on the comparison of outcomes provided by ten time-independent hazard models at about 70 accelerometric sites in Italy, characterized by a long recording history (>25 years). Maxima observed Peak Ground Accelerations (PGA) in a control period (1979-2004) have been compared with the hazard estimates, after that a site-specific correction has been applied accordingly to the Italian and European regulations. In particular, by considering a control period of 25 years, we compared the number of sites where reference PGA values (i.e., the PGA values characterized by a given exceedance probability) have been empirically exceeded, with the one expected on the basis of the relevant hazard model.
This comparison allows scoring the most effective computational models and identifying those providing outcomes in contrast with observations, that should therefore be discarded. The analysis shows that most of hazard estimates so far proposed for Italy are not in contrast with observations gathered in the 1979-2004; some models, however, perform significantly better than the others do, but the same computational scheme can perform very differently, depending on the region considered and on the average return time analysed. The models collected span about 20 years of PSHA practice in Italy and Europe; not necessarily the most recent models perform better than the older ones. The site-specific characterization of accelerometric stations is a critical element for which additional studies should been planned in the future.

Keywords: *Probabilistic seismic hazard analysis, Validation, S2-2012 DPC-INGV Project.*

1. Introduction

This paper shortly describes some results obtained by Task 6 "Model validation" during the project S2-2012 "Constraining Observations into Seismic Hazard", one of the six annual projects funded in the frame of the decennial agreement between the National Civil

Department (DPC) and the Istituto Nazionale di Geofisica e Vulcanologia (INGV), in Italy (http://istituto.ingv.it/l-ingv/progetti/progetti-finanziati-dal-dipartimento-di-protezione-civile-1). S2-2012 aimed at ranking PSHA results with respect to instrumental ground motion observations available at the project's beginning (2012). Despite the projects have been asked to focus on two priority areas (Po Plain, Southern Apennines), the S2-2012 analyses moved soon into a national-wide perspective, in order to increase the results representativeness.
Operating in a frame of cooperative and coordinated activities, PSHA models have been collected and archived by the Politecnico of Milan Research Unit (Deliverable 1.1, Faccioli and Vanini, 2013); Excel files that represent nearly 20 years of PSH estimates in Italy have been stored on https://sites.google.com/site/ingvdpc2012progettos2/deliverables/d1-1, a public accessible folder. On the experimental side, instrumental observations have been selected by the INGV Milan Research Unit (Deliverable 2.3, Pacor et al., 2013) from the ITACA database (Pacor et al., 2011) maintained by the same researchers' team too.
Most of the collected models are time-independent, and therefore they may be used for any reference time window of observations: conversely, the time-dependent results are given with respect to a starting date (Jan 1, 2010 for the models gathered) thus limiting their usage in testing. A full description of method and data is given in recently published papers (Albarello et al., 2014; Albarello & D'Amico, 2015), and presented at conferences and meetings too (see materials stored on https://sites.google.com/site/ingvdpc2012progettos2/deliverables/d6 and on Task6 folder, at https://sites.google.com/site/ingvdpc2014progettos2/tasks/task-6). Here, we gather, in an informal way, additional materials and sensitivity analyses performed by using the same datasets of Albarello et al., 2014, still not disseminated. Two topics that we believe crucial, for establishing the superiority of a PSHA model on another one, have been investigated: a) the sensitivity to site-specific corrections; and b) the completeness assumption adopted on instrumental observations.
All the considerations here depicted are propedeutical to the betterment of scoring methods and observations, pursued especially in the second, still ongoing, annual phases of S2 Project, namely S2-2014; the full track of activities, whose final results are expected in mid-2015, can be followed on the project web site (https://sites.google.com/site/ingvdpc2014progettos2/).

2. Shortcuts to the scoring test

Imagine you toss a hundred dices at once: how many dices are expected to exceed for example the score five? We performed a similar comparison on outcomes provided by time-independent hazard models at M Italian accelerometric sites, with respect to the ground motion observed during a recording period of Δt years (testing time). A set of PSH models is considered each providing Peak Ground Accelerations (PGAs) values expected to be exceeded with given probabilities p_i in given exposure times ΔT_i (usually, 10% in 50 years are the reference values for PGA analyses, corresponding to a unique return period RT = 475 years). In general, the time span Δt, period of activity of accelerometric sites, does not correspond to the exposure time ΔT considered in PSH models. However, since all the considered PSH models assume that seismicity is Poisson process, the probability $p(\Delta t)$ can be easily computed from $p_i(\Delta T_i)$ by the formula

$$p(\Delta t) = 1 - e^{\frac{\Delta t}{\Delta T_i}\ln(p_i - \Delta T_i)} \qquad [1]$$

As a first approximation, widely accepted by hazard modellers, we assume that outcomes of the PSH model at the M sites are mutually independent. In this case, one can compute the expected number Ne of sites where the reference PGA is exceeded as $Ne=M\Sigma p_i$. The relevant variance will be $\sigma^2(Ne)=Mp(1-p)$. To score the considered PSH model, the Z statistics is computed in the form:

$$Z=(N^*-Ne)/\sigma(N) \qquad [2]$$

where N^* is the observed number of sites where the reference PGA value has been actually overcame during the control period of 25 years. Numerical simulations show that Z is roughly distributed as a standardized normal: Z values near to 0 identify best performing models. In general, negative Z values indicate that the hazard is overestimated by the *i-th* model since the actual number of exceedances is lower than the observed one. The reverse is true for positive Z values. One could consider the outcomes of the i-th model "not supported" by observation when the absolute value of Z is greater than 2. A more extensive discussion about this scoring procedure can be found in Albarello and D'Amico (2015).
The scoring procedure delineated above can be considered just a first order approximation to testing since the independence of hazard estimates is not warranted. It can be demonstrated that the value of *Ne* value is not affected by this bias, but $\sigma(N)$ may be underestimated (by an amount monotonically increasing with M) since the eventual covariance among exceedances expected at neighbouring sites is not accounted for. This may increase the probability of rejecting a correct model (Type I error) since Z is biased towards higher values. A more extensive analysis of this problem is currently under study and is part of the second year of activity currently in progress in the frame of the S2-2014 project.

3. Application to PSH estimates on Italy

Pre-processing on the results stored in the PSHA repository (Faccioli and Vanini, 2013) consists in:
1) the selection of adequate space/ground motion parameters (longitude, latitude, PGA, or Spectral Acceleration –SA- at given periods) in the original files as most of the models have multiple sheets of results,
2) the recovery of the return period the results have been built for, from the combination of probability level and observation time declared in the literature,
3) the selection of the nearest node of given results, with respect to the coordinates of the point with available observed data (station location), and
4) the computation of site-specific correction coefficients, that in this test are based on site characterization (given as soil categories in ITACA v. 1.0) and on the rules of current Italian regulation (NTC, 2008) and Eurocode 8 (EN 1998-1, 2004).
Maximum observed PGAs at 71 Italian accelerometric stations in the period 1979-2004 have been therefore considered: this peculiar subset of stations and time-window have been chosen to maximize the number of contemporaneously active stations with a long operational status, among the ones belonging to the Italian Accelerometric Network (Rete Accelerometrica Nazionale RAN), operating in Italy since the 70'ies. Before applying the Z scoring procedure, complementary aspects of site-specific hazard, completeness and representativeness of the time frame used in the testing procedure must be addressed.

3.1 Site-specific seismic hazard assessment

Most of the accelerometric sites considered for testing cannot be considered representative of reference soil conditions. In particular, out of the 71 sites considered, about 1/3 are of Type A by following the EC8 soil classification. This implies that observed ground motion cannot be compared with the one provided by the PSH procedures that, in nearly all the cases, refers to a reference soil condition. In order to reduce this possible bias, a site correction factor has been tentatively applied to the non-reference sites by taking into account the soil classification provided in the ITACA dataset for all the accelerometric sites.
This classification is provided according to two procedures, namely:

a) the rules established by the current Italian regulation (NTC, 2008): it states that if no specific information about site response are given, a simplified method should be applied in order to define the seismic action, in particular the maximum spectral acceleration at period T=0 s is:

$$a_{\max} = a_g \cdot S_S \cdot S_T \qquad [3]$$

Tabella 3.2.V – *Espressioni di* S_S *e di* C_C

Categoria sottosuolo	S_S	C_C
A	1,00	1,00
B	$1,00 \le 1,40 - 0,40 \cdot F_o \cdot \frac{a_g}{g} \le 1,20$	$1,10 \cdot (T_C^*)^{-0,20}$
C	$1,00 \le 1,70 - 0,60 \cdot F_o \cdot \frac{a_g}{g} \le 1,50$	$1,05 \cdot (T_C^*)^{-0,33}$
D	$0,90 \le 2,40 - 1,50 \cdot F_o \cdot \frac{a_g}{g} \le 1,80 \cdot$	$1,25 \cdot (T_C^*)^{-0,50}$
E	$1,00 \le 2,00 - 1,10 \cdot F_o \cdot \frac{a_g}{g} \le 1,60$	$1,15 \cdot (T_C^*)^{-0,40}$

a)

Tabella 3.2.VI – *Valori massimi del coefficiente di amplificazione topografica* S_T

Categoria topografica	Ubicazione dell'opera o dell'intervento	S_T
T1	-	1,0
T2	In corrispondenza della sommità del pendio	1,2
T3	In corrispondenza della cresta del rilievo	1,2
T4	In corrispondenza della cresta del rilievo	1,4

b)

Figure 1. Stratigrafic (a) and topographic (b) site-specific coefficients (tables taken from NTC, 2008)

where the stratigraphic (S_S) and topographic (S_T) components of amplification factor (see cap. 3.2.2 of NTC, 2008) can be obtained according to the hereinafter reported tables (Figure 1), and a_g and F_o are tabulated values (Annex Tabella 1 to the law).

b) in terms of the soil classes defined in EC8.

In both method the soil type category (Categoria sottosuolo) is obtained by Vs profiles available at each accelerometric site from experimental data, or, in most cases (marked by a "*" identifier), from information deduced by large-scale geological mapping.

The coefficients provided by both NTC08 and EC8 rules have been applied to reduce available PGA values to a virtual reference soil condition. This solution can be considered a very preliminary analysis, and a more detailed study is mandatory for a correct testing of PSH models.

The comparison of the global amplification coefficients at the 71 accelerometric sites is given in Figure 2; note that several stations exhibit a site-specific amplification coefficients higher than 1.25, if Italian regulation is adopted.

3.2 Completeness of observations and stationarity of seismicity

Completeness is always a thorn in the flesh. We estimated the "incompleteness" of our maximum observed PGA by comparing observed PGA (as given by the ITACA v.1.0 release, available at the moment of elaborations the paper refer to) with theoretical values obtained by using the Italian earthquake catalogue CPTI11 and GMPE from Italian data (Bindi et al., 2011), using differentiated soil type accordingly with stations classes. The maximum computed value in the reference period (1979-2004) is taken if the (mean minus one standard deviation) exceed the sensitivity threshold of accelerometric stations of that period, commonly assigned at 0.01 g. Figure 3 represents the available data, sorted for increasing values of observed-calculated PGA.

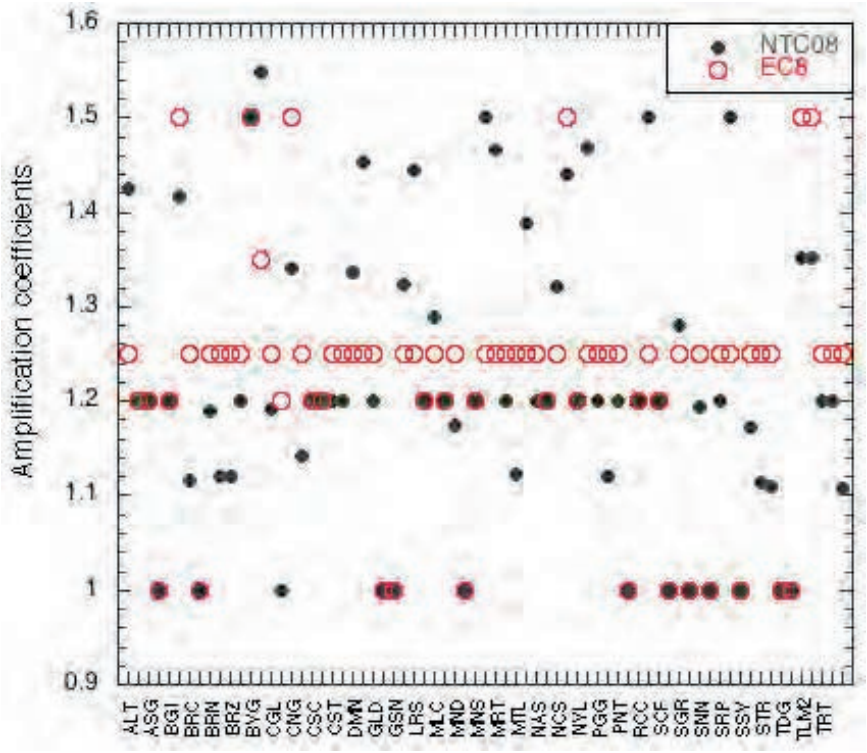

Figure 2. Amplification coefficients for the investigated accelerometric sites: black dots refer to NTC, 2008; red circles to Eurocode 8.

Note that about 50% of the stations have positive residuals thus implying that the observations exceed the theoretical calculated values; among those having negative residuals, only for four stations (ARI, SRP, LNG, MRN; 4/71=6%) incompleteness should be invoked in observations (no records), even if the expected values (40-60 cm/s^2) are still inside an acceptable intrinsic variability due to source/site effects. These results confirm the inadequacy of simplified site characterization as reported in ITACA by now, and consequently the weakness of the coefficients for soil type, as accounted for in the derived GMPE.
In order to evaluate the possible role of this incompleteness on our results, a sensitivity test was performed to check the effects of different levels of incompleteness on the final scores. For this purpose, a large number of artificial data sets has been generated by a Monte Carlo procedure including a randomly varying number of "incomplete" stations. In each run, "incomplete" stations were randomly selected with a fixed probability (0.05, 0.1, …) representative of the relevant incompleteness level. When a station is assigned as affected by incompleteness, the maximum acceleration actually observed is substituted by the sensitivity threshold (9.8 cm/s^2). For each "artificial" data set, the score was obtained by comparing "observations" with forecasts. In this way, the average "scores" (e.g., the number exceedances) was obtained for each "incompleteness" probability. The average score and the respective standard deviation has been than associated to each "incompleteness" level (e.g. incompletes probability). This analysis shows that, final results are not significantly affected by incompleteness levels lower than 20%.

3.3 Application of the Z test to Italian Accelerometric sites

The results, in terms of expected and observed PGAs, and absolute scoring factor for the nation-wide set of stations, and two regional subsets are depicted in Figs. 7 and 9 in Albarello et al., 2014. Here a summary table of Z scores is given, adding to the previous analyses a subset of 22 stations focussed in Central Italy, never presented before.

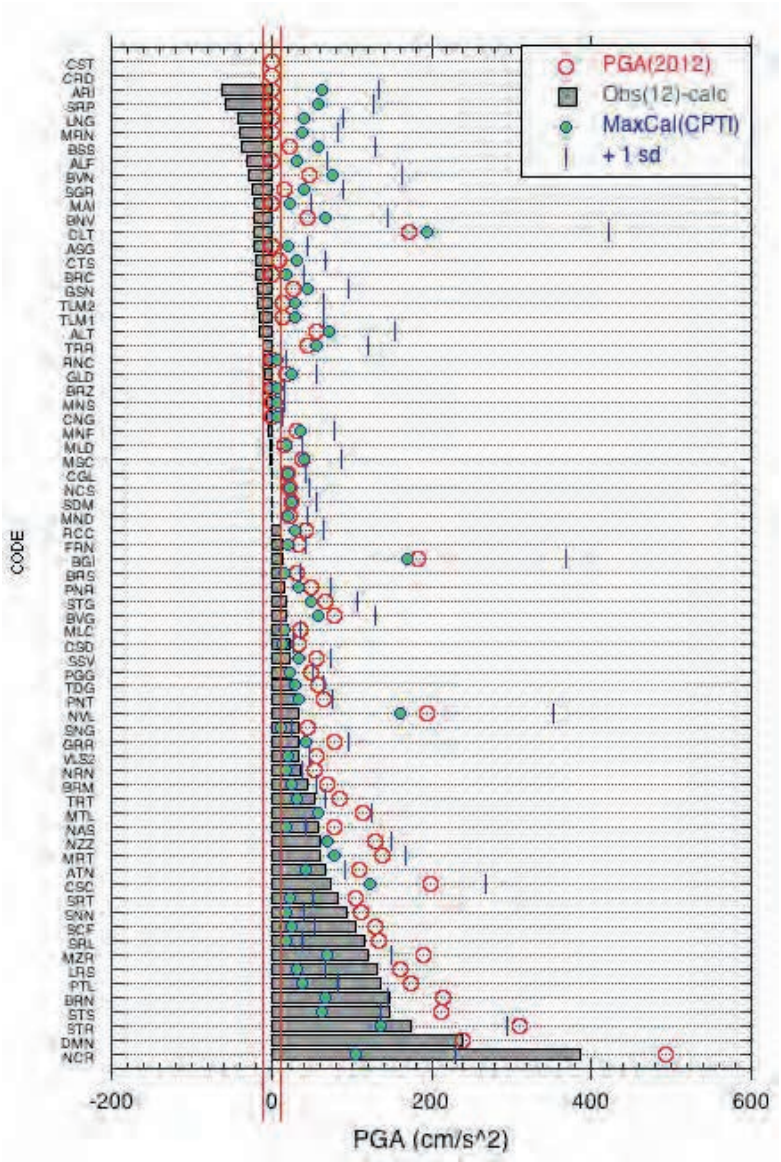

Figure 3. Observed and computed PGA values at some stations in the time frame 1979-2004.

Note that the scoring factor Z is here given with its sign, thus allowing to recognize the cases of overestimation of models on observations (positive values), with respect to the underestimation (negative); the best performing model is given in red; the models we consider inadequate (according to eq. [2]) are highlighted in yellow. Some considerations arise, by comparing the scores of different models at the national and regional scale. The hazard estimate that fits better the observation during the 25 years 1979-2004, on the whole set of 71 stations, is the one obtained at intermediate return period (ID 1 T284, corresponding to 10% of exceedance in 30 years) by an elaboration of 1996 (Slejko et al., 1998), done with the earthquake catalogue that ends in 1980 and ground motion prediction equation (GMPE) for undifferentiated soil conditions (Ambraseys, 1995). Using the NTC08 site-specific amplification coefficients, all the models are compatible with the observations, some of them overestimate the observed shakings (e.g. the same ID 1 model at 10% in 10 years), some underestimate them (e.g. the predictions released in the frame of the actual Italian regulation map at the longer return period, ID3 T475 and ID4 T2475, Gruppo di Lavoro MPS, 2004; Meletti & Montaldo, 2007; Stucchi et al., 2011). Conversely, the same long prediction model appears to be the most adequate to represent observations if applied in Northern Italy, while the other realizations of the same model at shortest return period (ID4 T101, ID3 T475) and

the most recent elaborations released in the frame of S2-2012 Project (ID8 and 8s) exhibit strong underestimation of ground motion, and are considered not compatible with observations. Noteworthy, for Southern Italy and Central Italy, where significant earthquakes occurred during the testing time frame used (e.g. the 1980 Irpinia earthquake with about 3,000 casualties in Southern Apennines; the 1997-98 Colfiorito sequence, in Central Italy), none of the models is rejected; the best performing models are based on a recent GMPE (Cauzzi & Faccioli, 2008); notably, in Central Italy, very different earthquake model assumptions (such as seismotectonic sources of ID 5 model, or smoothed seismicity of ID 6) behave the same.

Table 2. Z-scores as given in Albarello et al., 2014 for several PSHA models on different set of stations; in red the best performing model, highlighted in yellow the models rejected. The Z scores have been obtained using site-specific coefficients of Italian regulation (NTC08). For additional descriptions of PSHA models see also the supplementary material given on Task6 folder at https://sites.google.com/site/ingvdpc2014progettos2/tasks/task-6

Models	Whole Italy (71 stations)	Southern Italy (21 stations)	Northern Italy (12 stations)	Central Italy (22 stations)
ID 7 T30		0.059		
ID 1 T94	1.574	0.987	-1.794	1.082
ID 4 T101	-0.703	-1.267	-2.451	-0.609
ID 1 T284	-0.015	0.601	-1.079	0.652
ID 1 T475	0.335	1.062	-0.014	0.118
ID 2 T475	-0.744	1.062	-1.327	0.118
ID 3 T475	-1.823	0.07	-2.639	-0.851
ID 7 T475		1.062		
ID 9 T475	0.874	1.062	0.014	0.118
ID 10 T475				0.118
ID 5 T484	-0.79	1.051	-1.338	0.098
ID 6 T484	-0.79	0.050	-0.014	0.098
ID 8s T484			-3.951	
ID 8 T484			-3.951	
ID 7 T975		0.734		
ID 5 T984	-0.171	0.734	-0.004	0.751
ID 6 T984	-0.931	0.734	-0.004	-0.615
ID 4 T2475	-1.539	0.461	-0.001	0.471
ID 7 T2475		0.461		

4. Discussion and conclusive remarks

Figure 4 graphs the differences in Z scores due to the utilization of Italian or European simplified amplification factors. The effect of site-specific adjustments on scoring is not negligible if the whole dataset of accelerometric stations is considered (Fig. 4a) as 6 on 12 models change scores; on sub-regional datasets the impact is limited to one-few models only. Nonetheless we cannot reckon a systematic bias, by using the EC8 simplified coefficients or the NTC08 ones; in the considered study cases, the best model (the Z-score nearest to zero) is invariant to the changes in site-specific correction coefficients adopted.

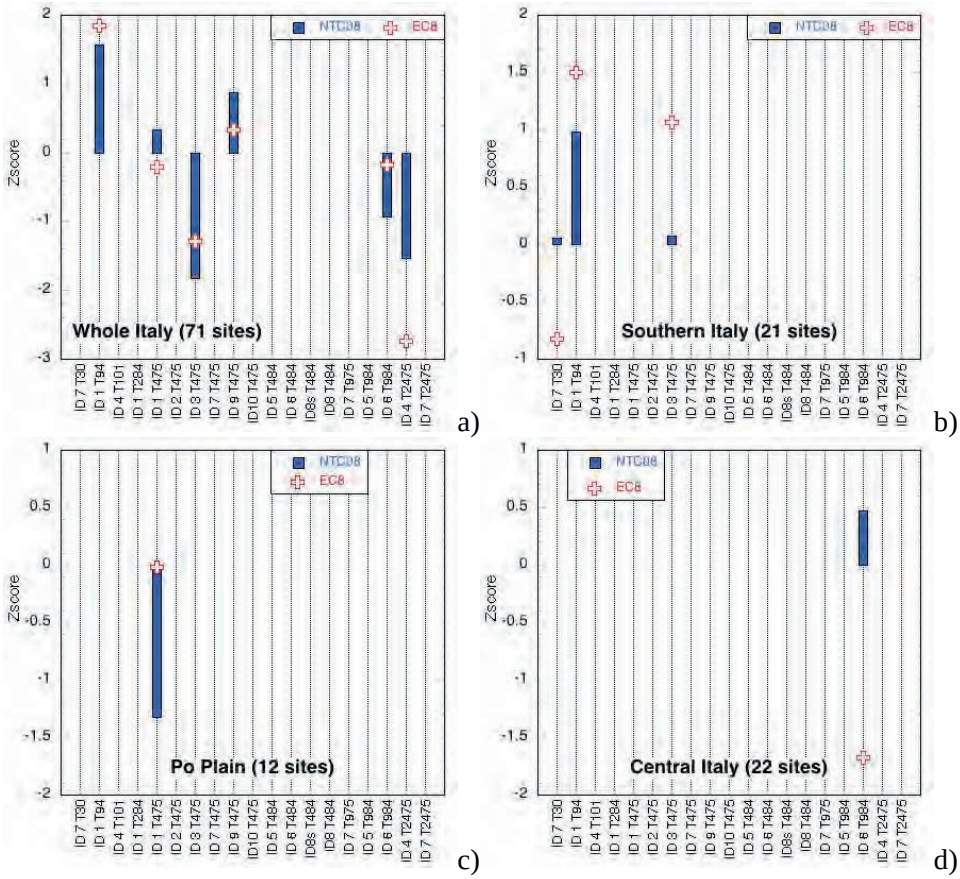

Figure 3. Effect of site-specific seismic hazard assessments on scoring. Z-scores of models that change scoring using EC8 the site-specific amplification coefficients instead of NTC08; representation on different sets of accelerometric stations; a) whole Italy, b) Southern Italy and c) Northern Italy and d) Central Italy.

Completeness of observations is negligible if the maximum shaking is considered in a fairly long time window (20 years and more). This consideration cannot be exported to the whole series, or to limited testing times. A re-evaluation of a GMPE derived from available Italian accelerometric data has to be considered, after that more precise information on site-specific response is given.

Last but not the least, the scoring procedures exhibit several advantages and some disadvantages too: a synthetic value that accomplishes the model effectiveness as whole is given, but there are several open questions (e.g. accounting for correlation among expected exceedances at the considered accelerometric sites, completeness of recordings, etc.) that need further investigations. We aim at facing some of them in the second phase of S2-2012-14 Project.

Acknowledgements This study has benefited from funding provided by the Italian Presidenza del Consiglio dei Ministri – Dipartimento della Protezione Civile (DPC), Project S2-2012. This paper does not necessarily represent DPC official opinion and policies.

REFERENCES

Albarello D., L. Peruzza, and V. D'Amico (2014) A scoring test on probabilistic seismic hazard estimates in Italy. Nat. Hazards Earth Syst. Sci. Discuss., 2, 5721–5757, 2014, www.nat-hazards-earth-syst-sci-discuss.net/2/5721/2014/, doi:10.5194/nhessd-2-5721-2014

Albarello and D'Amico (2015) Scoring and testing procedures devoted to Probabilistic Seismic Hazard Assessment. Survey of Geophysics, Submitted

Ambraseys N N (1995) The Prediction of Earthquake Peak Ground Acceleration in Europe, Earthquake Engineering and Structural Dynamics, 24, 467-490.

Bindi D., Pacor F., Luzi L., Puglia R., Massa M., Ameri G. & Paolucci R. (2011): Ground Motion Prediction Equations Derived from the Italian Strong Motion Data Base, Bull Earthquake Eng 9:1899–1920.

Cauzzi, C., and E. Faccioli (2008). Broadband (0.05 to 20 s) prediction of displacement response spectra based on worldwide digital records, J. Seismol., 12, 453–475.

EN 1998-1 Eurocode 8 (2004) Design of structures for earthquake resistance – Part 1: General rules, seismic actions and rules for buildings [Authority: The European Union Per Regulation 305/2011, Directive 98/34/EC, Directive 2004/18/EC]

Faccioli E. and Vanini E. (2013) D1.1 – PSHA Repository. Internal Report of DPC-INGV S2-2012 Project "Constraining observations into Seismic Hazard" available at https://sites.google.com/site/ingvdpc2012progettos2/deliverables/d1-1

Gruppo di Lavoro MPS (2004). Redazione della mappa di pericolosità sismica prevista dall'Ordinanza PCM 3274 del 20 marzo 2003, Rapporto conclusivo per il dipartimento di Protezione Civile, INGV, Milano—Roma, 65 pp. +5 appendici. Website: http://zonesismiche.mi.ingv.it/elaborazioni/ - in Italian.

Meletti C. and Montaldo V., (2007) Stime di pericolosità sismica per diverse probabilità di superamento in 50 anni: valori di ag. Progetto DPC-INGV S1, Deliverable D2, http://esse1.mi.ingv.it/d2.html

NTC (2008) Norme tecniche per le costruzioni, Ministero delle Infrastrutture e dei Trasporti, Decreto Ministeriale del 14 gennaio 2008, Supplemento ordinario alla G.U. n. 29 del 4 febbraio 2008

Pacor F., Luzi L., Puglia R., D'Amico M., Bindi D. (2013) D2.3 – Strong motion parameters of selected events (update the national database ITACA v1.1), revised GMPE. Internal Report of DPC-INGV S2-2012 Project "Constraining observations into Seismic Hazard" available at https://sites.google.com/site/ingvdpc2012progettos2/deliverables/d2-3-updated-strong-motion-data

Pacor, F., R. Paolucci, L. Luzi, F. Sabetta, A. Spinelli, A. Gorini, M. Nicoletti, S. Marcucci, L. Filippi, and M. Dolce (2011) Overview of the Italian strong motion database ITACA 1.0, Bull Earthquake Eng, 9(6), 1723–1739. Doi: 10.1007/s10518-011-9327-6

Slejko, D., L. Peruzza, and Rebez A. (1998) Seismic hazard maps of Italy. Annali di Geofisica 41(2): 183-214.

Stucchi, M., Meletti, C., Montaldo, V., Crowley, H., Calvi, G.M. and Boschi E. (2011) Seismic hazard assessment (2003-2009) for the Italian building code. BSSA, 101, 1885-1911.

CSNI Workshop on "*Testing PSHA Results and Benefit of Bayesian Techniques for Seismic Hazard Assessment*"
4-6 February 2015, Eucentre Foundation, Pavia, Italy

Revision of Earthquake Catalogues on Probabilistic Terms: Consequences on PSHA Validation

Marco Mucciarelli
CRS-OGS, Italy, mmucciarelli@inogs.it

SUMMARY

A previous work performed in the frame of the project SIGMA (SeIsmic Ground Motion Assessment) concluded that the uncertainty on Mean Return Times caused by problems in intensity definition for site seismic histories is of the order of 25-30%. The analysis of the rates from seismogenic zones suggest that the uncertainty due to epicentral intensity estimate is again about 25%, a relative error that will propagate in further steps of PSHA. This uncertainty could be reduced with a thorough revision of the catalogue in a probabilistic fashion, defining with the help of historians a "degree of belief" on each single intensity degree. In this study, the historical catalogue of the Po Plain has been revised on probabilistic terms, with an expert judgement that used probability to express the degree of belief in different possible epicentral intensities. Mean return times were then calculated from this new catalogue, and compared with the result of a standard approach that forces uncertain intensities on nearest integer values. The outcome showed that the variation in the estimate of MRT is ranging from 15 to 30% for intensities comprised between VII and IX. The presence of this uncertainty should be considered in the validation activities of PSHA estimates.

Keywords: *PSHA validation, Probabilistic Catalogues, Bayesian updating.*

1. Introduction

This study is the follow up of a research performed in the framework of the project SIGMA (SeIsmic Ground Motion Assessment), that was concerned with the preliminary earthquake recurrence models with extensive use of site data. The previous study (Mucciarelli, 2014) concluded that the uncertainty on Mean Return Times caused by problems in intensity definition for site seismic histories is of the order of 25-30%. The analysis of the rates from seismogenic zones suggest that the uncertainty due to epicentral intensity estimate is again about 25%, a relative error that will propagate in further steps of PSHA.This uncertainty could be reduced with a thorough revision of the catalogue, possibly in a probabilistic fashion, defining with the help of historians a "degree of belief" on each single intensity degree.

2. The data

The data for revising the catalogue of the test area (Po Plain , Italy) and put it in a probabilistic format were taken from the
Italian Parametric Catalogue (CPTI, Catalogo Parametrico dei Terremoti Italiani) and from the Italian database of Macroseismic Intensity (DBMI, Data Base Macrosismico Italiano), both available from INGV web page (www.ingv.it).
Some of the earthquakes to be revised do not have an associated intensity map. Another important feature to be described concerns the number of intensity point associated to each earthquake when a map is available.
It is worth noting that 15% of the revised events are known for just a single locality with associated intensity, and slightly less than 50% have a map with 10 points or less. This means that any automated procedure for parametrizing epicentral data will encounter problems due to the limited number of points available.
Moreover, for the single point earthquakes, the only way to solve the uncertainty associated to epicentral intensity (and thus converted magnitude) would be to carry on a reappraisal of the original source behind this single point.
The inspection of intensities maps revealed some recurrent problems confirmed with interviews with historical seismologists:

1) the uncertainty in epicentral intensity due to the fact that the points are few, scattered and with large “jumps” in intensity values.
2) the uncertainty is attributed to the role of site effects, assuming that this is the cause of a single or few, higher values among a rather homogeneous distribution of lower intensity.
3) the uncertainty is due to an apparent “anomalous” small area affected by high intensity with no or little evidence of lower values

The revision of a catalogue becomes then an expert judgement, using probability to express the degree of belief, that should be subjected to simple “conversion rules” such those listed in the EMS-98 scale for the definition of quantity such as “many”, “few”, or “most” (see Mucciarelli, 2014, for a possible conversion rule)

Table 1. The probabilistic catalogue of the Po Plain test area

			Prob				
Year	**Int**	**Np**	**V**	**VI**	**VII**	**VIII**	**IX**
1065	7		1	1	1	0	0
1117	9.5	57	1	1	1	1	1
1222	8.5	18	1	1	1	1	0.5
1249	6.5	4	1	1	0.5	0	0
1285	6.5	1	1	1	0.5	0	0
1323	5.5	5	1	0.7	0	0	0
1334	5.5	4	1	0.5	0	0	0
1345	5.5	1	1	0.5	0	0	0
1365	6.5	1	1	1	0.5	0	0
1365	5.5	1	1	0.5	0	0	0
1396	7.5	2	1	1	1	0.5	0
1399	7		1	1	1	0	0
1402	6		1	1	0	0	0

			Prob				
Year	**Int**	**Np**	**V**	**VI**	**VII**	**VIII**	**IX**
1403	6		1	1	0	0	0
1409	6		1	1	0	0	0
1410	6.5	3	1	1	0.5	0	0
1425	6		1	1	0	0	0
1433	6		1	1	0	0	0
1438	8		1	1	1	1	0
1445	5.5	3	1	0.5	0	0	0
1455	7.5		1	1	1	0.5	0
1455	7		1	1	1	0	0
1465	6.5	11	1	1	0.5	0	0
1471	5.5		1	0.5	0	0	0
1474	6		1	1	0	0	0
1483	8		1	1	1	1	0
1483	5.5	1	1	0.5	0	0	0
1491	7.5		1	1	1	0.5	0
1501	8.5	20	1	1	1	1	0.8
1505	7		1	1	1	0	0
1505	5.5		1	0.5	0	0	0
1508	6		1	1	0	0	0
1521	6		1	1	0	0	0
1540	6		1	1	0	0	0
1547	7		1	1	1	0	0
1561	5.5	5	1	0.5	0	0	0
1570	7.5	60	1	1	1	0.8	0
1572	7		1	1	1	0	0
1574	7		1	1	1	0	0
1576	6		1	1	0	0	0
1586	6		1	1	0	0	0
1591	6.5	6	1	1	0.6	0	0
1591	6		1	1	0	0	0
1593	6.5	1	1	1	0.5	0	0
1606	6.5	1	1	1	0.5	0	0
1608	6		1	1	0	0	0
1624	7.5	18	1	1	1	0.5	0.1
1628	7		1	1	1	0	0
1642	6.5	11	1	1	0.5	0	0
1660	5.5		1	0.5	0	0	0
1661	7		1	1	1	0	0
1666	6		1	1	0	0	0
1671	7		1	1	1	0	0
1688	9		1	1	1	1	1
1688	7		1	1	1	0	0
1689	6		1	1	0	0	0

			Prob				
Year	**Int**	**Np**	**V**	**VI**	**VII**	**VIII**	**IX**
1693	7		1	1	1	0	0
1695	5.5	1	1	0.5	0	0	0
1732	6		1	1	0	0	0
1738	7		1	1	1	0	0
1743	6.5	1	1	1	0.5	0	0
1756	5.5	1	1	0.5	0	0	0
1771	6		1	1	0	0	0
1771	6		1	1	0	0	0
1774	6		1	1	0	0	0
1780	6.5	9	1	1	0.5	0	0
1780	5.5	5	1	0.5	0	0	0
1781	6.5	11	1	1	0.7	0	0
1783	6.5	4	1	1	0.5	0	0
1787	5.5	3	1	1	0.5	0	0
1796	7		1	1	1	0	0
1799	6.5	12	1	1	0.6	0	0
1801	5.5	6	1	1	1	0	0
1802	8		1	1	1	1	0
1806	7		1	1	1	0	0
1810	7		1	1	1	0	0
1810	6		1	1	0	0	0
1811	7		1	1	1	0	0
1815	5.5	3	0.5	0	0	0	0
1818	7.5		1	1	1	0.5	0
1826	5.5		1	0.5	0	0	0
1831	7.5	25	1	1	1	0.6	0
1832	7.5	98	1	1	1	0.6	0
1834	5.5	12	1	1	1	0	0
1836	7.5	26	1	1	1	0.9	0
1839	6		1	1	0	0	0
1850	6		1	1	0	0	0
1857	6.5	22	1	1	0.6	0	0
1864	6.5	13	1	1	0.6	0	0
1866	7		1	1	1	0	0
1868	6	5	1	1	0.5	0	0
1869	7.5	5	1	1	1	0.6	0
1869	6.5		1	1	0.5	0	0
1873	6.5	15	1	1	0.6	0	0
1876	7		1	1	1	0	0
1877	6.5	6	1	1	0.6	0	0
1879	5.5	6	1	0.5	0	0	0
1881	6.5	24	1	1	0.8	0	0
1882	7		1	1	1	0	0

			Prob				
Year	**Int**	**Np**	**V**	**VI**	**VII**	**VIII**	**IX**
1882	6.5	37	1	1	0.6	0	0
1884	6		1	1	0	0	0
1886	6		1	1	0	0	0
1889	6		1	1	0	0	0
1891	8.5	403	1	1	1	1	0.6
1891	6		1	1	0	0	0
1891	6		1	1	0	0	0
1892	7		1	1	1	0	0
1892	6.5	100	1	1	0.6	0.1	0
1892	6		1	1	0	0	0
1894	7		1	1	1	0	0
1894	6.5		1	1	0.5	0	0
1894	6.5	116	1	1	0	0	0
1895	6		1	1	0	0	0
1895	6		1	1	0	0	0
1895	6		1	1	0	0	0
1895	6		1	1	0	0	0
1896	6		1	1	0	0	0
1897	5.5	47	1	0.5	0	0	0
1898	6.5	313	1	1	1	0.2	0
1898	6.5	73	1	1	0.8	0	0
1898	5.5		1	0.5	0	0	0
1901	8		1	1	1	1	0
1904	6		1	1	0	0	0
1907	6		1	1	0	0	0
1908	6		1	1	0	0	0
1908	6		1	1	0	0	0
1908	4.5	18	0.5	0	0	0	0
1909	6.5	799	1	1	0.3	0	0
1909	6		1	1	0	0	0
1913	5		1	0	0	0	0
1915	6		1	1	0	0	0
1918	6		1	1	0	0	0
1923	6		1	1	0	0	0
1927	6		1	1	0	0	0
1928	6.5	35	1	1	0.6	0	0
1929	7		1	1	1	0	0
1930	6		1	1	0	0	0
1932	7.5	21	1	1	1	0.7	0
1934	5.5	29	1	1	0	0	0
1936	6		1	1	0	0	0
1937	6.5	34	1	1	1	0	0
1937	6		1	1	0	0	0

			Prob				
Year	**Int**	**Np**	**V**	**VI**	**VII**	**VIII**	**IX**
1940	6		1	1	0	0	0
1940	5		1	0	0	0	0
1942	6		1	1	0	0	0
1943	6.5	29	1	1	1	0	0
1943	6		1	1	0	0	0
1947	6		1	1	0	0	0
1948	5		1	0	0	0	0
1951	5	154	1	1	0.5	0	0
1956	6		1	1	0	0	0
1957	6		1	1	0	0	0
1960	6		1	1	0	0	0
1961	6		1	1	0	0	0
1962	6		1	1	0	0	0
1965	5.5	32	1	0.1	0	0	0
1965	5		1	0	0	0	0
1966	6		1	1	0	0	0
1967	6		1	1	0	0	0
1967	6		1	1	0	0	0
1967	5.5	47	1	0.4	0	0	0
1967	5		1	0	0	0	0
1968	6		1	1	0	0	0
1968	5		1	0	0	0	0
1969	5.5	15	1	0.4	0	0	0
1970	6		1	1	0	0	0
1970	6		1	1	0	0	0
1970	6		1	1	0	0	0
1971	7.5	229	1	1	1	0.9	0
1972	6		1	1	0	0	0
1975	5.5		1	0.5	0	0	0
1976	7		1	1	1	0	0
1983	6.5	850	1	1	0.7	0	0
1986	6		1	1	0	0	0
1987	6		1	1	0	0	0
1987	6		1	1	0	0	0
1989	6		1	1	0	0	0
1995	5.5		1	0.5	0	0	0
1996	7		1	1	1	0	0
1999	5		1	0	0	0	0
2004	7.5		1	1	1	0.1	0
2012	7.5		1	1	1	0.5	0

3. Comparing Estimates of MRT

The previous study concluded that the uncertainty on Mean Return Times for seismogenic zones in the Po Plain is about 25%. The estimates obtained for the probabilistic catalogue are here compared with standard ones.
When dealing with semi-integer data, there are two customary approaches, either assigning all the intensities to the lower or to the higher value. The relevant results are described in the following as the Min and Max respectively.
Figure 1 reports the comparison between the Mean Return Times for the three different catalogues obtained using the approach for intensity data described in Albarello and Mucciarelli (2002)

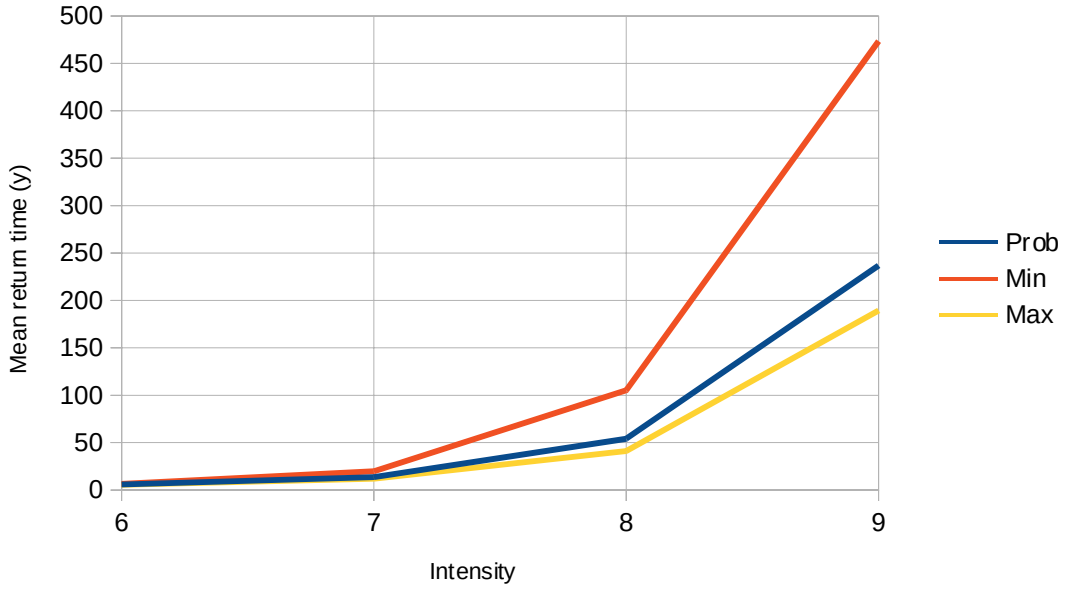

Figure 1. Comparison between the MRTs for three different catalogues

It is possible to note that the probabilistic approaches returns results closer to the Max approach, while the Min catalogue gives rather under-conservative values.
To better appreciate the relation between the different estimates for increasing intensities, Fig. 2 reports the variation between the estimates, calculated as:

%(M-Prob)/M

where M can be Min or Max.
With respect to the Max approach, the variation for the intensities between VII and IX is in the range 15-30%, thus confirming the results on uncertainties estimated for synthetic catalogues in Mucciarelli (2014)

4. Conclusions

The revision of the historical data to provide a probabilistic approach to the epicentral intensities highlighted some problems in parametrisation of intensity catalogues.
A expert judgement formalised as a probability intensity vector allowed for the calculation of Mean return times. These values were then compared with the result of a standard approach that forces uncertainty on intensity on nearest integer values.

The outcome showed that the minimum variation in the estimate of MRT is ranging from 15 to 30% for intensities comprised between VII and IX.
After this exercise, some open questions remain:

1) it is difficult to parametrise intensities in a quantitative, formal scheme when the original data is scarce;
2) it would be interesting to compare the results obtained here with those that can be derived from an alternative probabilistic estimates of intensity provided from another, independent expert judgement;
3) a deeper reappraisal of the catalogue could be performed including also non-semi-integers epicentral intensity considering that also integer values could be attributed with a large associated uncertainty.

The presence of uncertainty in PSHA estimates obtained from intensity data should be considered in the validation activities foreseen in Project SIGMA.

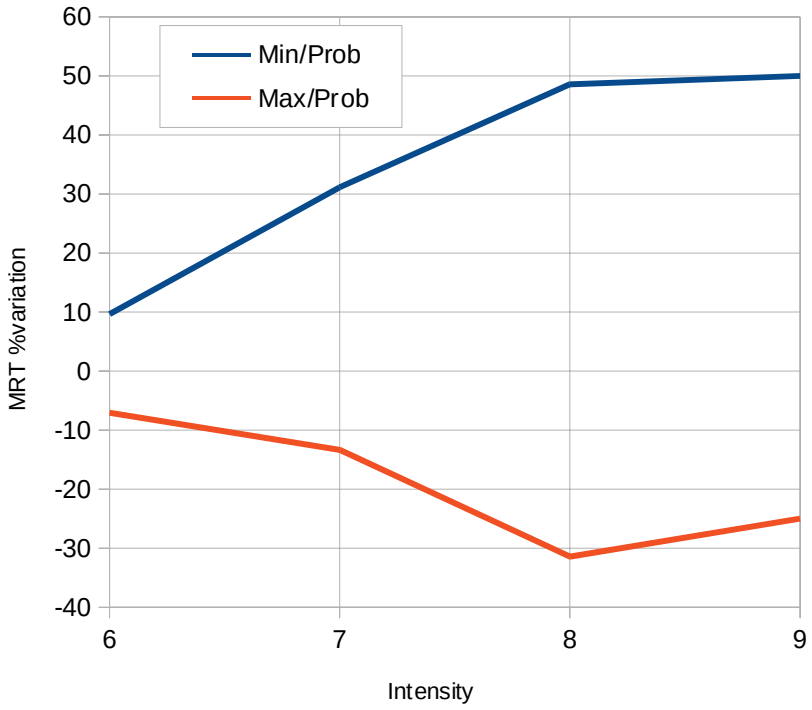

Figure 2. Variation between MRT for probabilistic and standard catalogue

REFERENCES

Mucciarelli M. (2014) Uncertainty in PSHA related to the parametrization of historical intensity data, Natural Hazards and Earth System Science, 14, 2761–2765, doi:10.5194/nhess-14-2761-2014

Albarello D. and Mucciarelli M.(2002) Seismic hazard estimates from ill-defined macroseismic data at a site, Pure Appl. Geophys. 159, 1289–1304.

CSNI Workshop on "*Testing PSHA Results and Benefit of Bayesian Techniques for Seismic Hazard Assessment*"
4-6 February 2015, Eucentre Foundation, Pavia, Italy

Testing Probabilistic Seismic Hazard Estimates Against Accelerometric Data in two countries: France And Turkey

H. Tasan[1], C. Beauval[1], A. Helmstetter[1], A. Sandikkaya[2], P. Guéguen[1]

[1]ISTerre, Université Grenoble Alpes, IRD, CNRS, OSUG, BP 53, F-38041 Grenoble, France, celine.beauval@ujf-grenoble.fr

[2]METU, Department of Civil Engineering, Earthquake Engineering Research Center, Middle East Technical University, K6 Building, 06800 Ankara, Turkey

SUMMARY

Probabilistic seismic hazard models (PSHM) are used for quantifying the seismic hazard at a site or a grid of sites. In the present study, we test these models by comparing the expected number of sites with exceedance with the observed number, considering an acceleration threshold at a set of recording sites. The method is applied to France and Turkey. The results show that the MEDD2002 and AFPS2006 PSH models over-estimate the number of sites with exceedance for low acceleration levels (below 40 $cm.s^{-2}$) or short return periods (smaller than 50 yrs for AFPS2006 and 475 yrs for MEDD2002). For larger acceleration levels, there are few observations and none of the models is rejected. In Turkey, the SHARE hazard estimates can be tested against ground-motion levels of interest in earthquake engineering. As the completeness issue is crucial, the recorded data at each station is analyzed to detect gaps in the recording. As most accelerometric stations are located on soil, accelerations at rock are estimated using a site-amplification model. Different minimum inter-site distances and station configurations are considered. The observed numbers of sites with exceedance are within the bounds of the predicted distribution for accelerations between 103 and 397 $cm.s^{-2}$. For higher levels, both the observed number and the predicted percentile 2.5 are zero, and the model cannot be rejected.

Keywords: *Probabilistic seismic hazard analysis, Statistical seismology*

1. Introduction

Probabilistic seismic hazard maps are now the basis for establishing seismic building codes in most parts of the world. These maps provide at geographical locations the ground motions with given probabilities of being exceeded in a future time period. Validation of these hazard maps with observations at a single site is challenging due to the limited duration of observations compared with the return time of interest for civil engineering. But by considering many sites

simultaneously, we can compensate for the short duration of observations. This work builds on previous studies (Papazachos *et al*. 1990; Ward, 1995; Stirling and Petersen, 2006; Albarello and D'Amico 2008; Mucciarelli *et al*. 2008; Stirling and Gerstenberger, 2010) that used observations to test hazard maps. We develop a method for testing probabilistic seismic hazard estimates available at the sites of an accelerometric network, and for exploring the uncertainties of the method. The aim here is to test the final output of the probabilistic calculations, the hazard curve.

In the first part of this article, we present the method used to test probabilistic hazard estimates. The method is first applied in metropolitan France, a low-to-moderate seismicity region, using the French Accelerometric Network (RAP). Then, the same methodology is applied to a more active region, Turkey, using accelerometric data recorded by the Turkish Strong-Motion network. More details on this work are given in Tasan et al. (2014).

2. Method for testing PSH models against observations

The French and Turkish accelerometric networks have been built progressively, since 1995 in France and since 1973 in Turkey, and lifetime of stations varies from a few months to a few decades. The test must be able to handle varying station lifetimes to take advantage of the full database. We consider the number of sites with exceedance, rather than the exact number of exceedances, although both studies are possible. At each site, the expected number of exceedances follows a Poisson distribution characterized by its mean ($\lambda_i t_i$), where t_i is the station lifetime. Monte Carlo simulations are performed to sample the site-specific Poisson distributions and generate numbers of acceleration exceedances for all sites, for a virtual network having the same number of stations and the same lifetimes as the accelerometric network. We thus obtain the distribution of the expected number of sites with exceedances, which is then compared with the observed number.

3. Testing PSHA in France

3.1 Accelerometric database

In France, the first stations of the accelerometric network were installed in 1995 (French Accelerometric Network, RAP, Péquegnat *et al*. 2008). Since then, the number of stations has increased, reaching at present a total of 142 sites in Metropolitan France. Out of these 142 sites, 69 are identified as 'rock sites' ($V_{S30} \geq 760$ m/s). Stations in buildings and boreholes are not used, yielding a total of 62 rock stations, mostly located in regions with the highest seismic hazard in metropolitan France. The database extends over 16 years, from June 1995 to July 2011. We first selected 2207 records with Peak Ground Acceleration (PGA) higher than 1 $cm.s^{-2}$, whatever the magnitude of the earthquake. We checked carefully the database and corrected several issues: bad association of records with responsible earthquake, bad station clock, shift of signal baselines, truncation of records, and low signal-to-noise ratio. To ensure independency of sites, stations located closer than 10 km to another rock station have been discarded (7 stations). In this case, we kept the station with the largest expected number of exceedances during the station lifetime. Twenty-eight stations have been recording between 5 to 10 years and 29 stations have been recording between 10 to 16 years. Three rock stations have recorded a PGA>100 $cm.s^{-2}$. At 15 rock stations, no ground motion higher than 1 $cm.s^{-2}$ occurred during their lifetime, these stations

are nonetheless included in the analysis. The final dataset used for testing PSH models contains 701 records detected at 47 rock sites corresponding to 551 earthquakes (Fig. 1).

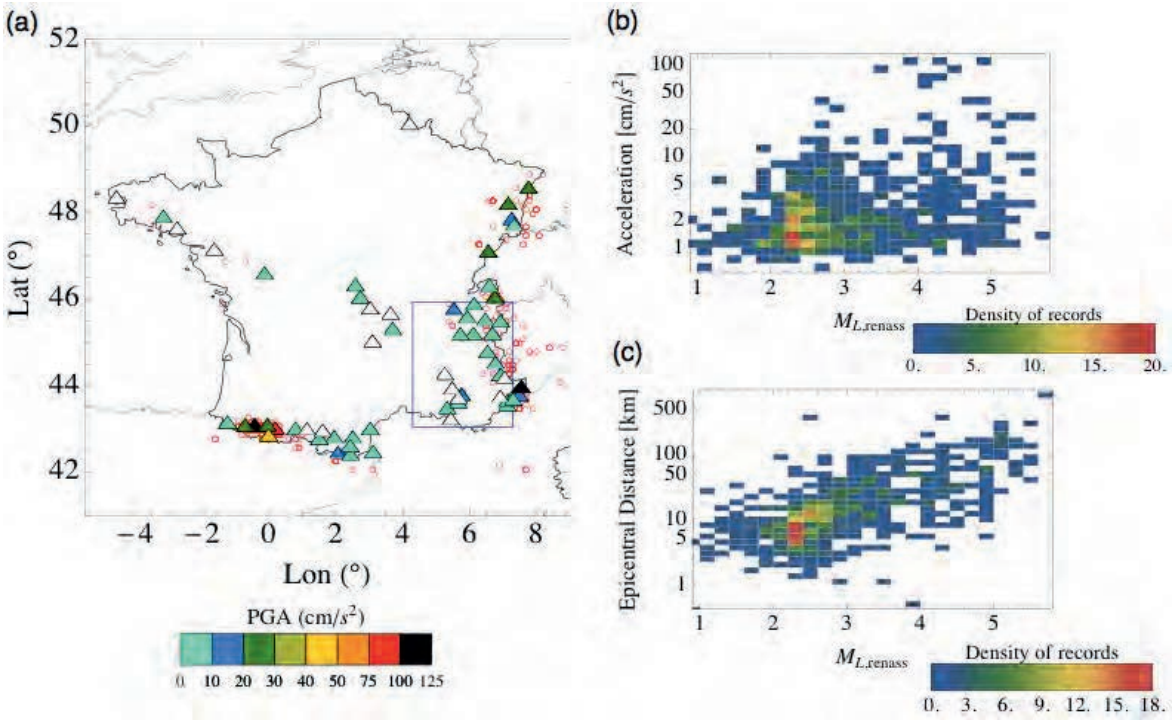

Figure 1: The accelerometric dataset built from the RAP raw database, for testing PSHA in France. (a) Colored triangles: the 47 rock stations which have experienced at least one PGA ≥1 cm/s^2 during their lifetime, white triangles: 15 remaining rock stations. Color scale: maximum acceleration recorded at each station. Circles: responsible earthquakes. (b) Distribution of all PGA amplitudes against the magnitude of the corresponding earthquake (M_{L_Renass}). (c) Distribution of epicentral distances of these records against the magnitude of the corresponding earthquake.

For our analysis, it is of primary importance to use a complete database, or at least to identify gaps in the recording. We identified potential gaps by analyzing the inter-event times (times between successive earthquakes) of the acceleration sequence, based on the raw RAP database (no threshold on the acceleration). Average inter-event times were calculated, and inter-event times larger than 10 times the mean were considered as gaps in the recording. Station lifetimes were shortened accordingly. We obtain a total corrected lifetime of 449 years. Another test can be applied to check the completeness of our database, using an earthquake catalog and a GMPE. Using the Cauzzi and Faccioli (2008) equation, which fits well the French dataset (Beauval *et al*. 2012), we looked for earthquakes in the Renass earthquake catalog that should have produced a median acceleration larger than 10 cm.s^{-2} at the stations considered. From 58 records, 8 were missing. Five of them occurred within previously identified gaps. For the three remaining earthquakes, we found no explanation for the missing record. This suggests that the fraction of missing records (after correcting from identified gaps in the monitoring) is around 5% (3/58).

3.2 PSH models

Two PSH models are considered in the present study. The MEDD2002 model has been derived for the official French seismic building code (Martin *et al.* 2002). The AFPS2006 model was developed later on (Martin and Secanell 2006). Both models rely on the same seismicity models; the main difference in AFPS2006 with respect to MEDD2002 is the treatment of magnitude conversions and the ground-motion prediction equations used. The AFPS2006 study predicts hazard values that are always lower than or equal to the values of MEDD2002 model. The hazard values are given on a grid of 0.1°x0.1° and are estimated at the location of each accelerometric station by averaging the values at the 4 closest cell's nodes. Minimum magnitudes used in the probabilistic calculations vary for each PSH model. In MEDD2002 study, the minimum magnitude is $M_{L,LDG}$=4 in local LDG magnitude. In AFPS2006 study, the minimum magnitude varies with the GMPE used, between 2.5 ($M_{L,LDG}$) and 5 (M_S). In the present study, all accelerations recorded at the stations are taken into account, regardless of the magnitude of the earthquake. The PSH models provide median hazard curves as well as percentiles deduced from the logic tree, but we only consider the median curves.

3.3 Testing results at the RAP sites

The AFPS2006 study provides accelerations for 10 return periods between 5 and 10,000 years. Obviously, the accelerations corresponding to these return periods vary from one site to the other. For this model, we use a fixed acceleration threshold, common to all sites. The useful range is defined by the maximum of minimum accelerations of hazard curves (23 cm.s^{-2} for the return period 5 yrs), and by the minimum of maximum accelerations of hazard curves (130 cm.s^{-2} for 10,000 yrs). The example in Fig. 2 shows the results for 23 cm.s^{-2}. The 7 sites with exceedance are highlighted on the map and the responsible earthquakes are indicated. The probability distribution of the expected number of sites with exceedance is very close to a binomial distribution. The percentiles 2.5 and 97.5 correspond respectively to 9 and 21 sites with exceedance. For this threshold PGA≥23 cm.s^{-2}, the model thus predicts more sites with exceedance than observed (7). The MEDD2002 study provides hazard results only for 4 return periods starting from 100 years to 1975 yrs. There is no common acceleration range between the 62 RAP sites. For this reason, this model is tested for a fixed return period rather than a fixed acceleration threshold.

Results of the test are shown in Fig. 3. For model AFPS2006 (Fig. 3a), observations are consistent with the model, i.e. within the percentiles 2.5 and 97.5, for PGA≥40 cm.s^{-2}. For the two lowest levels tested (23 and 30 cm.s^{-2}), the observed number of sites with exceedance is much lower than predicted by the model. We tested AFPS2006 also at fixed return periods (Fig. 3b). The AFPS2006 model predicts more exceedances than observed at 20 years return period. Between 50 and 200 years, the model is consistent with the observations. Results for MEDD2002 model are shown for 100, 475 and 975 years (Fig. 3c). The observed number of sites with exceedance (1) is lower than the 2.5 percentile at 100 years (2 sites) and the model is rejected. For 475 and 975 years, the model is not rejected, however there is no exceedance, and the 2.5 percentile is also zero. This is not surprising, since these return periods are larger then the total length of the observations (449 yrs). In such a case, very different models may be consistent with the observations. In order to obtain meaningful results, we need longer time windows or a larger number of sites so that the expected total number of exceedances is larger than zero.

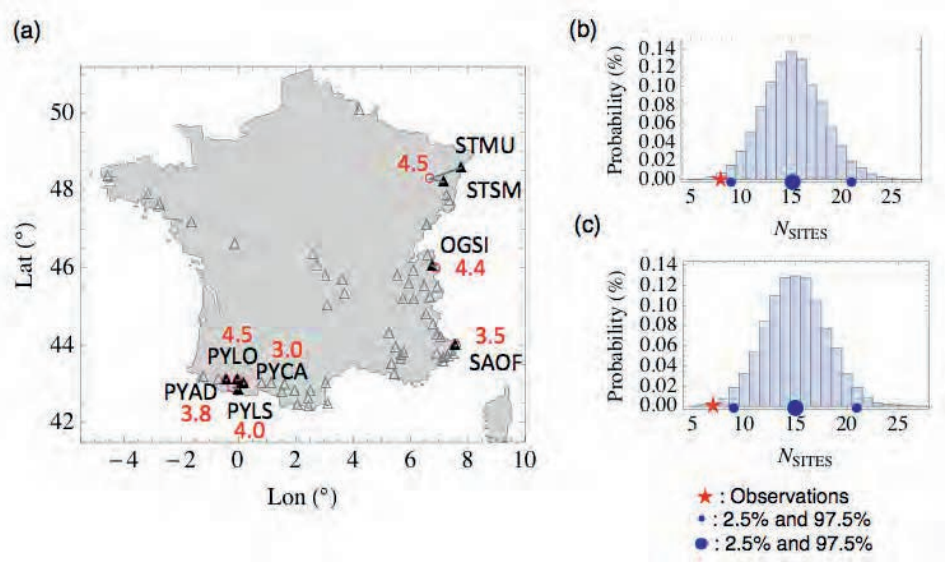

Figure 2: Testing the AFPS2006 model for the acceleration threshold A_0= 23 cm/s^2. (a) Locations of the 8 stations, out of 62, which recorded a PGA≥A_0 (black filled triangles), and responsible events (circles, M_w indicated). b) observed number of sites with exceedance superimposed on the probability distribution predicted by the PSH model. In this example, the model over-predicts the observations; c) two records producing exceedance are related to the same earthquake (stations STMU and STSM), excluding one station from the analysis does not change the conclusions (predictions are for 61 stations).

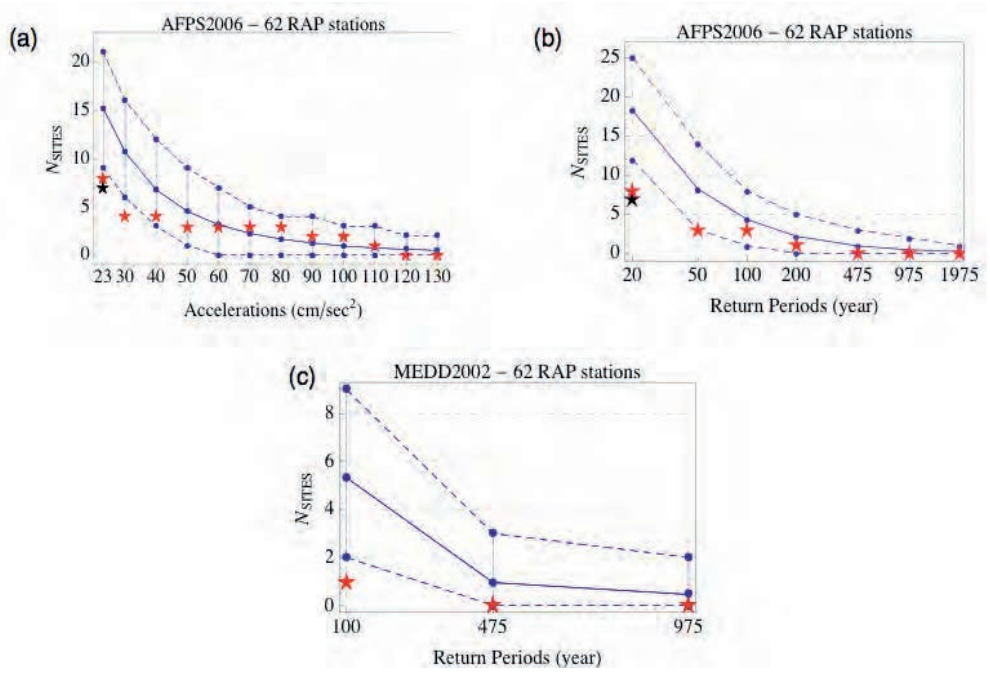

Figure 3: Predicted and observed number of sites with exceedance. Blue curves: median and percentiles 2.5 and 97.5 of the predicted distributions, red stars: observed number of sites, black stars: reduced number of sites in the case of double-counting (see Fig. 2). Results for the AFPS2006 PSH model considering (a) a range of acceleration thresholds and (b) a range of return period thresholds. (c) Results for MEDD2002 model, considering 3 return periods.

The testing method assumes that all events are independent. To reduce the correlation between records, stations closer than 10 km from each other have been excluded prior to the analysis. Moreover, the list of earthquakes responsible for the threshold exceedances was systematically checked. In a few cases when two records at two stations were produced by the same earthquake, we simply discarded the site with the lowest acceleration recorded. We also checked that the database used for the test contains no aftershock.

4. Testing PSHA in Turkey

A similar study is led in Turkey, a region of much higher seismic activity, where hazard estimates can be tested for higher accelerations, of greater interest in earthquake engineering. We consider the probabilistic seismic hazard results produced during the SHARE project (Giardini et al. 2013, www.share-eu.org). The minimum magnitude used in the probabilistic calculation is M_w 4.5. Hazard estimates corresponding to the logic-tree mean are tested against accelerometric data.

4.1 Accelerometric dataset

In Turkey, the first strong-motion instruments were installed in 1973. At the beginning of 2009, the total number of strong motion stations in the national network was 327. The majority of the events in the database are shallow crustal earthquakes (depths less than 15 km) associated with the North and East Anatolian transform faults. The main source of our accelerometric dataset is the RESORCE ground-motion database (Akkar et al. 2014). RESORCE is a single integrated accelerometric databank for the broader European area, consisting of earthquake and station metadata information, and accelerometric data. The Turkish component of RESORCE relies strongly on the T-NSMP strong-motion database, covering the time window between 1976 and 2011, and including ground motions from magnitudes 2.8 to 7.6 (Mw). We selected 56 records with PGA≥50 $cm.s^{-2}$ from RESORCE database, recorded at stations with known V_{S30}. We also included 44 records from the Turkish Strong Motion network (TR-NSMN, http://kyh.deprem.gov.tr) to extend the time window until 2013/3/13. In total, we used 100 records at 291 stations with known V_{S30}. The database is illustrated in Fig. 4.

The SHARE probabilistic seismic hazard curves are calculated for rock sites (V_{S30}=800 m/s), whereas less than 6% of the Turkish stations are actually located at rock. Sandikkaya et al. (2013) developed a site-amplification function using a subset of the strong-motion SHARE database. This equation was used to estimate the PGA_{750} at rock from the recorded PGA.

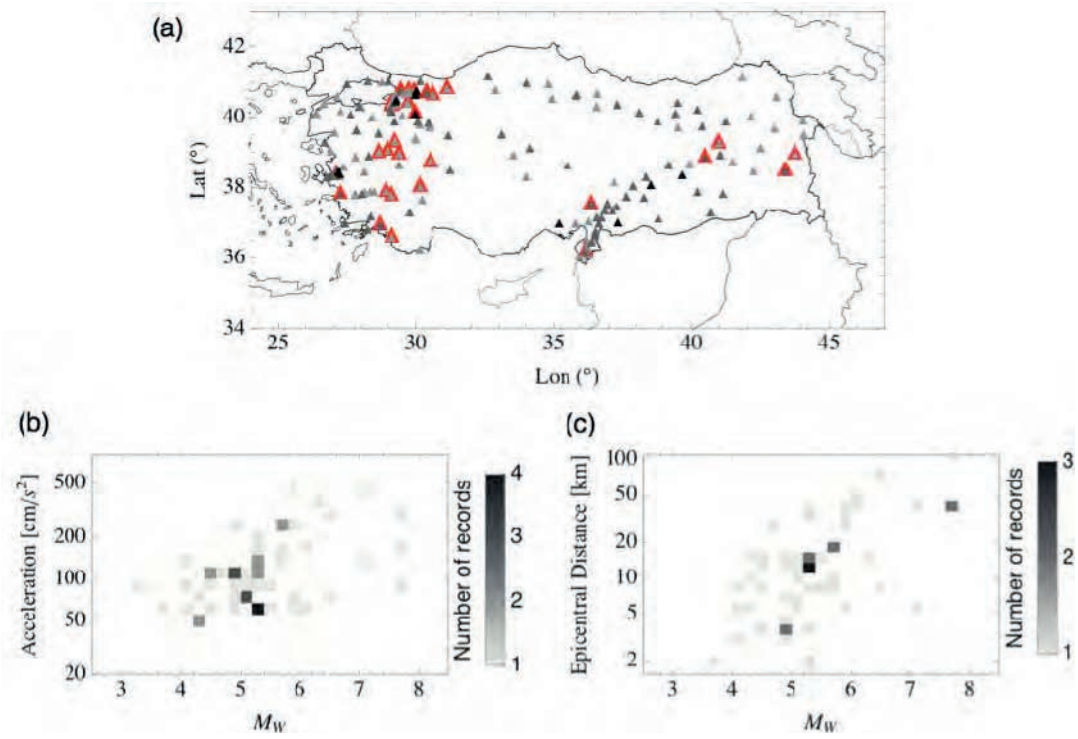

Figure 4: (a) map of the 189 selected accelerometric stations. Red Triangles: 30 stations that observed a $PGA_{750} \geq 50$ cm.s^{-2}. Distribution of the final 56 records with $PGA_{750} \geq 50$ cm.s^{-2}, (b) in terms of PGA versus M_w of the earthquake ; (c) in terms of epicentral distance versus M_w.

For testing PSHA against observations, completeness is a key aspect. Operating lifetime of stations must be known, as well as the periods when the stations were out of order. Unfortunately, this information is not available. A quick look at the data shows that some stations have been operating only a few months, sometimes with years apart. The gaps in the data can only be estimated from the recording histories. Two methods are proposed here which provide two sets of complete time windows. These methods use the (raw) data recorded at the stations, without any threshold amplitude. At 87 stations (out of 291), less than 2 records are available, and nothing can be inferred from this data about their operating lifetime. These stations are discarded. Applying the methods for detecting gaps, 15 stations are left with observation time window equal to zero. Therefore, our dataset is finally made of 189 stations and 56 records with PGA≥50 cm.s^{-2}. But only 30 stations recorded a PGA higher or equal to 50 cm.s^{-2} (Fig. 4).

4.2 Detecting gaps in the data

The first method is the same as that used for the French accelerometric database. The gaps in the (raw) data are detected based on the average inter-event time, estimated using a declustered catalog, without any threshold on PGA. All inter-event times longer than 10 times the average are considered as gaps. In the second method, gaps in the data are identified thanks to synthetic

accelerations, obtained by coupling a ground-motion prediction equation (Akkar and Çağnan, 2010) with the earthquake catalog used in SHARE and EMME projects for Turkey. Here gaps are identified whenever one or more acceleration higher than or equal to 10 cm.s^{-2} is missing in the recorded data. The gap is defined as the time elapsed between two consecutive observations including the missing records. Unlike the first method relying on inter-event times, this technique can detect gaps even when the stations recorded very few data. The method based on synthetic data identifies more gaps (total corrected lifetime of 892 yrs) than the method based on inter-event times (total corrected lifetime of 1177 yrs). The true total lifetime is likely between these bounds. Corrected lifetimes of stations vary from a few months to 22 years at maximum.

4.3 Testing results

We use the same testing method as for the French database. The results are shown in Figure 5. Considering both methods used to identify gaps, we found that observations are consistent with the model for PGA≥103 cm.s^{-2}. However, at 74 cm.s^{-2} and 52.7 cm.s^{-2}, the observed number of sites with exceedances is much lower than the 2.5 predicted percentile. Imposing a minimum inter-site distances of 10 km, the number of stations is reduced from 189 to 137, but the conclusions are the same.

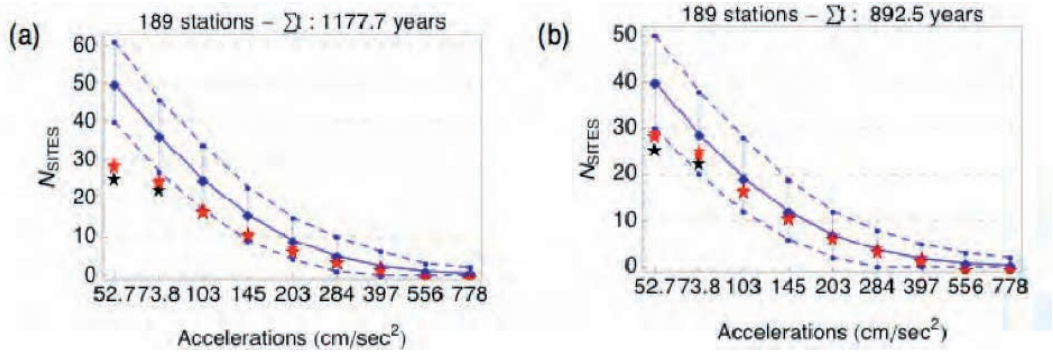

Figure 5: Comparison of the observed and predicted number of sites with exceedance at different acceleration levels, using (a) the 1st set of corrected lifetimes (1177 years in total); or (b) 2nd set of corrected lifetimes (889 years in total). Blue curves: median and percentiles 2.5 and 97.5 of the predicted distributions; Red stars: observations. Black stars: reduced number of sites in case of double-counting.

5. Conclusions

We have tested probabilistic seismic hazard models against accelerometric datasets in France and Turkey. In France, we found that the AFPS2006 PSH model is consistent with the observations of the RAP network for PGA≥40 cm.s^{-2} and for 50-200 years return periods (62 sites, 449 yrs in total), but this model overestimates the number of exceedances for smaller accelerations. The MEDD2002 PSH model is provided all over France only for 4 return periods, from 100 to 1975 years. For 100 years, there is only one site with exceedance, which is less than predicted. For longer return periods (475 and 975 years), both observed and predicted numbers equal zero and the model cannot be rejected. To compensate for the short duration of the RAP database (449 yrs in total), we also tested both models with a synthetic dataset, build by coupling an earthquake

catalog (LDG) with a GPME. This extends the total lifetimes to 2108 yrs but does not change the conclusions. The results for France are thus very limited, as only low accelerations have been recorded (≤0.1g) which are not of real interest in earthquake engineering. Most important, these results show that conclusions obtained for a given acceleration level cannot be extrapolated to other (higher) levels. Moreover, although AFPS2006 and MEDD2002 provide different hazard curves, the observations available do not permit to discriminate between these models. Applying the same method in Turkey enable to test probabilistic seismic hazard estimates over an acceleration range useful for earthquake engineering (~0.1 to 0.5g). As the completeness issue is crucial, the recorded data at each station is analyzed to detect potential gaps in the recording. As most accelerometric stations are located on soil, the recorded PGA are converted to PGA at rock using the site-amplification of Sandikkaya et al. (2013). The test is carried considering all stations (189), then 137 stations with a minimum inter-site distance of 10 km. All tests provide comparable results: the SHARE PSHA mean model is consistent with the observations between 103 and 397 $cm.s^{-2}$ but overestimates the number of exceedances for 53 $cm.s^{-2}$. For PGA>400 $cm.s^{-2}$, both the observed number and the predicted percentile 2.5 are zero. More work should be led to analyze why all PSH models studied here overestimate observations for low accelerations.

REFERENCES

Akkar, S., Çağnan, Z., Yenier, E., et al., 2010. The recently compiled Turkish strong motion database: preliminary investigation for seismological parameters. *J. Seism.*, 14(3), 457–479.

Akkar, S., et al., 2014. Reference database for seismic ground-motion in Europe (RESORCE). *Bull. seism. Soc. Am*, 12(1), 311–339.

Albarello, D. & D'Amico, V., 2008. Testing probabilistic seismic hazard estimates by comparison with observations: an example in Italy, *Geophys. J. Int*., 175, 1088–1094.

Beauval, C., et al. 2012. On the Testing of Ground Motion Prediction Equations against Small Magnitude Data., *Bull. seism. Soc. Am.*, 102, 1994–2007.

Cauzzi, C. & Faccioli, E., 2008. Broadband (0.05 to 20 s) prediction of displacement response spectra based on worldwide digital records, *J. Seism.*, 12, 453–475.

Giardini, D., et al. 2013. Seismic Hazard Harmonization in Europe (SHARE): Online Data Resource, doi:10.12686/SED-00000001-SHARE.

Martin, C., et al. 2002. Révision du zonage sismique de la France: étude probabiliste, Geoter Report, GTR/MATE/0701-150.

Martin, Ch. & Secanell, R., 2006. Développement d'un modèle probabiliste d'aléa sismique calé sur le retour d'expérience, Phase 2: Calculs et cartographie suivant l'arbre logique défini par le groupe « zonage », Geoter Report, GTR/CEA/0306-294, 39 pages (in French).

Mucciarelli, M., Albarello, D. & D'Amico, V., 2008. Comparison of Probabilistic Seismic Hazard Estimates in Italy., *Bull. seism. Soc. Am.*, 98, 2652–2664.

Papazachos, B.C., 1990. Seismicity of the Aegean and surrounding area, *Tectonophysics*, 178, 287–308.

Pequegnat, C., et al., 2008. The French Accelerometric Network (RAP) and National Data Centre (RAP-NDC)., *Seism. Res. Lett.*, 79, 79–89.

Sandıkkaya, M. A., Akkar, S. & Bard, P., 2013. A Nonlinear Site-Amplification Model for the Next Pan-European Ground-Motion Prediction Equations, *Bull. seism. Soc. Am.*, 103 (1), 19–32. doi:10.1785/0120120008.

Stirling, M. & Gerstenberger, M., 2010. Ground Motion–Based Testing of Seismic Hazard Models in New Zealand., *Bull. seism. Soc. Am.*, 100, 1407–1414.

Stirling, M. & Petersen, M., 2006. Comparison of the Historical Record of Earthquake Hazard with Seismic- Hazard Models for New Zealand and the Continental United States., *Bull. seism. Soc. Am.*, 96, 1978–1994.

Tasan, H., C. Beauval, A. Helmstetter et al., 2014. Testing probabilistic seismic hazard estimates against accelerometric data in two countries: France and Turkey, Geoph. Journal Int., 198(3), 1554-1571, ISSN 0956-540X

Ward, S.N., 1995. Area-based tests of long-term seismic hazard predictions. *Bull. seism. Soc., Am.*, 85, 1285–1298.

CSNI Workshop on "*Testing PSHA Results and Benefit of Bayesian Techniques for Seismic Hazard Assessment*"
4-6 February 2015, Eucentre Foundation, Pavia, Italy

Regulatory View on Challenges in PSHA in Low Seismicity Areas

Janne Laitonen*, Jorma Sandberg, Pekka Välikangas
Radiation and Nuclear Safety Authority (STUK), Finland, * janne.laitonen@stuk.fi

SUMMARY

Finland, especially the southern part, lies in a seismically very quiet intraplate area with old bedrock at the surface. No destructive earthquakes have been observed and the earthquakes cannot be connected with know fault zones (diffuse seismicity).

When the operating nuclear power plants (NPPs) were built, there were no requirements for seismic design in the Finnish regulations. The current Guide YVL B.7 (Provisions for internal and external hazards at a nuclear facility) requires, however, that probabilistic seismic hazard assessment (PSHA) shall be used in the estimation of the design basis earthquake for NPPs. The return period shall be at least 10^5 years with median confidence level but the peak ground acceleration (PGA) shall be at least 0.1 g. The Guide does not contain explicit requirements on the methods or standards to be used. The licensees choose the method and the nuclear regulatory authority (STUK) evaluates its applicability case-by-case. Today, seismic design is not required in conventional Finnish building projects. Therefore, the seismic engineering community is small and the methods for seismic hazard assessment have not been established. Also, the amount of national data suitable for determining ground motion prediction equations is limited and international data has to be used.

The capacities of the operating NPPs to resist earthquakes have been analyzed in the probabilistic risk assessment (PRA) framework. The current estimates for PGA are at Loviisa site 0.06 g and at Olkiluoto site 0.085 g (return period 10^5 years and median confidence level). The biggest seismic risk contributors in Loviisa NPPs are steam generators and feed water tanks whose HCLPF (High Confidence of Low Probability of Failure) values are close to the estimated site PGA. Hence, albeit low seismic core damage frequency (CDF), it can be assumed that the estimate for seismic CDF is sensitive for the seismic hazard estimate due to small safety margin.

The revision of the seismic hazard is on-going in Finland: The licensees of the operating NPPs (TVO and Fortum) are jointly revisiting the seismic hazard for southern Finland (Loviisa and Olkiluoto sites). The licensee of the Pyhäjoki green field site (Fennovoima) continues the hazard assessment for northern Finland in co-operation with Finnish and Swedish organizations, e.g., the Helsinki University Institute of Seismology, Finland and the Uppsala University, Sweden. Results of the preliminary studies done for the alternative sites at the earlier stage of the project indicate that the PGA values for the northern Finland may be considerably higher compared to southern Finland, up to about 0.35 g. Especially for northern Finland, some PSHA calculations

have resulted in unexpectedly high PGA values. Therefore, the possible methods for testing PSHA results are of interest in Finland.

Keywords: *Probabilistic seismic hazard analysis, risk assessment, nuclear power plant*

1. Introduction

Finland is situated in the north-western part of Europe and belongs to the Baltic shield. Especially the southern part of Finland lies in a seismically very quiet intraplate area with old bedrock at the surface. No destructive earthquakes have been observed and the earthquakes cannot be connected with know fault zones (diffuse seismicity). The most severe instrumentally registered earthquake in the vicinity of the Finnish sites is the magnitude 4.7 earthquake in Estonia in 1976 [1]. Altogether about ten earthquakes with magnitude higher than 4.5 have been observed in Finland [1]. Albeit the low seismic activity, seismic risk analyses of the operating Finnish nuclear power plant (NPP) units have shown that seismic risks may be significant if seismic loads have not been considered in the design.

The four operating NPP units are located in southern Finland: Loviisa site, with two 500 MWe VVER 440/213 units (LO1 and LO2), is operated by Fortum and Olkiluoto site, with two 840 MWe BWR units supplied by Asea-Atom (OL1 and OL2), is run by Teollisuuden Voima (TVO). All units, commissioned in 1977–1982, use seawater as the ultimate heat sink and have been constructed on hard crystalline bedrock. On both sites there are fresh and spent fuel storage facilities and final disposal facilities for low and intermediate level radioactive waste.

The unit under construction at the Olkiluoto site, Olkiluoto 3 (OL3), is a 1600 MW EPR type pressurized water reactor. In addition, the Finnish Government has granted decisions in principle for a fourth unit at the Olkiluoto site (OL4) and for one unit (FH1) to be built by a new utility, Fennovoima, on a green field site located in Pyhäjoki, northern Finland. The underground final repository for the spent fuel will be constructed in Olkiluoto in hard crystalline bedrock by Posiva (co-owned by Fortum and TVO).

As for seismic events and their risks on the NPPs, the interest is often on vibrations, measured by peak ground acceleration (PGA) or perhaps by absolute velocity, but for the underground final repository for the spent fuel, the attention has focused mainly on shifts and associated relative displacements. Hence, Posiva focuses on finding out possible correlations between shifts and earthquake magnitudes.

The current understanding among the Finnish nuclear regulatory authority (STUK) and the licensees is that the risks due to seismicity seem to be on an acceptable level. But, the three beyond design basis seismic events (Kashiwazaki-Kariwa 2007, Fukushima 2011, and North Anna 2011) have made STUK concerned whether the underlying assumptions and the current seismic hazard assessments are up-to-date in Finland. In addition, STUK has got an impression that the seismic hazard estimates have increased globally, possibly due to the aforementioned events, and some hazard assessments for northern Finland have resulted in unexpectedly high PGA values. Nowadays, also the instrumentation to measure seismicity is better than before in Finland and there have been some present events in Fennoscandia that may be utilized in verification of the ground motion prediction equations (GMPE) or that may cause the need to revisit or revise the seismic hazard curves, e.g., the earthquake of magnitude about 4.2 in Central-

Sweden on 15th September 2014 [2]. Hence, the possible methods for testing the probabilistic seismic hazard assessment (PSHA) results and Bayesian techniques are of interest in Finland.

The aim of this paper is to mainly provide information on the PSHA results in Finland and to describe some of the challenges that the regulatory authority has faced in the decision making on the acceptability of the seismic design versus the estimated seismic hazard (e.g., low safety margin and possible sensitivity for the uncertainties associated with the current hazard estimates).

The paper is organized as follows: Next, the regulatory requirements for probabilistic risk assessment (PRA) and seismic design are described briefly. Then, the backgrounds and some results from probabilistic seismic hazard assessment in Finland are provided after which a few case examples from the seismic PRAs are given. Conclusions end the paper.

2. Regulatory requirements for PRA and seismic design

The requirements on PRA have been included in the mandatory legislation since 1988. The general requirements are set forth in the Nuclear Energy Decree and in the Government Decree on Nuclear Safety. The detailed requirements on the use of PRA are given in the Regulatory Guide YVL A.7 (probabilistic risk assessment and risk management of a nuclear power plant, 15.11.2013 [3]) that specifies the following probabilistic safety goals:

- Mean value of the core damage frequency (CDF), as estimated from a comprehensive level 1 PRA, is less than 10^{-5} / year.
- Mean value of a large radioactive release (more than 100 TBq Cs-137) frequency (LRF), as estimated from a comprehensive level 2 PRA, is less than 5×10^{-7} / year.

The Guide requires an up-to-date, full-scope PRA for power operation and low-power and shut-down states, including internal events, fires, floods, seismic events, harsh weather conditions and other external events. The given safety goals apply as such to new NPP units. For operating units, the principle of continuous improvement is applied.

There were no requirements for seismic design in the Finnish regulations when the operating NPPs were built and the seismic verification of the operating units is based on a comprehensive PRA. The Regulatory Guide YVL B.7 (provisions for internal and external hazards at a nuclear facility, 15.11.2013 [3]) requires, however, that probabilistic seismic hazard assessment (PSHA) shall be used in the estimation of the design basis earthquake for NPPs. In the estimation, the return period shall be at least 10^5 years with median confidence level but the peak ground acceleration (PGA) shall be at least 0.1 g. The Guide does not contain explicit requirements on the methods or standards to be used. The licensees choose the method and STUK evaluates its applicability case-by-case.

To reach the probabilistic safety goals for CDF and LRF, it is essential that the fragilities of the components are small and that the reliability of the containment is high also above the design basis PGA. Hence, it is important to evaluate the fragilities of structures and components at accelerations higher than the design basis.

Due to the low seismic activity, only the safe shutdown earthquake is relevant in Finland. In areas with higher seismic activity, an operating basis earthquake with recurrence period comparable to the operating life of the plant is defined as another seismic design value. The normal operation of the plant should be possible in the case of an operating basis earthquake. In Finland the operating

basis earthquake would be so weak that it would not result in any practical requirements for the plant systems.

3. Seismic hazard assessment in Finland

Finland is situated on the Baltic shield, which is the one of the seismically quietest areas in the world. The push from the North Atlantic Ridge in the NW-SE direction seems to be the major source for the stress field related to the seismicity of Finland. Other factors of the stress field, such as post-glacial rebound and local seismotectonics, are more local. Earthquake recurrence rates in Fennoscandia are very low if compared with plate boundary regions worldwide. Nonetheless, Fennoscandia is an active seismic region, although at low earthquake recurrence rates and with relatively low magnitudes. [4]

The earthquake catalog for Northern Europe (FENCAT – Fennoscandian earthquake catalog [1]), maintained by the Institute of Seismology of the University of Helsinki, has been utilized for source term calculations in order to obtain PSHA results for the Finnish NPP sites. The catalog includes all documented earthquakes in Fennoscandia and adjacent areas since 1375. Instrumental earthquake observations started in Finland in the 1920's and local short period recordings started in 1956. The events in Finland and in Fennoscandia have been predominantly instrumentally located since the mid 1960's. The instrumental magnitudes are based on the Richter's classical local magnitude scale, M_L, modified for the Fennoscandian region. The uncertainty of macroseismic magnitudes is assumed to be 10% at best. [4] Figure 1 shows the distribution of the earthquake epicenters in Finland and surroundings according to FENCAT [1].

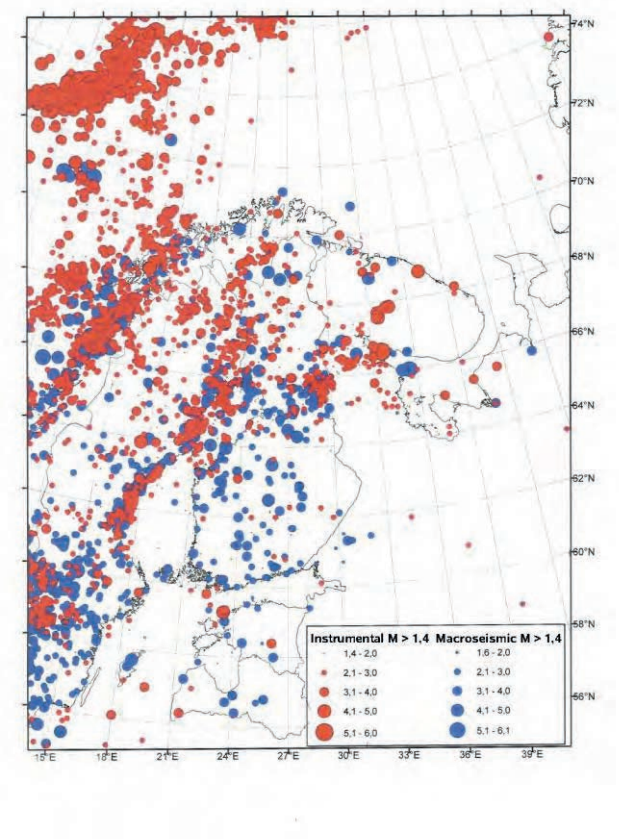

Figure 1: The distribution of the earthquake epicenters in Finland and surroundings in FENCAT [1]. Picture taken from [5].

In the early 1990's, seismic hazard analysis was done for Loviisa and Olkiluoto NPP sites in order to perform seismic PRAs although not required by the Finnish regulations. However, the shape of the ground response spectrum was taken from Swedish literature. Approximately ten years later, the Finnish regulations had advanced and required seismic design for NPPs. Therefore, seismic hazard was estimated for southern Finland by determining GMPEs and source terms by Varpasuo [6, 7, 8] in order to obtain seismic design specifications for OL3 NPP -project. Because there were no registered strong motion acceleration recordings of earthquakes in Finland, the earthquake recordings from Saguenay and Newcastle regions in Canada and Australia were taken as sources of initial data because of their geological and tectonical similarity to Fennoscandia. Site effects are not relevant in Finland as the sites are located on solid bedrock. The calculated horizontal PGA was about 0.06 g at Loviisa site and 0.085 g at Olkiluoto site (return period 10^5 years and median confidence level). But, the minimum design PGA is 0.1 g at both sites.

In 2008, the seismic hazard was assessed for the three alternative sites of the Fennovoima NPP project, two sites in northern Finland (Pyhäjoki and Simo) and one in southern Finland in the immediate vicinity of the Loviisa site. The analysis was done for Fennovoima by the Finnish Institute of Seismology. The delineation of seismic source areas differed from the one used in the earlier hazard assessment for southern Finland, e.g., the whole southern Finland was considered as one source area whereas in the analysis by Varpasuo the same region consisted of approximately four source areas. Possibly due to this difference, the results were unexpectedly high also for Loviisa and Olkiluoto sites. Therefore, STUK financed a comparative study [5] that used the same assumptions as Varpasuo (source area delineation and GMPEs) along with the Cornell's PSHA methodology and SEISRISKIII code. Figure 2 shows the calculated PGA values from this study. Hazard studies were continued by Fennovoima in co-operation with Finnish and Swedish organizations, e.g., the Helsinki University Institute of Seismology, Finland and the Uppsala University, Sweden. Preliminary results indicate that the PGA values for the northern Finland are considerably higher compared to southern Finland, up to about 0.35 g. Fennovoima will deliver to STUK the final results along with the construction license application by the end of June 2015.

In parallel with the studies by Fennovoima, TVO and Fortum are jointly revisiting the seismic hazard for southern Finland. The work was initiated due to the possible fourth unit to be built in Olkiluoto. But, it can also be utilized in the safety assessment of the underground final repository for the spent fuel to be constructed in Olkiluoto (although the interest focuses mainly on shifts and associated relative displacements instead of PGA) and in up-dating the seismic PRAs of the operating units.

Due to the low seismicity, seismic design is not required in conventional building projects (exceptions for this are export industry and possibly future high-rises) and therefore the Finnish seismic engineering community is small and the methods for PSHA have not been established. In addition, some PSHA studies have resulted in unexpectedly high PGA values. Figure 2 illustrates quite high differences between PGA values in southern Finland and high rise of PGA estimation between Pyhäjoki (FH1 site) and about 100 km north at Simo. Nowadays, also the instrumentation to measure seismicity is better than before in Finland and some present events in Fennoscandia may be utilized in verification of the GMPEs or may cause the need to revisit or revise the seismic hazard curves. Hence, the possible methods for testing the probabilistic seismic hazard assessment (PSHA) results and Bayesian techniques are of interest in Finland.

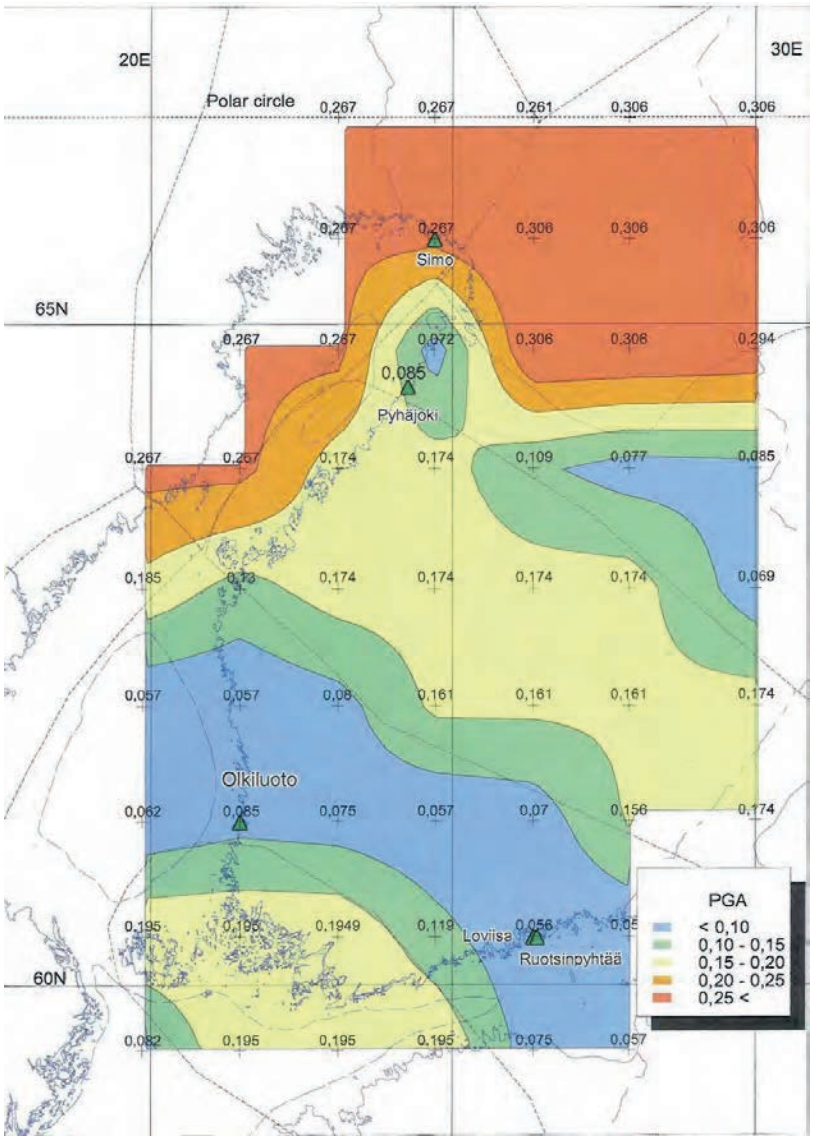

Figure 2: PGA values for southern and northern Finland according to [5].

4. Results from seismic PRAs

When the operating NPPs were built, seismic design was not required in the Finnish regulations. The capacities of the operating NPPs to resist earthquakes have been analyzed later in the probabilistic risk assessment framework. The first seismic PRA for Loviisa NPP units was done in 1992 and it was up-dated in 2010. For Olkiluoto NPP units 1 and 2 seismic risks were analyzed in 1997 and up-dated in 2008.

The current estimates for PGA are at Loviisa site 0.06 g and at Olkiluoto site 0.085 g (return period 10^5 years and median confidence level). The CDF due to seismicity is approximately 1.3×10^{-7} / year for Loviisa NPP units, 1.7×10^{-7} / year for Olkiluoto NPP units 1 and 2, and 1.3×10^{-8} / year for Olkiluoto NPP unit 3 which is seismically designed. The share of seismic risks is around or less than 1 % of the total CDF for all units.

Previously, the seismic risk for Olkiluoto units 1 and 2 was higher but the vulnerabilities were removed by plant modifications. The risk was mainly due to poor supports of batteries, rectifiers and inverters of direct current systems. When the supports were improved, the seismic risk was reduced to a fraction. The remaining risk was mainly due to relay chatter possibly resulting in dangerous combinations of spurious signals that could lead, in the worst case, to simultaneous opening of reactor relief valves and isolation of emergency core cooling systems. Plant modifications were later implemented to fix the problem.

For Loviisa NPP, the most vulnerable components are steam generators and feed water tanks whose HCLPF (High Confidence of Low Probability of Failure) values are close to the estimated site PGA. The break in steam generators leads to loss of coolant accident and the break of a feed water tank is considered to lead to core damage with high probability. Hence, albeit low seismic core damage frequency (CDF), it can be assumed that the estimate for seismic CDF is sensitive for the seismic hazard estimate due to small safety margin. The small safety margin, the uncertainties related to the seismic hazard assessments as described in the previous section, and the events mentioned in the introduction have made STUK concerned if the seismic hazard assessments are up-to-date and what methodologies there are to test the results.

5. Conclusions

Seismic risk analyses of the operating Finnish NPP units have shown that seismic risks may be significant even in a region with low seismic activity if seismic loads have not been considered in the design. The most serious risks have been due to inadequate anchorage or supports of electric and electronic equipment. It has been possible to remove most of these risks by relatively simple hardware modifications. For new power plant units, extensive seismic design analyses, qualification and risk studies will be carried out.

The possibly small safety margin of the Loviisa NPP units, the uncertainties related to the seismic hazard assessments, and the three beyond design basis seismic events (Kashiwazaki-Kariwa 2007, Fukushima 2011, and North Anna 2011) have made STUK concerned whether the underlying assumptions and the current seismic hazard assessments are up-to-date in Finland and what methodologies there are to test the results.

Because the seismic hazard has a direct impact on seismic risk STUK has considered that it is important to understand and study the uncertainties related to these hazards. Therefore, STUK has promoted the rather small seismic engineering community in Finland to study this subject, e.g., some Finnish seismologists participated the meeting on SSHAC-methodology in South-Africa and the Finnish Research Programme on Nuclear Power Plant Safety (SAFIR) includes research projects on seismic safety of nuclear power plants (SESA).

REFERENCES

[1] FENCAT – Fennoscandian earthquake catalog. Institute of Seismology, University of Helsinki. Available on-line: http://www.seismo.helsinki.fi/fi/bulletiinit/catalog_northeurope.html.

[2] Earthquakes recorded by the Finnish seismic network. Institute of Seismology, University of Helsinki. Available on-line: http://www.seismo.helsinki.fi/fi/havainto/maanjaristykset/pohjoiseurooppa.html.

[3] The Finnish nuclear legislation and the regulatory YVL Guides are available on www.stuk.fi > In English > StukLex – the legal database: http://plus.edilex.fi/stuklex/en/lainsaadanto/luettelo/ydinvoimalaitosohjeet/

[4] J. Sandberg and P. Välikangas. The Finnish Approach to Seismic Hazard Analysis – Case Loviisa. On workshop proceedings: Recent Findings and Developments in Probabilistic Seismic Hazards Analysis (PSHA) Methodologies and Applications. Lyon, France. 7-9 April 2008.

[5] J. Saari et al. Estimation of Seismic Hazard in Territory of Finland. ÅF-Consult Ltd. 18.11.2009.

[6] P. Varpasuo, Estimation of Seismic Hazard in the Territory of Southern Finland, Proceedings of the 8th International Conference on Structural Safety and Reliability (ICOSSAR). Los Angels, USA, 17-23 June 2001.

[7] P. Varpasuo, Probabilistic seismic hazard assessment for OL3 plant site in Finland, Proceedings of the CSNI Workshop: Specialist Meeting on the Seismic Probabilistic Safety Assessment of Nuclear Facilities, Jeju Island, Korea, 6-8 November 2006.

[8] P. Varpasuo, the Seismic Site Hazard Assessment for OL3 NPP in Finland, 18th International Conference on Structural Mechanics in Reactor Technology (SMiRT 18), Beijing, China, August 7-12, 2005, SMiRT18-KM01_2.

CSNI Workshop on "*Testing PSHA Results and Benefit of Bayesian Techniques for Seismic Hazard Assessment*"
4-6 February 2015, Eucentre Foundation, Pavia, Italy

A Method for Testing PSHA Outputs against Historical Seismicity at the Scale of a Territory; Example of France

Pierre B. Labbé
EDF, France, pierre.labbe@edf.fr

SUMMARY

In order to test PSHA outputs against historical seismicity data, the seismic risk is first introduced in terms of annual probabilities of occurrence of given damage degrees (EMS98 scale) on a conventional masonry building. Then out puts of seismic risk estimate from two methods are compared. The first method considers historical earthquakes of epicentral Intensities I_0 = V to IX, and statistics of affected areas. The second one is based on convolution of seismic hazard and masonry building fragility curves. Seismic hazard is described in the form of 3 different maps of the metropolitan French territory. Fragility of masonries is described in the form of a log-normal distribution of the probability of exceedance of a given damage versus the PGA. Compared to historically observed risk, a first map leads to a tremendous overestimate of the risk, a second one leads to a slight underestimate while the third one is in the middle. This approach could be used for reducing uncertainties of PSHA outputs in areas where sufficient historical data are available.

Keywords: *Seismic risk, Historical seismicity, Fragility curves, Probabilistic seismic hazard assessment, testing, hazard map.*

1. Introduction

In November 2006, the OECD-NEA (Nuclear Energy Agency) convened an expert meeting on Seismic Probabilistic Safety Assessment. As it is the rule for such NEA meetings, recommendations were made by the experts to improve engineering practices of the subject under consideration, including that "PSHA results should be compared to all available observations, especially for return periods where records are available, in order to get an objective comparison and to improve the confidence in the results, at least in that range of return periods." (*OECD 2007*). In a country like France, and in many other countries, reliable historical records are available on a rather long period of time (around a millennium). The purpose of this paper is to present a methodology to process both historical data and PSHA outputs so as to make them comparable and meet the OECD-NEA recommendation. The methodology is exemplified on the case of the metropolitan France and could be easily applied to other countries with a similar historical background.

For this purpose, it is first necessary to introduce the concept of seismic risk. In this paper the seismic risk is defined as the probability that a conventional masonry building experiences a damage grade 2 or 3 according to the definition of the European Macroseismic Scale (EMS98). Then the core of the method consists of calculating the seismic risk by two different approaches:

- The first one derives a risk evaluation from historical seismicity. It is based on a statistic analysis of earthquakes felt in France and of isoseismical maps.
- The second one evaluates the risk by convolution of hazard maps with fragility curves.

Finally the two risk estimates are compared and conclusions are drawn from this comparison. In the case of France we have 3 maps of seismic hazard at our disposal. The conclusion consists of identifying which one is the more consistent with the historical seismicity.

2. Seismic risk evaluate based on historical seismicity.

2.1. Areas Yearly Affected by a Given Intensity

2.1.1. Principle of calculation

We consider a territory with a seismic activity homogeneous (in space) and stationary (in time). Taking the example of intensity V, we denote A_V the average area of this territory yearly affected by an intensity equal to or larger than V. Conceptually, would we have at our disposal comprehensive macro-seismic data on a very long period of time (T years), calculating A_V would be easily achieved as follows : For every event i, occurring during the period of time T, we denote $\mathcal{A}_{i,V}$ the area affected by an intensity larger than or equal to V. Then

$$A_V = \mathcal{A}_V / T \quad \text{with } \mathcal{A}_V = \Sigma\, \mathcal{A}_{i,V} \tag{1}$$

Practically we do not have at our disposal the above-mentioned ideal comprehensive information. However, taking the example of the French territory, we can build on historical data as follows: We denote :

- n_{I0} ($I_0 \geq V$) the number of events of epicentral intensity I_0, felt in France during a reference period of time T, practically a century.
- $A_{I0,V}$ the average area affected by an intensity larger than or equal to V for an event of epicentral intensity I_0.

Then an estimate of A_V reads :

$$A_V = \Sigma\, n_{I0}\, A_{I0,V}, \quad I_0 = \text{V to IX} \tag{2}$$

It can be introduced in Eqn.(1) to get an estimate of A_V . Other A_I can be estimated similarly.

2.1.2 Application to the metropolitan French territory for I=V

On the basis of available data, the period of time 1895-1994 has been selected as the best documented, representative of a century of seismicity. In particular, events with an epicentre out of the French territory and felt in France are reported by *Lambert et al (1996)* and *Sisfrance (2005)*, and counted in the Table 1 (numbers are rounded-up).

Table 1 : Average number of events ($I_0 \geq V$) felt per century on the French metropolitan territory

Epicentral Intensity, I_0	V	V-VI and VI	VI-VII and VII	VII-VIII and VIII	VIII-IX
Number of events, n_{I0}	350	150	70	10	1

For the purpose of calculating $A_{I0,V}$ values, a catalogue of 140 isoseismical maps, compiled by *Levret et al. (1996)*, was processed. We do not present in this paper the detail of the statistical processing, including the treatment of extreme events *(Labbé 2007)*. A major output is that, for a given epicentral intensity, areas affected by intensity higher than or equal to V are log-normally distributed. Average values of these areas are presented in the Table 2.

Table 2 : Average area affected by an intensity ≥V for a given epicentral intensity

Epicentral Intensity, I_0	V	V-VI and VI	VI-VII and VII	VII-VIII and VIII	VIII-IX
Average affected area(km²)	180	1020	5300	16300	103000
Area inside the French metropolitan territory	120	620	2940	8790	21800

Applying the Eqn. (2) formula with data included in the Tables 1 and 2 leads to: A_V = 4500 km² on the metropolitan French territory.

2.1.3. Other intensities and variability of seismic activity in the territory

In the above presentation of the proposed methodology, we referred to the metropolitan French territory. However seismic activity cannot be regarded as homogeneous on this territory. Nevertheless it is possible to identified zones with a reasonable homogeneous seismicity. In the frame of this study, the territory was divided into two zones: a 'less prone to earthquake zone' and a 'more prone to earthquakes zone'. According to data provided by *Lambert et al., (1996)*, the later zone comprises 15% of the territory (on the basis of an administrative zoning as presented in the Fig. 1) and concentrates 56% of the activity. For both zones, areas affected by intensities V to VIII are reported in the Table 3.

Table 3. average annual value of areas (km²) affected by a given intensity (or higher)

	V	VI	VII	VIII
French metropolitan territory (538 000 km²)	4500	470	58	3,7
more prone to earthquakes zone (79 000 km²)	2500	260	32,5	3,7
less prone to earthquakes zone (459 000 km²)	2000	210	25,5	0

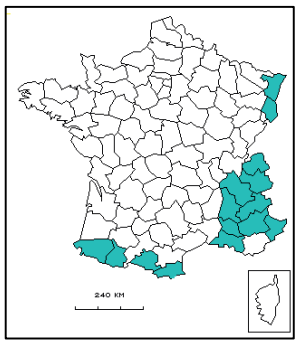

Figure 1 : More prone to earthquake zone of the metropolitan French territory (dark area)

2.2 Annual probability of a damage of grade 2 or 3 on masonry buildings

The EMS98 scale classifies types of buildings according to their sensitivity to seismic input motion and introduces a definition of damage grades. According to this scale, the proportion of masonry buildings that undergo a grade 2 or grade 3 damage is related to the intensity as reported in the Table 4. Definition of terms *some*, *many* and *most* is based on fuzzy set techniques. It leads to quantify the terms as follows: *some* is equivalent to 8%, *many* to 35% and *most* to 80%.

Table 4 : Damage rate to masonry buildings *vs* Intensity

	VI	VII	VIII
D=2 (damage grade 2)	some	many	most
D=3 (damage grade 3)	/	some	many

For evaluating the probability that a building undergoes a given damage grade, the probability it is exposed to intensity VI VII or VIII should first be established. This probability is directly derived from data presented in the Table 3. For instance, in average on the metropolitan territory the annual probability that a building is exposed to an intensity VII or higher is around $58 / 538000 = 1{,}1\ 10^{-4}$. In the more prone to earthquakes zone it is around $32{,}5 / 79200 = 4{,}1\ 10^{-4}$.

Table 5 : Annual probability that a masonry building undergoes a grade 2 or 3 damage on the basis of historical seismicity data

Damage grade	D=2	D=3
Average value in the metropolitan territory	$1{,}1\ 10^{-4}$	$1{,}1\ 10^{-5}$
Average value in the more prone to earthquakes zone	$4{,}5\ 10^{-4}$	$4{,}9\ 10^{-5}$

3. Seismic Risk based on hazard maps and fragility curves

3.1. Methodology

3.1.1 Principle of calculation

In the frame of this work, it is admitted that seismic hazard is described in the form of a hazard map derived from a PSHA of the territory under consideration. According to the usual practice, the map at our disposal provides Peak Ground Acceleration (PGA) values associated to a given return period. On any site of the territory, the annual probability that the observed PGA is greater than a is denoted $P_e(a)$[1]. Consequently the annual probability that a PGA with a value comprised between a and a+da occurs on this site is equal to $p_e(a)\,da$, so that :

$$p_e(a)\,da = -P_e'(a)\,da\ . \qquad (3)$$

Regarding a given type of buildings, its fragility is described by the probability it suffers a damage of degree D (or larger) in case it undergoes a seismic input motion, the PGA of which is equal to a. This conditional probability is denoted $P_{f,D}(a)$. The annual probability that a building of the considered type suffers a damage of degree D (or larger) is derived as follows :

$$p_D = \int_0^\infty p_e(a)\,P_{f,D}(a)\,da\ . \qquad (4)$$

[1] $P_e(a)$ is linked to the return period on the site, T(a), by : $P_e(a)=1-\exp(-1/T(a))$, or $P_e(a)=1/T(a)$ for rare events.

3.1.2. Classical forms of P_e et $P_{f,D}$ functions

It is genrally considered that $P_e(a)$ can be represented by a function of the form[2]: $P_e(a) = (a/A)^{-n}$ (practically n is in the order of 2 or 3), leading to :

$$p_e = n/A\ (a/A)^{-(n+1)} \tag{5}$$

It is also generally accepted that building fragility is log-normally distributed. It means that the population of PGAs corresponding to a damage grade greater than or equal to D is log-normally distributed; its median value is denoted a_D and the standard deviation of its natural logarithm β_D, leading to:

$$P_{f,D}(a) = \Phi\left[\frac{1}{\beta_D}\,\mathrm{Ln}\left(\frac{a}{a_D}\right)\right] \quad \text{with} \quad \Phi(u) = \frac{1}{\sqrt{2\pi}}\int_{-\infty}^{u}\exp(-t^2/2)\,dt \tag{6}$$

On the basis of these assumptions, it is possible to derive an analytical formula of p_D :

$$p_D = \left(\frac{A}{a_D}\right)^n k_D \quad , \quad k_D = \exp\frac{n^2\beta_D^2}{2} \tag{7}$$

3.2. Application to the metropolitan France, considering masonry buildings

3.2.1. Hazard data

Three hazard maps are considered, every of them deemed corresponding to a 475 y. return period : the MEDD-2002 map (*Martin and al., 2002*), the LDG-2004 map (*Marin and al., 2004*) and the AFPS-2006 map (*Martin and al., 2005*). For a given site, the PGA value read on the map is denoted a_{475} (a grid of 146 sampling sites was used). The average value of a_{475} is reported in the Table 6 for each map. The discrepancy is significant and reveals a dramatic variability in the evaluation of the seismic hazard in France, depending on the authors.

Table 6 : Average value of a_{475} for the three maps under consideration.

MEDD-2002 map	LDG-2004 map	AFPS-2006 map
0.95 ms^{-2}	0.14 ms^{-2}	0.48 ms^{-2}

At every site of the territory, $P_e(a)$ is given in the form indicated by Eqn. (8). (Selection of n values is discussed in the appendix.)

$$P_e(a) = \frac{1}{475}\left(\frac{a_{475}}{a}\right)^n \quad . \tag{8}$$

3.2.2. Fragility data

There is a lack of fragility data for conventional masonry buildings in France. Fragility data retained in the present study come from two sources. The first one (source a) is the Risk_UE project. This European project addressed the seismic risk assessment for 7 cities of the Southern

[2] Formally this formula cannot be a probability because it gives values larger than 1 in case a is lower than A; it means practically for very small PGAs. However the contribution of these very small PGAs to p_D is negligible, so that the proposed formula pertains. (On a formal view point this is valid for the annual rate of exceedance, which is the inverse of the return period).

Europe. Risk_UE established a methodology for building classification and characterization of their fragility by types. Masonry buildings were examined by the Skopje University, which has estimated values of a_D and β_D reported in the Table 7 for this type of buildings in Balkan countries (*Risk_UE 2002*). The second source (source b) is a paper by *Rota et al. (2010)*, in which fragility curves of Italian masonry buildings are presented. a_D and β_D values derived from these curves are also reported in the Table 7. We have selected damage grades 2 and 3 so as to get results comparable to those derived from historical seismicity.

Table 7 : Fragility data for masonry buildings ; left source a ; right source b

Damage grade	a_D	β_D	a_D	β_D
D=2	1.76 ms^{-2}	0.50	1.97 ms^{-2}	0.29
D=3	2.83 ms^{-2}	0.55	2.68 ms^{-2}	0.29

Concurrence of both sources on a_D values, both for damage grades 2 and 3, is remarkable and provides a certain confidence on these values, at least on their order of magnitude. However discrepancies on β_D values should also be mentioned because, in spite of concurrence on a_D values, it leads to a significant discrepancy in risk calculation (see formula 7 and calculation outputs in the next section).

3.2.3. Calculated risk

Eventually the risk is calculated according to Eqn. (9). (n values are discussed in the appendix.)

$$p_D = \frac{1}{475}\left(\frac{a_{475}}{a_D}\right)^n k_D \qquad (9)$$

On the basis of this formula, p_D values are calculated for the three maps introduced in the section 3.2.1. Average values of p_D are derived, for the metropolitan French territory as a whole and for the more prone to earthquake zone[3]. Outputs of these analyses are presented in the Tables 8-a and 8-b for fragility data of source a and source b respectively. It is pointed out that, to a very large extent, discrepancies between these two tables are due to discrepancies in β_D between source a and source b. Comparison with outputs of historical seismicity are discussed in the next section.

Table 8-a : Annual probability that a masonry building undergoes a grade 2 or 3 damage (p_D values)on the basis of hazard maps and fragility data of source a

	MEDD-2002 map		LDG-2004 map		AFPS-2006 map	
Average value in	D=2	D=3	D=2	D=3	D=2	D=3
metropolitan territory	14.6 10^{-4}	48.5 10^{-5}	0.31 10^{-4}	1.06 10^{-5}	2.83 10^{-4}	8.45 10^{-5}
more prone to earthquakes zone	47.6 10^{-4}	170 10^{-5}	1.02 10^{-4}	3.59 10^{-5}	16.0 10^{-4}	53.7 10^{-5}

[3] Practically the more prone to earthquake zone is variable from a map to the next one. For each map the boundary of this zone was determined on the basis of a criterion on the PGA. The boundary PGA is so that the area included in the more prone to earthquake zone is very close to the 79200 km^2 calculated in the section 2.

Table 8-b : Annual probability that a masonry building undergoes a grade 2 or 3 damage (p_D values) on the basis of hazard maps and fragility data of source b

Average value in	MEDD-2002 map		LDG-2004 map		AFPS-2006 map	
	D=2	D=3	D=2	D=3	D=2	D=3
metropolitan territory	$5.49\ 10^{-4}$	$21.9\ 10^{-5}$	$0.16\ 10^{-4}$	$0.72\ 10^{-5}$	$0.96\ 10^{-4}$	3.52E-05
more prone to earthquakes zone	$19.2\ 10^{-4}$	$81.2\ 10^{-5}$	$0.54\ 10^{-4}$	$2.44\ 10^{-5}$	$6.08\ 10^{-4}$	$24.3\ 10^{-5}$

4. Sensitivity study on hazard map return periods

There is a significant gap between the risk assessment based on historical data and the risk assessment based on convolution of hazard and fragility. In order to reconcile these two estimates, a sensitivity study has been carried out assuming that the return period, T, of a given map is not necessarily 475 years, so as to answer the following question: Which value should given to T so that the resulting risk (calculated as per section 3 approach) be consistent with the historically observed risk? Of course the answer is not unique. It depends on the damage grade (D=2 or 3) and on the source of fragility data (source a or b). Outputs of the four possible combinations are presented in the Table 9 for each hazard map (It is reminded that each map is deemed to represent a 475 y return period).

Table 9 : Return period (years) to be attributed to hazard maps so that the corresponding calculated risk fits the historically observed risk

	MEDD-2002 map		LDG-2004 map		AFPS-2006 map	
	D=2	D=3	D=2	D=3	D=2	D=3
Source a	7000	20000	120	450	1000	3500
Source b	2000	8000	80	300	400	1200

5. Conclusions

It is clear in the above table that fitting return periods vary widely, depending on the considered damage grade and the considered source. However, in spite of this variability, there is also a clear trend that the MEDD-2002 map considerably overestimates the hazard, while the LDG-2004 map underestimates it. Eventually, on the basis of available data at the moment for fragility of masonry buildings, it is reasonable to conclude that the AFPS-2006 map is the most in compliance with the historical seismicity of the metropolitan French territory.

Beyond the case of metropolitan France, the opinion of the author is that the proposed methodology could be successfully implemented in any country with a similar sufficiently documented historical seismicity. Consolidated fragility data for the conventional buildings of the type encountered in the country under consideration would be highly desirable. The author is convinced that checking the seismic risk value derived from hazard and fragility data against the seismic risk derived from historical seismicity, as presented in this communication, is a possible manner of complying with the recommendation of the OECD presented in the introduction. It is also a promising way of reducing uncertainties in PSHA implementation.

REFERENCES

Labbé P. (2007), Evaluation du risque sismique observé historiquement en France, *7th French National Conference on Earthquake Engineering, AFPS-2007*, Châtenay-Malabry, 4-6 juillet 2007.

Lambert J., Levret-Albaret A, (1996) Mille ans de séismes en France, Ouest Éditions, Nantes, France.

Levret A., Cushing M., Peyridieu G., (1996) Recherche des caractéristiques de séismes historiques en France, Atlas de 140 cartes macrosismiques, IPSN, France.

Marin S., Avouac J-Ph., Nicolas M., Schlupp A.(2004), A probabilistic approach to seismic hazard in metropolitan France, *Bulletin Seismological Society of America*, Dec. 2004; v. 94; no. 6; 2137-2163.

Martin Ch., Secanell R., (2005) Développement d'un modèle probabiliste d'aléa sismique calé sur le retour d'expérience, phase 1, Groupe Zonage, document de travail, GTR-CEA-1205-279, AFPS, Paris, France

Martin Ch., Combes Ph., Secanell R., Lignon G., Carbon, D., Fioravanti A., Grellet, B. (2002) Révision du zonage sismique de la France, Etude probabiliste. GTR/MATE/0701-150, MATE, Paris.

OECD (2007), Specialist meeting on SPSA for nuclear facilities, NEA/CSNI/R(2007)14, Paris

Risk_UE (2002). The European Risk_UE project: An advanced Approach to Earthquake Risk Scenarios with Application to Different European Towns. 12th ECEE, London 2002, Special session.

Rota M., Penna A., Magenes G., A methodology for deriving analytical fragility curves for masonry buildings based on stochastic non linear analyses. *J. Engineering Structures*, 32 (2010), 1312-1323.

SisFrance (2005). Catalogue des séismes français métropolitains, BRGM, EDF, IRSN, www.sisfrance.net

APPENDIX

About n value to be included in the P_e function

The formula adopted for $P_e(a)$ means that PGAs (denoted by a) and return periods (denoted by t) are linked by a relationship of the type $(t/t_0) = (a/a_0)^n$, which should be plotted as a straight line in logarithmic coordinates. Actually it is not exactly the case. Examination of hazard curves leads to the conclusion that n value depends on t (or on a) in a manner that fits the following formula:

$$n = n_{475} + \Delta n \log(t / 475) \qquad (10)$$

Practically, in the present study, n was not recalculated at every sampling site of the maps. For each map average values of n_{475} and Δn were calculated and used at every point of the territory when dealing with the map under consideration.

Table 10 : n and Δn values considered in the present study

	MEDD-2002 map	LDG-2004 map	AFPS-2006 map
n_{475}	2.7	1.75	2.7
Δn	0.3	0.25	0.3

CSNI Workshop on "*Testing PSHA Results and Benefit of Bayesian Techniques for Seismic Hazard Assessment*"
4-6 February 2015, Eucentre Foundation, Pavia, Italy

Comparison of PSHA Results with Historical Macroseismic Observations in South-East France

A. Rosti
UME School, IUSS Pavia, Italy, annalisa.rosti@umeschool.it

M. Rota
European Centre for Training and Research in Earthquake Engineering (EUCENTRE), Pavia, Italy, maria.rota@eucentre.it

A. Penna
Department of Civil Engineering and Architecture, University of Pavia and EUCENTRE, Pavia, Italy, andrea.penna@unipv.it

E. Fiorini
EUCENTRE, Pavia, Italy, emilia.fiorini@eucentre.it

G. Magenes
Department of Civil Engineering and Architecture, University of Pavia and EUCENTRE, Pavia, Italy, guido.magenes@unipv.it

SUMMARY

This paper presents a methodology for comparing the results of probabilistic seismic hazard analysis (PSHA) with historical observations, in terms of macroseismic intensities. Mean damage is identified and hence selected as the measure of the comparison. The comparison is intended to be performed by a procedure based on the use of empirical fragility curves, representative of the seismic vulnerability of the building stock at the time of macroseismic observations. Different sources of uncertainty are accounted for by the implementation of a logic tree approach. The comparison of PSHA results with observed intensities is first carried out at individual sites. Nonetheless, to make up for the limited availability of macroseismic data, a procedure for aggregating multiple sites, assuming they are affected by independent observations, is developed. Examples of application are also provided for the study area (i.e. South-East France) to better explain the methodological phases of the proposed procedures.

Keywords: *Probabilistic seismic hazard analysis, Macroseismic observations, Fragility curves.*

1. Introduction

The number of probabilistic seismic hazard analysis (PSHA) studies has been recently increasing, with significant research effort towards the definition of more precise methodologies for the quantification of seismic hazard. However, it appears that nowadays PSHA techniques are not yet mature enough to provide outputs reasonably insensitive to expert judgment [1]. This is particularly true for the case of moderate seismicity regions, such as metropolitan France, for which a lack of representative data was highlighted, with the consequence of introducing significant uncertainties in the PSHA results. Despite important technical and scientific progresses in the recent years, it is still difficult in the French seismotectonic context to identify potentially seismogenic faults and to determine the characteristics of the ground motions that such faults could generate. Therefore, the evaluation of seismic hazard for France includes very significant uncertainties related to the insufficiency and the inhomogeneous quality of the data, but also with the availability of very different methodologies and tools and the lack of a general consensus on the assumptions to be adopted in the analysis. These are some of the reasons why multiple hazard estimations, sometimes in disagreement with each other, can be found for the same region of the world. The case of France represents this lack of maturity: three different maps were established, in 2002, 2004 and 2006, leading to significant variations in the hazard assessment of the metropolitan French territory [1]. The French scientific and industrial community recently agreed on the need for an improvement of the knowledge on PSHA methodologies and of the reliability of PSHA results. This gave birth to the Project SIGMA, oriented to obtaining robust and stable estimates of the seismic hazard in France, through a better characterization of the uncertainties involved. This paper presents a methodology, accounting for several sources of uncertainty, to compare PSHA results (obtained within the SIGMA Project, [2]) with historical observations. The procedure, developed within the framework of the SIGMA project, is tentatively applied to the South-East quadrant of France. Since mean damage is selected as a measure of the comparison between PSHA predictions and historical information, a procedure to make macroseismic observations and PSHA results comparable is presented. The comparison is carried out first at single sites and then by aggregating multiple towns. In the first case, the empirically-derived rates of exceedance of predefined damage levels are simply plotted against the PSHA predictions. Conversely, when several municipalities are aggregated, the comparison is performed in terms of number of sites with exceedance of selected mean damage levels.

2. Conversion of macroseismic intensities into mean damage values

The proposed methodology starts with the identification of sites for which more complete and detailed information on macroseismic observations and building stock are available. Macroseismic observations, characterizing the seismic history of a site, should be sufficient in terms of number, entity and distribution over time to allow pertinent comparison with PSHA results. Also, it is essential to collect information on the building stock at the time of the historical events. Its subdivision into different building typologies is then accounted for by appropriate weights, depending on the environmental context of the site itself. Four masonry building typologies have been selected for the study area (i.e. South-East quadrant of France), as deemed to be representative of the historical building stock. All the typologies consist of undressed stone masonry buildings with flexible floors (Table 1). Differences concern the number of storeys (i.e. 1-2 storeys and >2 storeys) and the presence or absence of tie-rods and/or tie-beams. Table 2 reports the weights attributed to the four building typologies based on expert judgment and considering the environmental context of each considered site (i.e. cities, villages in the Alps and smaller villages). The French historical catalogue [3] attributes a different code to each macroseismic intensity, based on the reliability of the observation. Reliability of the reported intensities is expressed by codes A, B or C, according to the quality of the information linked to the observation. Code A corresponds

to a certain intensity, code B to a fairly certain intensity, whilst code C denotes an uncertain intensity value.

Table 1. Building typologies relevant for the study area

Typ. 1	Undressed stone masonry – flexible floors – w/ tie-rods and/or tie-beams– 1-2 storeys
Typ. 2	Undressed stone masonry – flexible floors – w/o tie-rods and tie-beams – 1-2 storeys
Typ. 3	Undressed stone masonry – flexible floors – w/ tie-rods and/or tie-beams – >2 storeys
Typ. 4	Undressed stone masonry – flexible floors – w/o tie-rods and tie-beams – >2 storeys

Table 2. Weights of the selected building typologies based on the environmental context

Environmental Context	w_{typ1}	w_{typ2}	w_{typ3}	w_{typ4}
City	0.05	0.50	0.15	0.30
Village in the Alps	0.10	0.60	0.10	0.20
Smaller village	0.10	0.70	0.15	0.05

In order to account for these uncertainties, a discrete distribution of intensity values, whose dispersion depends on the reliability of the observation, is defined. In particular, in the case of certain macroseismic intensity, only the value reported in the catalogue is considered. In the case of fairly certain intensity, the reported intensity value I and the intensity levels $I\pm0.5$ are defined, whereas in the case of uncertain intensity, the reported intensity value I and the intensity levels $I\pm0.5$ and $I\pm1$ are taken into account. Each discrete intensity value is then associated with a weight. In the case of codes B and C, weights are defined by assuming normal distributions centred on the reported intensity value and with a standard deviation of 0.25 and 0.50, respectively. According to this procedure, discrete intensity values are made to correspond to percentiles of the associated normal distribution. Weights are then obtained by integrating the area subtended by the normal distribution and bounded by midway percentiles (Figure 1). Table 3 reports the weights, attributed to each intensity level, depending on the reliability of the observation.

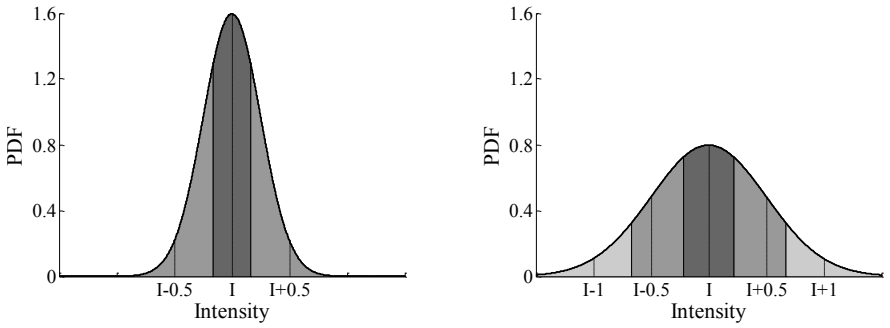

Figure 1. Normal distributions centred on the reported intensity level: codes B (left) and C (right)

Table 3. Weights attributed to the intensity levels depending on the reliability code

Intensity Level	Code A	Code B	Code C
I - 1	0	0	0.09
I - 0.5	0	0.26	0.24
I	1	0.48	0.34
I + 0.5	0	0.26	0.24
I + 1	0	0	0.09

Based on this approach, each macroseismic intensity, characterizing the seismic history of a site, is hence converted into a discrete distribution of intensity values, as shown in Figure 2. Notice that the colour of the markers correspond to the colour of the weights associated to each discrete intensity value, in accordance with Figure 1.

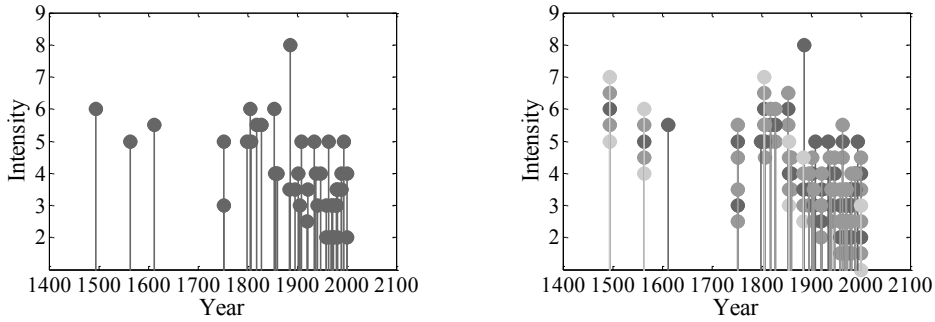

Figure 2. Seismic history (left) and seismic history accounting for the uncertainty on the macroseismic intensities (right) of a generic site

The macroseismic method proposed by Lagomarsino and Giovinazzi [4] is then applied to convert the seismic history of the site, accounting for the uncertainty in the observed intensities, into an equivalent mean damage catalogue. In particular, a closed-form analytical expression correlating mean damage and intensity, as a function of the assessed vulnerability, is used to compute the mean damage corresponding to a given intensity level, for a selected building typology. Uncertainties in the attribution of different typologies to the EMS-98 [5] vulnerability classes are accounted for by appropriate vulnerability indexes. According to the macroseismic method, for a given building typology, five vulnerability index values are derived from the corresponding membership function through a defuziffication process [6].

Differently from the macroseismic method, in this work, the five vulnerability indexes of each typology are defined as percentiles of the associated membership function (Figure 3, left). A weight is then attributed to each single index, consistently with the procedure adopted in the case of intensities. For a given building typology and intensity level, five mean damage values are therefore computed (Figure 3, right). Table 4 reports the values of the vulnerability index for each selected building typology and the corresponding weight.

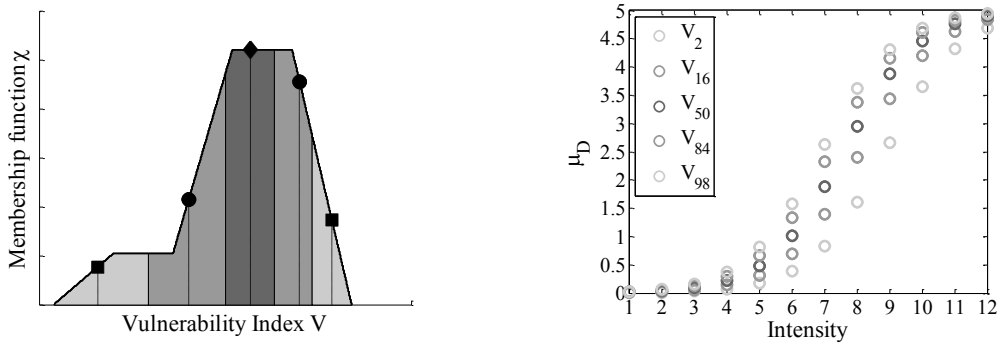

Figure 3. Membership function of building typology 4 and weights of different vulnerability indexes (left). Mean damage values versus intensity levels (right)

A critical aspect concerning the conversion of intensities into mean damage values is represented by the fact that macroseismic intensities can be expressed by different scales. In Sisfrance [3], macroseismic intensities are expressed according to the MSK scale [7], whereas the macroseismic method refers to the EMS-98 scale [5]. In this work, it has been assumed that the mean values of

each intensity class can be considered equivalent in the two macroseismic scales (consistently with literature studies [8]) whereas the uncertainty in the estimate of the intensity values is explicitly considered.

Table 4. Vulnerability indexes of the selected building typologies and corresponding weights

Index	Typology 1	Typology 2 and 3	Typology 4	Weight
V_2	0.650	0.711	0.679	0.09
V_{16}	0.686	0.773	0.801	0.24
V_{50}	0.737	0.833	0.884	0.34
V_{84}	0.794	0.870	0.950	0.24
V_{98}	0.821	0.897	0.994	0.09

To account for the several sources of uncertainty (i.e. the uncertainty in the reported intensity values, in the building stock and in the attribution of the building typologies to the different EMS-98 vulnerability classes), steps discussed so far are implemented through a logic tree approach, whose outcome is an equivalent mean damage catalogue (Figure 4). Each mean damage value is associated to a date (i.e. the year of the corresponding observed macroseismic intensity) and to a probability, given by the product of the weights of the logic tree branches.

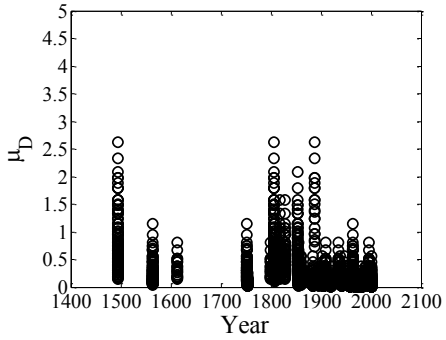

Figure 4. Equivalent mean damage catalogue for a generic site

On the other side, to allow the comparison with historical observations, the rates of exceedance obtained from PSHA studies for different PGA thresholds need to be connected to mean damage values. To this aim, PGAs are converted into mean damage values by means of fragility curves. Based on the similarity between the South-East French and Italian building stock, empirical fragility curves, derived from the statistical elaboration of post-earthquake damage data gathered after Italian earthquakes (1980-2002) [9] and then integrated by data collected after L'Aquila event (2009), are used for the conversion. The integrated dataset includes approximately 150000 buildings and allows the extension of the range of validity of the existing fragility curves [9] from 0.3g to 0.5g. For each selected building typology, the probabilities of reaching different damage levels are computed from the corresponding fragility curves. Under the assumption of a binomial distribution of the different damage grades, a mean damage curve is obtained as a function of PGA:

$$\mu_D = \sum_{k=0}^{5} p_k k \qquad (1)$$

where p_k represents the probability of having damage grade D_k (k=0÷5).
Given a PGA level, a value of mean damage can then be derived from the PGA-μ_D curve of each building typology. This step is repeated for each selected building typology providing, for a given PGA threshold as many mean damage values as the selected building typologies are. A single value of mean damage is then derived as weighted average of the different values. The conversion of PGA thresholds into mean damage values hence allows to associate PSHA rates of exceedance to

mean damage levels. These steps are sketched in Figure 5. In particular, on the left the hazard curves of a generic site are shown, whereas the mean damage curve as a function of PGA is depicted in the middle. On the right, curves connecting PSHA rates of exceedance to mean damage levels are reported.

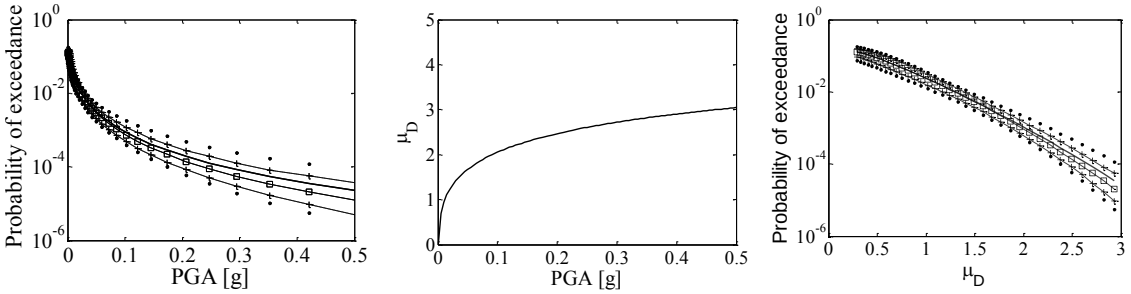

Figure 5. PSHA curves of different percentiles (left), weighted mean damage curve (middle), rates of exceedance of mean damage levels (right) of a generic site

3. Comparison at individual sites

A procedure for comparing PSHA results with historical observations at individual sites is first discussed. The comparison is carried out in terms of rates of exceedance of predefined mean damage levels. Monte Carlo method is used to sample mean damage values from the equivalent catalogue resulting from the implementation of the logic tree approach. At each run and for each predefined mean damage level, the observation period and the best estimate of the annual rate of exceedance (i.e. number of exceedances of the selected mean damage level over the corresponding observation period) are computed. Also, the 90% confidence bounds of the population proportion (i.e. number of exceedances over the number of observations in the observation period) are determined, under the assumption of binomial distribution. These limits are then converted into bounds of the best estimate of the empirically-derived rates of exceedance. Since Monte Carlo approach is repeated several times, statistics of the best estimate of the empirically-derived rates of exceedance and of its 90% confidence bounds are computed and plotted against the PSHA predictions.

4. Example of application of the methodology for individual sites

An example of application of the methodology for the comparison at individual sites is provided. Within the study area, the site of Annecy has been selected as, with respect to other towns, its seismic history shows a significant number of observations exceeding intensity level 5 (Figure 6, left). The seismic history of Annecy accounting for uncertainty in the macroseismic intensities is depicted in the middle of Figure 6. Based on the environmental context of Annecy, weights equal to 0.05, 0.50, 0.15 and 0.30 have been attributed to the selected building typologies (Table 1). An equivalent mean damage catalogue (Figure 6, right) is then obtained by applying the equation proposed by Lagomarsino and Giovinazzi [4] to each macroseismic intensity value and considering each building typology. Each mean damage value is hence associated with a probability.
As explained in a previous section, each PGA level for which PSH rates of exceedance are available is converted into a mean damage value by using empirical fragility curves. Mean damage levels can hence be associated to the rates of exceedance of the corresponding PGAs as depicted in Figure 5. Empirically-derived rates of exceedance of predefined damage levels are computed by sampling from the equivalent catalogue and statistics are plotted against the PSHA predictions (Figure 7).

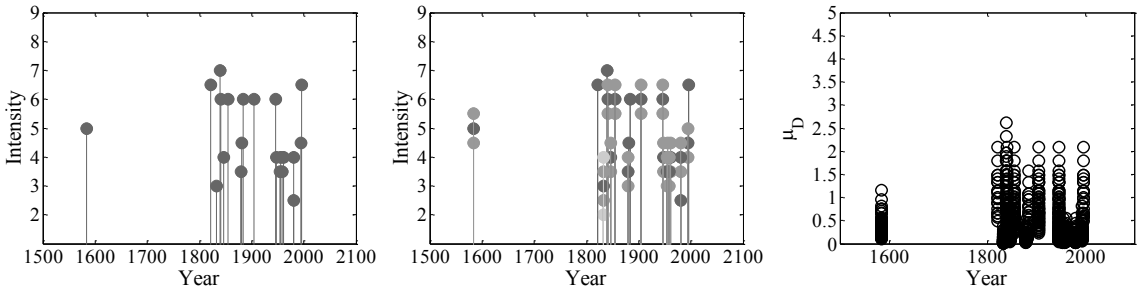

Figure 6. Seismic history (left), seismic history accounting for the uncertainty in the macroseismic intensity (middle), equivalent mean damage catalogue (right) of Annecy

In this example, ten damage thresholds, ranging from 0.5 to 2.75 with an increment of 0.25, have been selected. In the figure, red corresponds to the average empirically-derived rates of exceedance, whilst black and green correspond to the 90% confidence limits. Circles correspond to the median, diamonds to the average, whereas the error bars represent the variability over the several Monte Carlo runs (i.e. 5th and 95th percentiles). It is noted that, although the average empirically-derived rates of exceedance tend to underestimate the PSHA results, their trend is similar and close to the PSHA predictions. These rates are obviously limited by the number of observations available in the period of observation. It is also observed that uncertainties on the best estimate are smaller at low mean damage levels, whilst they increase at higher mean damage thresholds. This could be explained by the higher number of low intensity macroseismic observations (corresponding to low mean damage values), which allow to reach a higher confidence in the empirically-derived rates of exceedance.

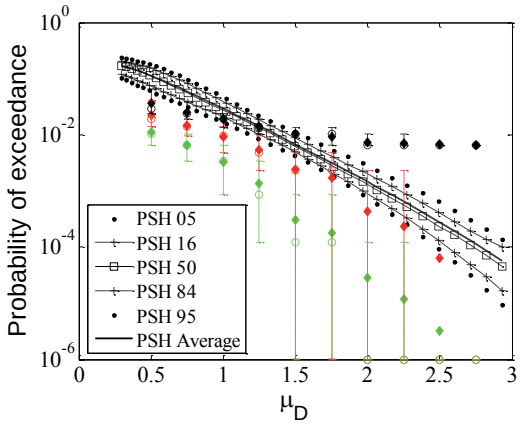

Figure 7. Comparison of PSH predictions of different percentiles with meaningful statistics of the best estimate (red) and of the upper (black) and lower (green) 90% confidence limits of the empirically-derived rates of exceedance of predefined mean damage levels (Annecy). Diamonds: average; circles: median; error bars: 5th and 95th percentiles.

5. Comparison on aggregated sites

Preliminary applications of the comparison at individual sites have shown that results are essentially affected by the seismic history of the selected places, most often characterized by a limited number of observations and/or by low intensity levels. Hence, a procedure to aggregate multiple sites has been developed. Similarly to the work of Tasan et al. [10], also developed within the SIGMA project, the aim of this methodology is to compare the observed with the predicted number of sites with exceedance, for predefined mean damage thresholds. Under the assumption

that the process of earthquakes' occurrence is ergodic, time and space can be swapped. Since the number of observations at individual sites may not be sufficient, several places are aggregated and treated as a single one. Provided that the different sites are affected by independent observations (i.e. observations generated by independent seismic events), the assumption of ergodicity allows to enlarge the observation time window. According to the procedure for converting macroseismic intensities into mean damage values, equivalent mean damage catalogues of the sites to be aggregated are fist generated. Mean damage values are then sampled from the corresponding catalogues through Monte Carlo approach. At each run, dependent observations are removed by keeping only the strongest observed mean damage value generated by each event at the sites of interest. For each preselected mean damage level, the observation period and the observed number of sites with exceedance are computed. Statistics of the observed number of sites with exceedance over the several Monte Carlo runs are then calculated. Under the assumption that the process of earthquakes' occurrence can be modeled as a Poisson process, for each site and for a predefined mean damage threshold, the expected mean number of exceedances is:

$$N_{mean} = T_{obs} \cdot \lambda \qquad (2)$$

where T_{obs} is the observation period and λ is the rate of exceedance, sampled from a lognormal distribution accounting for epistemic uncertainty in the hazard [11]. Under the assumption of Poisson process, the probability of observing n mean damage values above the selected threshold is then given by:

$$P(n) = \frac{(N_{mean})^n \cdot \mathrm{e}^{-N_{mean}}}{n!} \qquad (3)$$

According to Eq. (3), for each site the probability distribution of the number of exceedances is computed and numbers of exceedances, compatible with the PSH model, are generated by Monte Carlo approach. At each run, the number of sites with at least one exceedance is evaluated and by combining the results of the different Monte Carlo runs, a distribution of the expected number of sites exceeding a predefined mean damage level is derived (Figure 8).

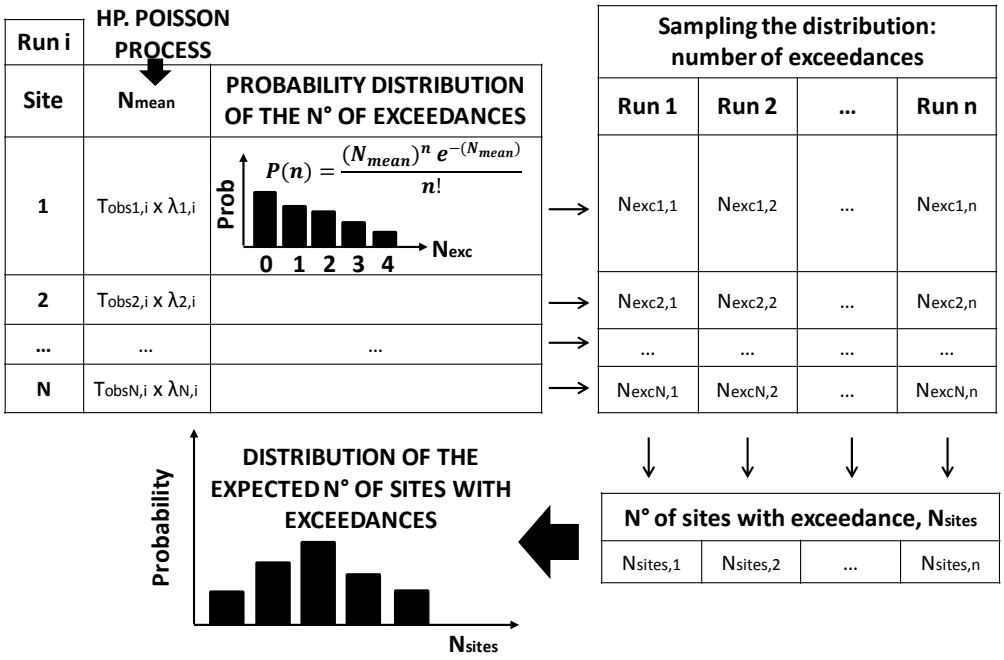

Figure 8. Sampling of site-specific Poisson distributions and generation of numbers of exceedances compatible with the PSH model. Calculation of the number of sites with exceedance and of its distribution for a mean damage level

As this procedure is repeated each time observation periods and PSH rates of exceedance are sampled, statistics of the expected number of sites with exceedance are computed and then compared with results derived from historical observations. Macroseismic observations are deemed to be consistent with PSHA predictions if falling within the 5th and 95th percentiles of the predicted distribution.

6. Example of application of the methodology for aggregated sites

An example of application of the methodology for aggregated sites is presented. Seven sites within the study area have been selected, i.e. Annecy, Albertville, Draguignan, Beaumont de Pertuis, Digne, La Mure and L'Argentières La Bessée. Based on the collected information, sites have been subdivided into different environmental categories (Table 5). This classification is essential for the attribution of the different weights to the four selected building typologies (Table 1).

Table 5. Environmental categories attributes to each site

Site	Category	Site	Category
Annecy	City	Digne	Smaller village
Albertville	Village in the Alps	La Mure	Village in the Alps
Draguignan	City	L'Argentières La Bessée	Smaller village
Beaumont de Pertuis	Smaller village		

The seismic history of each site is first transformed into an equivalent mean damage catalogue based on the procedure previously discussed. Monte Carlo approach is then used to sample mean damage values from the equivalent catalogue of each site and dependent observations, generated by the same seismic event at different places, are removed. At each run, the observed number of sites with exceedance is computed for each mean damage threshold (ten mean damage thresholds, ranging from 0.5 to 2.75 with an increment of 0.25). Distributions of the observed number of sites with exceedance are hence calculated.

On the other side, according to the procedure discussed in the previous section, distributions of the expected number of sites with exceedance are obtained for each selected mean damage level and significant statistics (i.e. median and 5th – 95th percentiles) are computed. Figure 9 shows the results obtained from this trial application of the methodology.

It is observed that, at low mean damage levels, the number of sites with exceedance derived from the observations is not consistent with the PSH model. In particular, the probability of having a smaller observed number of sites with exceedance is larger than the corresponding probability predicted by the PSHA. The opposite occurs for the higher number of sites with exceedance, for the low mean damage levels. Conversely, starting from a μ_D level of 1.75, observations are consistent with the PSH model, as they fall within the 5th and 95th percentiles of the predicted distributions.

Figure 10 (left) shows the results of the comparison for all the selected mean damage levels. On the right, the same results are plotted versus PGA values. It is observed that, for these seven sites, the PSH model gives results coincident with those derived from observations, for PGA exceeding 0.09g. For smaller PGAs (larger than 0.02g), results are still within the 5th and 95th percentiles.

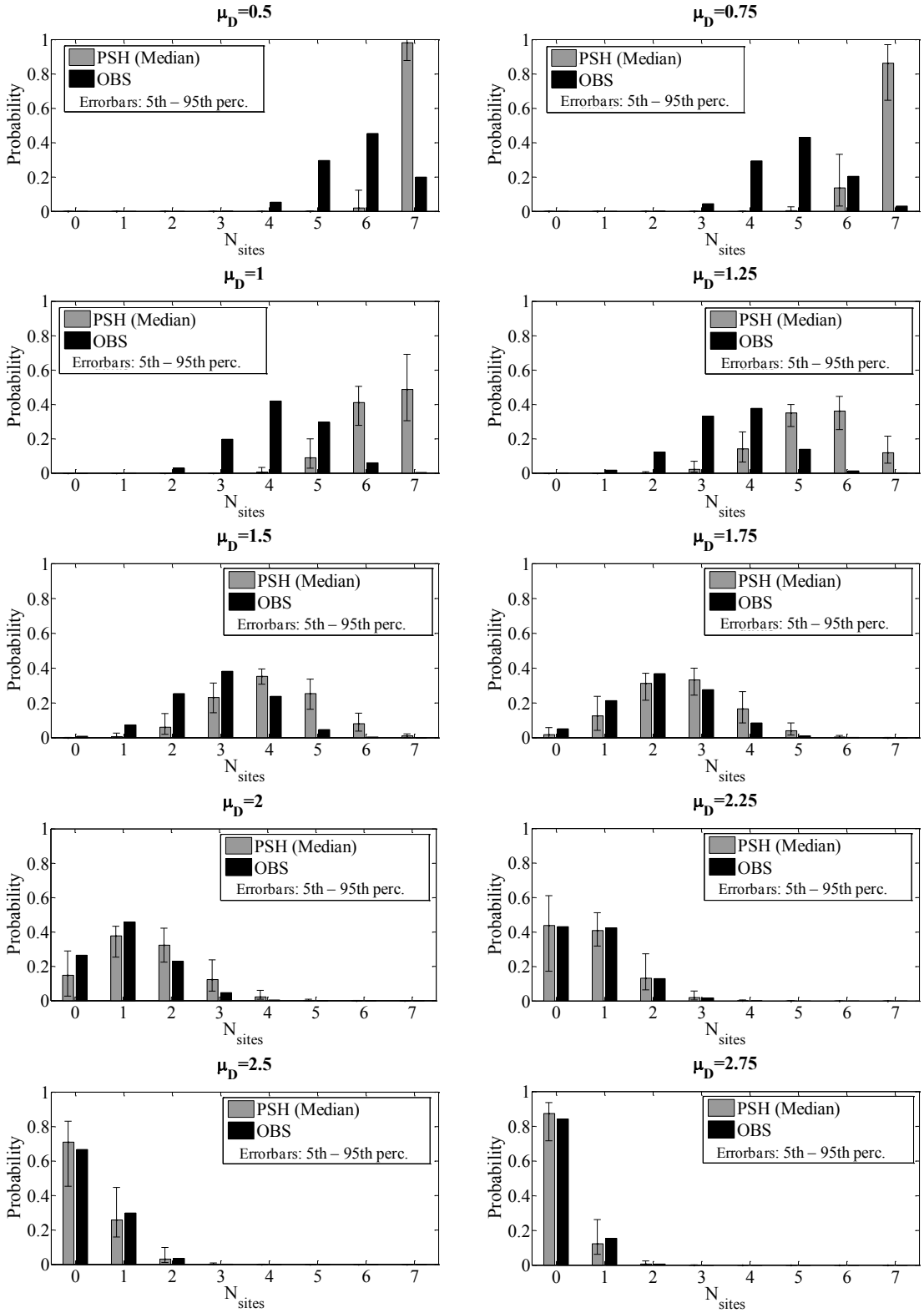

Figure 9. Comparison of the expected with the observed number of sites with exceedance for each mean damage level

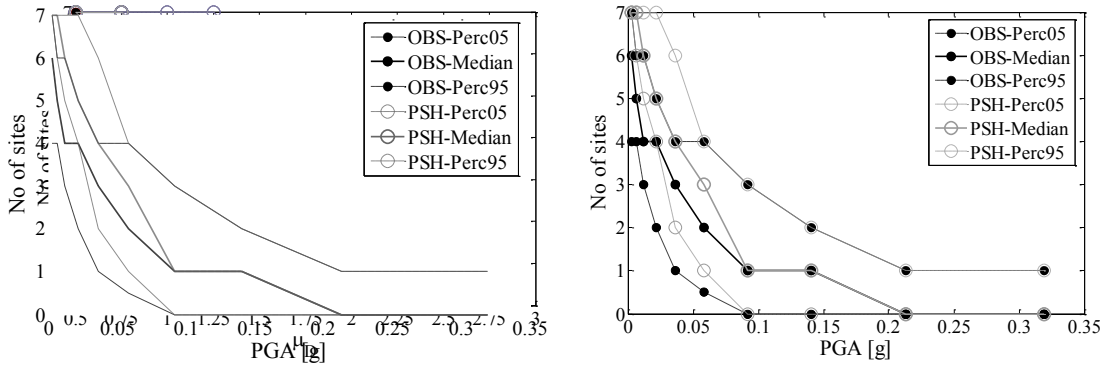

Figure 10. Summary of the comparison of the expected and observed number of sites with exceedance for all the mean damage levels (left) and the corresponding PGAs (right)

7. Conclusions

Although the probabilistic methods used for seismic hazard predictions have been continuously developed and improved over the last decades, for regions with low-to-moderate seismicity like France, the reliability of these methods can still be improved through a better quantification of the uncertainties. The quality of the results can then be estimated by comparing predictions with observations. A methodology for comparing PSHA results with macroseismic observations is here presented. Since mean damage is selected as a measure of the comparison, macroseismic observations and PSHA predictions are treated to allow the comparison in terms of mean damage. The originality of this procedure lies in the use of fragility curves to convert PGA levels, for which PSH rates of exceedance are provided, into mean damage values. The comparison of PSHA results with historical observations is first carried out at single sites. As shown by preliminary results, the comparison for single sites is strongly affected by the seismic history, which represents a critical aspect in the application of the method. Indeed, places with few observations and/or low macroseismic intensity levels, which are the large majority of the sites in France, do not allow to obtain meaningful results and to compare them with PSHA predictions. Based on these considerations, a procedure for aggregating several towns is also presented. This approach, focusing on the number of sites exceeding predefined mean damage thresholds, represents an attempt to compensate for the lack of macroseismic data available at the municipality level. The results of the comparison for aggregated sites seem promising, as they actually allow to overcome the limitations related with the number and entity of macroseismic observations at single sites. This suggests the opportunity of exploring a methodology allowing to carry out the comparison at a larger scale. The approach to be followed could be similar to the one proposed by Labbé [1], allowing the comparison at the regional scale level.

ACKOWLEDGEMENTS

This work was carried out within the Project Sigma, under the financial support of Areva. The work benefited from several useful discussions with Mr. Thiry of Areva, Dr. Senfaute of EDF, Dr. Martin of Geoter and Prof. Bazzurro of IUSS Pavia.
Very useful revisions of a previous version of the work were provided by Prof. Faccioli and Dr. Gurpinar.

REFERENCES

[1] Labbé PB. PSHA outputs versus historical seismicity Example of France. In: Proceedings of the 14th European Conference on Earthquake Engineering, Ohrid, Macedonia; 2010.

[2] Carbon D, Drouet S, Gomes C, Leon A, Martin C, Secanell R. Probabilistic analysis for France's southeast ¼ to produce a preliminary "classical" hazard map. Report Sigma WP4 T4-1, 2012.
[3] Sisfrance – Catalogue des séismes français métropolitains, BRGM, EDF, IRSN, www.sisfrance.net.
[4] Lagomarsino S, Giovinazzi S. Macroseismic and mechanical models for the vulnerability and damage assessment of current buildings. Bulletin of Earthquake Engineering 2006; 4: 415-443.
[5] Grünthal G. (ed). European Macroseismic Scale 1998 (EMS 1998). Council of Europe, Cahiers du Centre Européen de Géodynamique et de la Sismologie 1998; Vol 15.
[6] Dubois D, Prade H. Fuzzy Sets and Systems. Academic Press, New York; 1980.
[7] Medvedev S, Sponheuer W, Karník V. Neue seismische Skala Intenisty scale of earthquakes, 7. Tagung der Europäischen Seismologischen Kommission vom 24.9. bis 30.9.1962. In: Jena, Veröff. Institut für Bodendynamik und Erdbebenforschung in Jens, Deutsche Akademie der Wissenschaften 1964; 77: 69-76.
[8] Musson RMW, Grünthal G, Stucchi, M. The comparison of macroseismic intensity scales. Journal of Seismology 2010; 14(2): 413-428.
[9] Rota M, Penna A, Strobbia CL. Processing Italian damage data to derive typological fragility curves. Soil Dynamics and Earthquake Engineering 2008; 28 (10): 933-947.
[10] Tasan H, Beauval C, Helmstetter A. Testing probabilistic seismic hazard estimates against observations: application in France using accelerometric data. Paper draft to be submitted to the Bulletin of the Seismological Society of America 2014.
[11] Rota M, Penna A, Magenes G. A framework for the seismic assessment of existing masonry buildings accounting for different sources of uncertainty. Earthquake Engineering and Structural Dynamics 2014; 43(7): 1045-1066.

CSNI Workshop on "*Testing PSHA Results and Benefit of Bayesian Techniques for Seismic Hazard Assessment*"
4-6 February 2015, Eucentre Foundation, Pavia, Italy

An Application of Bayes Theorem to Test Macroseismic Intensity Data

Fiorini E.
Eucentre, Italy, Emilia.fiorini@eucentre.it

Bazzurro P.
IUSS, Italy, Paolo.Bazzurro@iusspavia.it

SUMMARY

In this work we present an application of a Bayesian updating methodology to test the credibility of available Macroseismic Intensity (MI) data at locations where secondary effects (e.g., hydrogeological effects) have been reported in the SisFrance database. The hypothesis we intend to test is whether the reported MI values may be overestimated because of damage occurrences that are not directly related to the earthquake generated ground shaking.
This Bayesian updating application, which stems from a work of Ebel and Wald [1], was developed within the framework of the SIGMA project (http://projet-sigma.com/organisation.html). The method uses Bayes theorem to estimate the probability that a certain level of a ground motion intensity measure (IM), here PGA, is experienced at a site where a given MI value has been reported. This is done by combining the probability that buildings at that site have experienced a certain MI level given that the site has observed a specific ground motion value, with the "prior" probability that such ground motion level is caused by the given earthquake at the site of interest. A number of locations in the SisFrance database where secondary effects are reported have been tested with this methodology, by generating conditional distributions of PGA|MI and comparing such distributions with the values obtained through exogenously derived Intensity-to-Ground-Motion Conversion Equations (IGMCEs) already existing in the literature. For each historical earthquake we also carried out a second check by generating at each considered site *i* a distribution of PGA conditional on the inferred PGA values at all other *n-1* sites, *j=1, 2,…, i-1,i+1,…, n*, where MI data were available. The conditioning PGA values at the *n-1* sites were independently simulated from the site-specific probability distribution of PGA|MI obtained through Bayesian estimation. The distribution of (log) PGA at site *i* conditional on (log) PGA at the other *n*-1 sites is a Gaussian distribution. For each earthquake an empirical estimate of the Gaussian distribution of PGA at site *i* (and at any other site, for that matter), can be extracted from a large set of spatially correlated random fields constrained by the *n-1* PGA values. The test gave indications that the MI values reported in 3 out of 4 localities may actually be overestimated, and in the SIGMA project the seismic history in the selected localities was corrected accordingly.

Keywords: *Probabilistic seismic hazard analysis, Bayesian updating.*

1. Introduction

The amount of damage caused by the ground motion generated by an earthquake may be in some cases increased by the occurrence of secondary effects associated with the earthquake itself, such as the occurrence of liquefaction, tsunamis or landslides. In such cases any Macroseismic Intensity (MI) data that may be available at the locations where the secondary effect occurred would not only reflect the intensity of the ground shaking, but also the damage caused by such secondary effects. In other words, this cumulative cause of damage may lead to an overestimation of the level of ground shaking inferred from the MI data for historical earthquakes, especially when no Intensity Measures (IM) are available (e.g., PGA from nearby recording stations) to possibly correct the reported MI value. In the SIGMA project, WP4 Task 3, PSHA estimates in southern France, expressed in terms of PGA, are compared with historical observations of damage, expressed in terms of the MI values reported in the SisFrance database. [2]. In this context it is assumed that damage data are related to the level of ground shaking alone. Therefore the occurrence of secondary effects can clearly affect the results obtained in the PSHA validation. The purpose of this work is, therefore, to test the credibility of the intensity estimates of historical earthquakes at locations where secondary effects were reported in the SisFrance database. Of course, the preferred way would be to perform a reassessment of the historical sources from which the original data was derived. However, this is a cumbersome and time-consuming task and is rarely possible to carry out in general. Here we propose a probabilistic methodology that is based on: a) the conversion of MI values at the considered locations into PGA, which is the IM of interest in the present application, and b) on the comparison of such PGA values with those obtained with Intensity-to-Ground-Motion Conversion Equations (IGMCE), such as the one by Worden *et al.* [7] or the one by Faenza and Michelini [8]. For the conversion of MI to PGA, we apply the Bayesian updating methodology proposed by Ebel and Wald [1]. Such a method allows one to take into account in the conversion process not only the probability distribution of PGA for each MI value obtained from empirical datasets of PGA-MI pairs, but also the probability distribution of PGA caused at a given site by the occurrence of a specific earthquake scenario. Of course, this PGA probability distribution takes into account magnitude and distance of the causative earthquake and the amplification due to site effects.

2. Methodology

The method proposed by Ebel and Wald to convert MI values into PGA (or other IM of interest) estimates the probability, $P(PGA_0|MI)$, that a certain ground motion level, PGA_0, is experienced at a site where a given macroseismic intensity, *MI*, has been reported using the Bayes theorem

$$P(PGA_0|MI) = \frac{P(MI|PGA_0)P(PGA_0)}{\sum_{GM} P(MI|PGA)P(PGA)}$$

where $P(MI|PGA_0)$ is the probability that buildings at a given site have experienced a certain *MI* level given that the site has observed a given PGA_0 value. This probability is extracted from empirical datasets of macroseismic intensity (here MMI) and ground motion (here PGA) pairs from 8 California earthquakes, with moment magnitude, Mw, ranging from 5.8 to 6.9 and Modified Mercalli Intensity (MMI) values ranging from IV to IX. *P*(*PGA*) is the "prior" probability that such ground motion level is caused by the given earthquake at the site of interest as predicted by a Ground Motion Prediction Equation (GMPE).

This method has been applied here to test the credibility of available MI data for the events in Table 1 at locations where secondary effects (e.g., hydrogeological effects) have been reported in the SisFrance database [3]. To compute P(*MI*|*PGA*) we made three assumptions.

1. First we assumed that the work of Ebel and Wald [1] applies in this context, namely that the level of damage in old French buildings when subject to any specific level of ground motion is similar to that of California (mostly woodframe) buildings when subject to the same level of ground motion.
2. Second we assumed the equivalency of MMI and MSK intensity scales. This is necessary because Ebel and Wald worked in MMI while the macroseismic intensity values available in the SisFrance database are in MSK scale. We did not make any attempt to convert one scale into the other because these conversions are ridden of uncertainties that are not easily quantifiable.
3. Third we assumed that the IGCMEs that we used here as benchmarks for the probability distributions of PGA|MI are applicable to the context of old French buildings damaged by historical earthquakes occurred in Southern France.

To test the observed MI intensities we estimated the 'prior' probability distribution of PGA for each location and event reported in Table 1 using the GMPE of Akkar *et al*. [4]. The site conditions were evaluated based on the Vs30 map for France developed by the U.S. Geological Survey (http://earthquake.usgs.gov/hazards/apps/vs30/predefined.php#Europe).

Table 1. Sites at which secondary effects and macroseismic intensity values were reported in the SisFrance database. Legend: Repi = epicentral distance; n. Mi = number of sites with MI observations (with MI >= 4).

EQ ID	Date	Mw	Loc	Vs30 (m/s)	MI	n. MI	R_{epi} (km)	Secondary effect
1130045	23/02/1887	6.62	Nice	404	8	505	60.9	Tsunami
1130003	31/01/1612	4.77	Nice	404	5.5	3	92.6	Hydrogeological
60010	20/07/1564	5.5	Nice	404	5	16	33.6	Tsunami
840015	20/03/1812	4.86	Beaumont de Pertuis	431	7.5	7	2.3	Hydrogeological

The plausibility of MI observations at these four sites is further checked with a second approach. We produced spatially correlated random fields of PGA for all the earthquakes listed in Table 1, conditioned on the MI observations available at all locations surrounding the four of interest. Although the constrained random fields of PGA are developed according to a well-established methodology ([5], [6]), some explanatory words are in order. This methodology allows the generation of spatially correlated random fields of a ground motion IM (here PGA), constrained to recorded observations at some stations. In the application at hand there are no available recordings because the historical events predate instrumentation. For each earthquake however there are MI "observations" at *n* sites, where *n* varies from earthquake to earthquake (see Table 1). Included in the *n* sites for each earthquake there is also one of the four test locations in Table 1. Hence, for each one of the four earthquakes, we generated a set of *n*-1 "imperfect" PGA observations probabilistically derived from the MI observations that are available at all the *n*-1 locations, *j=1, 2,…, i-1,i+1,…, n,* other than the i^{th} site listed for each earthquake in Table 1.

The *n*-1 imperfect PGA observations have been separately simulated from the distributions of PGA|MI at all sites where MI observations are available, except for the location that is to be tested, using the Bayesian estimation method in the equation above. We used each simulated sets of PGA|MI as a constraint for simulating a large number of PGA random fields from which we extract the PGA values at the four test sites in Table 1. The empirically derived distribution of

(log) PGA at each test site, which is normally distributed, is conditioned not only on the parameter of the given earthquake scenario (magnitude, distance and site effects), but also on the values of PGA estimated at surrounding sites where an MI value is available for the same event.

3 Results from the Bayesian Estimation Approach

Figure 1 shows the median PGA ±σ of the updated PGA|MI distribution (blue dot showing the median PGA with error bars for ±σ) obtained with the Bayesian estimation procedure, compared with the PGA obtained using the IGMCE of Worden et al. (Worden2012) [7]. The median PGA ±σ of the IGMCE is shown in red continuous and broken lines, respectively, in the figure. The updated distribution of PGA|MI at the tested sites of Beaumont de Pertuis and Nice for Earthquakes ID 840015 and ID 1130045, respectively, fall within ±σ of the median PGA obtained with the Worden2012 conversion equation for the MI intensities reported for these events at those sites. However in both cases the updated median PGA|MI is lower than the median PGA of the Worden2012 IGMCE. Hence, supposing that the assumptions mentioned above do not insert any bias in the derived PGA|MI distributions, one could conclude that the original MI estimates of 8 and 7.5 could be lowered to MI 7 at Beaumont de Pertuis, and 7.5 at Nice, respectively.

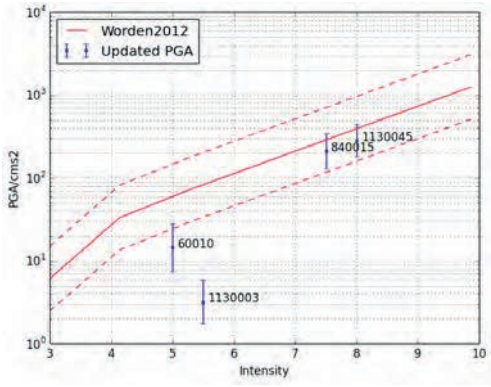

Figure 1. PGA|MI distribution (blue dot for median estimate with error bars for ±σ), obtained with the proposed Bayesian estimation procedure, compared with median PGA ±σ (continuous and broken red lines, respectively) of the Worden2012 IGMCE. See Table 1 for the name of the earthquakes with ID values written by the blue vertical lines.

For Earthquakes ID 60010 and ID 1130003, however, the median PGA|MI values, both reported for the same site at Nice, are lower than the values obtained with the Worden2012 conversion equation by more than one σ. In this case the PGA|MI estimates in Nice obtained with the proposed Bayesian estimation procedure for these two earthquakes seem to support significantly lower MI values (of 4 or less) than those reported in the SisFrance database.

To test the sensitivity of these considerations on the IGMCE selection, in Figure 2 the same comparison is carried out using as benchmark the median PGA ±σ (black continuous and broken lines, respectively) derived this time from the Faenza and Michelini IGMCE [8] (FM2010). In this case the median PGA ±σ values of the updated distribution at the 4 tested sites fall within the median PGA ±σ of the IGMCE for three out of four sites. As before, the median PGA of the updated distribution of PGA|MI at Nice for earthquake ID 1130003 is more consistent with a lower MI estimate than the one reported in the SisFrance database. For this earthquake, the MI value at Nice could be lowered to 4 or less.

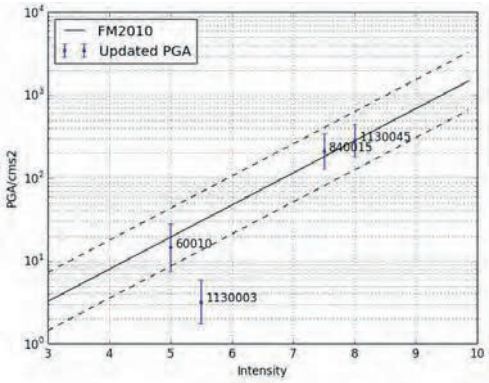

Figure 2. PGA|MI distribution (blue dot for median PGA with error bars for ±σ), obtained with the proposed Bayesian estimation procedure, compared with median PGA ±σ (black continuous and broken lines respectively) of the FM2010 IGMCE. See Table 1 for the name of the earthquakes with ID values written by the blue vertical lines.

4. Results from Spatially Correlated Random Fields

Figure 3 shows the median PGA ±σ (blue dot showing the median PGA with error bars for ±σ) obtained through conditional simulation performed for three (ID 60010, ID 840015 and ID 1130045) of the four events reported in Table 1. The remaining earthquake did not have enough MI observations to appreciably constrain the PGA random fields. The results from both IGMCEs of Worden2012 and of FM2010 are shown in Figure 3 in red and black lines, respectively, continuous for the median PGA and dashed for the ±σ.

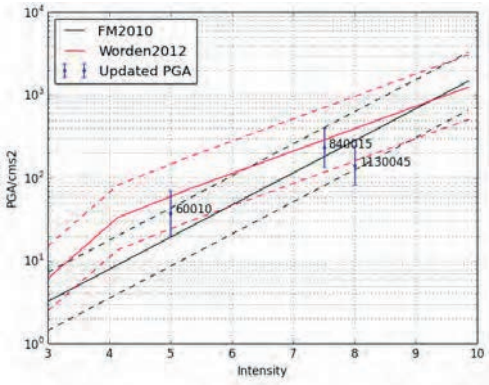

Figure 3. PGA|MI distribution (blue dot for median PGA with error bars for ±σ), obtained with spatially correlated random fields, conditioned on all the other observations available for the same event. Median PGA ±σ is shown as continuous and broken lines respectively for the Worden2012 and FM2010 IGMCE

For earthquake ID 840015 the simulation did not yield very different results from those obtained with the Bayesian updating. For this event the PGA obtained at Beaumont de Pertuis with both methods seems to be consistent with the MI value of 7 to 8 reported in the SisFrance database. The conditional PGA obtained instead for earthquake ID 1130045 for the location of Nice is lower than that obtained with the Bayesian estimation. The random field simulation approach yields a PGA at Nice that is more consistent with a MI value of 7, when comparing the median PGA of the conditional distribution with the median PGA of the FM2010 IGMCE, or even lower

when the comparison is made with the Worden2012 IGMCE. Finally for event ID 60010, which had a reported MI value of 5 in Nice, the median PGA obtained with conditional simulation is higher than the one obtained with Bayesan updating alone. In this case we could estimate a MI value of 4 to 5 when comparing with the Worden2012 IGMCE, or 5 to 6 when comparing with the FM2010 IGMCE.

5. Discussion and Conclusions

In this work we presented an application of the Bayesian estimation methodology proposed by Ebel and Wald in 2003 and used it to convert MI values to PGA values at specific locations, with the purpose of evaluating if these PGA values (or, rather, their distributions since they are random variables) were compatible with the values of MI reported in the SisFrance database at the same locations. The locations selected for testing were those where the database flags that the reported MI values for a given earthquake may have been affected by secondary effects, such as tsunamis or hydrogeological phenomena. Two kinds of test were carried out. In the first one a simple Bayesian estimation was performed for the selected locations and events. At each location the reported MI value was converted into a PGA distribution by considering both the probability that a given MI value is generated by a given level of PGA (based on a relationship derived from empirical datasets of MI-PGA pairs) and the probability that the given causative earthquake produced such PGA level at the specific site, given its magnitude, the source-to-site distance and the local soil conditions at the site. In the second test we assumed that no information of any kind to infer the ground shaking level was available at the locations to be tested. In this second approach we produced spatially correlated random fields of PGA, constrained to all other "imperfect" observations of PGA available at nearby sites. These imperfect PGA observations were generated, again, by converting MI into PGA using the Bayesian estimation technique and sampling the resulting distributions.

The advantage of the first method is that it is simple to implement and it requires only basic data on the causative earthquake and local site conditions. This Bayesian estimation approach seems to suggest that there is one event (ID 113003) for which the MI value, MSK = 5.5, reported at Nice is severely overestimated. This overestimation is supported by both the benchmark MI to PGA conversion IGMCEs of Worden2012 and FM2010. For the other 3 earthquakes and locations the PGA|MI distribution displays a better fit with the distribution of PGA obtained with both IGMCEs and especially with the FM2010 IGCME. This better consistency with the FM2010 equation is likely due to the fact that the FM2010 IGMCE is based on Italian data, unlike the Worden2012 one that is based on US data. The seismic response of old French buildings in southern France is more likely to be more similar to that of Italian buildings than that of US ones, whose majority is made of timber.

The second method used is mathematically more complex and also requires the availability of either instrumental or macroseismic observations to constrain the PGA simulated at the locations where we wish to test the credibility of the reported MI estimate. While the simulation did not change the final considerations for earthquake ID 840015, the conditional median PGA at Nice obtained for earthquake ID 1130045 was sensibly lower than the median PGA|MI obtained through the Bayesian estimation technique. Based on these results the MI estimate in Nice for this earthquake could be lowered to 7, based on comparison with the FM2010 IGMCE, or even lower than 7 based on comparison with the Worden2012 IGMCE. For event ID 60010 the median PGA obtained in Nice through conditional simulation was again different, and this time higher, than the one resulting from the Bayesan updating alone. The corresponding MI value could be estimated to be between 4 and 5 based on comparison with the Worden2012 IGMCE, and between 5 and 6 based on comparison with the FM2010 IGMCE.

Table 2 reports a summary of the results, displaying the reassessed MI value for the events and locations reported in Table 1, based on comparison of the median PGA obtained with the two methods, with those from the FM2010 IGMCE. The results displayed are relative to the estimation performed with the random fields technique, except for event ID 1130003 for which only the Bayesan updating results are available.

Table 2. Reassessed Mi values at the four tested sites. Legend: R_{epi} = epicentral distance.

EQ ID	Date	Mw	Loc	Repi (km)	Secondary effect	Original MI	Reassessed MI
1130045	23/02/1887	6.62	Nice	60.9	Tsunami	8	7
1130003	31/01/1612	4.77	Nice	92.6	Hydrogeological	5.5	< 4
60010	20/07/1564	5.5	Nice	33.6	Tsunami	5	5.5
840015	20/03/1812	4.86	Beaumont de Pertuis	2.3	Hydrogeological	7.5	7.5

It should be emphasized, however, that this study focused on testing the credibility of MI values reported at locations where secondary effects were reported in the SisFrance database. The original hypothesis was that such phenomena might have caused an increased level of damage above and beyond the damage directly caused by the ground shaking. Of course, nothing of what done here can be used to support the claim that the overestimation that we found at some of the test sites localities is actually caused by these secondary effects. The overestimation, if indeed real, can be due to any other reason. Note also that, for example, for earthquake ID 1130003 a location with MI value of 5.5 is reported at 180 km from the epicenter. No secondary effect is flagged in this case, but this MI value is surely quite unlikely. Our methodology would have certainly identified a severe overestimation of MI at that site. Moreover, our approach implicitly assumes that the magnitude and the epicenter location of the historical events were correct, while an erroneous assignment of either of such parameters could have been a possible real cause of the overestimation found at some sites.

Whatever the reason for the inconsistencies highlighted by this analysis, the methodology presented here may help to identify cases for which a reassessment of the historical sources, leading to the originally assigned MI values, and/or of the event parameters might be needed. If nothing else, this approach can be used at least to investigate the reliability of the available MI data of historical events.

REFERENCES

[1] Ebel J.E and Wald D.J. Bayesian estimations of Peak Ground Acceleration and 5% Damped Spectral Acceleration from Modified Mercalli Intensity Data, *Earthquake Spectra* 2003; 19, 3, 511-529.

[2] Rosti A, Rota M, Penna A, Fiorini E, Magenes G. Comparison of PSHA Results with Historical Macroseismic Observations in South-East France. In: Proceedings of the CSNI Workshop on "Testing PSHA Results and Benefit of Bayesian Techniques for Seismic Hazard Assessment", Pavia, Italy; 2015

[3] Sisfrance – Catalogue des séismes français métropolitains, BRGM, EDF, IRSN, www.sisfrance.net.

[4] Akkar S, Sandıkkaya M A, Bommer J J. Empirical ground-motion models for point- and extended-source crustal earthquake scenarios in Europe and the Middle East, *Bull. Earthquake Eng.* 2014; 12, 1, 359 – 387

[5] Park J, Bazzurro P, and Baker J.W. Modeling spatial correlation of ground motion intensity measures for regional seismic hazard and portfolio loss estimation. In: *10th International Conference on Application of Statistic and Probability in Civil Engineering* (ICASP10), Tokyo, Japan, 8 pp; 2007

[6] Fiorini E and Bazzurro P. Macroseismic intensity constraint for probabilistically based shakemaps. In Proceedings of the 2ECEES (*Second European Conference on Earthquake Engineering and Seismology*), Istanbul, Turkey, August 24-29, 2014

[7] Worden C B, Gerstenberger M C, Rhoades D A. and Wald D. J. Probabilistic Relationships between Ground-Motion Parameters and Modified Mercalli Intensity in California. *Bulletin of the Seismological Society of America* 2012; 102, 1, 204–221

[8] Faenza L and Michelini A. Regression analysis of MCS intensity and ground motion parameters in Italy and its application in ShakeMap. *Geophys. J. Int*. 2010; 180, 1138–1152

CSNI Workshop on "*Testing PSHA Results and Benefit of Bayesian Techniques for Seismic Hazard Assessment*"
4-6 February 2015, Eucentre Foundation, Pavia, Italy

Thirty-Year Bayesian Updating of PSHA for Hinkley Point NPP

Gordon Woo
RMS, UK, Gordon.Woo@rms.com

Willy P. Aspinall
Bristol University, UK, Willy.Aspinall@bristol.ac.uk

SUMMARY

Where a PSHA is undertaken for a critical installation, such as a nuclear power plant, it needs not only to be reliable and conform to the state-of-the-art in PSHA, but also be robust against developments over the coming decades in seismological data acquisition, earthquake occurrence, and advances in engineering seismology. Given the operational lifetime of critical installations, PSHA results should be robust for at least thirty years. Although it is difficult to assess and test a current PSHA for its fitness for purpose thirty years into an unknown future, robustness can be tested retrospectively for PSHA studies undertaken three decades ago. One such PSHA study was undertaken by the CEGB Seismic Hazard Working Party for the Hinkley Point NPP in southwest England. The authors were principal seismic hazard analysts for this study. Taking the probabilistic inputs for this study as priors, Bayesian updating methods can be applied to construct posterior distributions that account for new information obtained relevant to the site seismic hazard. The results of the Bayesian updated PSHA are compared with those of the former study, and lessons are drawn on the value of retrospective updating of hazard assessments for PSHA testing.

Keywords: *Probabilistic seismic hazard analysis, Bayesian updating, nuclear plant*

1. PSHA undertaken for CEGB

The first generation of UK nuclear power plants was not designed with earthquake loading in mind. The first UK nuclear power plant to be specifically designed for earthquake loading was the Sizewell B pressurized water reactor. Before construction began, there was a lengthy public enquiry from 1982 to 1985. A seismic safety case for Sizewell B was presented as part of this public enquiry. The fact that a rigorous seismic hazard assessment was undertaken for Sizewell B was deemed by the chairman of the nuclear utility, the Central Electricity Generating Board (CEGB), as a powerful way of conveying to the British public the thoroughness of nuclear safety measures. With the 1979 Three Mile Island partial meltdown in recent memory, there was a pressing need for public reassurance of nuclear safety, as there has been after the Fukushima partial meltdown in 2011.

It was appreciated at the outset by CEGB that a deterministic approach to seismic hazard assessment was inappropriate for UK. Given the possibility of a Magnitude 6 earthquake with an epicentre very close to a nuclear site, the low occurrence probability should be taken into account in the definition of a Maximum Credible Earthquake. As the first UK probabilistic seismic hazard analysis (PSHA) for a civil nuclear site, the Sizewell B seismic hazard, completed in 1982 in time for the public enquiry, was subject to the most intense scrutiny, and arguably remains the most important because of its nuclear safety context and its dependence on a re-evaluated historical earthquake catalogue. The historical development of the British earthquake archive was reviewed by Woo [1] as a contribution to the memorial volume for N.N. Ambraseys, who made a salient contribution to the methodology for UK seismic hazard assessment, which was established in the early 1980s.

The first operational nuclear power plant for which a PSHA was undertaken was at Hinkley Point in the southwest county of Somerset. A microtremor network was installed in May 1985, and data acquired from this network up to the end of 1986 informed the PSHA for Hinkley Point, which adopted the methodology used for Sizewell. This assessment was carried out by the CEGB Seismic Hazard Working Party (SHWP), of which the two authors were specialist consultants.

2. Magnitude Felt Area Correlation

Under the guidance of Ambraseys at Imperial College, London, the entire UK historical earthquake catalogue was reconstructed in 1981 by Principia Mechanica Ltd. In order for historical earthquakes to make their due contribution to an assessment of seismic hazard, their magnitudes need to be estimated. Without a robust and reliable method of magnitude assignment, time spent hunting down original old earthquake reports would have been in vain. Fortunately, Ambraseys had honed such a method in Iran. The blueprint for this method is to be found in the chapter on instrumental data in ‘The History of Persian earthquakes’ by Ambraseys and Melville [2]. This method is based on correlating magnitude with macroseismic felt area. Ambraseys and Melville regarded with suspicion attempts to estimate magnitude from peak intensity; a practice which had hitherto been quite widespread.

Using those events for which both instrumental and macroseismic data are available, the felt area correlation can be constructed. Yet such a correlation would be poor unless both instrumental and macroseismic data were meticulously researched. In a country such as Britain where seismicity is sparse, and where some of the most notable earthquakes affecting the country occurred in the first half of the twentieth century, the development of a reliable magnitude–felt area correlation depends crucially on acquiring early seismological station bulletins and even original seismograms. This research was undertaken by Principia Mechanica Ltd. in 1981. The

preferred choice of magnitude for seismic hazard assessment is governed by the magnitude – felt area correlation. Since the antique seismometers recording the notable 1927 Viking Graben and 1931 Dogger Bank earthquakes enabled surface wave magnitude to be estimated, it was the M_S scale that was used to categorize the magnitudes of all British earthquakes. From the reassignment of surface wave magnitudes and felt areas within isoseismals III and IV for the principal 20th century British earthquakes, the following correlations were constructed [3].

$$M_S = -0.356 + 1.00\ Log\ A_{III} \quad (\sigma = 0.12)$$
$$M_S = 0.91 + 0.818\ Log\ A_{IV} \quad (\sigma = 0.13)$$

The logarithmic dependence on felt area renders these correlations notably robust and stable for assigning magnitudes. Errors, ambiguities and gaps in drawing isoseismals are damped by the application of the logarithmic function. This is especially significant for intraplate regions such as Britain where moderate earthquakes are felt over a wide area. The 1982 PML magnitude-felt area correlations were the earliest of a subsequent series of European correlations generated using the Ambraseys principles of intensive and meticulous data acquisition. These yield broadly similar results.

3. Ground Motion Prediction Equation

Using the above M_S – felt area correlations, the drawing of isoseismal maps for all UK historical earthquakes then allowed M_S assignments to be made for the UK earthquake catalogue. Recognizing the significant errors that may be introduced through magnitude conversion, M_S was the natural choice of magnitude for peak ground acceleration attenuation relation (now called ground motion prediction equation).

Few published peak acceleration attenuation relations had M_S as a scaling parameter, and none had a magnitude range that encompassed the moderate magnitudes which are dominant for UK seismic hazard. Furthermore, given the dearth of UK neotectonics, hypocentral distance is the optimal distance metric. Accordingly, Principia Mechanica Ltd. [3] constructed a new peak acceleration attenuation relation, characterized by M_S and hypocentral distance, using as a strong motion database records of earthquakes from magnitude 4 upwards, without restriction on hypocentral distance. The choice of magnitude 4 for the lower threshold is significant; earthquakes of magnitude 4 provide an important contribution to UK seismic hazard. GMPEs are routinely constructed with magnitude 5 as the lower threshold, and are appropriate for more seismic environments than UK.

Nonlinear regression analysis in terms of M_S and hypocentral distance R yielded the following formula for acceleration A, measured in cm/sec.

$$Ln(A) = 5.72 + 0.59M_S - 1.26\ Ln(R + 2.13\exp(0.25M_S))$$

In the thirty year time interval since this peak acceleration attenuation relation was constructed, there has been only one strong ground motion recorded in UK in excess of 5% g. On 28 April 2007, a damaging earthquake (M_S 4.0) at a shallow depth of 5 km occurred at the coastal town of Folkestone in the southeastern English county of Kent. In Folkestone, cracks appeared in walls and some chimneys collapsed. The peak ground acceleration of 10%g close to the epicentre was and remains the highest ever recorded for a UK earthquake. This is a significant observation for the seismic safety of nuclear installations, because of the concern that a common type of event of

magnitude 4 might generate high levels of impulsive peak acceleration that could trigger some system malfunction.

The 1982 peak acceleration attenuation yields a median PGA of 14%g. With a sigma of 0.553, this is within a standard deviation of 10%g. By comparison, a number of recent GMPEs have under-predicted the peak acceleration, including a UK stochastic model by Rietbrock et al. [4], which has a median prediction just less than 1%g. The actual recorded level was more than two standard deviations higher. The GMPE of Rietbrock et al. is based on the results of numerical simulations using a stochastic point-source model calibrated with parameters derived from local UK weak-motion data. However, the parameters are as yet too poorly constrained to be reliable for practical UK usage.

Looking back over the past thirty years, it is reassuring from a nuclear safety perspective that no UK ground acceleration has been recorded which might have even remotely indicated or suggested that the 1982 Principia Mechanica Ltd. peak acceleration attenuation relation was under-conservative. For the Hinkley Point logic-tree, weights of 0.2, 0.5 and 0.3 were assigned to alternative sigma values of 0.5, 0.553 and 0.6. The central value is that obtained directly from the regression; the outer values reflect judgement as to the epistemic uncertainty over the extent of PGA variability. Bayesian updating of these weights would produce a slight shift towards higher sigma values, which would make the observed over-estimation of PGA a more likely outcome.

Looking forward over the next thirty years, the methodology for generating GMPEs is anticipated to change even more than it has over the past three decades. The 1982 Principia Mechanica Ltd. peak acceleration attenuation relation has been shown to be robust with respect to three decades of strong motion observations. Now consider a modern GMPE used alone, or within a logic tree suite, for a nuclear installation seismic hazard analysis in 2015. It would be disconcerting if, during the lifetime of a nuclear installation, any recorded ground motion in the surrounding region were to exceed the median prediction by more than one standard deviation. If the median prediction were exceeded by more than two standard deviations, the integrity of the seismic hazard analysis might be called into question. Some engineering seismologists may doubt whether it might be possible to make robust GMPE projections over thirty years; but it has been achieved.

4. Individual fault modelling

In the Hinkley Point seismic source model, one specific geological structure close to the site was modelled explicitly. This is the Watchet-Cothelstone-Hatch Fault zone. At its closest, it passes 10km from the site. The parameterization of this fault was based on very limited data, in respect of which a weight of 0.5 for the fault being active was assigned. The activity rate was calculated from the tentative association with the Taunton earthquake of 4 January 1868.
More recent geological study of the Watchet-Cothelstone-Hatch Fault by Glaser and Smith [5] has identified several aspects of the development of the fault, e.g. a splitting into several antithetic normal faults in Mesozoic cover, which suggest that this prior weight is high and might be updated to a lower value.

5. Seismic zonation

The principal seismic source modelling follows the standard area zonation approach of Cornell and McGuire. The area source zonation for Hinkley Point comprised two quadrilateral zones shown below in Figure 1, supplemented by a UK average background region. The open triangle marks the site location. The northern zone encompasses the marked seismic band of South Wales

extended up to Herefordshire, but not east of the Malvern Axis. The southern zone covers much of Somerset, north Devon and Dorset, with its southern boundary drawn to reflect approximately the northern edge of the Dorset Basin. A statistical constraint on the partition boundary was the requirement that the seismicity was un-clustered according to the Clark-Evans nearest neighbour test.

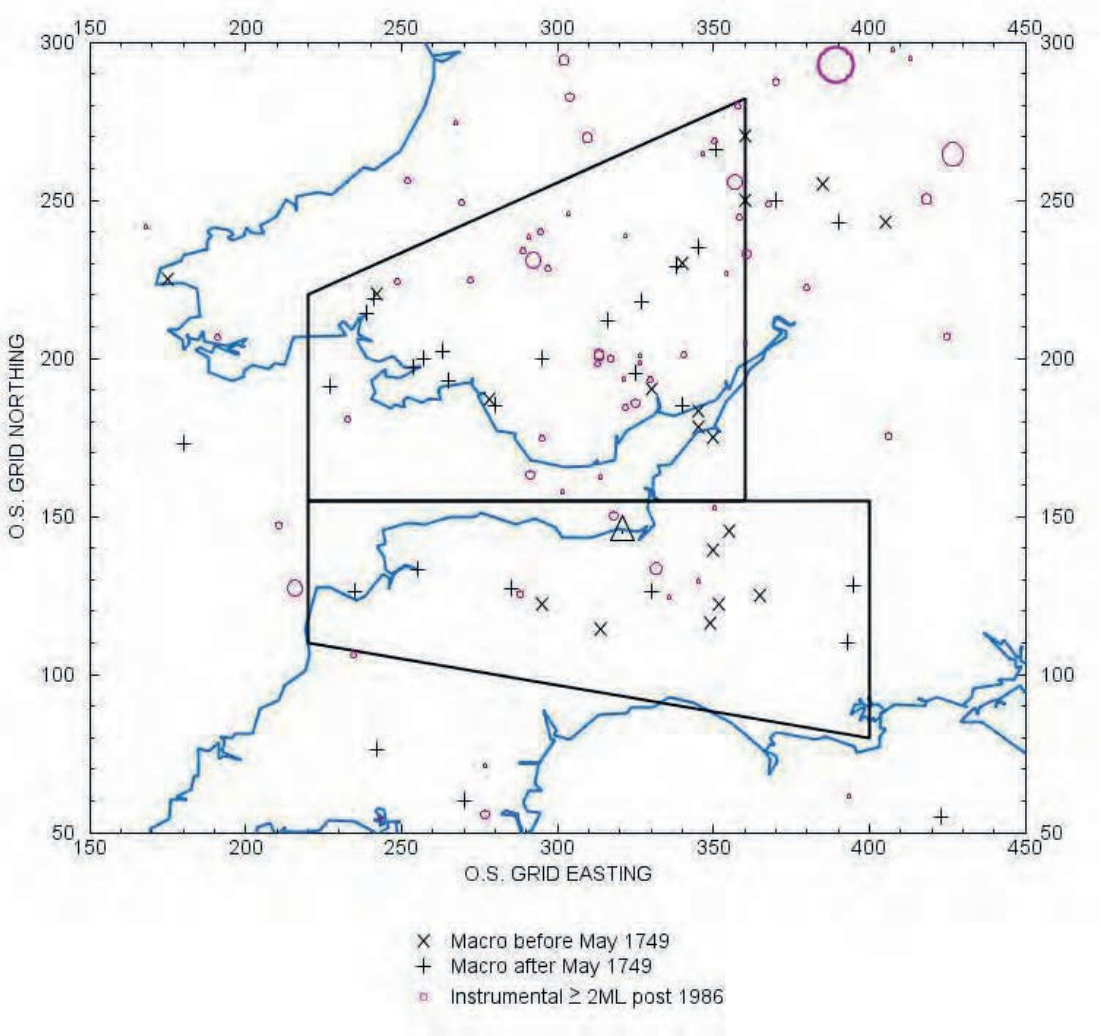

Figure 1. Seismic zonation around Hinkley Point

5.1 Spatial patterns of instrumental earthquakes

It is a fundamental fact of PSHA that the locations of pre-instrumental historical earthquakes are generally much less well-constrained than more recent instrumental observations, especially with respect to depth of focus. However, the instrumental record is much shorter, and seldom captures a good sample of events for larger magnitudes. The question can be asked: given these limitations, what information can be gleaned from instrumental earthquake locations?

Here we explore one way in which spatial patterns of instrumental locations may be analysed objectively to inform the geometrical definition of diffuse seismicity area source zones in a

seismic hazard model. We use as reference the Hinkley Point case history, and illustrate the sensitivity of PGA hazard to two alternative zonations: the original model, and one with site neighbourhood area sources modified in the light of recent instrumental data. The basis of our spatial analysis approach is *K*-means cluster analysis, outlined next.

5.2 K-means cluster analysis

Within the Euclidean zonation constraints of the Cornell-McGuire approach and with real hypocentral data of variable quality it is often difficult, if not impossible, to define multiple zones each of which enjoys statistical uniformity and complete spatial randomness. Because of these limitations, it is usually sufficient in the first instance to apply a simple procedure for separating hypocentres into a limited number of clusters on the basis of their spatial proximity to one another; a suitable approach for this purpose is the *K*-Means Clustering Algorithm [6]. This is an algorithm for partitioning (or clustering) N data points into K disjoint subsets S_j containing N_j data points such that the division minimizes the following sum-of-squares criterion:

$$J = \sum_{j=1}^{K} \sum_{x \in S_j} \left| x_n - \mu_j \right|^2$$

here x_n is a vector representing the nth data point and μ_j is the geometric centroid of data points in S_j. It may be noted that, in general, this algorithm does not necessarily achieve a global minimum of J over the K assignments, since the procedure uses discrete assignment rather than a continuous parameterization. Despite this limitation, the algorithm is used frequently because its basis for cluster selection is objective, within the limitations noted, and because it is an easy procedure to implement.

The algorithm consists of a simple re-estimation procedure as follows: initially, the data points are assigned at random to the K sets. In the first step, the centroid is computed for each set. In the next step, every point is assigned to the cluster whose centroid is closest to that point. These two steps are iterated successively until a stopping criterion is met, e.g. when no re-assignment of any data point to a different set takes place.

In addition, the *K*-means algorithm allows certain constraints to be applied to the partitioning process: for instance, the analyst can set a minimum size (in terms of number of members) at which further subdivision of a cluster ceases. In the present case, this constraint can be used to prevent the algorithm generating partitions on length scales that are too small for the context of seismotectonic regionalization; given the limited size of the dataset, a minimum cluster size of five earthquakes is chosen.

For a three-dimensional analysis using mixed co-ordinate measures (e.g. latitudes and longitudes in degrees, and depths in km) it is necessary to apply some form of normalization to the data, to prevent the clustering process being dominated by differences in the value scales involved. In the present case, it is appropriate to give hypocentral depths – which range from 0 km to 25 km - a balancing weight to compensate for the larger numerical values associated with northings and eastings, spanning more than 100 km. Weighting depth ten times more influential than epicentral co-ordinates produced a suitable outcome in terms of normalizing within-variable data variance and achieving a balance between lateral scatter of epicentres and depth scatter of hypocentres. Other weightings are possible, but trials indicated the present cluster partitioning was not sensitive to modest changes in relative weights.

5.3 Spatial hypocentre clusters near Hinkley Point

In the present application, a derivative of a FORTRAN program implementation of the *K*-means algorithm due to Hartigan [7] is used to disaggregate recent instrumental seismicity located in the two main area source zones of the original Hinkley Point model into a fixed number of spatially-related clusters. (This code has been used in the past by the authors for a number of site-specific PSHAs; the same concept has been applied by Weatherill & Burton [8]).

For the Hinkley Point zones, the instrumental data comprise 37 individual hypocentres with magnitudes 2MLs or greater – a cautious threshold of completeness, chosen above that ascribed by BGS to this region (1.5ML). With the constraints mentioned above, the *K*-means algorithm identified four separate, depth-related spatial clusters, as shown in Figure 2.

The spatial extents of these clusters are shown in Figure 2, with outline boundaries which define four 'new' area sources for hazard modelling purposes. Also noted on the plots are the proportions of the joint activity in the two main zones of the original model that are redistributed into these revised zonations - pro-rata with the number of instrumental events in each cluster. For this sensitivity test, all other external area sources and the single fault source of the original model remain in place, unchanged.

With the revised zonation, the calculated hazard is marginally higher than before, with the expected 10^{-4} p.a. PGA level 0.25 g, compared to 0.22 g in the former model. There are various factors contributing to this difference: the increase is mainly due to the fact that the site is enclosed in the new model within two zones of shallow focus events which spatially extend to include more active areas in South Wales. The reduced areal extent of these two source zones, compared to the original northern zonation, also results in significantly higher spatial densities of shallow activity in the vicinity of the site.

This simple alternative model updating exercise demonstrates the crucial sensitivity of a site-specific PSHA to local area zonation boundary definitions. It invites discussion on how any objective analysis of instrumental data spatial patterns can be utilized to modulate a seismic hazard zonation model. The Bayesian updating of seismic source model weights is discussed in section 7.

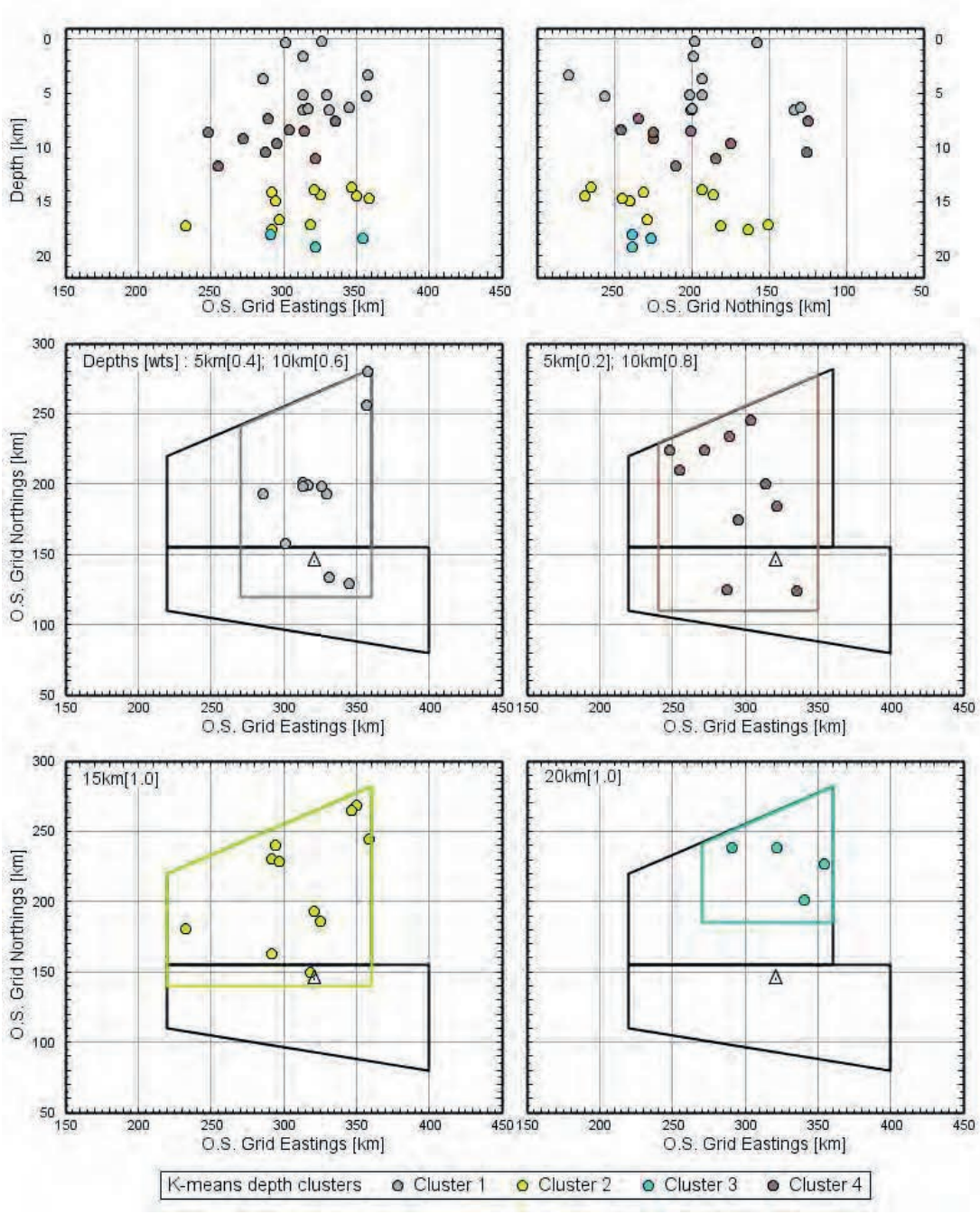

Figure 2. Seismicity clusters around Hinkley Point, with outline boundaries defining alternative zone boundaries for seismic hazard modelling.

6. Seismicity updating – monitoring data

In this analysis, we examine potential indicators for activity rate estimation that might be gleaned from recent instrumental earthquake monitoring around the Hinkley Point site. Taking BGS National Catalogue data for 1986 to 2011 inclusive, we find 347 earthquakes reported for the area of the map in Figure 1 (i.e. 150kmE to 450kmE; 050kmN to 300kmN O.S. Grid co-ordinates). BGS [9] indicate a contemporary magnitude completeness of 1.5ML in this area, under average noise conditions.

Of the total recorded events, 28 were magnitude 2.5ML or greater, and 79 were 2.0ML or greater, and either dataset can be presumed complete or close-to-complete for the period 1986 to present. Taking the Hinkley Point northern zone area specifically, there have been eight events in the monitoring interval with magnitude 2.5ML or greater which unquestionably can be considered to comprise a complete instrumental dataset.

On the basis of the original SHWP activity rate and b-value parameterizations from the macroseismic record, and incorporating the associated rate and b-value uncertainties in calculations, by back-extrapolation a distribution for a magnitude completeness threshold - for an expected eight events in 27 years in the northern zone - is determined as shown on Table 1, together with conversions to equivalent ML values using two alternative relations for the UK and for Europe (see notes in section 9):

Table 1: Magnitude threshold for expected 8 'complete set' events in 27 years

Model	5% confidence	50% confidence	95% confidence
Original SHWP Model	3.35 Ms	3.20 Ms	3.00 Ms
UK ML-Ms conversion	3.55 ML	3.38 ML	3.16 ML
Ambraseys (1990)	3.80 ML	3.70 ML	3.55 ML

In the 27 years from 1986 – 2011, there have been just two events recorded in the northern zone with ML magnitudes exceeding the converted lower (95% confidence) value of 3.16ML: i.e. 1999/10/25 Sennybridge 3.6ML, and 2008/10/26 Bromyard 3.5ML; and only one of these was above the equivalent Ambraseys [10] lower converted threshold of 3.55ML. If eight events are expected to exceed the (lower) completeness threshold in 27 years, the probability of observing just two is less than 1%; the probability of only one is about 0.1%, and for zero is diminishingly small.

Two factors may contribute to this apparent shortfall of observed activity: conversions between ML and Ms may be much less reliable than the relationship uncertainties imply; or, magnitude-frequency self-similarity scaling may break down at these low- to moderate magnitudes, as suggested by Mayeda et al. [11], Morasco et al. [12], Kumar et al. [13], and others. If the latter is a factor then it sets limits on the validity of the usual Gutenberg-Richter linearity assumption, with important implications for using recent monitoring data to extrapolate activity rates from

low- to medium or high magnitudes, or for testing prior activity parameterizations and validating PSHAs.

To illustrate this in terms of estimating an M4 exceedance activity rate, if for a given region the Gutenberg-Richter relative frequency distribution were linear and valid from M6.5 down to M2.5, say, then 27 years of complete recording at M2.5 and greater would be equivalent to more than 2,000 years of complete recording at M4 and greater. In the case of the Hinkley Point region, which has a longer historical record than for many parts of the world, the effective duration of historical event completeness at M4 or above is about 880 years.

In this case, it would be difficult to argue persuasively that low-magnitude activity rates adduced from a few years of instrumental monitoring could be sufficiently compelling to modify inferences from centuries of data with multiple samples of larger magnitude events. If, however, the instrumental data for the northern zone in the Hinkley Point case has some evidential worth in this context, then it can only serve to emphasize the relative conservatism of the original PSHA model.

6.1 Bayesian updating of b-value

In the SHWP Hinkley Point logic tree, three *b*-values were adopted for both zones, centred on a *b*-value of 1.28 derived from UK M_S data, with weights as follows:

1.25 [0.3] 1.28 [0.5] 1.30 [0.2]

Here, these weights are taken as priors and updated with the recent data MLs values for both zones, jointly. A fundamental assumption in what follows is that there exists a Gutenberg-Richter relation that is for earthquakes in the two zones which, when taken jointly, is linear from some completeness threshold Mc up to M_{MAX} (i.e. 6.5Ms), and that both the historical M_{SA} and modern instrumental MLs data are representative and mutually consistent samples of this distribution. For sensitivity purposes, the two alternative completeness thresholds Mc noted above, i.e. 2.0MLs and 2.5MLs, are each used, and the prior *b*-value weights updated by the instrumental data for both cases. The results of this exercise are summarized on the following, Table 2:

Table 2: Updating b-values using recent instrumental data

			***b*-value / weights**		
Case	**No. of Data**	**Data *b*-value**	**1.25**	**1.28**	**1.30**
SHWP prior	-	-	0.3	0.5	0.2
Zones Mc = 2.0ML_S	37	1.23	0.303	0.500	0.197
Zones Mc = 2.5ML_S	11	1.19	0.304	0.499	0.197
Area Mc = 2.5ML_S	26	1.08	0.327	0.491	0.182

Thus, *b*-value updating for the Hinkley Point provides negligible evidence for changing these prior weights, even when based on the more plentiful Zones data for Mc = 2ML_S or the whole area for Mc = 2.5ML_S (weights to three decimal places are shown to illustrate the point, not to imply such precision is meaningful).

7. Bayesian updating on source model weights

Notwithstanding the geological and statistical arguments supporting the delineation of the zone boundaries, there is a substantial degree of arbitrariness in their definition, especially in regions of low or moderate seismicity. After more than a decade of seismic hazard assessment experience at most of the UK nuclear plants, which included constructing multiple alternative zonations, the concept of zoneless seismic source modelling was introduced [14].

The essential observation underlying this approach is the recognition that the geometry of earthquake epicentres hardly ever satisfies the constraints of spatial uniformity, as presumed by the standard Euclidean zonation method, but rather has a far richer, more structured, fractal characterization. Apart from the inevitable errors in earthquake magnitudes and epicentres, nonlinear dynamical effects on the seismogenic system will cause perturbations in the size and location of future events. These recording errors and irreducible dynamical perturbations require a smoothing operation to be performed on the seismicity data, such as can be implemented using statistical kernel techniques.

Over the past several decades, kernel smoothing seismic source models have been introduced quite widely into seismic hazard assessment, often as a residual complement to fault models, but the subjective weight assigned to them in source model logic trees has been generally rather low, e.g. of the order of 0.2. Furthermore, it is still common for a zero logic tree weight to be assigned to zoneless source models. Marzocchi and Jordan [15] have pointed out that logic tree weights formally reflect the degrees of belief in a finite subset of possible alternatives. But there is a principle in decision analysis known as Cromwell's Rule [16]: it is inadvisable to assign a prior zero probability to a contingency, because the posterior probability will also be zero, regardless of the strength of subsequent evidence.

The logic tree weight assigned to zoneless modelling would be a prime candidate for Bayesian updating, so as to make the weight less subjective and more evidence-based. Consider the accumulation of supplementary seismicity data around a site. The prior weight assigned to zoneless modeling could be updated using the likelihood ratio:

$$R = P(Seismicity\ Data \mid Zoneless\ Model) / P(Seismicity\ Data \mid Zonal\ Model)$$

In the case of Hinkley Point, the seismic hazard assessment predated by almost a decade the development of kernel smoothing techniques in 1994 by one of the authors, so the prior weight to zoneless modelling was zero. In accordance with Cromwell's Rule, no updating is formally possible. Suppose however that the ratio of the prior weights assigned to the zoneless model to the zonal model is W. Then the Bayesian updated ratio is: $R*W$.

In the period from 1986 to 2014, there have been no earthquakes of magnitude 4 or more within 150km of the site. (The Dudley earthquake of 22 September 2002 was just outside this range). Given the Poisson model for earthquake occurrence, the chance of this null outcome is about 20%, according to the area source zonation model. This comparatively low figure may be explained as follows. The zone boundaries are weakly constrained geologically. Given the ambiguity and the need to demonstrate robustness, the boundaries are delineated to avoid latent under-conservatism.

Furthermore, the area surrounding the two principal zones is assigned UK average seismicity, which itself is a conservative assumption.

Within the zoneless model, the chance of no earthquakes of magnitude 4 or more within 150km of the site within the period 1986 to 2014 is about 70%, so that the likelihood ratio $R = 3.5$. The structure of the zoneless model is independent of the site of interest, so there is no subjective bias introduced through identifying a specific site. If the prior weights had been 0.8 for the zonal model and 0.2 for the zoneless model, as might have been assigned, then the Bayesian updated weights for the zonal and zoneless models would have been approximately the same. It might be noted that for a seismic hazard study in southern India [17], the weight assigned to the zoneless model was 0.4.

Within the logic tree framework, averaging of the results of the zonal and zoneless models would reduce the hazard at Hinkley Point slightly: at the 10^{-4} annual probability of exceedance level, the kernel smoothing model yields a PGA a few %g lower than the zonal model.

8. Conclusions

The probabilistic seismic hazard assessment methodology for UK nuclear installations was established thirty years ago. The application of this methodology to Hinkley Point followed within a couple years [18], and has been reviewed here within the context of Bayesian updating. The principal seismological observation has been an absence of events within the PSHA magnitude range of M_S 4.0 and above, within 150 km of the site. Furthermore, there has also been a dearth of regional instrumental seismicity, relative to expectation from the activity rates defined for the hazard model.

For NPP applications of PSHA, ambiguity and uncertainty in parameterization is often handled through adopting a conservative position. Bayesian updating provides a systematic means for modifying inputs according to empirical data observations acquired post hoc. If the original model parameters were on the side of conservatism, this updating may output reduced hazard results. This is the situation at Hinkley Point, where updating of the weights for source models would suggest a reasonable weight for a zoneless model.

9. Notes on ML-Ms conversion

The original SHWP Hinkley Point PSHA was conducted in terms of macroseismic surface wave magnitude M_{SA}, therefore a conversion is needed if comparisons are to be made of recent instrumental data in ML with the seismicity parameters in SHWP. For UK instrumental data, Musson [19] provides an orthogonal regression of Ambraseys [20] M_S values for 17 British Isles and Scandinavian earthquakes against corresponding BGS ML values for the same events.

For the Musson dataset, and adding 1 sigma uncertainties equivalent to 0.1 magnitude unit to values on both scales, a revised orthogonal regression, with uncertainties, is obtained here:

$$ML_S = 0.18 \pm 0.02 + (0.89 \pm 0.01) * ML$$

with ML_S denoting a magnitude converted from ML to an equivalent M_S value by this regression. The slope of this relation is slightly lower than Musson's 0.99, and the intercept positive and smaller than his -0.42.

At low magnitudes (i.e. less than about 2ML) – and accepting for present purposes that such small M_S values may not have real physical meaning - this modified MLs/ML relation gives very similar numerical M_S and ML magnitude values, with deviations increasing above 4ML. For instance, the largest event in the modern instrumental dataset, the 4.7ML Dudley earthquake of 22 Sept 2002, is ascribed magnitude $4.4M_S$ by this relation. This accords with findings from other studies essaying ML/M_S conversions of such modest magnitudes.

Ambraseys [9] also provided a revised relation for European earthquakes:

$$0.80 * ML – 0.60 * M_S = 1.04 (+/- 0.22)$$

Overall, at low magnitudes the Ambraseys relation indicates higher ML value conversions from Ms, relative to those from the relation, above, adapted from Musson [19]. For sensitivity purposes, Ambraseys [10] is used here also, as an alternative to the adapted British Ms/ML conversion.

ACKNOWLEDGEMENT

W.P. Aspinall was partly supported at Bristol University by the Natural Environment Research Council (Consortium on Risk in the Environment: Diagnostics, Integration, Benchmarking, Learning and Elicitation - CREDIBLE; grant number NE/J017450/1).

REFERENCES

[1] Woo G. (2013) Historical development of the British and Scandinavian earthquake archives. *Bull. Seism*. doi: 10.1007/s10518-013-9487-7.
[2] Ambraseys N.N., Melville C.P. (1982) *A history of Persian earthquakes*. Cambridge University Press, Cambridge.
[3] Principia Mechanica Ltd. (1982) *British earthquakes*. PML Report for CEGB, BNFL and SSEB.
[4] Rietbrock A., Strasser F., Edwards E. (2011) A stochastic earthquake ground-motion prediction model for the United Kingdom. *Bull. Seism. Soc. Amer*., **103**, 1, pp. 53-77.
[5] Glaser L., Smith P. (2012) Probabilistic seismic hazard assessment for Hinkley Point. *AMEC Geomatrix* 15118/TR/0019.
[6] Bishop C. (1995) *Neural networks for pattern recognition.* Oxford University Press, Oxford.
[7] Hartigan, J.A. (1975) *Clustering algorithms*. John Wiley & Sons, Inc., New York; 84-108.
[8] Weatherill, G., Burton P.W. (2009). Delineation of shallow seismic source zones using K-means cluster analysis, with application to the Aegean region. *Geophys J. Int.* **176**, 565–588.
[9] Galloway D.D. (ed.) (2012) Bulletin of British earthquakes 2011. *British Geological Survey Internal Report* OR/12/041. 44pp.
[10] Ambraseys, N.N. (1990) Uniform magnitude reevaluation of European earthquakes associated with strong-motion recordings. *Earthquake Engineering Structural Dynamics*, **19**, 1–20.
[11] Mayeda K., Gök R., Walter W.R., Hofstetter A. (2005) Evidence for non-constant energy/moment scaling from coda-derived source spectra. *Geophys Res Lett* 32:L10306. doi:10.1029/2005GL022405.
[12] Morasca P., Mayeda K., Malagnini L., Walter W.R. (2005) Coda derived source spectra, moment magnitudes, and energy-moment scaling in the western Alps. *Geophys J. Int.* 160:263–275.
[13] Kumar M., et al. (2015) Evidence for non-self-similarity in the Mw 7.7 2001 Bhuj earthquake sequence. *Natural Hazards* **75**, 2, 1577-1598.
[14] Woo G. (1996) Kernel estimation methods for seismic hazard area source modeling, *Bulletin of the Seismological Society of America* **86**, 2, 353–362.
[15] Marzocchi W., Jordan T.H. (2014) Testing for ontological errors in probabilistic forecasting models of natural systems, *Proc. Nat. Acad. Sci*. , doi: 10.1073/pnas.1410183111.
[16] Lindley D.V. (1990) *Making decisions*. John Wiley & Sons, London.

[17] Ornthammarath T., Lai C.G., Menon C., Corigliano M., Dodagoudar G.R, Gonavaram K.K. (2008) Seismic hazard at the historical site of Kancheepuram in Southern India. *Proc. 14 WCEE*, Beijing.
[18] SHWP (1987) *Hinkley Point seismic hazard assessment*. Report for CEGB.
[19] Musson R.M.W. (2013) Updated intensity attenuation for the UK. *British Geological Survey Open Report* OR/13/029, 19pp.
[20] Ambraseys N.N. (1988) Engineering seismology. *Earthq.Eng.Struct.Dyn.,* 17, 1-105.

Past is the Key of the Present. A Geological Principle as Bayesian Philosophy Applied for Seismic Hazard Analysis.

José G. Sanchez-Cabañero[1]; Mª José Crespo[2]; Raúl Pérez[3]

1.- CSN, Consejo de Seguridad Nuclear, Geosciences Branch, Madrid, Spain, jsc@csn.es.
2.- PRINCIPIA Ingenieros Consultores, Madrid, Spain, maria.crespo@principia.es
3.- IGME, Instituto Geológico y Minero de España, Geological Hazard Division, Madrid, Spain, r.perez@igme.es.

ABSTRACT

Current licensing process of the European reactors in operation requires analyzing site seismic hazards. After the Fukushima accident, reviewing the scope of that process has become more essential; especially, to identify and characterize seismogenic structures able to threaten the reactor safety. The most relevant Bayesian approach to constrain the characterization of seismic sources based on historical or recorded seismicity, tries to incorporate new source data preserved in the geological record by surveying primary (surface or near surface displacement) and secondary (liquefaction, subsidence, landslides, rock failing, tsunami…) seismic effects from known and unknown sources. Different methodologies have been developed for identifying past seismogenic activity not represented in seismic catalogues. Incorporating this information following a Bayesian approach for estimating statistical distributions of earthquake sizes and recurrences is the key of the numerical modeling of a Seismic Hazard Analysis (SHA).

Application of a Bayesian approach is rational in any case, but it is especially needed for regions with low to medium seismicity rate as is the Western Europe, crossed from the Valencia Trough to the North Sea by the European Rift which is a very large seismogenic structure, along which a significant number of European reactors are sited. As recommended by the ENSREG at 'European Stress Test Results', methods like the ones proposed in IAEA SSG-9 are good procedures for extending the seismic catalogue backwards or enriching the seismic activity characterization by other means. In the Spanish context, a couple of examples can be cited: a recent reevaluation of the national seismic hazard map was carried out considering paleoseismic information for estimating the maximum magnitude of seismic zones; and secondly, a proved methodology for incorporating paleoearthquakes in zoneless seismic hazard calculations will be briefly described in this paper.

Key words: Seismic Hazard Analysis, seismic source, seismic effects, paleoseismic information, paleoearthquakes.

INTRODUCTION

The world occurrence of earthquakes, even in regions with high seismicity rates like Japan, shows that the time span of historic seismicity is too short to capture seismic source parameters relevant for hazard prediction purposes especially at low probability levels; examples of these parameters are the maximum magnitude and the seismicity rate. This fact becomes more critical in regions with low to moderate seismicity rates like Western Europe, where its slower behaviour implies a great challenge to identify and characterize existing seismic sources.

Some recent or ongoing EU projects in relation with seismic hazard Analysis (SHA) are GSHAP[1] (1992–1999), PALEOSIS[2] (1997–1999), FAUST[3] (1998–2000), SESAME[4] (1996–2000), ESC–

1 Giardini, D. Editor 1999; "The Global Seismic Hazard Assessment Program 1992-1999. Spetial Issue. Annali Geofis., 42 (6). UN/IDNDR demonstration program.

SESAME[5] (1996–2002), or more recently TOPO–EUROPE[6] (2006–) or SHARE[7] (2009–2012). A general common objective in these projects has been to improve classical approaches by incorporating new data like past historic and prehistoric strong events, in addition to unifying methodologies at a European scale. To support the SHARE project, two initiatives have appeared in the Iberian Peninsula: the IBERFAULT[8] initiative and the QAFI[9] (Quaternary Active Faults, V. 2.1) database.

The object of these studies is generally to determine the design seismic action of a new structure. Normally more than one level of occurrence probability is to be considered, with different performance requirements. For conventional structures, it is usual to employ a 10% probability of occurrence over 50 years, which corresponds to a return period of 475 years. This means that the previously dedicated efforts for conventional applications are far from the site specific needs demanded by the safety of critical industries like gas and nuclear installations, where it is common to work with lower return periods (2475, 4975, 10,000, 100,000 years or even more), and to consider site-effects and uncertainties analysis performed with technically sophisticated approaches.

A question then arises as to how reasonable it is to produce results for return periods that far exceed the time range covered by the historical catalogue. Instrumental data will span a century at best; the historical catalogue is more variable depending on country, but will never be long enough to contain more than one event with a mean recurrence period on the order of those mentioned in the previous paragraph. The seismic source characterization obtained out of the catalogue, needs to be supplemented with paleoseismic information.

CURRENT EUROPEAN NPPs FLEET STATUS

During past seismic design process of most European NPPs, the knowledge on strong earthquake occurrences was very limited if compared to the current state of the art. In general, almost exclusively historical data were used without carrying out nascent paleoseismic surveys, which are needed to better characterize strong events with low frequency rates. Additionally seismic records available to design at that time were few and of low damage capacity if compared with records available at present.

The European Stress Tests[10] process, carried out in 2011-2012 after the CN Fukushima Daiichi accident, emphasized the relevance of assessing the adequateness of existing NPPs design bases to deal with the worst credible scenario originated by natural phenomena. Their results addressed the necessity to develop guidance on seismic hazard, and the assessment on margin beyond the initially considered design basis of each site, involving the best available expertise. The Western

2 PALEOSIS; ENV4-CT97-0578 (DG12-ESCY: http://ssgfi.geo-guide.de/cgi-bin/ssgfi/anzeige.pl?db=geo&nr=000891&ew=SSGFI

3 FAUST; ENV4-CT97-0528: http://faust.ingv.it/

4 Jiménez M.J., Giardini D., Grünthal G., et al; “Unified Seismic Hazard Modelling Throughout The Mediterranean Region”, Boll. Geof. Teor. Appl., 42, 3-18. IGCP (International Geological Correlation Program nº 382), SESAME (Seismotectonics and Seismic Hazard Assessement of The Mediterranean Basin, 1996-2000).

5 ESC–SESAME (European Seismological Commission): http://www.ija.csic.es/gt/earthquakes/

6 TOPO EUROPE: http://www.topo-europe.eu/

7 SHARE, Seismic Hazard Harmonization in Europe; FP7, WP4: http://www.share-eu.org/

8 Iberian meetings on active faults and paleoseismologya, Sigüenza, October 27th-29th, 2010 & Lorca, October 22th-24th 2014: www.iberfault.org

9 http://info.igme.es/qafi/

10 ENSREG, ‘Post-Fukushima Accident. Stress Test Peer Review Board. Stress Tests Performed on European NPPs’, Final Report, v12i, March 25th 2012: http://www.ensreg.eu/node/407

European Nuclear Regulators Association (WENRA) has finished a process to harmonize this topic by producing Reference Levels[11&12] to new define or revaluate Design Basis Event (DBE) matching a low frequency level resulting from a probabilistic seismic hazard analysis (PSHA). Furthermore, those results encourage the process of Periodic Safety Review (PSR) to develop consistent approaches for assessing seismic margins beyond the DBE. Additionally, to take into account in new reactor designs the lessons learned from this huge accident, the nuclear regulation harmonization process conducted by WENRA, considers a specific section[13] dealing with natural phenomena, including earthquakes. All over these processes, the concern about the correctness or definition of seismic design basis is being of paramount importance in order to assess technical basis which guarantees the safety of European Nuclear Safety Regulators Group (ENSREG) Nuclear fleet[14&15].

An appropriate framework to assess the current seismic design basis and allow estimating margins, is to carry out a PSHA which opens the door to a risk informed decision making, based on the best available science. For this task, it becomes essential to know if there are seismogenic structures threatening reactor sites, by analyzing the geological record from a paleosismic point of view, as addressed in new approaches like the IAEA SSG-9 (August 2010) and was stated by ENSREG[16&17].

From the above statements and after reading all ENSREG country peer review reports, especially those from plants reviewed under IAEA regulations, it is apparent that SHAs performed within the European NPPs licensing processes, should be updated in most cases by considering both, paleoseismic surveys and the current knowledge on active tectonic in Europe.

In the particular case of Spain, the Conclusion 8 of the Final National Report[18] reads: '*The CSN shall introduce a programme to update seismic site characterisation studies, following the IAEA's most recent regulations*'; and the requirement I1 of the National Action Plan[19], includes as a ITC (Complementary Technical Instruction): '*Implementation of the necessary improvements to*

11 WENRA Report on 'Safety Reference Levels for Existing Reactors', 24th September 2014: http://www.wenra.org/media/filer_public/2014/09/19/wenra_safety_reference_level_for_existing_reactors_september_2014.pdf

12 WENRA Statement regarding the revision of the Safety Reference Levels for existing reactors taking into account the lessons learned from the TEPCO Fukushima Dai-ichi Nuclear Accident, October 2014: http://www.wenra.org/media/filer_public/2014/11/13/wenra_statement_on_updated_srl_2014.pdf

13 RHWG Report on 'Safety of new NPP designs', 03.6 Position 6: External hazards, March 2013: http://www.wenra.org/media/filer_public/2013/08/23/rhwg_safety_of_new_npp_designs.pdf

14 69 sites: Belgium (2), Bulgary (1), Czech Republic (2), Germany (12), Finland (2), France (19), Hungary (1), Netherlands (1), Romania (1), Slovakia (4), Slovenia (1), Spain (6), Sweden (3), Switzerland (4), Ukraine (4), United Kingdom (8).

15 156 reactors in operation: Belgium (7), Bulgaria (2), Czech Republic (6), Germany (1)7, Finland (4), France (5)6, Hungary (4), Netherlands (1), Romania (2), Slovakia (4), Slovenia (1), Spain (8), Sweden (10), Switzerland (5), Ukraine (1), United Kingdom (18). Under decommission or new (Finland 1, France 1, Slovakia 2, Ukraine 2, United Kingdom 2) reactors are not included. To see IAEA data base: http://pris.iaea.org/PRIS/CountryStatistics/CountryStatisticsLandingPage.aspx.

16 4.3... it is therefore recommended that national regulators consider how best to ensure that specific requirements (e.g. IAEA safety standards and WENRA reference levels) for all three topical areas under investigation (Earthquakes, flooding and other extreme weather conditions) are adequately maintained. ENSREG, 'Post-Fukushima Accident. Stress Test Peer Review Board. Stress tests Performed on European NPPs', v12i, 2012: http://www.ensreg.eu/node/407.

17 5.2.3... 'With regard to hazards, particularly seismic, it would appear that techniques and available data are still developing. It is recommended that regulators should consider co-operation with other agencies in order to develop a consistent approach across Europe, taking account of updates in methodology, new findings and any relevant information from continuous research on active and capable faults in the vicinity of NPPs. ENSREG, 'Post-Fukushima Accident. Stress Test Peer Review Board. Stress tests Performed on European NPPs', v12i, 2012.04.25: http://www.ensreg.eu/node/407.

18 'Stress tests carried out by the Spanish nuclear power plantsFinalReport', 30th December 2012: http://www.ensreg.eu/sites/default/files/Spain_Stress-Tests.pdf

19 SPAIN, 'National Action Plan', Attachment 1: 'Requirements included in the CSN Instructions ITC-STS', Table A-1.1: 'Generic Requirements', December 19th, 2012: http://www.ensreg.eu/node/690

increase the seismic resistance capacity of equipment relating to the following to 0.3g: a) The two "safe shutdown paths" defined in the IPEEE, b) Containment integrity, c) Mitigation of station blackout (SBO) situations, and d) Severe accident management'.

The updated National Action Plan[20], informs that plant responses to the ITC was completed at December 2014 (Table A-1.1), and an action related to the former Conclusion 8 is foreseen for the first quarter of 2015: '*Issuing by the CSN of a new ITC that will require a reassessment by the licensees of the seismic risk of each site. This assessment will take into account geological and palaeo-seismological data characterising relevant active faults*'.

GEOTECTONIC SETTING OF WESTERN EUROPE

According to the SSG-9 (IAEA, 2010), the first goal in evaluating seismic hazards at any nuclear site, is to build a sound database of geologic, geophysical, geotechnical and seismologic data collected at four distance scales each with an appropriate degree of detail. The information derives from both, past and new surveyed data, to construct a reliable and coherent seismotectonic model (and alternative models if needed).

Any seismotectonic model consists of two types of seismic sources: a discrete set of identified seismogenic structures, and diffuse seismicity that is not attributable to specific structures. This second type, typically represented as zones, has been the only one used in classical approaches, supported by historic seismicity. The overall bottom line, is that tectonic events of interest for Earthquake Engineering are generated by fault ruptures, even if sometimes the faults are not identified. In order to reduce uncertainty, it is necessary to discover the roll of each fault or fault system, especially if they are close to nuclear sites or located further but representing a potential threat.

Seismogenic structures can consist of isolated faults, or more frequently a particular fault can be part of a master system (a bigger structure or a fault system) whose movement is conducted by the master behaviour along some geologic stages. In other words, following the Bayesian philosophy, classical approaches constrain the seismicity occurrence, at any scale, as an aleatory phenomenon, but Nature has memory.

In order to minimize both dualities, mainly to identify seismogenic structures, it is needed to carry out paleoseismic surveys that let us discover known and unknown seismogenic structures. The challenge will remain as an unresolved issue in the near future, especially if seismicity rates are low or medium and other bayesian constrains from paleoseismicity surveys and updated knowledge on active tectonic are not considered.

At intraplate domains like Western Europe, according to the IAEA SSG-9, in order to increase the knowledge on geodynamic setting where NPP sites are located, the recommended tasks include: to identify master structures, current/past tectonic regime and the depth/width of the seismogenic layer, as well as to carry out paleoseismic surveys as far as earlier Pliocene. Additionally, historic seismicity is usually located around towns but actual sources can be located away from towns: in this respect also landscape features affected by past strong events, can provide useful source information if they are preserved, by applying the INQUA Environmental Seismic Intensity Scale 2007 – ESI 07 (Michetti et al 2007).

20 SPAIN, 'National Action Plan', Rev. 1, Attachment 1: 'Requirements included in the CSN Instructions ITC-STS', Table A-1.1: 'Generic Requirements', and Attachment 2: 'Recommendations and Suggestions of the ENSREG Peer Reviews carried out in Spain', December 17th 2014: http://www.ensreg.eu/sites/default/files/Spain%20-%20NAcP%20rev.1%202014.pdf

Most WENRA countries are located on an intraplate domain, where the regional geotectonic setting is driven by two main actors: the Alpine orogene, formed by a belt of ranges (Betic-Alps-Carpathians-Balkanides to the north, and Rift-Appenines-Dinarides-Hellenides to de south) with a high seismicity rate and its passive foreland or intraplate domain with low-moderate seismicity rate (Figure 1). The passive foreland has several main cortical features. One of them is the European Rift, an extensional structure more than 2,000 km long and with variable width, that extends from the North Sea between the United Kingdom and Norway all the way to the Valencia through (even more). Some master systems gradationally separated can be differentiated (Yeats 2012): Mediterranean and North Sea basins, Rhenish Massif, Jura transfer zone, and grabens of Bresse-Rhone, and Lower and Upper Rhine (Figures 2 and 3).

The European Rift was introduced by Maurice Mattauer (1973). It is a structure active since the Cenozoic, having today a low deformation rate (Yeats, 2012). Along its trace there was Quaternary and Holocene volcanism (Figures 3 and 5), and also strong seismicity has happened along its body, highlighting the existence of potentially seismogenic faults (Figure 4). In addition to strong events discovered by paleoseismic surveys (Camelbeeck et al, 2007; Cushing et al, 2000; Masana et al, 2000), from 1356 year until today, more than a dozen historical strong earthquakes with EMS intensities as high as VIII–X took place in Netherlands, Belgium, France, Spain and Switzerland[21]. Along the European Rift there are located nearly 19 sites with 41 operating reactors in Belgium, Germany, France, The Netherlands, Spain, Switzerland and United Kingdom (afps 1996; BRGM 1979, 1980, 1981, 1985; IGN 2002). Closer in time, a couple of events with intensity VII (EMS) shutdown Biblis (13.04.1992) and Fessenheim (15.07.1980) both NPPs being located on the Lower Rhine graben.

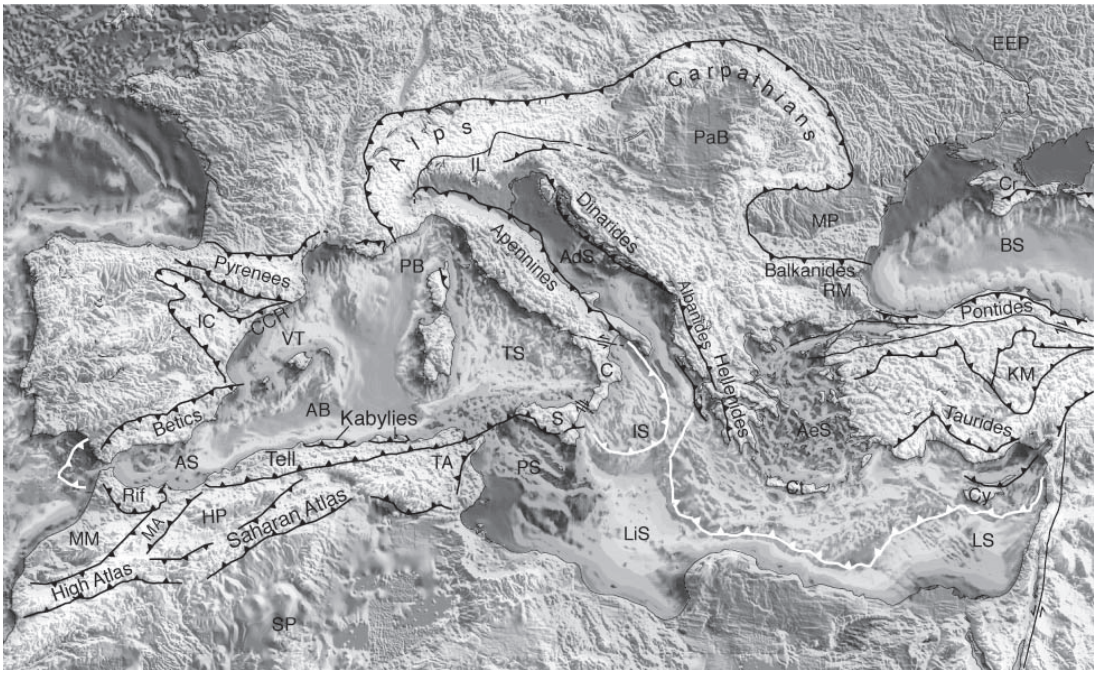

Figure 1. Terrain digital model of the Mediterranean region with simplified mayor geological structures. Quoted from Cavazza and Wezel (1983).

21 North Sea South (VII-VIII, May1382), Basel (IX, October 1356), Remiremont (VIII, May 1682), Buguey-Chautagne (VIII, February 1822), Vercors (VII-VIII, April 1962), Tricastin (VIII, January, February 1773, Agoust 1873), Trevaresse (IX, June 1909), Amer (VIII, March 1427), Olot (VIII-IX, May 1427), Queralbs (IX, February 1428), Enguera (IX-X, March 1748). Xátiva (VIII, November 1519), Tabernes (X, December 1396).

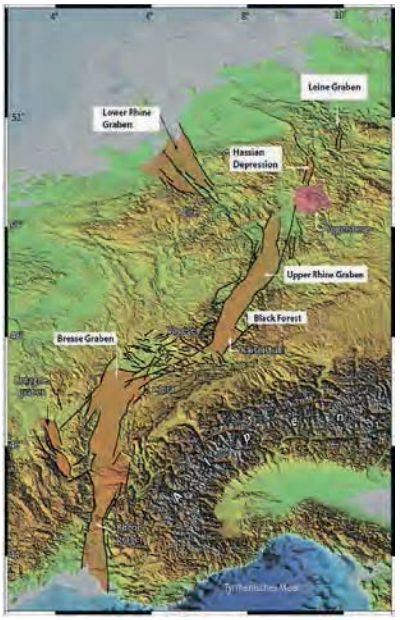

Figure 2. Grabens of Bresse, Lower and Upper Rhine, Limagne, Hassian and Leine. Quoted from Reicherter et al (2013).

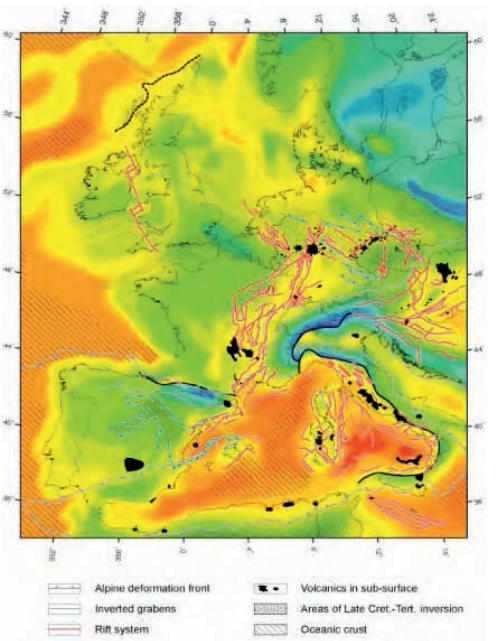

Figure 3. Red lines show the Rift system and black stains Quaternary volcanism. Quoted from Ziegler et al (2005).

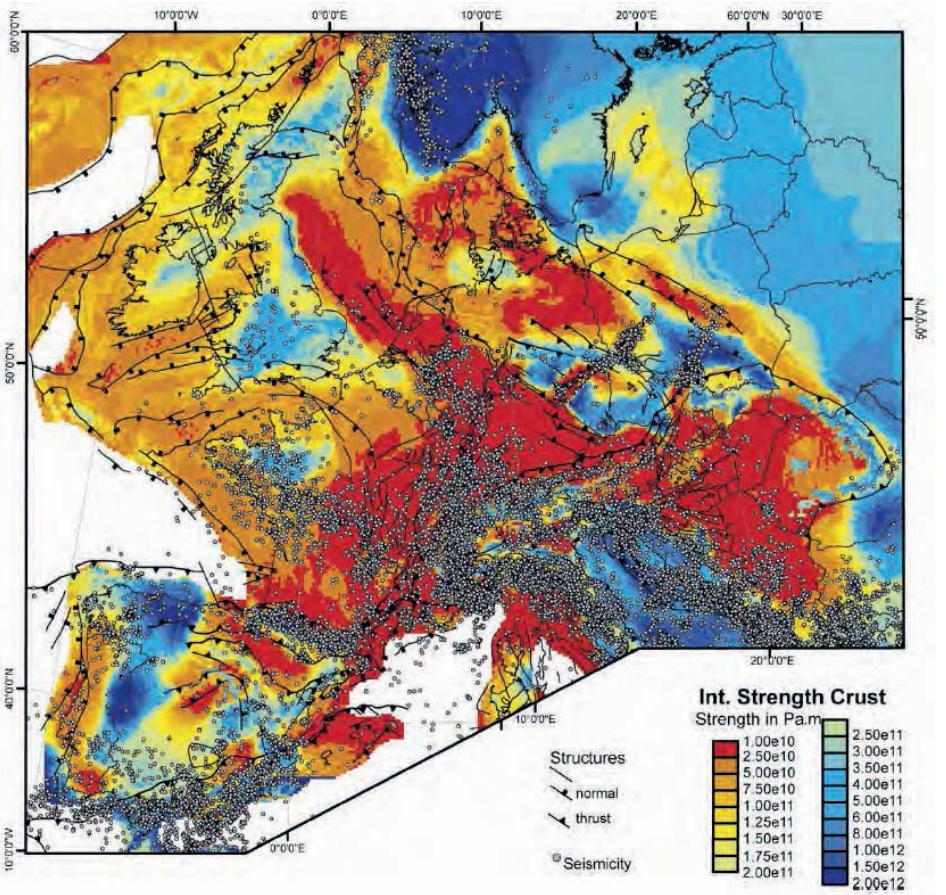

Figure 4. Integrated strength crust for intraplate Europe. Contours represent integrated strength in compression total lithosphere, mantle and crust, with superimposed distribution of current seismicity (green dots); The European Rift is belonged maximum values of strength (red color). Quoted from Tesauro et al (2007).

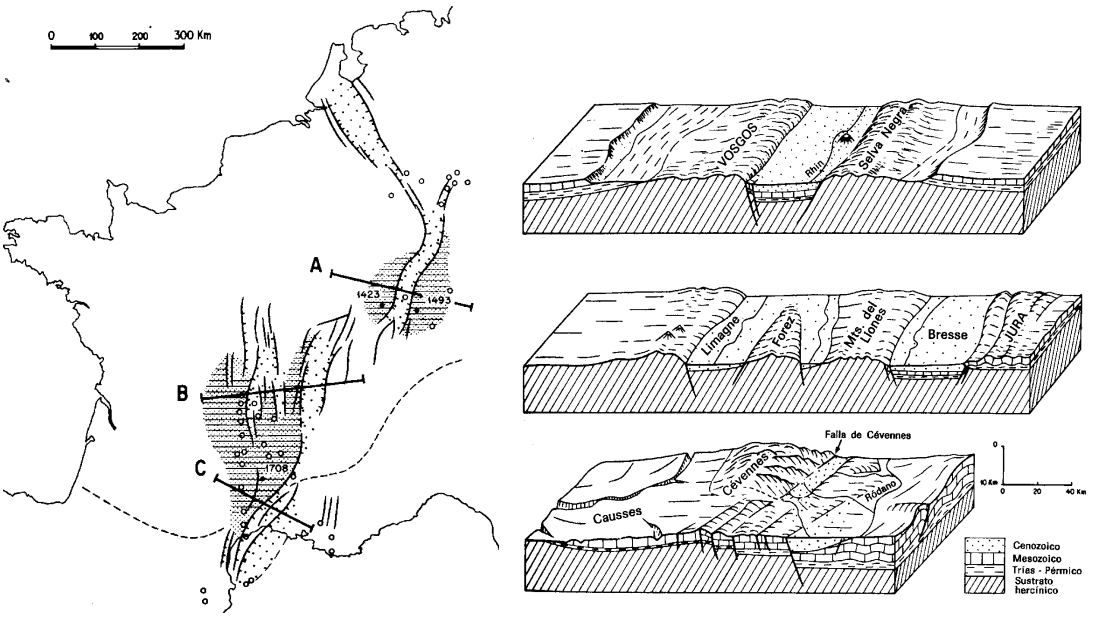

Figure 5. Early description of the European Rift System showing contours of Cenozoic basins, main faults, and volcanic outcrops locations (dots). Quoted from Mattahuer (1973).

Each master system along the European Rift has a different tectonic style that controls the mechanism of the faults included in each one; and from a Bayesian point of view, the movement rate of a particular fault will be conditioned by the movement of relative faults. The maximum magnitude of each master system will be bounded by both, the seismogenic layer depth/width and the particular fault length. This is a huge aim to carry out in next future, necessary to constrain some PSHA uncertainties related to source characterization.

In the Iberian Peninsula, as result of IBERFAULT initiative, causative faults of 44 historic strong events were identified, and the QAFI database was developed. Also, fault ruptures less than 100 km long, with maximum M_w between 6 and 7, and occurrences between 15,000 and 20,000 years ago have been found as of today by Iberian geologists.

Seismic hazard map for the new Spanish seismic building code has been developed following the classical zoned model, but assuming as maximum magnitude at some zones resulting M_w from paleoseismic surveys. In addition, a new method to incorporate paleoseismic information in zoneless approach is being developed. Both initiatives are showed below.

EXAMPLES OF INCORPORATING PALEOSEISMIC INFORMATION INTO A PSHA

Example 1: derivation of maximum credible magnitude of zones from paleoseismic information.

The seismic hazard map of the Spanish Seismic building code dates back from 2002. During 2011 the map was updated (Ministerio de Fomento, 2013) and this new map will be the basis for the one in the building code, which is going to be updated during 2015.

The maps published (Ministerio de Fomento, 2013) initially considered three zonations and a zoneless branch, although in the final logic tree only two of the three zonations had non-zero weights. All the zonations considered had the corresponding maximum credible magnitudes assigned to their zones, based mainly in the seismic information contained in the catalogue; however for the new maps, some of these maximum credible magnitudes were updated considering geological data, some of them recently compiled in the QAFI database.

Example 2: incorporation of paleoearthquakes in zoneless methodologies.

A zoned model can be supplemented with faults wherever the information is available. To describe their activity one can make use of the characteristic earthquake (Schwartz and Coppersmith, 1984), assuming that the fault can generate earthquakes over a certain range, with frequencies centred on a given magnitude. A second possibility is the maximum earthquake model (Wesnousky et al, 1993), which assumes that the fault can only produce earthquakes of a certain magnitude.

There is still ongoing research regarding the magnitude beyond which surface ruptures usually appear and hence their associated activity rate should be assigned to known faults, indeed this may even depend on location. For Spain, Rivas (2014) has recently presented information in this regard.

In zoneless methodologies such as that proposed by Woo (1996) using kernel functions, the seismic activity rate λ_k depends on magnitude M and location $\mathbf{x}$ and is constructed as:

$$\lambda_k(\mathbf{x}, M) = \frac{1}{H(M)^2} \sum_{i=1}^{n} \frac{K\left(\frac{\mathbf{x}-\mathbf{x}_i}{H(M)}\right)}{T(\mathbf{x}_i)}$$

This adds the kernel functions K centred on each catalogue event with location $\mathbf{x}_i$, and weighed with an effective period $T(\mathbf{X}_i)$; the result is a continuous function of location and magnitude that does not have a predefined shape. The bandwidth $H(M)$ depends on magnitude. Crespo et al (2014) describe this formulation in greater detail.

The kernel function K is a probability density function in a two-dimensional space. It is normally symmetric, but it can also be skewed.

Skewed density functions normally have two additional parameters to define an axis and the ratio between radial dimensions in two perpendicular directions. The axially symmetric formulation can be skewed simply by multiplying it by a function. For example, the symmetric bi-quadratic function is:

$$K_{axi}(r) = \frac{n-1}{\pi H^2}\left[1+\left(\frac{r}{H}\right)^2\right]^{-n}$$

where: n is a decay exponent
H is the bandwidth

A possible directional version, proposed by Woo, is:

$$K_{dir}(r,\Theta) = K_{axi}(r)\frac{1}{1+\frac{DL}{2}}\left[1+DL\left(\cos(\Theta)\right)^2\right]$$

where: DL describes the degree of anisotropy
T controls the orientation of that anisotropy

This formulation decouples the kernel size from its anisotropy, but is undefined at the origin. Figure 1 shows schematically isotropic and anisotropic versions of the kernel. There is currently ongoing work on an elliptic version of the kernel function that avoids the singularity.

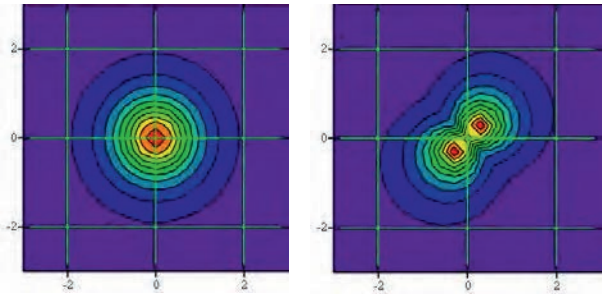

Figure 1 Kernel functions with and without anisotropy

When the kernel function sits on earthquakes without a known fault, axial symmetry is normally assumed. When the fault is known, the activity can be aligned with it by skewing the kernel function and reconsidering its reference period to be consistent with the recurrence period of the corresponding fault. It is worth noting that, even with symmetrical functions, the activity may tend to concentrate along the faults because of the locations of the earthquakes it generates, but this can be enhanced by the use of directional kernel functions.

As explained earlier each earthquake also has its own effective period. These can be assigned simply as a function of magnitude and location, or individually based on its specific characteristics. When the magnitude coincides with that associated to the fault, the effective period should be that estimated for such an earthquake. The effective period should be estimated from paleoseismic considerations and could be longer than the time span covered by the historic catalogue, a period in which not more than one such earthquake may have been experienced. In such cases the activity rate thus represented may correspond to time period longer than the time span of the catalogue.

Moreover, apart from the possibilities afforded by the kernel function and the effective period, new events can be incorporated to the catalogue to represent an activity that it does not reflect but can be transferred from paleoseismicity.

Taking as a reference the two best known models for incorporating faults in hazard studies (Schwartz and Coppersmith, 1984; Wesnousky et al, 1993), both would have here natural equivalent formulations. If the fault also produces lower magnitude events, those would be reflected in the catalogue hence accounted for by their corresponding kernel functions. If it only produces events around a given magnitude, its activity would be represented only via some already existing event in the catalogue or via added events.

The characteristics of the events added to represent activity deduced from paleoseismicity is given below, using the previous terminology:

- Epicentral location $\mathbf{x}_i$ centred on the fault or, if the fault is very long, via several events along it.

- Characteristic magnitude M of the fault and its uncertainty, which will be incorporated as a random variation when constructing the activity rates for different magnitudes.

- Effective period T equal to the recurrence period of the fault. If several events were placed, the effective period will be the recurrence period time by the number of events, so that the contributions are weighted with the recurrence period.

- The bandwidth H should be on the order of the width of the fault projection of the surface, though this may be influenced by the kernel function employed.

When the fault is made of several segments each can be represented with an event with the proper orientation. The paleoseismic study may lead to more than one possible interpretation: a single fault with a characteristic magnitude or several segments that practically behave as independent faults. Both can be adequately represented with added events.

The zoneless methodology based on non-parametric density estimators (kernel functions were described here) allows an easy and versatile integration of the seismic activity obtained from paleoseismicity, whether it is represented by catalogue events on known faults or by added events. Both alternatives require the fault geometry, its characteristic magnitude, and its recurrence period.

In regions of low to moderate seismicity with scarce neotectonics and few/low associated seismicity, activity rates cannot be derived from statistical analysis of historical earthquakes. In specific site studies, it is usually the case of having a priori information, with assigned probabilities that can be updated with the new information available after the site specific campaigns have been conducted. The combination of the new available evidence with the Bayes theorem is a quantitative mean for incorporating evidences, seismicity and geological information into a hazard assessment in a consistent way.

For generating the engineering input sought, it is worth analysing to what extent the alternatives (distributed zone, several independent faults) entail differences in the results. Indeed it may be best to adopt different strategies for different regions, depending on distance to the site, as some guides already suggest; this is for example the case of SSG-9 (IAEA, 2010).

CONCLUSIONS

The European Stress Tests results have emphasize the relevance of assessing the adequateness of existing NPPs design bases to deal with the worst credible scenario originated by natural phenomena, including earthquakes. Seismic design of most European NPPs were obtained using, almost exclusively historical data, and site seismic characterization should be updated in most cases by considering both, paleoseismic surveys and the current knowledge on active tectonic.

This finding was highlighted years ago by some events that took place near some nuclear sites in Japan and the IAEA SSG-9 (2010) was released as an approach to conduct necessary geologic surveys to support PSHA analysis. At present, five documents (two Safety Reports and three TecDocs) are in press to detail the SSG-9 approach.

Two examples have been summarised in which geological information is incorporated in seismic hazard analysis. The first one is a practical application of the incorporation of geological information for updating maximum credible magnitudes of zones whilst the second is a description of a methodological approach for incorporating geological information in zoneless methodologies. In both cases, the combination of new information with the Bayes theorem is a quantitative mean for incorporating geological information into a hazard assessment in a consistent way.

REFERENCES

- afps, '*Mille ans de séismes en France; catalogue d´épicentres, paramètres et references*', Ouest Editions, November 1996.
- BRGM, '*Les tremblements de terre en France*', Mémoire nº 96, 1979.

- BRGM, '*Introduction a la Carte Tectonique de la France*', Mémoire nº 110, 1980.
- BRGM, '*Carte Sismotectonique de la France*', Mémoire nº 111, 1981.
- BRGM, '*Nouveau zonage sismique de la France*', Octobre 1985.
- Cavazza W. & Wezel F.C., Episodes, Vol. 26, Nº. 3, September 1983.
- Crespo, M.J., Martínez, F. and Martí J. (2014) "Seismic hazard of the Iberian Peninsula: evaluation with kernel functions", Natural Hazards and Earth System Sciences, Vol. 14, pp. 1-15.
- IAEA, SSG-9, Specific Safety Guide 'Seismic Hazards in Site Evaluation for Nuclear Installations', Vienna, August 2010: http://www-pub.iaea.org/MTCD/publications/PDF/Pub1448_web.pdf
- IGN, '*Catálogo sísmico de la Península Ibérica (880 A.C.-1900)*', Monografía 18, 2002
- Mattauer, Maurice, '*Les Déformations des matériaux de l'écorce terrestre*', Herman, d'éditeurs des Sciences et des Arts, Paris, 1973.
- Masana E., Villamarín J.A., Sánchez-Cabañero J., Plaza J., & Santanach P., '*Seismological behavior of a fault with no historical seismicity: El Camp fault (northeastern Iberian península)*'. HAN2000-Potential for large earthquakes in low seismic activity regions of Europe, 101-104, 2000.
- Michetti, A.M., E. Esposito, L. Guerrieri, S. Porfido, L. Serva, R. Tatevossian, E. Vittori, F. Audemard, T. Azuma, J. Clague, V. Comerci, A. Gürpinar, J. Mc Calpin, B. Mohammadioun, N.A. Mörner, Y. Ota, and E. Roghozin (2007). *Intensity Scale ESI 2007*, in Mem. Descr. Carta Geologica d'Italia L. Guerrieri and E. Vittori (Editors), Servizio Geologico d'Italia, Dipartimento Difesa del Suolo, APAT, Rome, Italy, 74.
- Ministerio de Fomento (2003) *Norma de Construcción Sismorresistente Española, NCSE-02*
- Cushing M., Lemeille F., Cotton F.S., Grellet B., Audru J-Ch., Renardy F., '*Paleoearthquakes investigations in the Upper Rhine Graben in the framework of the PALEOSIS project*'. HAN2000-Potential for large earthquake in low seismic activity regions of Europe, 39-41, 2000.
- Reicherter K., Hinzen K.G., Salamon M., Mathes-Schmidt M., Fernández-Steeger T., Walter R. Rudersdorf A., '*Seismic Hazard, Critical Facilities and Slow Active Faults*', Field Trip Guide. 4th International INQUA Meeting on Paleoseismology, Active Tectonics and Archeoseismology, October 9th–15th, 2013.
- Rivas (2014) "Contribución Metodológica para Incorporar Fallas Activas en la Modelización de la Fuente Dirigida a Estimaciones de Peligrosidad Sísmica. Aplicación al Sur de España", Tesis Doctoral, Universidad Politécnica de Madrid.
- Schwartz, D.P. and Coppersmith, K.J. (1984) "Fault Behavior and Characteristic Earthquakes: Examples from the Wasatch and San Andreas Fault Zones", Journal of Geophysical Research, Vol. 89
- Tesauro M, Kaban M.K., Sierd A.P.L., Cloetingh S.A.P.L., Hardebol N.J., & Beekman F., '*3D strength and gravity anomalies of the European lithosphere*', Earth and Planetary Science Letters 263, 2007.
- Wilson M. & Bianchini G., '*Quaternary magmatism within the Mediterranean and surrounding regions*', Geol. Soc., London, Special Publications, 1999.
- Wesnousky, S.G., Scholz, C.H., Shimazaki, K., and Matsuda, T. (1983). "Earthquake Frequency Distribution and the Mechanics of Faulting", Journal of Geophysical Research, Vol. 88.
- Woo, G (1996) "Kernel Estimation Methods for Seismic Hazard Area Modelling", Bulleting

of the Seismological Society of America, Vol. 86, pp. 353-362.

- Yeats, Robert, '*Active Faults of the World*', Cambridge University Press, May 21th, 2012.
- Ziegler P.A. & Dèzes P., '*Crustal Evolution of Western and Central Europe*', Crustal Evolution of Europe, European Lithosphere Dynamic, D.G. Gee & R.A. Stephenson (eds.) Memoir of the Geological Society, London, 2003.

Bayesian update of a simplified PSHA model, comparison of different academic cases

L. Vaseux & J.M. Thiry

AREVA NP

ABSTRACT:

Probabilistic seismic hazard assessment for large return period leads to high uncertainty, a way to reduce this uncertainty is to use new information, observations for example, to constrain the predictions and update them using Bayesian techniques.

The presented study was performed with the aims to investigate how to optimize predictive seismic hazard results using the Bayesian update. It focuses on the estimation of the probability of acceleration exceedance, i.e. the probability that an earthquake's PGA exceeds a certain threshold α.

At first, a simplified Cornell-like methodology is implemented to derive the probability of exceedance at a selected site. Our estimations are based on a catalog of historical observations reported around the site. As always, the construction of hazard curves requires the estimation of several parameters (e.g., attenuation laws, Gutenberg-Richter parameters, maximum magnitude); all of these carry epistemic uncertainties. To account for this variability, we use a realistic logic tree whose output is a set of exceedance probability curves corresponding to different samples of the input parameters.

The results of the logic tree constitute a prior knowledge which we try to update in the light of synthetic PGAs. The simplified model, the results and the issues raised by this exercise are discussed in the paper.

Keywords: Cornell-like PSHA, Logic Tree, Bayes Updating, MCMC

1. INTRODUCTION

Cornell-like Probabilistic Seismic Hazard Assessment (PSHA) studies in low and moderate seismic regions often exhibit significant discrepancies. Considering the importance of characterizing seismic hazard for building design, the OECD/NEA highlighted the issue of consistency-checking the PSHA results.

When conducting a PSHA in term of Peak Ground Acceleration (PGA), the target quantity is the annual rate of exceedance of a certain PGA value α. The estimation process involves the specification of plenty parameters. Some of them can be estimated from the data, others rely on expert judgments. But in both case, they carry 'epistemic' uncertainties, which can be treated by a logic tree. The outputs are several estimates of the annual rate of exceedance constituting a prior knowledge. But the discrepancies between probabilistic and deterministic measures of the seismic hazard remain a major concern.

Using Bayesian updating methods to address this issue has been encouraged and several studies have investigated the subject (cf. Humbert and Viallet 2008, Viallet et al. 2008, Seva and Sandri 2013). Two limitations have been identified: (i) The period of observation is often too short to get meaningful improvements of the prior PSHA. (ii) In stable seismotectonic area, the acceleration records are too low to update the complete hazard curve.

To address these limitations, first, the temporal dimension is removed by only focusing on the distribution of the PGA; then, a parameterization of the hazard curves is introduced, allowing an update of the entire PSHA through an adjustment of the parameters.

The remainder of this article is organized as follows. In section 2, the prior model and the treatment of the uncertainties by the mean of a logic tree are described. Then the outputs are fitted by a parametrical model (section 3). In section 4 and 0, a specific and a more classical approach are presented to apply a Bayesian update of the parametrical model. Finally, section 6 gives the conclusion.

2. A SIMPLE CORNELL-LIKE PRIOR MODEL

In the Cornell-McGuire (1968, 1995) methodology, the annual rate of exceedance (denoted $\lambda^{(\alpha)}$) can be broken down into the product as follows:

$$\lambda^{(\alpha)} = \lambda_0 \rho^{(\alpha)}$$

with: - λ_0, the **activity rate** describing the number of earthquake[1] occurrences per year,
- $\rho^{(\alpha)}$, the **Probability of Acceleration Exceedance** (PAE), namely the probability for an earthquake of having a PGA greater than α (regardless the magnitude and the distance).

Our premise is that the estimation of $\rho^{(\alpha)}$ is totally independent of λ_0. The latest is therefore easily estimated by taking the average waiting time between two earthquake occurrences. That is the reason why our attention is focused on the estimation of the PAE, whose basic formulation is:

$$\rho^{(\alpha)} = P(A > \alpha) = \int_{M_{\min}}^{M_{\max}} \int P(A > \alpha | m,r) f_{M,R}(m,r) dr\ dm$$

where A denotes the random variable corresponding to the PGA, and $f_{M,R}(m,r)$ describes the distribution of magnitudes and source-to-site distances.

The database used for deriving a prior PAE gathers 82 historical observations within 200 km around a specific site in France (see Figure 7 in Appendix 1). Intensities have been changed into moment magnitudes (Mw), and epicentral distances (R_{epi}) have been derived. The minimum magnitude considered is Mw=4. Completeness periods have also been computed for 5 magnitude ranges by the method of slopes (see Suckale & Grünthal, 2009). There are summed up in the Table 1.

Table 1: Completeness period of the catalog for different magnitude ranges.

Magnitude range	4 – 4.5	4.5 – 5	5 – 5.5	> 5.5
Completeness period	1828-2005	1759-2005	1727-2005	1428-2005
Number of earthquakes	41	19	11	11

[1] Usually we consider only earthquakes of magnitude higher than a significant threshold (in this paper Mw > 4).

The magnitude is described by the Gutenberg and Richter (1944) law, whose parameters are estimated by the Weichert (1980) method[2], e.g.:

$$\hat{\beta} = 1.7104 \quad \text{and} \quad \hat{\lambda}_0 = 0.3780 \quad \text{for} \quad M_{max} = 6.6$$

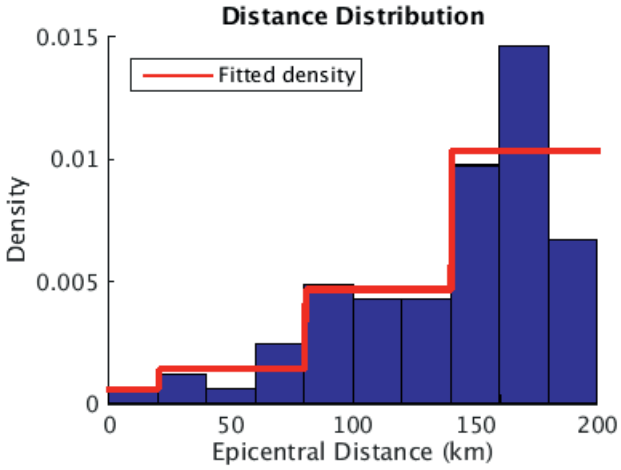

Figure 1: Step curve modeling the distance superimposed on the histogram derived from the catalog.

The distances are modeled by a simple circular zoning: the surrounding of the site of interest is grossly cut into 4 concentric annuluses (0 to 20, 20 to 80, 80 to 140 and 140 to 200km).
Then a uniform distribution on these intervals is assumed, weighted by the proportion of earthquakes belonging to each of them.
This model leads to the step function in red on the Figure 1.

To treat the uncertainties, a realistic logic tree is implemented with 5 GMPEs (Berge-Thierry et al. 2003; Atkinson & Boore 2006; Zhao et al. 2006; Cauzzi & Faccioli 2008; Akkar & Bommer 2010).

Uncertainties associated with the seismic parameters (β and M_{max}) have been treated with 400 secondary branches, where a gaussian distribution is assumed for β, and for M_{max}, a uniform distribution between 6.4 and 6.8.

Finally, the global logic tree is composed of 5x400 branches allowing the computation of 2000 estimates of the probability of exceedance for different thresholds α. From these results, a mean hazard curve and confident bounds at 16% and 84% can be derived (see Figure 2).

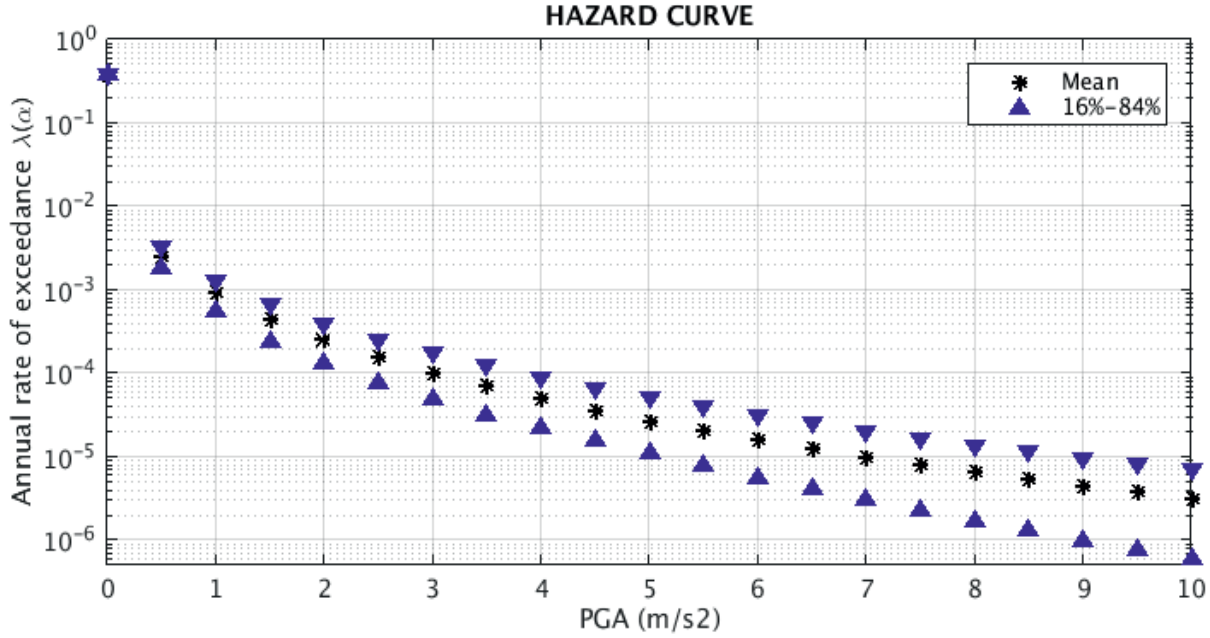

Figure 2: Hazard curves outgoing the logic tree. The probability of exceedance is multiplied by the activity rate λ_0 - which is not introduced in the logic tree - to obtain the annual rate of exceedance of different PGA levels.

[2] The estimation of λ_0 is given for information, since the study focus only on the PAE: we do not propose any update of the activity rate.

3. PARAMETRIZATION OF THE HAZARD CURVES

The logic tree previously described provides a prior knowledge consisting of 2000 estimation of the PAE. But classical Bayesian techniques apply on parameters. To address the absence of parameters to infer on, we try to fit a Weibull (1951) law with two positive parameters, k and η, describing respectively the shape and the scale of the exceedance function:

$$G(x) = 1 - F(x) = \exp\left(-\left(\frac{x}{\eta}\right)^{k}\right), \quad \text{for all } x > 0$$

This function can easily be linearized (relatively to k and η) by a change of variable:

$$\ln\left(-\ln\left(G(x)\right)\right) = k\ln(x) - k\ln(\eta)$$

Hence, an easy way of checking if a PAE can be modeled by a Weibull law is to plot ln(-ln($\rho^{(\alpha)}$)) versus ln(α). If the fit is good enough, the scatters plot is expected to form a straight line with slope k and y-intercept in –kln(η) (see Figure 3).

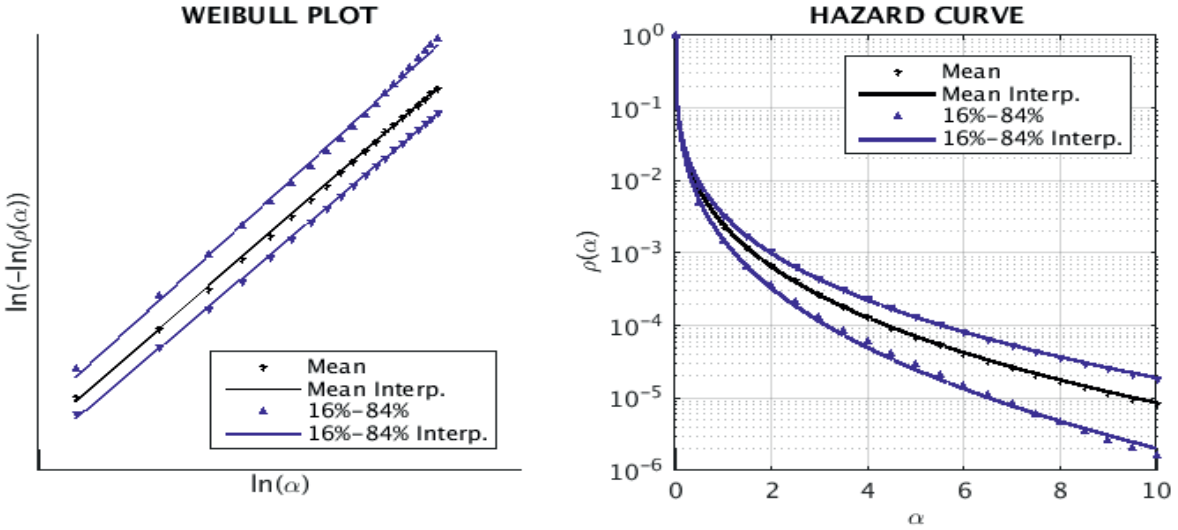

Figure 3: Hazard curves from the logic tree interpolated by a Weibull law on a special axis (left), and on a semi-log scale (right).

It is not a coincidence if the Weibull fits well the PAE computed by the Cornell-like method. First, the Weibull law has been widely used in the modeling of rare events (see Johnston 1985), furthermore the probability of exceedance seems polynomial when plotted in semi-log scale just like the exceedance function of Weibull. Moreover, the site studied is mainly affected by one major seismic source. This fact could explain why the shape of the probability of exceedance and the shape of the Gutenberg-Richter recurrence law are similar.

Following this process, the 2000 hazard curves from the logic tree can be transformed into 2000 estimations of k and η. But to come within the framework of Bayesian inference, the prior knowledge needs to be turn into a prior function. The point is that the pool of k and η does not form a homogenous well-known distribution due to the use of different GMPEs which give significantly different results (see Figure 5).
Fortunately, a specific approach of the Bayes estimator can allow us to get rid off this issue of deriving a prior distribution.

4. FAST UPDATE OF THE PROBABILITY OF ACCELERATION EXCEEDANCE

As said before the prior knowledge is constituted by the pool of 2000 (k_i, η_i). The aim is now to obtain a single estimation of (k, η), updated in the light of observations of PGAs at site.

At this moment, some extra accelerometric data are still needed to play the role of the observations. Unfortunately, data of that kind are not yet sufficient. And this lack of information is frequent in regions characterized by a moderate seismic activity. To address this issue, the catalog of 82 couples of magnitude-distance has been converted into 82 PGAs at site, thanks to the 5 GMPEs used above taking the mean value.

These synthetic PGAs are assumed to be independent and to follow a Weibull distribution[3]. Hence, the likelihood of the sample is given as follow:

$$L\left(A\middle|k,\eta\right)=\prod_{i=1}^{82}\frac{k}{\eta}\left(\frac{a_i}{\eta}\right)^{k-1}\exp\left(-\left(\frac{a_i}{\eta}\right)^{k}\right)$$

where $A=a_1,\cdots,a_{82}$ denotes the PGAs.

The two following formulas give a reasonable approximation of the Bayes estimator (i.e. the posterior mean) -- the detail of the justification is given in Appendix 2:

$$\tilde{k}_{fast}\approx\sum_{i=1}^{2000}k_i\varpi_i \quad \text{and} \quad \tilde{\eta}_{fast}\approx\sum_{i=1}^{2000}\eta_i\varpi_i \quad \text{with} \quad \varpi_i=\frac{L\left(A\middle|k_i,\eta_i\right)}{\sum_{j=1}^{2000}L\left(A\middle|k_j,\eta_j\right)}$$

The mathematical signification of those estimators is interesting: they can be seen as the mean of the k_i and the η_i weighted by a likelihood-based ratio ω_i.

[3] Assuming an other distribution would have been counterproductive since we have to be coherent with the prediction model which is Weibull.

5. CLASSICAL UPDATE OF THE PROBABILITY OF ACCELERATION EXCEEDANCE

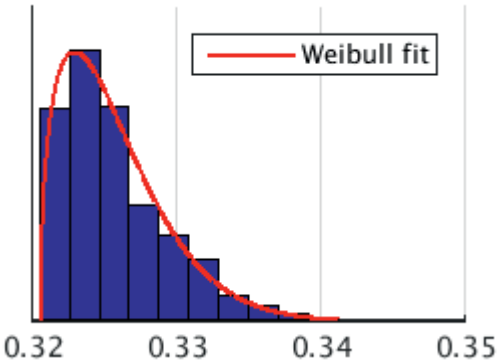

Figure 4: Distribution of the 400 k_i coming from the GMPE of Akkar and Bommer 2010, fitted by a Weibull law

In section 2, the difficulty of deriving a prior distribution from the outputs of the logic tree is highlighted. Indeed, one can observe that the distribution of the 2000 k_i and η_i (Figure 5) is far from being homogenous. But when the k_i and η_i are grouped by their GMPEs, more conventional distributions are observed and can be fitted by ordinary law such as a 3 parameters Weibull law[4] (see Figure 4). By combining the 5 fitted laws in a mixture distribution, two prior functions π_k and π_η can be built to translate the empirical distribution of the k_i and η_i (see red curves in Figure 5).

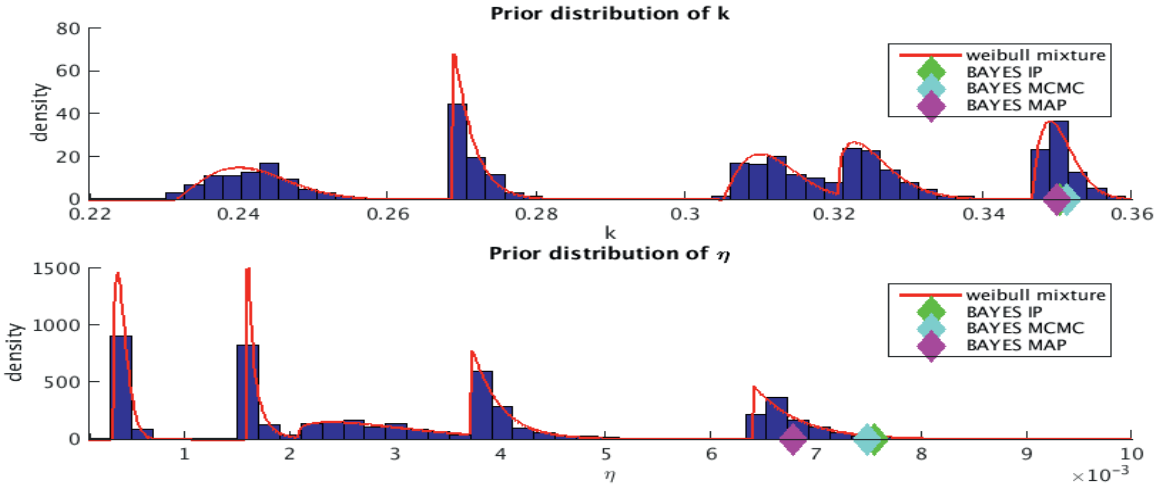

Figure 5: A mixture of Weibull distributions is superimposed on the histograms of the 2000 k and η. The posterior estimates coming from different methods are also plotted (colored diamonds).

Once the prior information has been expressed in a functional form, one can exhibit the posterior distribution of k and η thanks to the Bayes' theorem:

$$f\left(k,\eta|A\right)=\frac{L\left(A|k,\eta\right)\pi_k\left(k\right)\pi_\eta\left(\eta\right)}{\int\int L\left(A|k',\eta'\right)\pi_k\left(k'\right)\pi_\eta\left(\eta'\right)d\eta'\,dk'}$$

Two kinds of estimation can be derived from this posterior function. The most straightforward is the maximum a posteriori (MAP), i.e. the mode of the posterior distribution:

$$\left(\tilde{k}_{MAP},\tilde{\eta}_{MAP}\right)=\left(k,\eta\right)\text{ such that }f\left(k,\eta|A\right)=\max f\left(k',\eta'|A\right)$$

[4] We choose a Weibull law again for pratical reason since we had already implemented its functions, but an other model could have been considered.

The second is the posterior mean already discussed in the previous section and better known as "the Bayes' estimator":

$$\begin{cases} \tilde{k}_{bayes} = E_{f(k,\eta|A)}[k] = \int\int k \times f(k,\eta|A) dk\, d\eta \\ \tilde{\eta}_{bayes} = E_{f(k,\eta|A)}[\eta] = \int\int \eta \times f(k,\eta|A) dk\, d\eta \end{cases}$$

Due to the complexity of the posterior distribution, these double integrals have to be approximated by complex tools such as Markov Chain Monte-Carlo (MCMC) methods. These techniques generate a sample of values distributed accordingly to the posterior function. The sample's average give an estimation of the posterior mean and sample's quantiles can delimit confident bounds (cf. Table 2 and Figure 6).

Table 2: Summary of the different estimations of k and η in the order of their presentation and expected PGA (in m/s^{-2}) for different return period (1,000 years, 10,000 years, 100,000 years).

	Mean	16%	84%	FAST	MAP	MCMC	MCMC 16%	MCMC 84%	Empiric
k	0.2877	0.3051	0.2806	0.3503	0.3499	0.3513	0.3486	0.3540	0.9434
η	0.0020	0.0022	0.0020	0.0076	0.0068	0.0075	0.0067	0.0084	0.0343
1,000	0.979	0.814	1.220	1.220	1.102	1.191	1.101	1.278	N/A
10,000	3.075	2.290	3.836	3.110	2.812	3.029	2.820	3.226	N/A
100,000	7.037	5.152	8.919	6.286	5.688	6.109	5.720	6.472	N/A

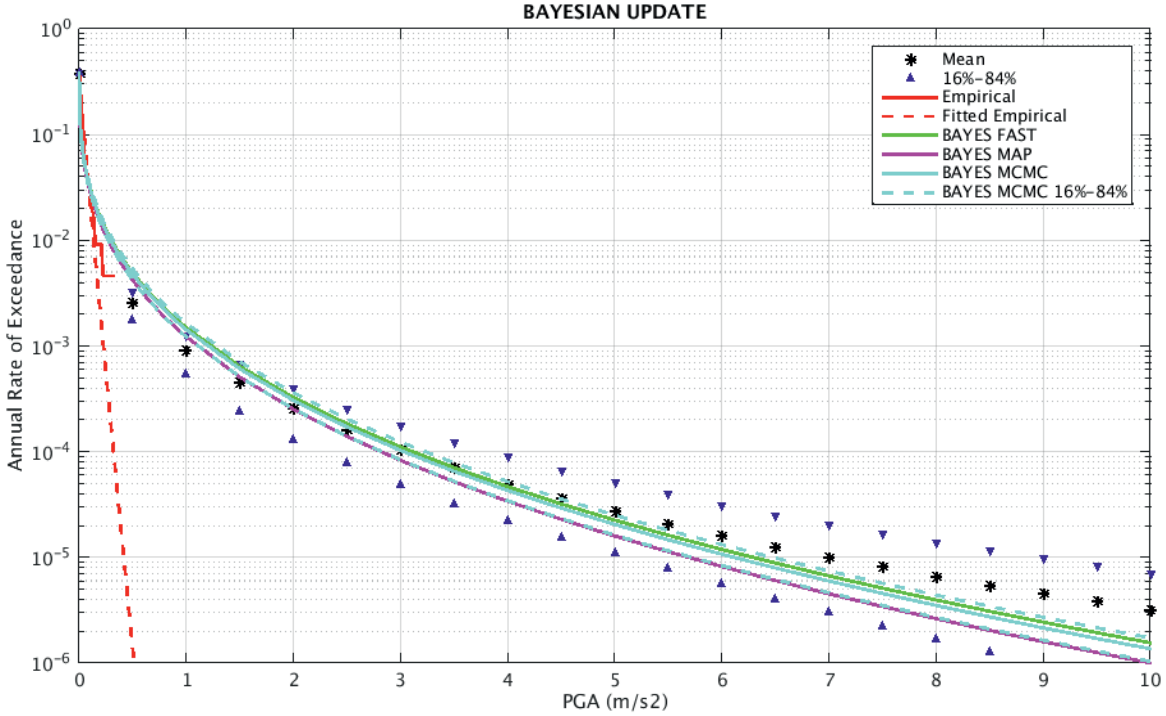

Figure 6: Hazard Curves updated by three different processes. N.B.: All the curves have been multiplied by the activity rate (λ_0) estimated in section 2 to get the annual rate of exceedance instead of the PAE.

The curves estimated by the fast method and the MCMC method are close together. This result is unsurprising since they both approximate the same quantity (i.e. the posterior mean). It is furthermore reassuring for 3 reasons: (i) it's a validation of the fast method, (ii) it's a justification of the modeling of the outputs by a mixture of Weibull, (iii) it's a validation of the implementation of the MCMC (here a Metropolis-Hastings algorithm is used).

The estimate of the MAP gives a slightly different curve, falling nonetheless within the bounds of the MCMC (see Table 2). However the use of this estimator is controversial due to its lack of robustness. Indeed, if the posterior distribution has multiple peaks, its maximization can become difficult.

Globally, the update tends to increase the annual rate of exceedance for small PGAs (i.e. below 3 $m.s^{-2)}$. At the opposite, for higher PGAs, the mean curve outgoing the logic tree seems to overestimate the risk by comparison with the three updated curves. Beyond that, the confident bounds given by the MCMC remain in the bounds fixed by the logic tree, and they show a significant reduction of the uncertainty, but convergence on the value of the confidence level have still to be verified.

6. CONCLUSION

The parameterization of the outputs of the logic tree allows us to enter within the Bayesian scope and to update the entire hazard curves. Three methodologies have been presented to update the parameters k and η of the Weibull law. They all have their own advantages and their own drawbacks:

FAST method	**MCMC method**	**MAP method**
+ Easy and fast implementation	+ Confident intervals	+ Easy and fast implementation
+ Functional prior not needed	- Functional prior needed	+ Gives an other kind of estimate
- No confident intervals	- Unreliable convergence	- No confident intervals
		- Not robust (initialization)

To sum up, the benefits of the Bayesian update within the parametric framework are listed below:

- Since the outputs of the logic tree are confronted with the likelihood of synthetic observations, **the update process gives a more legitimate hazard curve than the mean of the logic tree**.
- Unlike the previous tries to update PSHA result, **the parameterization of the hazard curves allows to update the PSHA for low to high PGA**.
- The analysis of the fast method's weights (i.e. the ω_i) could reveal much information on the logic tree weighted scheme that we could learn from.

These substantial advantages must nonetheless be appreciated in balance with the following limitations:

- The goodness of fit of the parameterization must be discussed for every PSHA. A mathematical proof has not been found to ensure that the Weibull model is universal.
- The conversion of the macroseismic catalog into synthetic PGAs might be source of disturbance.
- All the methods presented here make the assumption that the synthetic PGAs are independently distributed according to a Weibull law. This questionable hypothesis might also introduce a bias.
- The Bayesian update process ends up with a unique curve (except for MCMC) which may lead to believe that all the uncertainties have been erased. But that's far from being the case.
- The reduction of the uncertainty on the mean value can be due to lack of convergence of the MCMC process.

REFERENCES

Akkar, S., & Bommer, J. J. (2010). Empirical equations for the prediction of PGA, PGV, and spectral accelerations in Europe, the Mediterranean region, and the Middle East. *Seismological Research Letters*, *81*(2), 195-206.

Atkinson, G. M., & Boore, D. M. (2006). Earthquake ground-motion prediction equations for eastern North America. *Bulletin of the Seismological Society of America*, *96*(6), 2181-2205.

Cauzzi, C., & Faccioli, E. (2008). Broadband (0.05 to 20 s) prediction of displacement response spectra based on worldwide digital records. *Journal of Seismology*, *12*(4), 453-475.

Cornell, C. A. (1968). Engineering seismic risk analysis. *Bulletin of the Seismological Society of America*, *58*(5), 1583-1606.

Gutenberg, B., & Richter, C. F. (1944). Frequency of earthquakes in California. *Bulletin of the Seismological Society of America*, *34*(4), 185-188.

Humbert, N., & Viallet, E. (2008). A method for comparison of recent PSHA on the French territory with experimental feedback. In *Proceedings of Fourteenth World Conference on Earthquake Engineering* (pp. 07-0118).

Johnston, A. C., & Nava, S. J. (1985). Recurrence rates and probability estimates for the New Madrid seismic zone. *Journal of Geophysical Research: Solid Earth (1978–2012)*, *90*(B8), 6737-6753.

McGuire, R. K. (1995). Probabilistic seismic hazard analysis and design earthquakes: closing the loop. *Bulletin of the Seismological Society of America*, *85*(5), 1275-1284.

Selva, J., & Sandri, L. (2013). Probabilistic Seismic Hazard Assessment: Combining Cornell-Like Approaches and Data at Sites through Bayesian Inference. *Bulletin of the Seismological Society of America*, *103*(3), 1709-1722.

SisFrance (2005). Catalogue des séismes français métropolitains, BRGM, EDF, IRSN, www.sisfrance.net

Suckale, J., & Grünthal, G. (2009). Probabilistic seismic hazard model for Vanuatu. *Bulletin of the Seismological Society of America*, *99*(4), 2108-2126.

Weibull, W. (1951). A Statistical Distribution Function of Wide applicability. *Journal of applied mechanics*.

Viallet, E., Humbert, N., Martin, C., & Secanell, R. (2008). On the Use of a Bayesian Updating Technique to Get Probabilistic Seismic Hazard Assessment More Rugged. In *Proceedings of Fourteenth World Conference on Earthquake Engineering.*

Zhao, J. X., Zhang, J., Asano, A., Ohno, Y., Oouchi, T., Takahashi, T., ... & Fukushima, Y. (2006). Attenuation relations of strong ground motion in Japan using site classification based on predominant period. *Bulletin of the Seismological Society of America*, *96*(3), 898-913.

APPENDIX 1: THE MACROSEISMIC CATALOG

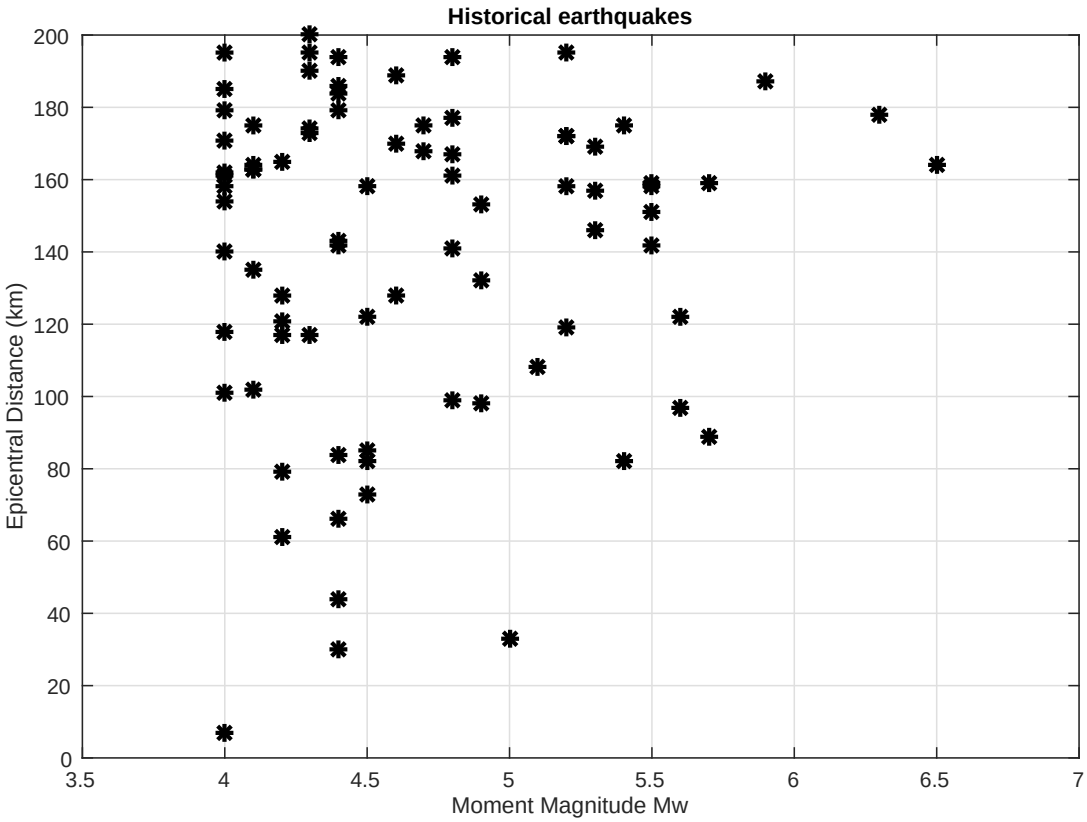

Figure 7: The macroseismic catalog: epicentral distances are plotted accordingly to the moment magnitudes.

APPENDIX 2: MATHEMATICAL VALIDATION OF THE SPECIFIC METHOD

The aim of this appendix is to give, step by step, the path which leads to the estimator used in the fast method. To simplify, a case involving only one parameter is presented.

Let's suppose that we want to estimate the mean θ of a normal law for which we have m iid.[5] observations $X = x_1, \cdots, x_m$. Their likelihood is given by the following -- the standard deviation is assumed to be one (σ=1):

$$L(X|\theta) = \prod_{i=1}^{m} \frac{1}{\sqrt{2\pi}} \exp\left(-(x_i - \theta)^2 / 2\right) \tag{1}$$

Now, we assume a uniform law between two scalars (a, b) as a prior distribution for θ, i.e.:

$$\begin{aligned} \pi(\theta) &= \frac{1}{b-a} \text{ if } \theta \in [a,b] \\ &= 0 \text{ otherwise} \end{aligned} \tag{2}$$

Hence the posterior distribution combines (1) and (2) using the Bayes theorem:

$$f(\theta|X) = \frac{L(X|\theta)\pi(\theta)}{\int L(X|\theta')\pi(\theta')d\theta'} \tag{3}$$

Since the denominator does not depend on θ, we denote it: $C = \int L(X|\theta')\pi(\theta')d\theta'$.

The Bayes estimator of θ is therefore the expected value of the posterior distribution:

$$\hat{\theta}_{bayes} = E_{f(\theta|X)}[\theta] = \int \theta \times f(\theta|X)\, d\theta \tag{4}$$

In our trivial example, (4) is easily calculable, but let's suppose that we want to use a Monte-Carlo simulation. One way to proceed is to simulate a sample of the posterior distribution and take the sample's average as an estimate of (4). But the major issue is that the posterior distribution (3) might be difficult to simulate. One option is to rewrite the Bayes estimator in a different way:

$$\begin{aligned} \hat{\theta}_{bayes} &= \int \theta \times f(\theta|X)\, d\theta = \int \theta \times \frac{L(X|\theta)\pi(\theta)}{C}\, d\theta \\ &= \frac{1}{C} \int \theta \times L(X|\theta)\pi(\theta)\, d\theta = \frac{1}{C} E_{\pi(\theta)}[\theta \times L(X|\theta)] \end{aligned}$$

[5] Independent and Identically Distributed

The expected value based on the posterior distribution has been transformed into an other expected value expressed accordingly to the prior distribution. The same trick can be made to compute C:

$$C = \int L\left(X\middle|\theta'\right) \times \pi\left(\theta'\right) d\theta' = E_{\pi(\theta)}\left[L\left(X\middle|\theta'\right)\right]$$

The interest of adopting such approach is that the prior distribution is much easier to simulate than the posterior one. Indeed, if we can generate a sample $\theta_1, \cdots, \theta_n$ following the prior distribution $\pi(\theta)$, reasonable approximations of C and $\hat{\theta}_{bayes}$ are given by:

$$C \approx \frac{1}{n}\sum_{i=1}^{n} L\left(X\middle|\theta_i\right) \quad \text{and} \quad \hat{\theta}_{bayes} \approx \frac{\sum_{i=1}^{n} \theta_i L\left(X\middle|\theta_i\right)}{\sum_{j=1}^{n} L\left(X\middle|\theta_j\right)}$$

An illustration of the method is given by Figure 8, for the following values: θ = 2, [a, b] = [1, 3].

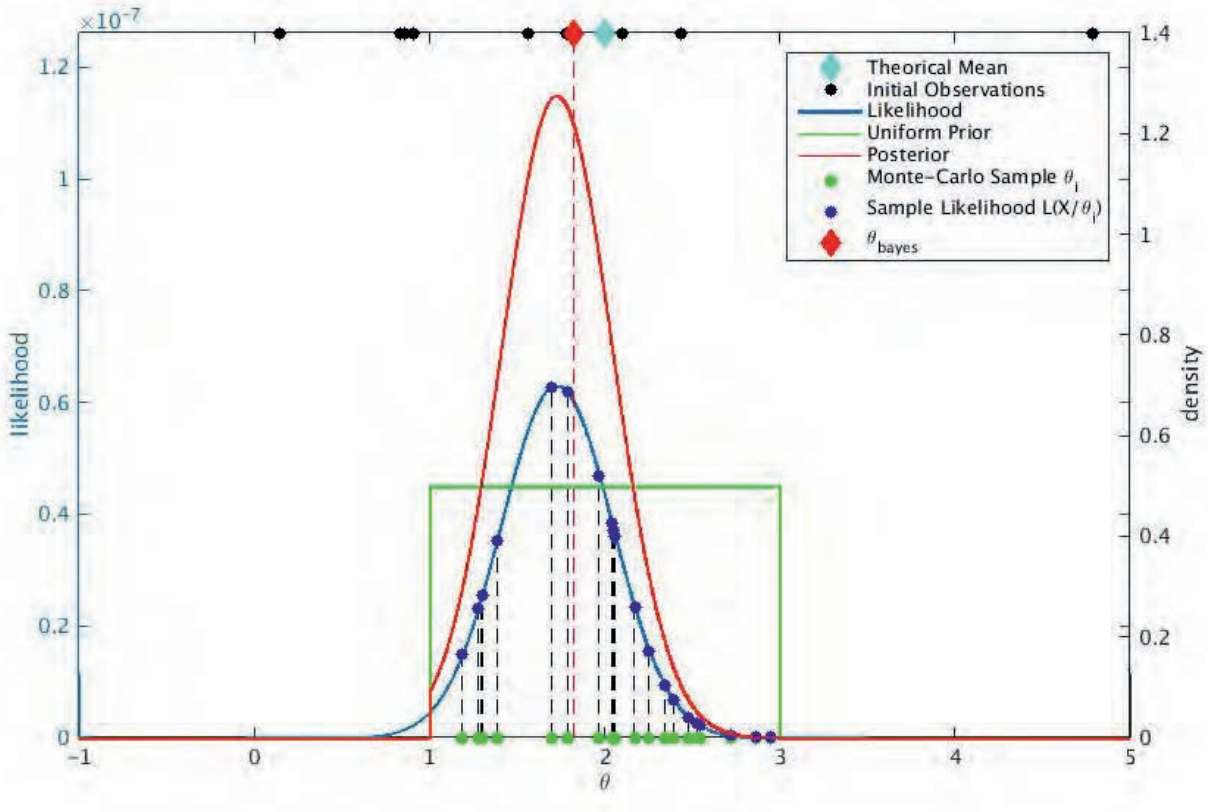

Figure 8: Illustration of the specific method on a trivial example: An initial sample (black dots) is drawn from a normal distribution with mean θ=2 (blue diamond). Its likelihood is given according to θ (blue line). Then, an other sample (green dots) is drawn from the prior distribution (green line); their likelihood (blue dots) is used to compute an approximation (red point) of the mean of the posterior distribution (red line).

CSNI Workshop on "*Testing PSHA Results and Benefit of Bayesian Techniques for Seismic Hazard Assessment*"
4-6 February 2015, Eucentre Foundation, Pavia, Italy

A Bayesian methodology to update the Probabilistic Seismic Hazard Assessment

Ramon SECANELL
FUGRO-GEOTER, France, ramon.secanell@geoter,fr

Christophe MARTIN
FUGRO-GEOTER, France, christophe.martin@geoter,fr

Emmanuel VIALLET
EDF, France, emmanuel.viallet@edf.fr

Gloria SENFAUTE
EDF, France, gloria.senfaute@edf.fr

SUMMARY

In this paper, we present a Bayesian methodology for updating the seismic hazard assessment (the seismic hazard curves) in a point of a geographical domain. The methodology is based on the comparison of predictive exceedance rates of a fixed acceleration level (given by the seismic hazard curves) and the observed exceedance rates in some selected sites.

The application of the methodology needs, firstly, the definition of a prior Probabilistic Seismic Hazard Assessment (PSHA) based in a logic tree. In this article, we used the logic tree defined for a preliminary PSHA of SIGMA[1] project. Each main branch corresponds to a probabilistic model of calculus of seismic hazard. The method considers that, initially (or a priori), the weights of all branches of the logic tree are equivalent.

Secondly, the method needs to compile the observations in the region. They are introduced in a database (here called REX, Return of Experience) containing the recorded acceleration data (normally during the instrumental period). Nevertheless, the instrumental period in stable zones (as France) shows only very low acceleration levels recorded during a short period of observation. In this study, we present a method to enlarge the REX taking into account the historical data. This article presents an approach to define "synthetic" accelerations in the sites of observation. The synthetic REX allows to expand the period of observation and to increase the acceleration thresholds used in the Bayesian updating process.

[1] Research and Development Program on Seismic Hazard Assessment (http://www.projet-sigma.com/)

The application of the Bayesian approach leads to a new and objective definition of the weights of each branch of the logic tree. The new weights of the branches (or posterior weights) are used to define new seismic hazard curves (mean, median and centile 15% and 85%). The Bayesian approach doesn't change the probabilistic models (seismic hazard curves). It only modifies the weights of each branch of the logic tee.

Finally, we present some updates of the seismic hazard using the Bayesian methodology developed, the logic tree of SIGMA project (as prior model) and the REX defined.

Keywords: *Bayes, probabilistic seismic hazard assessment.*

1. Introduction

In recent years, increasing efforts have been devoted to the assessment of the reliability of PSHA results. Different procedures have been tested and many publications have provided useful information on this subject (e.g. Selva and Sandri, 2013 [1]; Mezcua et al. 2013 [2]; Humbert and Viallet, 2008 [3]). Considering the high uncertainties in Probabilistic Seismic Hazard Assessments (PSHA) and the importance of PSHA results for the seismic design, it is pertinent to focus on the issue of consistency-checking of the PSHA results.

This article presents a Bayesian methodology for testing probabilistic seismic hazard analyses (PSHA) and for justifying an alternative approach to determine the logic tree weighting scheme. The goal of this article is to present only the general methodology, without presenting a formal application. This methodology has been developed in the spirit of updating any PSHA study.

We present a general Bayesian methodology in which the results of different probabilistic models included in a logic tree and the recorded data (which are independent from the data used in the PSHA) are used together to try reducing the uncertainties in a PSHA. In this sense, the main objective is not to develop a new PSHA model, but to allow, through a Bayesian approach, the explicit evaluation and comparison between predictions and observations to offer a rational approach to modify the prior weights of a logic tree.

This research has been done within the framework of the international research program: SIGMA

2. Methodology

The Bayesian approach developed to update the seismic hazard is based on the comparison of the exceedance rates of acceleration thresholds predicted by the probabilistic models of a logic tree (seismic hazard curves) and the exceedance rates observed from available records (recorded or synthetic) in a set of seismic network stations.

The method uses the Bayes theorem. Following this theorem, the conditional probability of occurrence of an event A, given that other event B was produced, is defined by:

$$P(A/B) = \frac{P(B/A).P(A)}{P(B)} \quad (1)$$

Applying the method to the seismic hazard, we can replace A by the exceedance rate of a fixed acceleration threshold predicted by a probabilistic model (this information is typically provided

by the seismic hazard curves) and B by the exceedance rate of the same acceleration threshold following the available observations (called here REX or Return of Experience). Then:

$$P(Model/Observation) = \frac{P(Observation/Model).P(Model)}{P(Observation)} \quad (2)$$

In a logic tree with N branches defining N input models of a seismic hazard calculation, the weight given to each branch of the logic tree is equivalent to the probability of the model, P(Model). The updating method consist on calculating the conditional probability of each model knowing the observations included in the REX, P(Model/Observation), that determines the posterior value of the weight of the logic tree branch.

If the method is initialized considering that the N branches of the logic tree are equivalent (equal probability), then the weight of each logic tree branch (or the probability of a model « i ») is:

$$P(Model_i) = \frac{1}{N} \quad (3)$$

The objective consists in quantifying the following part of equation (2):

$$\frac{P(Observation/Model)}{P(Observation)} \quad (4)$$

P(Observation) is independent on the models and is equivalent to a normalization factor. Then, the sum of $P(Model_i/Observation)$ is equal to 1 (sum of weights *a posteriori* = 1). Performing the integration of equation (2) on the set of N models/branches of the logic tree, we have that:

$$\sum_{i=1}^{N} P(Model_i/Observation) = \frac{1}{N} \times \frac{1}{P(Observation)} \times \sum_{i=1}^{N} P(Observation/Model_i) = 1 \quad (5)$$

Therefore,

$$\frac{1}{N} \times \frac{1}{P(Observation)} = \frac{1}{\sum_{i=1}^{N} P(Observation/Model_i)} \quad (6)$$

To define $P(Observation/Model_i)$, the model of earthquakes occurrence is supposed to follow a Poisson distribution with parameters λ and t :

$$P(n,t) = \frac{e^{-\lambda t}(\lambda(M)t)^n}{n!} \quad (7)$$

P(n,t) is the probability to observe n earthquakes of magnitude greater than M during a period of observation t, and λ is the annual exceedance rate of these earthquakes.

If the recording stations are supposed to be independent, the probability to observe the exceedance of an acceleration level follows a Poisson distribution law (Beauval et al., 2007 [4]).

Nevertheless, if the occurrence of an earthquake of magnitude M implies the exceedance of an acceleration level at some stations, then there is a correlation among the different stations. The exceedance of an acceleration level follows, in this case, a more general distribution, the negative binomial distribution:

$$P(Observation/Model_i) = \exp\left[\ln\Gamma\left(\frac{A_i}{k-1}+N_{REX}\right)-\ln\Gamma\left(\frac{A_i}{k-1}\right)-\ln\Gamma\left(N_{REX}+1\right)\right]\times\frac{1}{k}^{\frac{A_i}{k-1}}\times\left(1-\frac{1}{k}\right)^{N_{REX}} \quad (8)$$

- ✓ Ai is the number of exceedances of an acceleration level, A*, predicted by the probabilistic model « i » on the global set of sites of stations of REX :

$$A_i = \sum_{j=1}^{L}\lambda_{ij}\left(A^*\right)\times T_j \quad (9)$$

- ✓ L is the number of selected stations of REX, T_j is the cumulative number of years of observation at station « j », and λ_{ij} (A*) is the annual exceedance rate of acceleration level A* fixed by the seismic hazard curve calculated at the site of station « j » following the probabilistic model « i ».

- ✓ The parameter k is indicative of the correlation among stations of the REX. If k tends to 1, the negative binomial distribution goes towards a Poisson distribution. The parameter k is the average number of sites impacted by one earthquake.

- ✓ NREX is the number of total exceedances of the acceleration level A* observed (recorded) at L stations of REX.

We obtain finally that:

$$P(Model_i/Observation) = \frac{P(Observation/Model_i)}{\sum_{i=1}^{N}P(Observation/Model_i)} \quad (10)$$

And $P(Model_i/Observation)$ represents the weight of the model *i* in the logic tree.

The updating method of the seismic hazard modifies the “a priori” weight or probability of each probabilistic model $P(Model_i)=1/N$ with the “a posteriori” weight defined by equation (10). These updated or posterior weights are adopted to weigh the results and to calculate a new seismic hazard (median, mean and centiles 15% and 85%).

Therefore, the updating method of the seismic hazard doesn’t affect the individual calculation of the exceedance rates of the acceleration levels predicted by the prior probabilistic seismic hazard curves. It only adjusts the weights associated with each probabilistic model. Thus, the updating method only changes the final mean, median and centiles seismic hazard curves. These statistical values (seismic hazard curves) are affected by the weights assigned to the individual seismic hazard curves of the individual models.

The updating is performed using a comparison of probabilistic predictions with recorded and/or estimated observations (REX) at L stations. From this comparison we obtain new weights (or probabilities) of the N branches of the probabilistic logic tree. After the definition of the N posterior weights, we post-process the probabilistic results considering the new weighting scheme, to calculate new seismic hazard curves at the same observation points of the REX.

The choice of the stations for the analysis of the REX could have a significant impact on the posterior weights of the branches. The final seismic hazard curves could vary depending on the stations selected to build the REX.

For this reason, the selection of the REX is an important part of the updating method. The considered REX must be representative of the study region and, preferably, it should cover the largest possible period of observation.

3. Prior model used

With the objective to apply the described methodology to a case study, we adopted the logic tree developed during the initial phases of the SIGMA project (Carbon et al 2012a [5], Carbon et al 2012b [6]).

It contains 24 main logic tree branches (Carbon et al 2012b [6]) associated with three seismotectonic models, four GMPEs or attenuation relations (Akkar and Bommer 2010 [7]; Atkinson and Boore, 2011 [8]; Zhao et al., 2006 [9], Berge-Thierry et al., 2003 [10]) and two seismic catalogues. The combination of these hypothesis leads to the definition of 3 x 4 x 2 = 24 main branches.

As the purpose of our analyses is to verify the applicability of the Bayesian update, we decided to use only the main logic tree branches (24 main branches). Then, we didn't consider the secondary branches associated to other uncertainties (as λ and β of the Gutenberg-Richter law, maximum magnitude, Mmax, and thickness of the seismogenic crust, H). This choice was made to simplify the analysis of the results. Nevertheless, the Bayesian method can be applied to any more complex logic tree.

The minimum magnitude considered in the PSHA used for the test is Mw=4.5. For this reason, the REX (number of observations at the selected sites) should take into account only events with magnitudes greater than 4.5.

4. Definition of the REX database

The instrumental REX file including the acceleration records of the French seismic network (Réseau Accélérométrique Permanent, RAP) contains 970 acceleration records. 232 records come from earthquakes with magnitudes equal or greater than 4.5. The maximum PGA recorded (SAOF station) was 117 cm/s^2 and only 71 records have a PGA greater than 10 cm/s^2.

The French seismic network is composed of 84 stations across the entire French territory (Figure 1). The majority of the stations are located in the most active seismic areas of France: the Alps and the Pyrenees.

The historical REX, developed to enlarge the period of observation of instrumental period, was created using the Sisfrance database[2]. It contains 1700 intensity records from year 463 to end of 1961. 1141 records have an epicentral intensity equal or greater than V (Figure 2). Intensities lower than V were removed.

The objective of the historical REX is to calculate the hypothetical or synthetic acceleration values probably generated at the stations of the REX during the historical events. The generation of synthetic accelerations has been performed as follows:

- ✓ Calculation of epicentral distance from the earthquake epicenters to the recording station.

- ✓ Calculation of peak ground acceleration (PGA) values that would have been probably generated at the stations. The acceleration values can be obtained using 2 methods:
  - o Calculation of punctual (or site) intensities at the stations using intensity prediction equations defined in terms of epicentral intensities and epicentral distances (i.e. Mezcua et al., 2004 [11]; and Martin et al., 2008 [12]; Carbon et al 2007 [13]). Then, acceleration values are calculated using the punctual intensity and appropriate intensity-PGA relations (i.e. PS92; Gomez and Capera, 2007 [14]; Atkinson and Kaka, 2007 [15]; etc.).
  - o Calculation of acceleration values using GMPE's. We used the GMPE of Drouet, 2013 [16], specially developed for France during the SIGMA project, and Cauzzi and Faccioli, 2008 [17].

The historical REX database only retained those records with an epicentral distance lower than 150 km. For larger distances, the intensity and the peak ground acceleration at the site is too low to be considered for an updating process.

The final historical REX contains 12549 synthetic PGA records. These synthetic records correspond to the hypothetical recorded data at the RAP seismic stations located less than 150 km from the epicenter.

The analysis and filtering of the instrumental and historical REX lead to the definition of the number of observations. For example, analyzing the REX, we could find the number of observations in a selected set of stations, associated to earthquakes with magnitude greater than a defined threshold and exceeding a minimum PGA level.

[2] Database of the French historical earthquakes (http://www.sisfrance.net/)

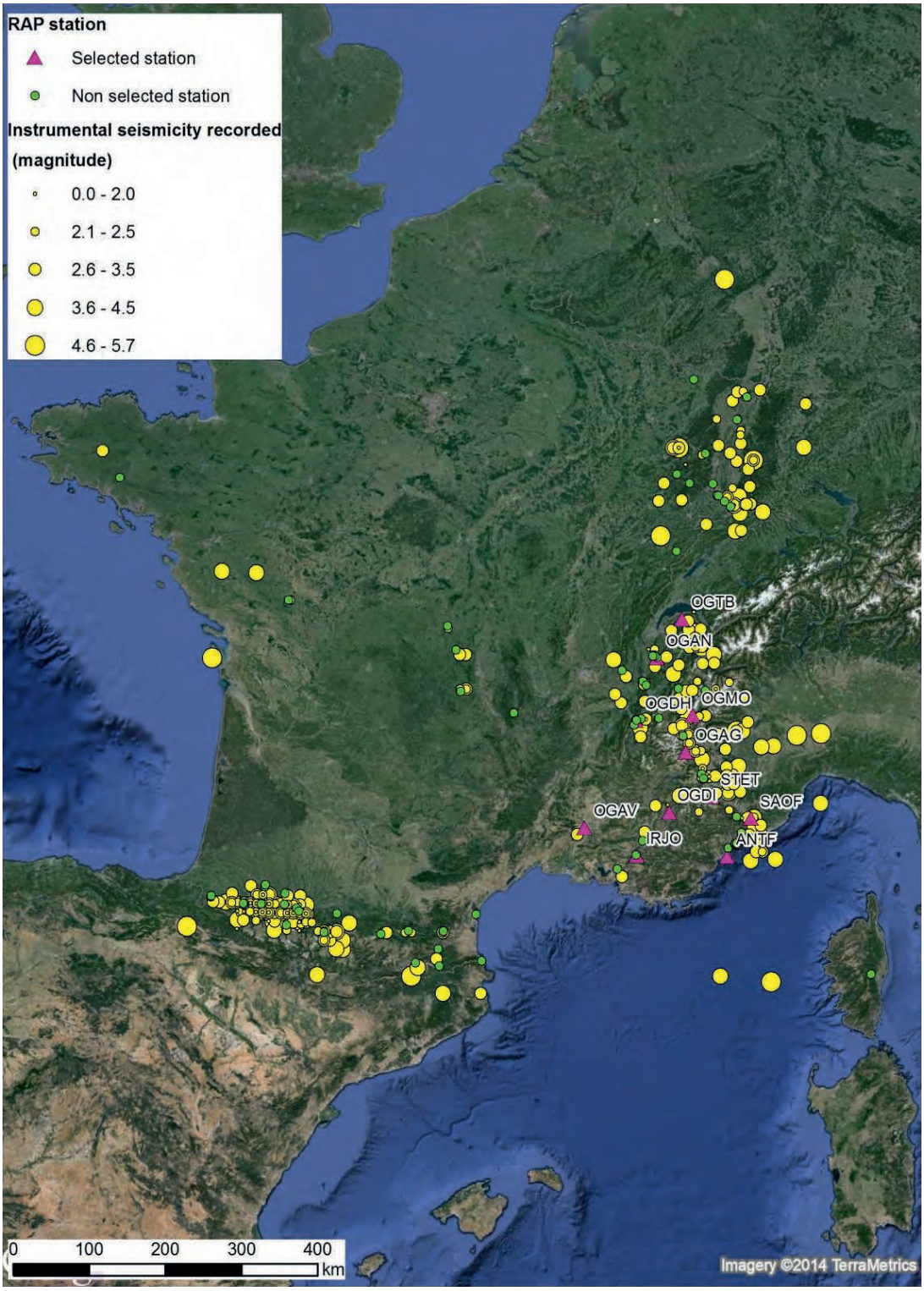

Figure 1. Seismic stations of the French seismic network, RAP (green dots) and earthquakes included in the instrumental REX (yellow dots). The pink triangles correspond to the selected RAP stations in the SIGMA region.

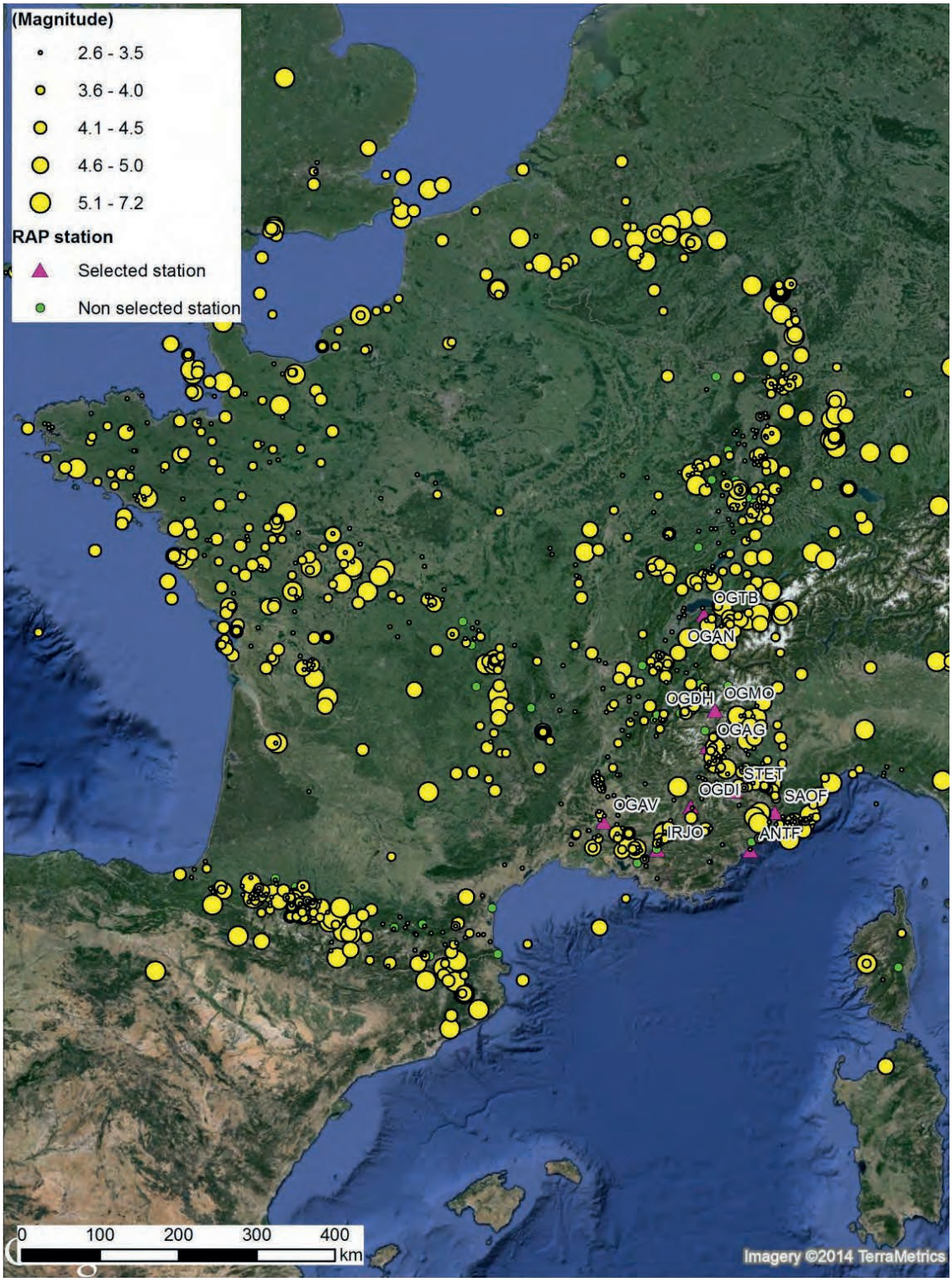

Figure 2. Seismic stations of the French seismic network, RAP (green dots) and earthquakes included in the historical REX (yellow dots). The pink triangles correspond to the selected RAP stations in the SIGMA region.

5. Application of the Bayesian updating of a PSHA in the South-East of France

To test the application of the Bayesian update to the seismic hazard and to assess its relevance, we performed a series of sensitivity tests to analyze the effects of the different input data in the updating process. For example, we analyzed the effect of the correlation among stations, the effect of the duration of the observation period in the updating process, the effect of the selection of a single site or a set of sites, the effect of the acceleration threshold and the effect of the use of instrumental and historical data, etc.

To perform these tests, we used the simplified logic tree composed of 24 branches and different REX (PGA observations) defined considering different hypothesis: instrumental or historical data, several acceleration thresholds, different equation to estimate accelerations from intensities, etc.

The interpretation of the tests is performed comparing the specific REX developed for the test (observations during a period of time) and the exceedance rates at the selected stations (i.e. Figure 3). The exceedance rates at the selected stations are obtained as follows: (i) multiplying the seismic hazard curve of each station by the number of years of observation and (ii) adding the results of each station.

For example, the Figure 3 shows the prior mean exceedance rate (bold blue line) predicted by 24 branches of the logic tree compared with the exceedance rates derived from the observations (REX red dots). The test of the figure was performed considering: 1) 11 stations, with 112 years of operation per station, 2) a historical REX obtained considering an acceleration threshold of 50 cm/s^2.

The updated mean exceedance rate (bold red line, Figure 3) shows that the mean posterior exceedance rates are closer to observations than the mean prior exceedance rate. In this case, the posterior exceedance rates are higher than the prior exceedance rates. It means that the updating of the seismic hazard lead to an increase of the seismic hazard.

The Figure 4 shows the same type of test considering : 1) 11 stations, with a total of 112 years of operation, 2) the instrumental REX obtained considering an acceleration threshold of 5 cm/s^2 .
The updated mean exceedance rate (bold red line, Figure 4) shows that the mean posterior exceedance rates are also closer to observations. However, in this case, the posterior exceedance rates are lower than the prior exceedance rates. Therefore, the updated seismic hazard is lower than the prior seismic hazard.

A battery of tests (similar to the previously described) was performed. They allow defining some basic rules to envision an application of the Bayesian updating method to the PSHA. The main rules to take into account during the application of the Bayesian updating method are the following:

- ✓ Logic tree: The logic tree should represent an exhaustive and mutually exclusive set of alternatives. In an ideal case, the observed or estimated REX should be into the range of predictions of the probabilistic models.

- ✓ Number of sites: The use of more than 1 site of observation in the updating process increases the number of observations. Nevertheless, the effects of the updating process could not be equivalent at all sites because of the different shape of the seismic hazard curves in different sites.

- ✓ REX: The number of observations (exceedances of a fixed acceleration level during a period of time) is important. Preferably, it should be highest as possible because the updating process is more effective.

- ✓ Period of observations: Greater the period of observation, higher the effect of the updating method.

- ✓ The threshold of acceleration used for the updating process. The updating process is always performed using a pre-defined acceleration threshold. Then, the results of the updating process are well defined for the accelerations of the seismic hazard curve near to the considered acceleration threshold. The level of the acceleration thresholds used should preferably be in agreement with the accelerations associated to the return periods of analysis.

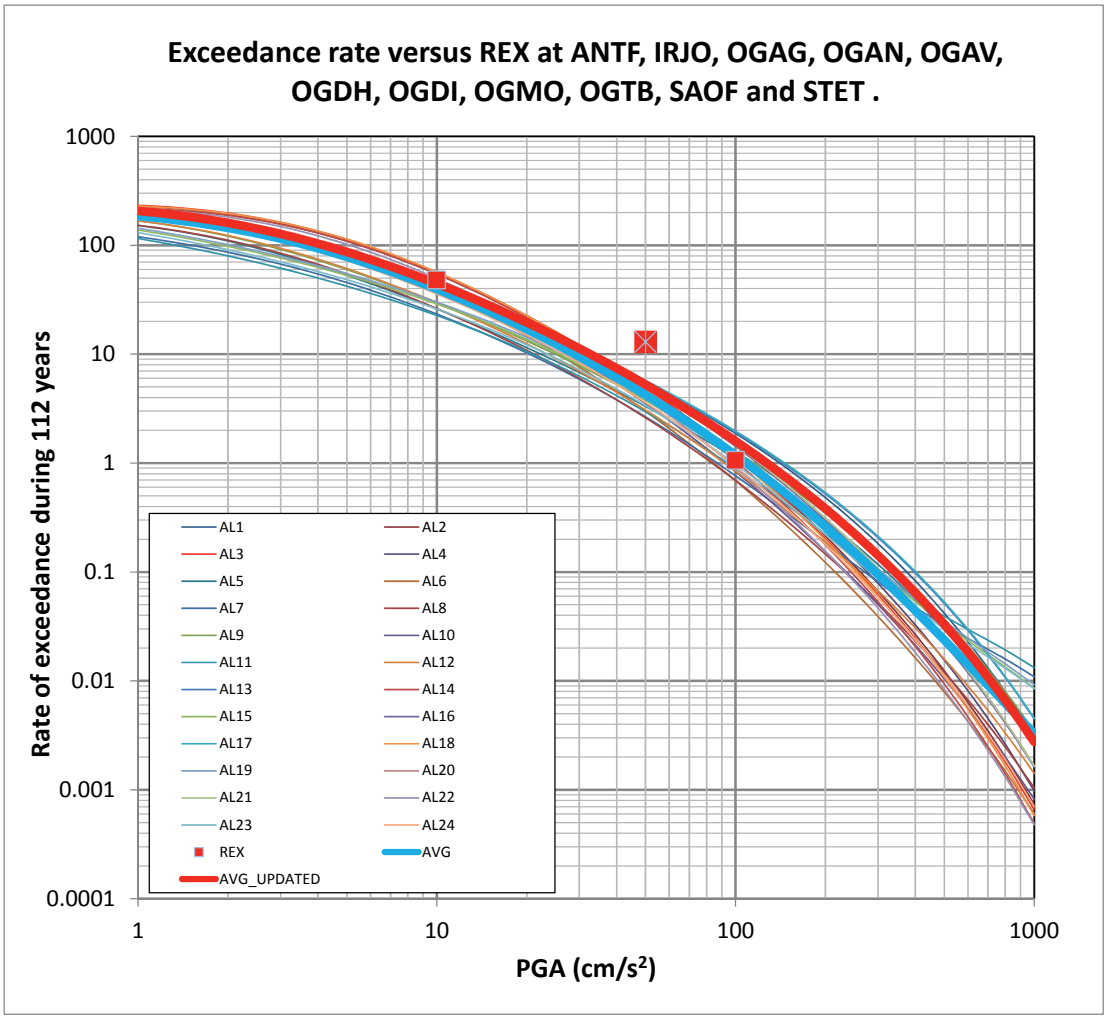

Figure 3. Comparison of exceedance rate during the working period of the selected stations and the historical REX. Set of 11 stations. Acceleration threshold = 50 cm/s2.

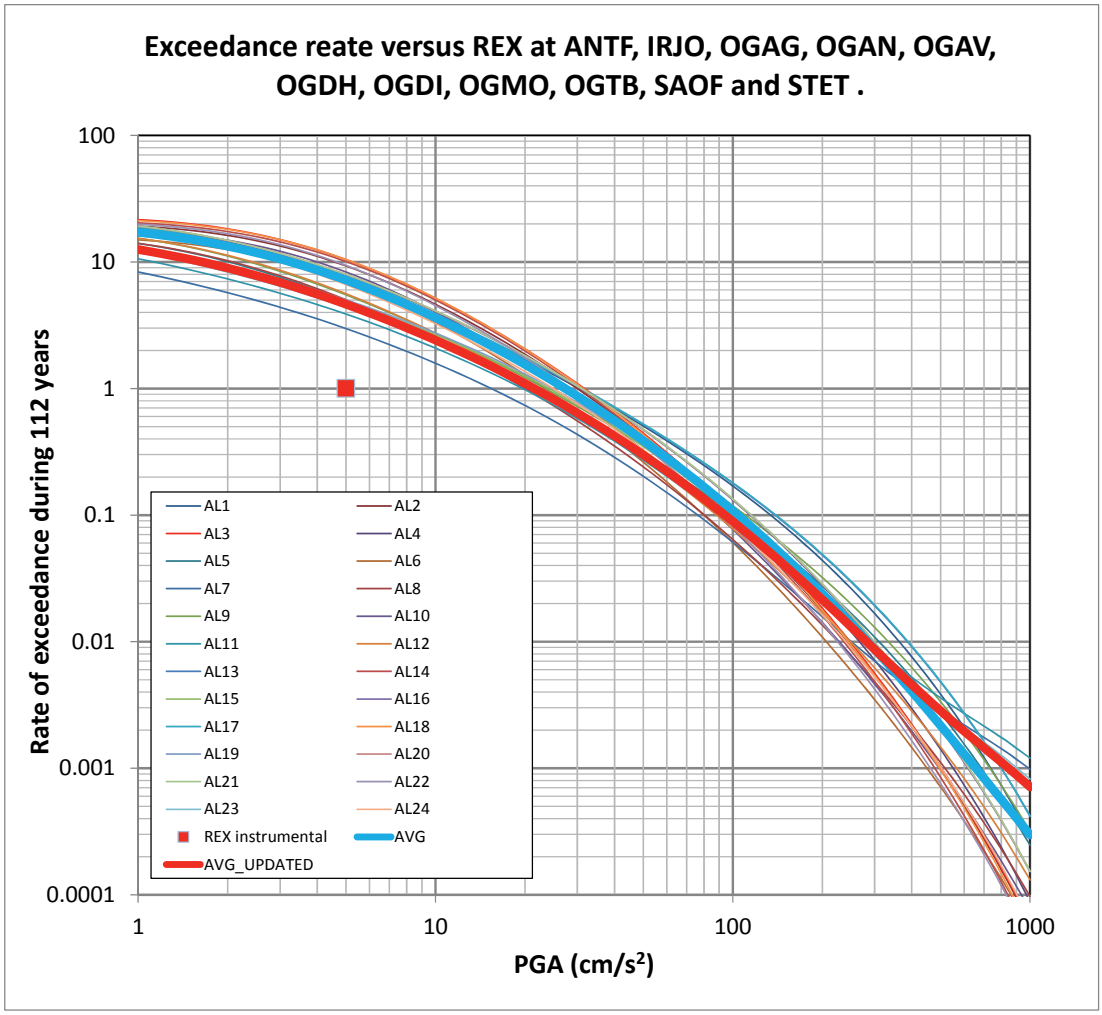

Figure 4. Comparison of exceedance rate during the complete period of the stations and the instrumental REX. Set of 11 stations. Acceleration threshold = 5 cm/s2

6. Conclusions

The method is justified from the mathematical point of view. It provides an objective way to define the weights of the different branches of the logic tree instead of using the common and subjective methodology based on expert judgment. The method can be applied in all cases and there are no mathematical constraints. The application of the method offers the possibility to use the data specific to the region and to decrease the uncertainties.

Globally, the effect of the Bayesian updating method is to give a higher weight to the probabilistic models that predicts exceedance rates closer to the observed data (REX) and a lower weight to the probabilistic models predicting exceedance rates far from the observed data.
Therefore, the global effect of the Bayesian updating process is to bring closer the predictive probabilistic model to the recorded (or estimated) data (REX).

There are, however, limitations in its application and we have to keep in mind constraints due to each context in which it is intended to be applied.

Some main rules to be taken into account during the application of the Bayesian updating method were defined. They are associated mainly to the definition of the prior logic tree, to the definition of the REX (number of observations) and to the definition of the threshold of acceleration used in the updating process.

REFERENCES

[1] SELVA JU., SANDRI L. (2013). Probabilistic Seismic Hazard Assessment: Combining Cornell-Like Approaches and Data at Sites through Bayesian Inference. Bulletin of the Seismological Society of America, Vol. 103, No. 3, pp. 1709–1722, June 2013, doi: 10.1785/0120120091.

[2] MEZCUA, J., RUEDA J, AND GARCÍA BLANCO R. M. (2013); Observed and Calculated Intensities as a Test of a Probabilistic Seismic-Hazard Analysis of Spain. Seismol Res Lett Vol 84, Num 5, doi: 10.1785/0220130020.

[3] HUMBERT & VIALLET, 2008. A method for comparison of recent PSHA on the French territory with experimental feedback. The 14th World Conference on Earthquake Engineering October 12-17, 2008, Beijing, China.

[4] BEAUVAL C., BARD, P.Y., HAINZL, S., GUEGUIN, Ph. (2007). Aléa sismique probabiliste : les limites d'une comparaison entre estimations et observations. 7ème Colloque National AFPS 2007 – Ecole Centrale Paris

[5] CARBON, D., DROUET, S., GOMES, C., LEON, A., MARTIN, C., AND SECANELL, R. (2012a). Final preliminary Probabilistic Hazard map for France's southeast 1/4. Technical Report Ref : SIGMA-2012-D4-18. 162 pages.

[6] CARBON, D., DROUET, S., GOMES, C., LEON, A., MARTIN, C., AND SECANELL, R. (2012b). Initial probabilistic seismic hazard model for France's southeast 1/4. inputs to sigma project for tests and improvements. Technical Report Ref : SIGMA-2012-D4-41, Seismic, 150 pages.

[7] AKKAR, S. AND BOMMER, J.J. (2010). "Empirical equations for the prediction of pga, pgv and spectral accelerations in europe, the mediterranean region and the middle east," seismological research letters, 81, 2, 195-206.

[8] ATKINSON G.M. AND BOORE D.M. (2011). Modifications to Existing Ground-Motion Prediction Equations in Light of New Data. Bulletin of the Seismological Society of America, Vol. 101, No. 3, pp. 1121–1135, June 2011, doi: 10.1785/0120100270

[9] ZHAO J.X., ZHANG J., ASANO A., OHNO Y., OOUCHI T., TAKAHASHI T., OGAWA H., IRIKURA K., THIO H.K., SOMERVILLE P.G., FUKUSHIMA Y. AND FUKUSHIMA Y. (2006). Attenuation relations of strong ground motion in japan using site classification based on predominant period. Bulletin of the Seismological Society of America, vol. 96, n° 3, p. 898-913.

[10] BERGE-THIERRY, C., GRIOT-POMMERA, D. A., COTTON, F. AND FUKUSHIMA, Y. (2003) "New empirical response spectral attenuation laws for moderate European earthquakes," Journal of Earthquake Engineering. 7(2), 193-222.

[11] MEZCUA, J., J. RUEDA, AND R. M. GARCÍA BLANCO (2004). Re-evaluation of historic earthquakes in Spain, Seismol. Res. Lett. 75, 75–81.

[12] MARTIN Ch., , R. SECANELL, E. VIALLET, N. HUMBERT, 2008. Consistency of PSHA Models in Acceleration and Intensity by Confrontation of Predictive Models to Available Observations in France. Working Group on Integrity of Components and Structures (IAGE) Recent Findings and Developments in Probabilistic Seismic Hazards Analysis (PSHA) Methodologies and Applications Lyon, France 7-9 April 2008.

[13] CARBON D., MARTIN C., SECANELL R. (2007) : Evaluation probabiliste de l'aléa sismique en intensité à l'échelle nationale. Lois d'atténuation en intensité, tests des modèles et confrontation au Rex. Rapport GEOTER – Ref n° GTR/EDF/0707-396.

[14] GÓMEZ CAPERA A.A., D. ALBARELLO E P. GASPERINI (2007). Aggiornamento relazioni fra l'intensità macrosismica e PGA. Progetto DPC-INGV S1, http://esse1.mi.ingv.it/d11.html.

[15] ATKINSON, G., S. KAKA (2007). Relationships between Felt Intensity and Instrumental Ground Motion in the Central United States and California. Bulletin of the Seismological Society of America, Vol. 97, No. 2, pp. 497–510, April 2007, doi: 10.1785/0120060154

[16] DROUET, S. (2013). Development of regional ground motion prediction equations covering a wide magnitude range based on stochastic simulations (application to the Alps, Pyrenees and Rhine graben regions in France). SIGMA report - Ref. SIGMA-2012-D2-33.

[17] CAUZZI C. and FACCIOLI E. (2008). Broadband (0.05 to 20 s) prediction of displacement response spectra based on worldwide digital records. Journal of Seismology, Vol. 12, n° 4, p. 453-475.

CSNI Workshop on "*Testing PSHA Results and Benefit of Bayesian Techniques for Seismic Hazard Assessment*"
4-6 February 2015, Eucentre Foundation, Pavia, Italy

Bayesian Estimation of the Earthquake Recurrence Parameters for Seismic Hazard Assessment

M. Keller
EDF R&D, France, merlin.keller@edf.fr

M. Marcilhac
PHIMECA, France, marcilhac@phimeca.com

T. Yalamas
PHIMECA, France, yalamas@phimeca.com

R. Secanell
GEOTER, Spain, ramon.secanell@geoter.fr

G. Senfaute
EDF, France, gloria.senfaute@edf.fr

SUMMARY

Seismic hazard curves provide the rate (or probability) of exceedance of different levels of a ground motion parameter (e.g.,the peak ground acceleration, PGA) in a given geographical point and for a given time frame. Hence, to evaluate seismic hazard curves, one needs an occurrence model of earthquakes and an attenuation law of the ground motion with the distance. Generally, the input data needed to define the occurrence model consists in values of the magnitude, experimentally observed or, in the case of ancient earthquakes, indirectly inferred based on historically recorded damages.

In this paper, we sketch a full Bayesian methodology for estimating the parameters characterizing the seismic activity in pre-determined seismotectonical zones, given a catalog of recorded magnitudes. The statistical model, following the 'peak over threshold' formalism, consists in the distribution of the annual number of earthquakes exceeding a given magnitude, coupled with the probability density of the magnitudes, given that they exceed the threshold. When several seismotectonical models, i.e., several possible segmentations of a geographical region in different seismotectonical zones, it is possible within the Bayesian formalism to weigh each model according to its posterior probability given the data recorded in the earthquake catalog, yielding a theoretically well-grounded method for model selection and/or averaging.

The proposed methodology is applied to the Bayesian estimation of the parameters of the magnitudes' distribution in several seismotectonical zones. Finally, when several attenuation laws are available, together with several seismotectonical models, we discuss the possiblility to weigh each resulting seismic hazard model by its posterior probability, given the data from both the earthquake catalog and a second catalog of accelerations recorder in several seismic observation stations.

Keywords: *Probabilistic seismic hazard analysis, Bayesian updating.*

1. Seismicity modeling

The seismicity of a given geographical zone is commonly defined by a parametric statistical model ruling (i) the frequency of occurrence and (ii) the magnitudes of the earthquakes. In common practice when assessing hazard risk at a national or regional scale, the territory is divided in a number of seismotectonical zones, inside which the parameters of the seismicity model (the so-called seismicity parameters) are constant. The definition of the seismotectonical zones is made under the basis of geological, geophysical, geotechnical and seismological considerations, prior to the statistical study. We will not deal here with this problem as we exclusively focus on the statistical issues of hazard risk assessment. As an example, Figure 1 shows the seismotectonical zoning of South-Eastern France we used as an input for the study presented hereinafter.

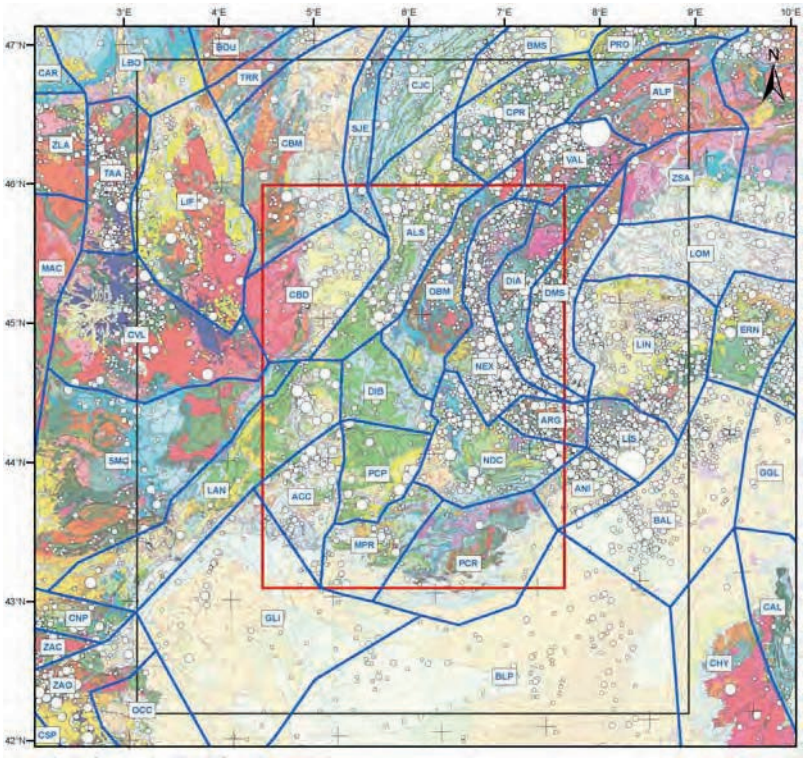

Figure 1. Seismotectonical zoning of South-Eastern France.

A commonly accepted hypothesis within the seismologists' community is that, inside any given zone, the number n of occurrences of earthquakes, the magnitude of which is greater than a given magnitude m, over a period of length t is Poisson-distributed:

$$p(n|\lambda) = \frac{(\lambda . t)^n e^{-\lambda . t}}{n!}$$

Generally t is taken equal to one year, so that λ is to be interpreted as the mean annual number of occurrences (it depends on m).

Another common assumption is that the magnitude of the earthquakes follows a truncated exponential distribution:

$$p(m|\beta, M_{min}, M_{max}) = \frac{\beta e^{-\beta m}}{e^{-\beta M_{min}} - e^{-\beta M_{max}}} \cdot \mathbf{1}_{[M_{min}, M_{max}]}(m)$$

In practice, the parameter of the Poisson model is chosen as the one corresponding to the lower threshold of the magnitude of the truncated exponential model. We will simply note: $\lambda=\lambda_{M_{min}}$. Hence, the seismicity of the zone, i.e. the probabilistic model ruling occurrences and magnitudes of earthquakes is completely determined by the four parameters: M_{min}, M_{max}, λ and β.

In practice, M_{min} and M_{max} are assumed to be known, under the basis of the available expert knowledge; hence, the seismicity of the zone thus relies on the two parameters λ and β. In the following sections we will focus on the statistical estimation of these parameters in the Bayesian framework.

2. Bayesian estimation

The ideal case for the statistical inference of (λ,β) is when the analyst has at her/his disposal a set of n independent and identically distributed (iid) values of observed magnitudes over a given period of observation. Bayesian inference in this case is then straightforward if one chooses Gamma prior distributions for both λ and β, as in Campbell[14]:

$$\lambda \sim Ga(n_0, t_0)$$
$$\beta \sim Ga(r_0, s)$$

Actually, the posterior distribution of λ is again a Gamma distribution, because of the well-known conjugacy property of the Poisson-Gamma statistical model. As far as β is concerned, because of the truncation of the Exponential distribution, the conjugacy property of the Exponential-Gamma model is lost and no closed-form expression exists for the posterior, which is only known up to a multiplicative constant. Nevertheless, Bayesian inference can easily be performed by generating random samples from the posterior distribution by means of Monte Carlo methods, such as Markov Chain Monte Carlo (MCMC) or Importance Sampling[18].

In practice however, data are much more heterogeneous: namely, the historical period over which magnitudes can be supposed to have been observed in their entirety differs according to the value of the magnitude itself: the higher the magnitude, the longer the observation period. Hence, available data are not iid with respect to the above model described above.
To overcome this issue, Weichert[8] proposed a modified version of the Poisson-Exponential model previously introduced, which is now a reference model within the seismologists' community. Weichert's model is based on a preliminary treatment of data, consisting in dividing the interval $[M_{min}, M_{max}]$ of observed magnitudes in to intervals of half-length δ. Let us note m_j the center of these $J=(M_{max} - M_{min})/2\delta$ intervals. Under the basis of expert considerations, seismologists assign a complete observation period t_j to each of the intervals.

Weichert's model is based on the same assumptions as the model described hereinbefore. Under the assumption that magnitudes are exponentially distributed, the probability for an earthquake to have a magnitude between m_j-δ and m_j+δ is:

$$p_j = \frac{e^{-\beta m_j}}{\sum_{k=1}^{J} e^{-\beta m_k}}$$

Hence, the number n_j of earthquakes of magnitude between m_j-δ and m_j+δ occurred in the corresponding complete observation period t_j follows a Poisson distribution, the parameter of which is $\lambda.m_j.t_j$.
Finally, under the assumption that earthquakes occur independently from one another, i.e. that the observed numbers n_j of earthquakes in each interval are independent, the likelihood of the data $D=\{t_j,n_j\}_{1\leq j\leq J}$, where J is the number of distinct magnitude classes $[m_j-\delta\ ;\ m_j+\delta]$, is given by:

$$L(D|\lambda,\beta) = e^{-\lambda\sum_j t_j p_j} \times \lambda^n \prod_j \frac{(t_j p_j)^{n_j}}{n_j!}.$$

According to Bayes' theorem, the posterior density of (λ,β) is, that is, the density of their conditional distribution given the available data D, is equal to:

$$\pi(\lambda,\beta|D) = \frac{L(D|\lambda,\beta)\pi(\lambda,\beta)}{ML(D)},$$

where $ML(D) = \int_{\lambda,\beta} L(D|\lambda,\beta)\pi(\lambda,\beta)d\lambda d\beta$ is known as the *marginal likelihood*, or the *evidence*. This is a central quantity in Bayesian model selection/model averaging[16], since it yields the posterior probability of a certain statistical model of the data, given a list of candidate models. We will develop this idea further in the next section.

Unfortunately, the integral defining the evidence $ML(D)$, hence also defining $\pi(\lambda,\beta|D)$, is not available in closed form. To overcome this issue, it is possible to use the Importance Sampling (IS) methodology developed by Keller[28] to generate a sample from the posterior distribution, along with Monte-Carlo estimates of all the associated quantities of interest.
In short, the IS approach consists in generating a large number I of so-called *particles* (λ_i,β_i) from the Gamma priors described above, then assigning the weight $w_i = L(D|\lambda_i,\beta_i)$ to each particle (λ_i,β_i). An approximately iid sample from the posterior density can then be obtained by sampling repeatedly from these particles, with probabilities proportional to their weights. Such a procedure, known as Sampling Importance Resampling (SIR) is very simple to implement, and avoids the tuning and convergence issues typical of MCMC approaches. Also, by simply averaging the weights w_i, a Monte-Carlo estimate of the evidence $ML(D)$ is obtained.

3. Multi-zone inference and model selection/averaging

The methodology presented in the previous section enables to sample from the posterior distribution of the earthquake recurrence parameters and calculate the marginal likelihood in a single zone of a given seismotectonical model (SM). Typically, such a model comprises a certain number N of zones, to which the above approach must be applied separately in order to estimate the full earthquake recurrence model for the entire region under study (here, the south-east of France). Since the seismic activity is considered independent across zones, the marginal likelihood (or evidence) for the full model is obtained simply as the product of the marginal likelihood for each zone:

$$ML(D|SM) = \prod_{k=1}^{N} ML(D_k|SM),$$

Where $ML(D_k|SM)$ denotes the marginal likelihood for the data in D_k zone k of the seismotectonical model SM.
In general, several competing SM's are available for a given region; the Bayesian model selection framework allows weighting each of these models according to their posterior probability given the data, making it possible to account for the uncertainty on the choice of seismotectonical zones, in the same manner the uncertainty tainting the earthquake recurrence parameters was assessed. Indeed, given prior probabilities $\pi(SM_i)$ on each seismotectonical model, reflecting the beliefs of

seismologist experts on each one of them, before consideration of the data *D* (here, the historical catalog), it can be shown that the posterior probabilities of these same SMs, reflecting the update of the prior beliefs given the available data, are given by:

$$P[SM_i|D] = \frac{ML(D|SM_i)\pi(SM_i)}{\sum_i ML(D|SM_i)\pi(SM_i)}$$

These Bayesian probabilities can be used either to select a single 'optimal' seismotectonical model, with maximal posterior probability, or to weight the predictions of interest quantities within each model in a model averaging approach[16], effectively integrating out the uncertainty on the seismotectonical model.

4. Illustration of the proposed methodology

We now apply the methodology presented above to three contiguous zones of south-eastern France. Each zone presents a different type of seismicity; one is high, denoted in the following zone 1, the other moderate, denoted zone 2, and the third one low, denoted zone 3. We also defined three sites of interest within each zone, chosen arbitrarily as the center of each, and which we will use in the following to assess seismic hazard curves. The zones and sites of interest are depicted in figure 2.

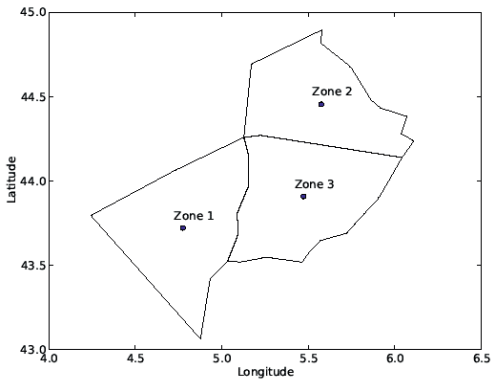

Figure 2. Boundaries of the three considered seismotectonical zones (solid lines) and sites of interest (circles).

Thanks to the SIR approach described in the previous section, we generated a sample of 10000 draws from the joint posterior distribution of the parameters λ and β for each considered zone. Scatterplots of these samples are depicted in figure 3. In particular, posterior dependence between λ and β is apparent from these graphs, the more so for the low seismicity zones 2 and 3. This dependence is a direct consequence of the incompleteness of the earthquake catalog, incompleteness which is aggravated in low seismicity zones, where only few earthquakes have been observed[28]. Intuitively, this can be explained by the fact that the number of observed earthquakes depends on their magnitude (the higher the magnitude, the larger the number of observed earthquakes). This mechanically creates a statistical dependence between the estimate of λ, which controls their number, and of β, which controls their magnitudes.

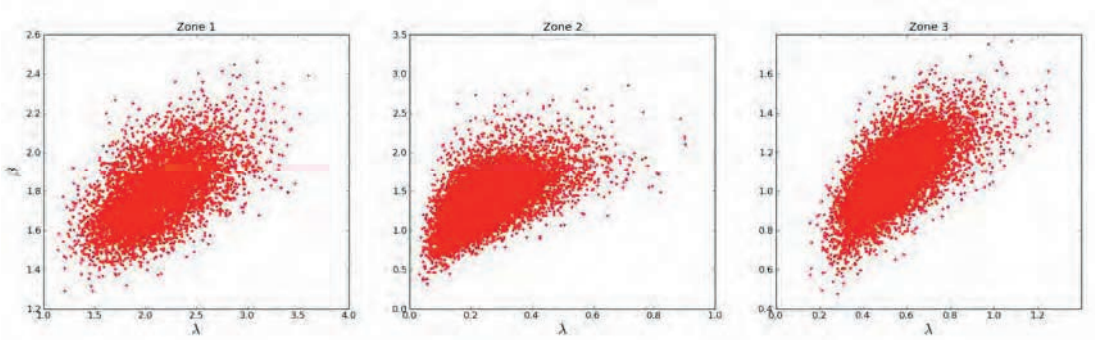

Figure 3. Bayesian estimation of the seismicity parameters: sample from the joint posterior distribution of λ and β.

Table 1 sums up the posterior mean values of the seismicity parameters whose posterior distributions are obtained using the SIR approach described above. From a practical viewpoint, 10000 draws have been found to be enough to build proper Monte Carlo estimation of the posterior mean and credibility bounds.

We have also included as an illustration of the methodology the Monte-Carlo estimates of the marginal likelihood (the evidence) for the statistical model within each considered zone, though we stress that the displayed values cannot be interpreted *per se*. As discussed in the previous section, once the evidence for each zone of a seismotectonical model is computed, multiplying them yields the complete evidence which can then be used in a straightforward way to weight several possible seismotectonical models according to their posterior probabilities.

Table 1. Evidence of the statistical model for each considered zone, posterior mean of the seismicity parameters along with 95% credible intervals

	Evidence		Posterior mean	Credible interval
Zone 1	6.73E-29	λ	2.135	[1.508 ; 2.885]
		β	1.801	[1.509 ; 2.115]
Zone 2	2.05E-10	λ	0.258	[0.091 ; 0.537]
		β	1.397	[0.813 ; 2.069]
Zone 3	1.16E-21	λ	0.555	[0.301 ; 0.896]
		β	1.088	[0.769 ; 1.409]

5. Discussion and perspectives

The methodology presented here, further developed by Keller[28], allows estimating the earthquake recurrence parameters in each zone of a given seismotectonical model for a region of interest, and a historical catalog of earthquakes. An important advantage of such a Bayesian approach, over more classical methods such as Weichert's[8], is a full description of the uncertainties, both aleatory and epistemic, surrounding the quantities of interest.
We have also sketched how such an approach could also encompass the task of selecting an appropriate seismotectonical model, or averaging over several possible such models, by estimating the posterior probabilities associated to each model, given the data. In principle, this boils down to including the choice of an appropriate data model as an additional, discrete, parameter, to which prior probabilities are assigned, then deriving the posterior probabilities according to Bayes' theorem.

We have not discussed here the construction of seismic hazard curves which account for the uncertainty on earthquake recurrence parameters, an important application of our proposed methodology[28]. Combined to the estimation of the seismic fragility curve of a given building[27], such seismic hazard curves can be used to estimate the building's failure probability[29].
The central ingredient to such applications is the attenuation law, such as the popular Berge-Thierry law[24]. However, as for seismotectonical models, many other attenuation laws have been proposed to date; hence, selecting an appropriate law from a list of candidates, or averaging over them, given a catalog of PGAs recorded in certain interest locations is an exciting perspective of our work. This is a challenging task, which could be tackled for instance using the methodology proposed by Selva et Sandri[30], based on a discretization of the range of accelerations similar to that of earthquakes' magnitudes used in Weichert's approach.

REFERENCES

[1] Cornell CA. Engineering seismic risk analysis. Bulletin of the Seismological Society of America 1968; 58(1):1583-1606.
[2] McGuire RK. Fortran computer program for seismic risk analysis. Open-File Report 76-67; United States Department of the Interior, Geological Survey, 1976.
[3] Beauval C. Analysis of uncertainties in a probabilistic seismic hazard estimation, example for France. PhD thesis; Grenoble University Joseph Fourier, 2003.
[4] Kramer SL. Geotechnical Earthquake Engineering. Prentice Hall: Upper Saddle River, NJ, 1996.
[5] Reiter L. Earthquake Hazard Analysis: Issues and Insights. Columbia University Press: New York, 1990.
[6] Bender BK, Perkins DM. Treatment of parameter uncertainty and variability for a single seismic hazard map. Earthquake Spectra 1993; 9:165{195.
[7] Lombardi AM, Akinci A, Malagnini L, Mueller CS. Uncertainty analysis for seismic hazard in Northern and Central Italy. Annals of Geophysics 2005; 48(6):853{865.
[8] Weichert DH. *Estimation of the earthquake recurrence parameters for unequal observation periods for different magnitudes.* Bulletin of the Seismological Society of America 1980; 70:1337-1356.
[9] Bernier J. Décisions et comportement des décideurs face au risque hydrologique / Decisions and attitude of decision makers facing hydrological risk. Hydrological Sciences Journal 2003; 43(3):301-316.
[10] Eckert N, Parent E, Faug T, Naaim M. Bayesian optimal design of an avalanche dam using a multivariate numerical avalanche model. Stochastic Environmental Research and Risk Assessment 2009; 23(8):1123-1141.
[11] Pasanisi A, Keller M, Parent E. Estimation of a quantity of interest in uncertainty analysis: some help from Bayesian decision Theory. Reliability Engineering and System Safety 2012, 100:93-101.
[12] Wells DL, Coppersmith KJ. New Empirical Relationships among Magnitude, Rupture Length, Rupture Width, Rupture Area, and Surface Displacement. Bulletin of the Seismological Society of America 1994; 84:974-1002.
[13] Kijko A, Graham G. Parametric-historic Procedure for Probabilistic Seismic Hazard Analysis Part I: Estimation of Maximum Regional Magnitude Mmax. Pure Applied Geophysics 1998, 152:413-442.

[14] Campbell KW. *Bayesian analysis of extreme earthquake occurrences. Part I. Probabilistic hazard model*. Bulletin of the Seismological Society of America 1982; 72(5):1689-1705.
[15] Stavrakakis GN, Drakopoulos J. Bayesian probabilities of earthquake occurrences in Greece and surrounding areas. Pure and Applied Geophysics 1995; 144(2):307-319.
[16] Rosenblueth E, Ordaz M. Use of seismic data from similar regions. Earthquake Engineering & Structural Dynamics 1987; 15(5):619-634.
[17] Bernal R. Estimacion Bayesiana del Peligro Sismico del Ecuador. PhD thesis; Escuela Politecnica Nacional, 1998.
[18] Marin JM, Robert CP. Bayesian Core: A Practical Approach to Computational Bayesian Statistics. Springer: New York, 2007.
[19] A. Gelman, J.B. Carlin, H.S. Stern, D.B. Dunson, A. Vehtari, and D.B. Rubin. *Bayesian Data Analysis, Third Edition*. CRC Press: Boca Raton, FL, 2013.
[20] Gutenberg B, Richter CF. Frequency of earthquakes in California. Bulletin of the Seismological Society of America 1944; 34(4):185-188.
[21] Lominashvili G, Patsatsia M. On the Estimation of a Maximum Likelihood of Truncated Exponential Distributions. Bulletin of the Georgian National Academy of Sciences 2013; 7(1):21-24.
[22] van der Vaart AW. Asymptotic Statistics. Cambridge University Press: Cambridge, UK, 2000.
[23] Solomos G, Pinto A, Dimova S. A Review of the seismic hazard zonation in national building codes in the context of Eurocode 8. Technical Report EUR 23563 EN-2008; JRC European Commission, 2008.
[24] Berge-Thierry C, Cotton F, Scotti O, Griot-Pommera DA, Fukushima Y. New empirical response spectral attenuation laws for moderate European earthquakes. Journal of Earthquake Engineering 2003; 7(2):193-222.
[25] Kass RE, Raftery AE. Bayes factors. Journal of the American statistical association 1995; 90(430):773-795.
[26] Wasserman L. *Bayesian model selection and model averaging*. Journal of Mathematical Psychology 2000; 44(1):92-107.
[27] Damblin G, Keller M, Pasanisi A, Barbillon P, Parent E. Approche décisionnelle bayésienne des incertitudes dans un contexte industriel. Application aux courbes de fragilité sismique. Journal de la Société Française de Statistiques 2014; 155(3):78-103.
[28] Keller M, Pasanisi A, Marcilhac M, Yalamas T, Secanell R, Senfaute G. *A Bayesian Methodology Applied to the Estimation of Earthquake Recurrence Parameters for Seismic Hazard Assessment*. Quality Reliability and Engineering International 2014; 30:921-933.
[29] Keller M, Pasanisi A, Marcilhac M, Yalamas T, Secanell R, Senfaute G. *Bayesian Estimation of the failure Probability of a Structure submitted to Seismic Hazard Assessment*. International Society for Bayesian Analysis World Meeting, (ISBA 2014) - 18 July, 2014 (poster).
[30] Selva J, Sandri L. *Probability Seismic Hazard Assessment: Combining Cornell-Like Approaches and Data at Sites through Bayesian Inference*. Bulletin of the Seismological Society of America, Vol. 103, No. 3, pp. 1709–1722, June 2013.

CSNI Workshop on "*Testing PSHA Results and Benefit of Bayesian Techniques for Seismic Hazard Assessment*"
4-6 February 2015, Eucentre Foundation, Pavia, Italy

PSHA Updating Technique with a Bayesian Framework: Innovations

N. HUMBERT
EDF – Hydro Engineering Center (CIH), France, nicolas.humbert@edf.fr

SUMMARY

The objective of this paper is to point out some difficulties that may appear in the development of PSHA studies and to propose an approach that may be used to address epistemic uncertainties. The innovating point of the process is the use of instrumental experience feedback to update the results of a PSHA. The method used is based on a Bayesian updating technique including real observations as a realization of a random variable. These observations are used as conditional events in a Bayesian approach.
This work proposes the development of a negative binomial model that avoids the ergodic assumption in the Bayesian approach by taking into account dependency between the feedback stations. This generalisation of the updating technique is evaluated with a test case in order to identify the efficiency of this updating method.

Keywords: *Probabilistic seismic hazard analysis, Bayesian updating.*

1. Context & Motivations

In the specific case of moderate and low seismicity areas, the lack of strong motion data lead to select an attenuation model built on strong motion data coming from high seismicity regions. These data are taken out of their context.
The assumption that the attenuation is coherent in active and moderate zones is strong and lead usually to scale conversion issues: for example the GMPEs are usually based on moment magnitude or surface moment magnitude while the magnitude used for the activity model is usually local magnitude for low seismicity context.
Surprisingly, in that context of lack of data the local seismic recording are not frequently used to calibrate the attenuation model. For example in the specific context of the French metropolitan territory, the data bases presented on figure 1 are not systematically used in the recent PSHA:

- the French broadband and accelerometric permanent network (more than 100 stations),
- CEA velocimetric network (since 1950 - 40 velocimetric stations),
- TGV network (French high speed train - 24 stations),
- nuclear power plants accelerometric stations (18 sites).

These data could be systematically used in PSHA in order to reduce epistemic uncertainties. The Bayesian updating is one of the methods able to include these additional data in the assessment. Bayesian updating for PHSA is not unusual: methods to update PSHAs are proposed since the

90th, for example in [1] to [7]. The following paragraphs generalize the method proposed in [3] or [7], taking into account dependence between stations.

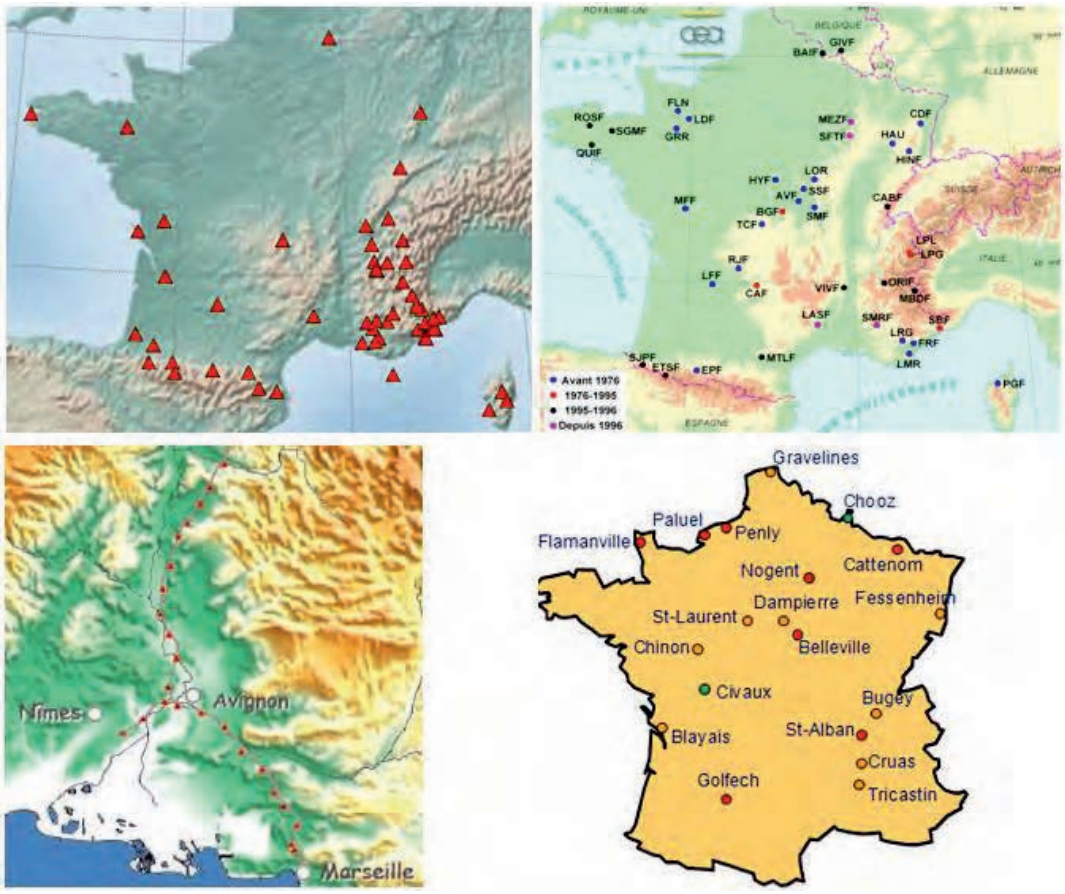

Figure 1. local accelerometric or velocimetric databases not systematically used in French PSHA: French broadband and accelerometric permanent network, CEA velocimetric network, TGV network (French high speed train) and nuclear power plants accelerometric stations

2. Theory and methodology of updating

The earthquake hazard for a site is usually expressed in terms of exceedance rates (λ), of a parameter of the ground motion: peak ground acceleration (PGA), spectral pseudo-acceleration (SPA) or macroseismic intensity…etc. The exceedance rate is the expected number of earthquakes per year which exceed a given value of the parameter of interest. If a Poisson model is assumed for earthquake occurrences in time, this rate includes all the information required to compute probabilities of exceedance during given time.

2.1 Single site of observation

As proposed by Albarello and D'Amico [7], in the case of one site of observation the probability recording n « events » during t years: P(n,t) is can be evaluated by the equation 1.

$P(n,t) = \frac{e^{\lambda t}(\lambda t)^n}{n!}$	(1)

This equation is used in a Bayesian updating technique to define the "likelihood function" and update the weight of each branch of the logic tree for a discreet approach (usual method in PSHA), or to update the input parameters in a continuous formulation (method used in §3 of this paper).
Note that the standard deviation is a function of the time of observation: $SD(P)=(1/t)^{0.5}$: so the longer the time of feedback is, the more precise the evaluation becomes. For this reason in a Bayesian updating, the sufficiency of time of feedback does not need to be checked or demonstrated, the occurrence model does it intrinsically.

2.2 Multiple independent sites of observation: Poisson distribution

If we formulate the hypothesis that sites are independent in term of seismic hazard, the total number of exceeding for the N sites follows a Poisson distribution too (equation 2).

$$P(n,t)=\frac{e^{A}(A)^{n}}{n!} \text{ with } A=\sum_{i\in sites}\lambda_i t_i \qquad (2)$$

The "A" coefficient is the cumulative exceedance rate: so the time of observation and the seismic rate do not have necessarily to be the same on each site. As for the single site, we notice that the standard deviation is a function of the cumulated time of observation for the whole network. $SD(P)=(1/T)^{0.5}$ with T the cumulated time of observation.

2.3 Multiple dependent sites of observation: Negative binomial distribution

The case of multiple dependent sites is more complicated, because an earthquake can be recorded by two or more stations: the Poisson theory is no longer applicable. In existing publications, such as Ordaz & Reyes [1], Fujiwara et al. [4], Stirling et Al [5] & Albarello et Al. [7] this case is not studied and the dependence is supposed negligible. This paper proposes a generalization of the Poisson model allowing taking into account the specific dependency between stations of a network. This model is based on Woo G. [8] and expressed with the negative binomial distribution (equation 3) (ie. Pòlya distribution).

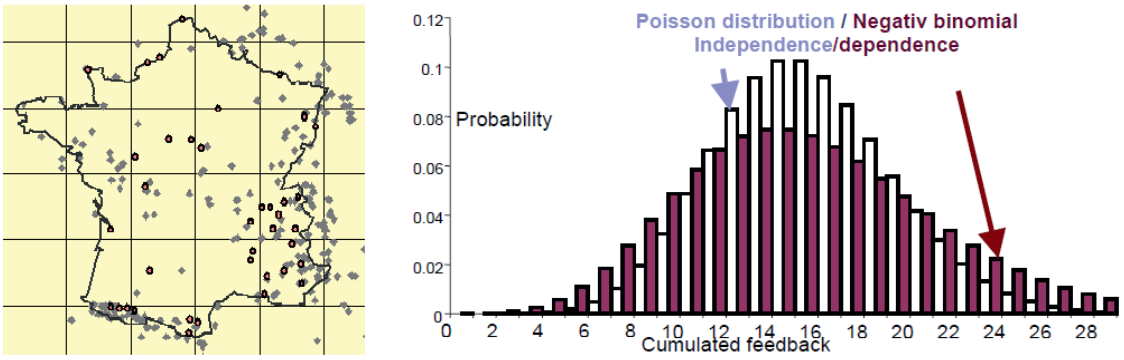

Figure 2. test case illustrating the effect of dependence between stations on likelihood function

$f(n;r,p)=\frac{\Gamma(n+r)}{n!\,\Gamma(r)}(1-p)^r\,p^n$ with n the number of event and r & p two parameters of the model	(3)

In case of dependent stations, the observations are over-dispersed with respect to a Poisson distribution for which the mean is equal to the variance. The distribution (3) is especially adapted this kind of configurations and can be used with independent stations too (equation 4).

Since the negative binomial distribution has one more parameter than the Poisson distribution, the second parameter can be used to adjust the variance independently of the mean. This distribution is validated on 12 test cases described in table 1 and based on the model that will be developed in §3. It fits the expected values in all cases.

$\forall n \in \mathrm{N},\ \lim_{r\to\infty} f(n;r,\frac{\lambda}{\lambda+r}) = Poisson(n;\lambda)$	(4)

Table 1. test cases of validation for the negative binomial distribution

	Number of sites	Dependence	Type of Seismicity	Total
Hypothesis	2 / 15 / 50	Low/high	Homogenous / heterogeneous	
Number of branches	3	2	2	12

2.4 Alternative parameterization: Natural logarithm of the gamma function

With this formulation, the parameters r & p are difficult to evaluate. The equation (5) gives an alternative parameterization of the same distribution. The K is the mean number of stations that record the same earthquake (K=1 for a network of independent stations / K=2 if an earthquake is recorded by a mean of 2 stations). The dependence between stations ("K") has no effect on the cumulative exceedance rate "A".

$f(n,t)=\exp\left[\ln\Gamma\left(\frac{A}{K-1}+n\right)-\ln\Gamma\left(\frac{A}{K-1}\right)-\ln\Gamma(1+n)\right]\frac{1}{K}^{\frac{A}{K-1}}\left(1-\frac{1}{K}\right)^n$ with $A=\sum_{i\in sites}\lambda_i t_i$ and $\ln\Gamma(x)=\ln\left(\int_0^\infty e^{-u}u^{x-1}du\right)$: natural logarithm of the gamma function	(5)

In terms of efficiency of the method, the higher the K parameter is, the less efficient the updating is. Figure 3 shows the effect of K on the "likelihood function": the standard deviation of the function in growing with K.

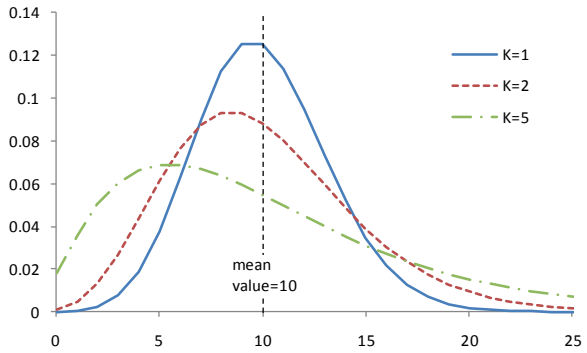

Figure 3. Effect of the dependence between sites of the network on the "likelihood function"

2.5 Methodology of application: Monte Carlo sampling

The value of A is assessed by the hazard curves of the PSHA. However to evaluate the K coefficient the integration has to be assessed simultaneously on the N stations. For this reason, a discrete simulation of seismic hazard has to be assessed instead of the continuous integration of activity expectation proposed by McGuire (1976).
The sampling of earthquake is developed following the same hypothesis of the PSHA:

- seismic activity is sampled for each seismotectonic zone with a Poisson random variable consistent with Mmin, activity model and time of observation,
- for each earthquake a realization of magnitude, location and ground motion prediction is generated with a random variable consistent with the PSHA model.

For a sufficient number of realizations (Monte Carlo sampling), the total number of impacted sites is evaluated. The mean value of this number is an approximation of "K".
The K parameter depends on all the PSHA parameters and varies for each branch of the logic tree. But based on the tests cases presented on table 1, it appears that K depends mainly on two hypotheses: the feedback (sites localization, number and time of recording) and the minimal magnitude for hazard integration (Mmin). For this reason K can be estimated as constant for the whole logic tree.

2.6 Simplified approach: Analytical approach

The K parameter can be evaluated in an analytical way including some simplifications. Assuming an homogenous spatial repartition of N sites on a territory with a surface St and an homogeneous seismic activity: for a given threshold "a", and a given magnitude M let's define the capable surface Sc(M) as the surface on which the threshold "a" is exceeded. The seismic activity follows a Gutenberg-Richter recurrence law. The effective capable surface Sc is obtained with equation (6). Based on average functions of acceleration versus magnitude in GMPEs, Sc can be simplified by a more simple equation (7) depending on Mmin. Finally, K can be estimated by the equation (8).

$Sc(M) = \dfrac{\int_M \dfrac{d\lambda(M)}{dM}.Sc(M)dM}{\int_M \dfrac{d\lambda(M)}{dM}dM}$ with $\lambda(M)$ the magnitude exceedance rate	(6)

$Sc \approx Sc(M_{MIN} + 0.5)$	(7)

$\mathrm{K} \sim 1 + \frac{N.Sc}{St} \sim 1 + \frac{N.Sc(M_{MIN} + 0.5)}{St}$	(8)

This simplified approach perfectly fits the "Monte Carlo" computed value of K for reasonably homogeneous network and homogeneous seismicity. It can be used to simply check the hypothesis of independence between the stations of a network. Note: the area covered by the network (St) must be limited to the neighborhood of the station coherent with the radius of the capable surface Sc.

2.7 GMPE updating

As presented in previous paragraphs, the Bayesian updating of the seismic activity creates some difficulties of integration for the Poisson distribution. A simplest method consists in the direct Bayesian updating of the GMPE logic tree. This method is developed in various works, as Ordaz in 1994 [1], or the NGA-West2 Research Program [9] that updates the NGA database for small, moderate and large magnitude events or the work of A. Runge [10] that proposes a method of elicitation of GMPEs in logic trees.
These methods have to be used before the integration step of the PSHA by the team in charge of the GMPEs selection whereas the method presented in previous paragraphs can be used at the end of the process to check the consistency of the overall PSHA with the feedback experience.

3. Application: Test case

In order to evaluate the effect of Bayesian updating on PSHA, a test case is developed hereinafter. The analysis is not limited to the description of updating on hazard curves but also tries to describe the efficiency of the method to update the assumptions of the PSHA. This is of major importance and can give an idea of the possibility of local earthquake recordings to update PSHA assumptions.

The test case is rather simple (Figure 4 and equation 9):

- the considered territory is a 1000km x 1000km square with 100 seismotectonic square zones,
- for each seismotectonic zone the occurrence model is a bounded Gutenberg-Richter recurrence law; the seismic activity considered is consistent with a moderate seismicity (~France),
- the GMPE is a model developed on the base of [11],
- usually different magnitude scales are used for the GMPE and the occurrence model: to take this into account, a bilinear relation is used to link this two magnitudes scales [12],
- the random model is lognormal with a constant sigma value consistent with a single site value.

On one hand the model is used in order to sample a feedback for a time of observation and series of recording stations with a Poisson occurrence model and the method presented in §2.5. On the second hand an epistemic variability is introduced and a PSHA is built including the uncertainty in a logic tree. Finally the Bayesian updating of the PSHA is assessed with the feedback of the "Monte Carlo" model.

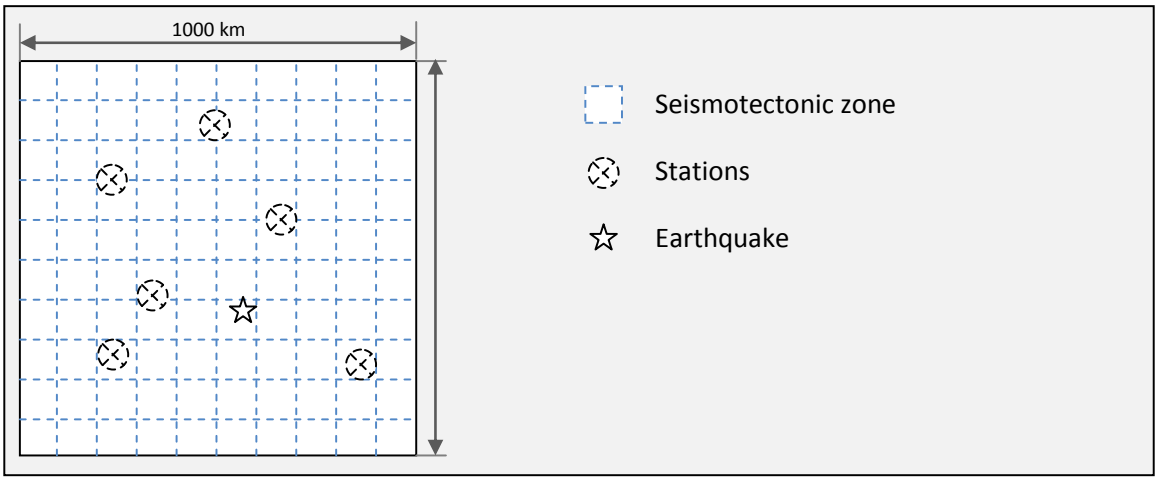

Figure 4. geographical description of the model

In the PSHA part, we assume that our knowledge of the seismic hazard is imperfect: for this reason all model parameters are considered as random variables. The methodology to evaluate the uncertainties is based on fuzzy regression with the methodology proposed in [11]. The input data comes from [14]. Equation 9 & table 2 describe the resulting model.

Activity: $N = 10^{a-bM} - 10^{a-bMax}$ with N the number of events having a magnitude > M, and a, b & Mmax epistemic variable normally distributed **Magnitude conversion:** $M_{GMPE} = 6 + \lambda(M-6)$ for M < 6 $M_{GMPE} = M$ for M > 6 (λ is normally distributed) **GMPE**: $Log(A) = \alpha_0 + \alpha_1 M + \alpha_2 M^2 + \alpha_3 R + (\alpha_4 + \alpha_5 M)\log\sqrt{R^2 + R_0{}^2} + \varepsilon$ with A the acceleration and $\alpha_0, \alpha_1, \alpha_2, \alpha_3, \alpha_4, \alpha_5$ & R_0 epistemic variable normally distributed **Random model**: ε=𝒩(0 ; σ) with σ epistemic variable normally distributed	(9)

Table 2. numerical value for the expected value and the epistemic variability

	a	b	Mmax
Mean	3.2	1	6
SD	0.5	0.17	1

lambda	aleatory
0.66	0.43
0.13	0.11

	alpha0	alpha1	alpha2	alpha3	alpha4	alpha5	Ro
Mean	2.08	0.18	0.0056	0.00029	-0.93	-0.0086	1.95
SD	0.82	0.28	0.02	0.001	0.34	0.05	4.6

The Table 2 gives the mean values and standard deviation of the α0, α1, α2, α3, α4, α5, Ro, λ and σ variables. However these parameters cannot be used as expressed because the variables are interdependent. These values are consistent with the variability observed in recent PSHA such as [13]. The objective in this test case is only to catch the degree of magnitude of the epistemic uncertainties observed in recent PSHA and observe the efficiency and the effect of updating in that context.

The three following paragraphs give the main conclusions of this exercise.

3.1. Time of observation

The more the time of observation grows the more the updating is efficient. If the time of observation is too short, the updating can nevertheless be used, but has absolutely no effect on PSHA.

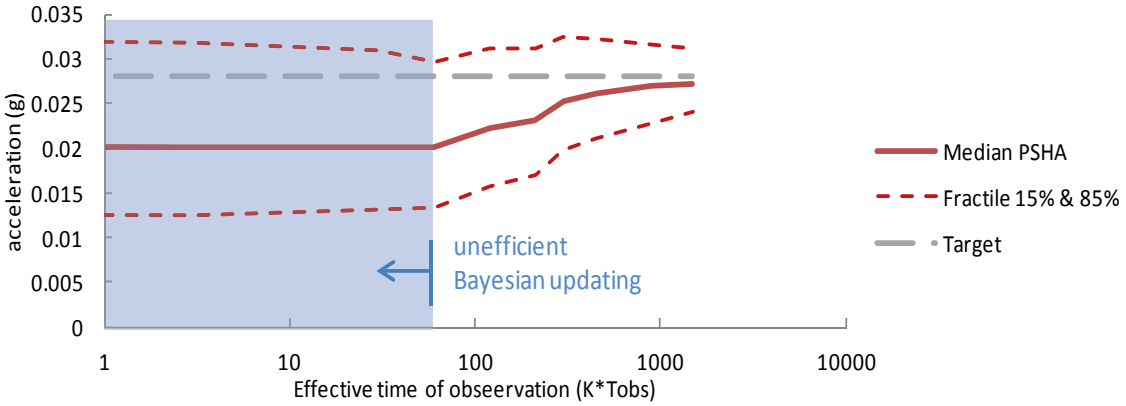

Figure 5. effect of the time of observation

3.2. Compensate lack of observation time by multiplying stations? (ergodicity assumption)

This exercise shows that it is possible to "trade some space for some time" by multiplying the number of stations, but this effect is limited by the size of the territory: as the number of stations increases, the cumulated time of observation increases, but the dependence coefficient K increases too (see §2.3 to §2.6), and so the "effective time" of observation saturates (Figure 5).

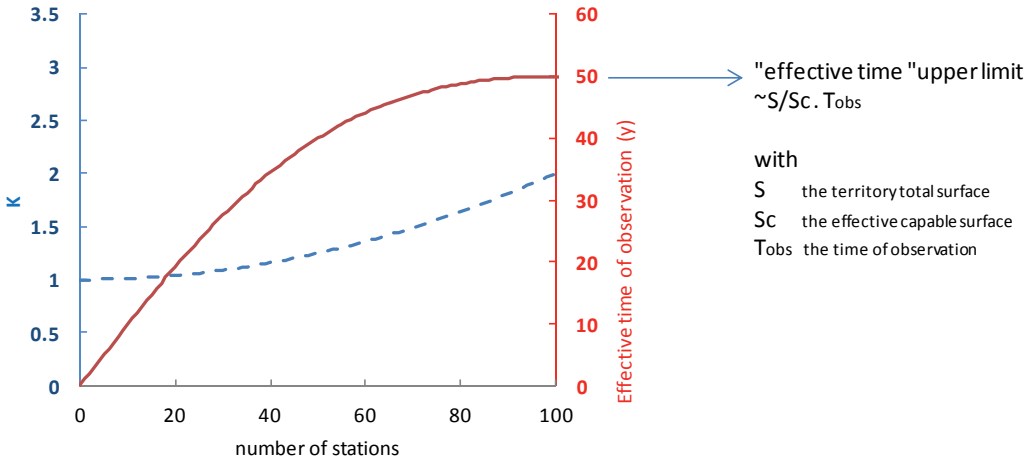

Figure 6. limit in the multiplication of stations on the updating technique (test case for 1 year of observation)

On this example, we can observe that it is possible to "accelerate" time of observation by a factor of 50, but no more (50 is the upper limit) because of correlation between stations.

3.3. Parameters updated by the technique

The effect of the updating technique is clear: as shown on figure 6 only a part of attenuation equation parameters and magnitude conversion equation parameters are updated. The Bayesian updating technique has no effect on seismic activity rates or random model. Consequently, the integration of the activity model in the updating process has no scientific interest: it limits the effect of updating because of the high variability of the Poisson occurrence model and is not updated by the method.

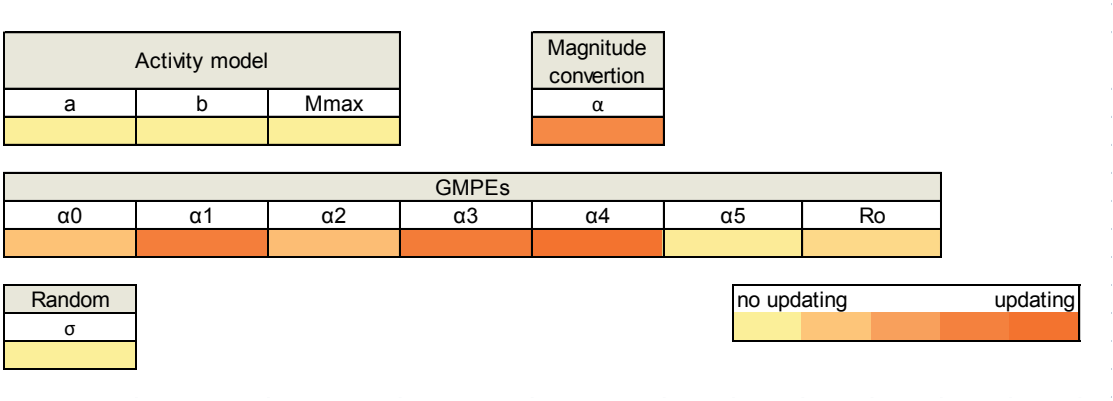

Figure 6. Effect of the updating on the input parameters of the PSHA (test case)

For this reason, we conclude that the direct Bayesian updating of the GMPEs logic tree (§2.7) is the most efficient way to integrate local data in PSHA and we recommend in the future PSHA to integrate this data before the integration of hazard.
However the method presented in this paper keeps an interest for the verification of the overall process at the end of the PSHA: for example for the branches including double counting of uncertainties.

4. Conclusion

The high level of uncertainties in PSHA for low to moderate seismicity contexts is usually attributed to a lack of local seismic data. However, seismic records are available for such areas but may not be used as input data in PSHAs (see French metropolitan territory example in §1).
The Bayesian updating process developed in this paper provides a systematic process to include these data in PSHA. The innovation presented here allows updating PSHA even with data coming from relatively dense station network including seismically dependent stations.
The main interest of this technique is the opportunity to use it after the integration of the PSHA, and consider it for example as a verification step in a QA process or for reducing epistemic uncertainties.
But as we see in the paragraph 3.3, the efficiency of the updating is reduced by the integration of an occurrence model in the process (and dependency of stations if any). This observation is confirmed by the fact that the Bayesian updating is nearly unable to update the activity model without sufficient time of observation.
For this reason, the most efficient method of updating PSHA consists in including this step before the integration of hazard, updating directly the GMPE logic tree (as [9] or [10]). This work will be extended in the future by performing a comparison of both ways of updating PSHA (before or after the integration process) in order to illustrate the performances of these two approaches.

REFERENCES

[1] Ordaz M, Singh S. K, Arciniega A, (2007) “Bayesian Attenuation Regressions: an Application to Mexico City”

[2] Wang M. and Tsuyoshi Takada T. (2006) “Site-specific prediction of seismic ground motion with Bayesian updating framework”, 4th International Conference on Earthquake Engineering Taipei, Taiwan

[3] Ordaz, M. & Reyes, C. 1999, "Earthquake hazard in Mexico City: Observations versus computations", Bulletin of the Seismological Society of America, vol. 89, no. 5, pp. 1379-1383.

[4] Fujiwara, H., Morikawa, N., Ishikawa, Y., Okumura, T., Miyakoshi, J., Nojima, N. & Fukushima, Y. 2009, "Statistical Comparison of National Probabilistic Seismic Hazard Maps and Frequency of Recorded JMA Seismic Intensities from the K-NET Strong-motion Observation Network in Japan during 1997-2006", Seismological Research Letters, vol. 80, no. 3, pp. 458-464.

[5] Stirling, M. & Petersen, M. 2006, "Comparison of the Historical Record of Earthquake Hazard with Seismic- Hazard Models for New Zealand and the Continental United States", Bulletin of the Seismological Society of America, vol. 96, no. 6, pp. 1978-1994.

[6] Stirling, M. & Gerstenberger, M. 2010, "Ground Motion-Based Testing of Seismic Hazard Models in New Zealand", Bulletin of the Seismological Society of America, vol. 100, no. 4, pp. 1407-1414.

[7] Albarello, D. & D'Amico, V. 2008, "Testing probabilistic seismic hazard estimates by comparison with observations; an example in Italy", Geophysical Journal International, vol. 175, no. 3; 3, pp. 1088-1094.

[8] Woo G. (2000). “The mathematics of natural catastrophes,” Imperial College Press.

[9] “NGA-West2: A Comprehensive Research Program to Update Ground Motion Prediction Equations for Shallow Crustal Earthquakes in Active Tectonic Regions”

[10] Runge A, Händel A, Riggelsen C, Scherbaum F, Kühn N, “A Smart Elicitation Technique for Informative Priors in Ground-Motion Mixture Modeling” M. EGU General Assembly 2013, held 7-12 April, 2013 in Vienna, Austria, id. EGU2013-990

[11] Humbert H, and Viallet E, “An evaluation of epistemic and random uncertainties included in attenuation relationship parameters”, 14 th WCEE 2008, Beijing, China

[12] Martin Ch, Secanell R, Viallet E, Humbert N (2008) “Consistency of PSHA models in acceleration and intensity by confrontation of predictive models to available observations in France”. CSNI Workshop on "Recent Findings and Developments in PSHA Methodologies and Applications". Lyon Congress Centre. Lyon – France. 7-9 April 2008

[13] Martin Ch., Secanell R., « Développement d’un modèle probabiliste d’aléa sismique calé sur le retour d’expérience, phase 1 », AFPS, Groupe Zonage, document de travail, GTR/CEA/1205-279, décembre 2005.

[14] Ambraseys, N.N. , Douglas J., Sarma S.K., Smit, P.M. “Equations for the estimation of strong motions from shallow crustal earthquakes using data from Europe and Middle East : Horizontal peak ground acceleration and spectral acceleration”. Bulletin of earthquake engineering (2005) 3: pp. 1-53.